Doctoral Program in Neuroscience

Deciphering apolipoprotein E-associated alterations in Alzheimer's Disease

_____

Matthew Paul Lennol

Director of the thesis
Dr. Javier Sáez Valero

Co-director of the thesis
Dra. Inmaculada Cuchillo Ibáñez

_____

Universidad Miguel Hernández de Elche

– 2023 –

This Doctoral Thesis, entitled "**Deciphering apolipoprotein E-associated alterations in Alzheimer's Disease"** is submitted under the format of **thesis by compendium** of the following **publications**:

- Lennol MP, Sánchez-Domínguez I, Cuchillo-Ibañez I, Camporesi E, Brinkmalm G, Alcolea D, Fortea J, Lleó A, Soria G, Aguado F, Zetterberg H, Blennow K, Sáez-Valero J. Apolipoprotein E imbalance in the cerebrospinal fluid of Alzheimer's disease patients. Alzheimers Res Ther. 2022 Nov 2;14(1):161. doi: 10.1186/s13195-022-01108-2. PMID: 36324176; PMCID: PMC9628034.

- Lopez-Font I †, Lennol MP †, Iborra-Lazaro G, Zetterberg H, Blennow K, Sáez-Valero J. Altered Balance of Reelin Proteolytic Fragments in the Cerebrospinal Fluid of Alzheimer's Disease Patients. Int J Mol Sci. 2022 Jul 7;23(14):7522. doi: 10.3390/ijms23147522. PMID: 35886870; PMCID: PMC9318932.

- Cuchillo-Ibañez I, Lennol MP, Escamilla S, Mata-Balaguer T, Valverde-Vozmediano L, Lopez-Font I, Ferrer I, Sáez-Valero J. The apolipoprotein receptor LRP3 compromises APP levels. Alzheimers Res Ther. 2021 Nov 2;13(1):181. doi: 10.1186/s13195-021-00921-5. PMID: 34727970; PMCID: PMC8565065.

Dr. Javier Sáez Valero, director, and Dr. Inmaculada Cuchillo Ibáñez, co-director of the doctoral thesis entitled **"Deciphering apolipoprotein E-associated alterations in Alzheimer's Disease",**

REPORT:
That Matthew Paul Lennol has performed, under our supervision, the work entitled **"Deciphering apolipoprotein E-associated alterations in Alzheimer's Disease",** pursuant to the terms and conditions established in the Research Plan and following the Code of Good Practices of the Miguel Hernández University of Elche, successfully meeting the objectives planned for its public defence as a doctoral thesis.

In witness whereof we sign for all pertinent purposes, in Sant Joan d'Alacant on

.... 2023

Thesis director   Thesis co-director

Dr. Javier Sáez Valero   Dr. Inmaculada Cuchillo Ibáñez

Dr. Elvira de la Peña García, Coordinator of the Doctoral Programme in Neurosciences

REPORTS:

That Matthew Paul Lennol has performed, under the supervision of our Doctoral Programme, the work entitled **"Deciphering apolipoprotein E-associated alterations in Alzheimer's Disease",** pursuant to the terms and conditions established in the Research Plan and following the Code of Good Practices of the Miguel Hernández University of Elche, successfully meeting the objectives planned for its public defence as a doctoral thesis.

In witness whereof I sign for all pertinent purposes, in Sant Joan d'Alacant on

.... 2023

Dr. Elvira de la Peña García
Coordinator of the Doctoral Program in Neurosciences

GRANT INFORMATION

INDEX

LIST OF ABBREVIATIONS

Aβ: Amyloid Beta

ABCA: ATP Binding Cassette transporter A

ABCG: ATP Binding Cassette subfamily G

AD: Alzheimer's Disease

ADAM: A Disintegrin And Metalloproteinase

AICD: APP Intra-Cellular Domain

AMPA: α-Amino-3-hydroxy-5-methyl-4-isoxazolepropionic acid receptor

APLP: APP-like protein

APP: Amyloid Precursor Protein

ApoE: Apolipoprotein E

BACE: Beta-site APP Cleaving Enzyme

BBB: Blood-Brain Barrier

CNS: Central Nervous System

CSF: Cerebrospinal Fluid

CTF: C-Terminal Fragment

Dab1: Disabled-1

ELISA: Enzyme-Linked Immunosorbent Assay

fAD: Familial Alzheimer's Disease

GFAP: Glial Fibrillary Acidic Protein

GSK3β: Glycogen Synthase Kinase Beta

HDL: High Density Lipoprotein

HSPG: Heparan Sulphate Proteoglycan

ICD: Intracellular Domain

IDE: Insulin-Degrading Enzyme

IP: Immunoprecipitation

iPSC: Induced Pluripotent Stem Cell

ISF: Interstitial Fluid

LDL: Low-Density Lipoprotein

LDLR: Low-Density Lipoprotein Receptor

LPS: Lipopolysaccharide

LRP: Low-density lipoprotein receptor-Related Protein

LXR: Liver X Receptor

MAPT: Microtubule Associated Protein Tau

MS: Mass Spectrometry

NfL: Neurofilament Light

NFT: Neurofibrillary Tangle

NMDAR: N-Methyl-D-Aspartate Receptor

P-tau: Phosphorylated tau

PET: Positron Emission Tomography

PHF: Paired Helical Filament

PI3K: Phosphoinositide 3-Kinase

PS: Presenilin

RXR: Retinoid X Receptor

sAD: Sporadic Alzheimer's Disease

sAPP: Soluble APP

SDS-PAGE: Sodium Dodecyl-Sulphate Polyacrylamide Gel Electrophoresis

SORL: Sortilin-related receptor

SP: Senile Plaques

T-tau: Total tau

TLR: Toll-Like Receptor

TNF-α: Tumour Necrosis Factor α

TREM2: Triggering Receptor Expressed on Myeloid cells 2

VLDL: Very Low-Density Lipoprotein

ABSTRACT

Alzheimer's disease (AD) is an age-related neurodegenerative disorder and the main cause of dementia, characterised by two specific pathological hallmarks: the extracellular deposition of neurotoxic amyloid beta peptides in the form of senile plaques, and the intracellular accumulation of hyperphosphorylated forms of the cytoskeletal protein tau in neurofibrillary tangles. Two forms of AD exist, early-onset AD, which occurs before the age of 65 years and is usually hereditary; and late-onset, or sporadic AD (sAD), which accounts for more than 95% of cases and is linked to a series of genetic and environmental risk factors. *APOE*, the gene encoding the apolipoprotein E (apoE) protein, is the most prominent genetic risk factor for sAD. Three allelic variants exist in humans: *APOE* ε2, the least common variant linked to a reduced risk of developing AD; *APOE* ε3, the most common variant considered to be risk-neutral; and *APOE* ε4, linked to an increased risk of AD. The isoforms encoded by the allelic variants differ in single amino acid substitutions at positions 112 or 158; with apoE4 presenting Arginine at both positions, thus being unable to form disulphide-linked dimers, the most effective form of apoE to interact with cellular receptors. ApoE is the most important cholesterol transporter in the brain, however it has many other functions, some of which are dependent on its interactions with receptors, including apoER2, the main ligand of which is reelin. Reelin is a large glycoprotein that regulates neuronal migration during brain development, and is implicated in synaptic transmission, plasticity, and memory in the adult brain.

In this doctoral thesis, we aimed to characterise altered patterns of apoE and reelin proteins in the cerebrospinal fluid (CSF) of AD patients, and to describe a relatively unknown apoE receptor, LRP3, and determine how it interacts with key proteins in AD. An imbalance of apoE glycoforms, with an increased abundance of immatures species, was detected in AD samples compared to controls, alongside the appearance, exclusively in AD samples, of an aberrant high molecular mass species that was compatible with dimers but resistant to reducing agents. ApoE4 also participates in these aberrant dimers, despite the inability of these isoforms to form disulphide-linked dimers. The apoE glycoform

imbalance was replicated in AD brain samples. Full-length reelin levels decreased in AD CSF and presented a different profile of fragments, characterized by increased C-terminal region cleavage and decreased N-terminal region cleavage, as compared with control subjects. Once again, aberrant complexes of high molecular mass, composed mainly of N-terminal reelin fragments, were also detected in AD, regardless of the *APOE* genotype. Regarding LRP3, we found a reduced presence of the receptor in the brain of AD patients and discovered that the expression of LRP3 is modulated by apoER2; and that LRP3 can in turn influence APP and Aβ levels. These results indicate a possible pathological situation in which modifications of the apoE and reelin proteins affect their protective functions and the efficiency of apoER2 signalling, thus contributing to the exacerbation of AD. These modifications can also affect mechanisms of co-regulation of key AD proteins, such as APP, thus implicating the LRP3 receptor. The apoE glycoform imbalance and the fragmentation profile of reelin, alongside the appearance of aberrant aggregates of both proteins, could serve as potential read-outs of impaired signalling, and may also have potential for AD diagnosis and progression.

RESUMEN

La enfermedad de Alzheimer (EA) es un trastorno neurodegenerativo asociado a la edad y la principal causa de demencia. Se caracteriza por dos rasgos patológicos principales: el depósito extracelular de péptidos neurotóxicos de beta amiloide en forma de placas seniles, y la acumulación intracelular de formas hiperfosforiladas de la proteína citoesquelética tau en ovillos neurofibrilares. Existen dos formas de EA: EA de inicio temprano (antes de los 65 años), que suele ser hereditaria, y EA de inicio tardío o esporádica, que representa más del 95% de casos y se asocia a factores de riesgo genéticos y ambientales. *APOE*, el gen que codifica la apolipoproteína E (apoE), es el factor de riesgo genético más importante para sAD. Existen tres variantes alélicas en humanos: *APOE* ε2, la menos frecuente y relacionada con un riesgo reducido de desarrollar EA; *APOE* ε3, la más común y neutra; y *APOE* ε4, relacionada con un mayor riesgo de padecer EA. Las isoformas codificadas por las variantes alélicas difieren en sustituciones de un aminoácido en las posiciones 112 o 158; y apoE4 presenta arginina en ambas posiciones, por lo que no puede formar dímeros por enlaces disulfuro, la forma más efectiva en la interacción con receptores celulares. ApoE es el transportador de colesterol más importante en el cerebro, pero tiene otras funciones, algunas asociadas a su interacción con receptores, como el apoER2, cuyo ligando principal es la reelina. La reelina es una glicoproteína involucrada en la migración neuronal durante el neurodesarrollo, y en el cerebro adulto participa en la memoria, y en la transmisión y plasticidad sináptica.

En esta tesis doctoral, nuestro objetivo fue caracterizar los patrones alterados de las proteínas apoE y reelina en el líquido cefalorraquídeo (LCR) de pacientes con EA, y describir la función de un receptor de apoE, LRP3, apenas caracterizado en el SNC. Encontramos un desbalance de las glicoformas de apoE, con una mayor abundancia de especies inmaduras en las muestras de LCR con EA, en comparación con los controles. También detectamos la aparición, exclusivamente en EA, de una especie aberrante de alto peso molecular, compatible con los dímeros pero resistente a agentes reductores. El apoE4 también participa en estos dímeros aberrantes, a pesar de su incapacidad

de formar dímeros por enlaces disulfuro. El desequilibrio de glicoformas de apoE se replicó en muestras de cerebro con EA. Los niveles de reelina, como proteína completa, sin procesar proteolíticamente, disminuyeron en el LCR de EA y presentaron un perfil alterado de fragmentos, debido a un aumento de fragmentación en la región C-terminal y una disminución en la región N-terminal, en comparación con los controles. Detectamos complejos aberrantes de 500 kDa compuestos principalmente por fragmentos N-terminales de reelina, independientemente del genotipo *APOE*. En cuanto a LRP3, detectamos niveles reducidos del receptor en el cerebro de pacientes con EA y descubrimos que la expresión de LRP3 está modulada por apoER2; y que LRP3 puede a su vez influir en los niveles de APP y del péptido beta amiloide a través de mecanismos de endocitosis. Estos resultados indican que modificaciones de las proteínas apoE y reelina podrían afectar a sus funciones protectoras y a la eficiencia de la señalización de apoER2, contribuyendo así a la exacerbación de la EA. Estas alteraciones pueden también afectar la co-regulación de proteínas claves en la EA, como APP, a través del receptor LRP3. El desequilibrio de las glicoformas de apoE y el perfil de fragmentación de reelina, junto con la aparición de agregados aberrantes de ambas proteínas, podrían servir como indicadores de señalización alterada y tener un uso potencial para el diagnóstico de la EA.

INTRODUCTION

ALZHEIMER'S DISEASE

Background

Alzheimer's Disease (AD) is a neurodegenerative disease characterized by memory loss and a progressive decline in cognitive abilities that was first described in 1907 in a case study reported by Alois Alzheimer of a 51-year-old patient with rapidly deteriorating memory (Alzheimer, 1907). Whilst a variety of progressive neurological conditions were known at that time, the early age of onset and a new pathological finding, the neurofibrillary tangles (NFT), made this condition unique. Over time, AD has been split into two clinical conditions depending on the age of onset. Early-onset AD is a rare condition that affects individuals under the age of 65, and nowadays is known to be mostly hereditary, thus it can also be referred to as familiar AD; on the other hand, a similar dementia in the elderly, in individuals over 65 years of age, is referred to as late-onset or sporadic AD, representing >95% of AD cases.

According to the World Health Organization, AD is the most common form of dementia, defined as a deterioration in cognitive function that surpasses the consequences associated to biological aging. AD is responsible for approximately 60-80% of cases of dementia and affects over 50 million people worldwide, with an increase in AD-associated deaths in recent years (Gauthier et al., 2021). The risk of developing AD greatly increases with age, affecting 5% of people aged 60-74 years, 13% of people aged 75-84, and 33% of people aged 85 or above (2022 Alzheimer's Disease facts and figures). Therefore, the disease constitutes a much larger burden on society than other common forms of dementia, such as dementia with Lewy bodies, frontotemporal dementia, or secondary dementia (caused by other primary factors, such as a stroke); and the associated economic burden of the disease has increased drastically in recent years (Wong, 2020).

In AD, the pathophysiological changes precede clinical symptoms by various years (Jack et al., 2010). The disease is characterized by two main pathological hallmarks: amyloid or senile plaques (SPs) that accumulate extracellularly, and the deposition of NFTs constituted of hyperphosphorylated tau within neurons. The role of these hallmarks has been largely discussed,

leading to both amyloid- and tau-driven hypotheses (reviewed in Ferrer, 2022). Although other animals may present Aβ deposits and tau pathology, the distribution and prevalence of these characteristic hallmarks are exclusive to humans (Ferrer, 2022).

The distribution and progression mainly of NFTs, but also SPs, in post-mortem brains allows the categorization of the severity of the pathology. Regarding NFTs, the most widely used stage categorization system is called Braak stages (Braak and Braak, 1991), which describe neurofibrillary degeneration. In Braak stages I & II NFTs appear in the entorhinal and transentorhinal cortex; at stages III and IV they appear in the hippocampus, limbic system and temporal cortex; and finally, in stages V and VI the NFTs spread across the majority of the neocortex (Braak & Braak, 1991; Braak & Del Tredici, 2011). Regarding the distribution of SPs, the stages are characterized as 0 (absence of SPs), A (low density SPs in the occipital, temporal and frontal cortex), B (SPs in neocortical association areas and hippocampus) and C (SPs in the primary sensory and motor areas) (Braak & Braak, 1997). The different progressive stages of AD are illustrated in **Figure 1**.
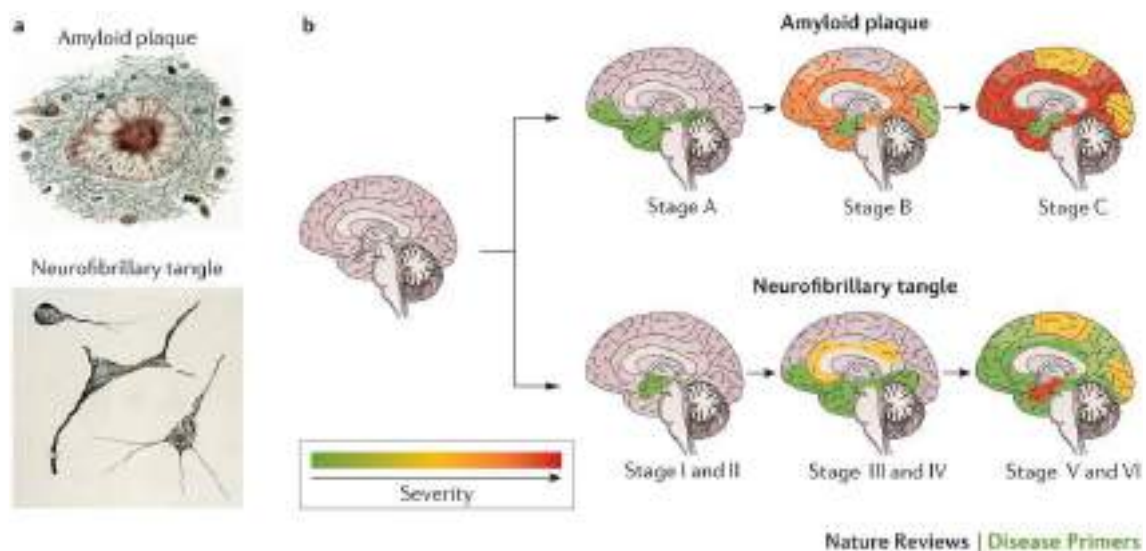

Nature Reviews | Disease Primers

Figure 1. **Progression of Aβ and tau pathology in AD. A**: Illustration of an amyloid plaque (above) and a NFT (below). **B**: Progression of amyloid (above) and tau (below) pathologies over the course of AD. Small amounts of amyloid plaques start to appear in the temporal, frontal and occipital cortex (Stage A), before expanding to the hippocampus and neocortical association areas (Stage B), and then finally to the primary sensory and motor areas (Stage C). NFTs first

appear in the entorhinal and transentorhinal cortex (Stages I & II), and then progress to the hippocampus, limbic system and temporal cortex (Stages III & IV), before occupying the majority of the neocortex (Stages V & VI). Extracted from Masters et al., 2015.

Amyloid-beta (Aβ)

The extracellular amyloid plaques, or SPs, are one of the main hallmarks of AD. SPs represent the accumulation of amyloid beta (Aβ) peptides, which are short peptides of 36–43 amino acids generated by the proteolytic processing of the so-called Amyloid Precursor Protein (APP), a large type I trans-membrane protein (Haass, 2012). APP belongs to a protein family alongside APP-like protein 1 (APLP1) and 2 (APLP2), which are all type-I transmembrane proteins that are processed in a similar manner; however, the Aβ domain is unique to APP (Wasco et al., 1993; Coulson et al., 2000). Despite being at the centre of many studies, the physiological function of APP has yet to be fully defined, probably because APP is rapidly processed by proteolytic enzymes. Nonetheless, APP appears to be crucial for adequate migration of neuronal precursors to the cortical plate in neurodevelopment (Young-Pearse et al., 2007), as well as many other different functions, such as neurite outgrowth and synaptogenesis (reviewed in Zheng & Koo, 2006).

The *APP* gene is located on chromosome 21, and three major isoforms can arise from alternate splicing: APP695, APP751 and APP770, which contain 695, 751 and 770 amino acids, respectively (Goate et al. 1991), all of which can generate Aβ. Even though the neuronal APP695 variant is the most abundant in the brain, levels of the APP751 and APP770 variants appear to be elevated in the AD brain and are associated with increased Aβ deposition (Menéndez-González et al., 2005). However, the relation between the expression levels of the different isoforms and their proteolytic processing is not well established.

The proteolytic processing of APP is carried out by enzymes known as secretases, which are responsible for the cleavage of many different substrates in addition to APP. Depending on the secretases involved, APP can be processed by two distinct pathways: the amyloidogenic pathway, which leads to the production of Aβ, and the non-amyloidogenic pathway, which does not. These pathways are illustrated in **Figure 2**. It is worth noting that under physiological

conditions both pathways are active in parallel, and that Aβ levels are maintained through a balance of production (amyloidogenic pathway) and clearance (Zhang et al., 2011).

APP non-amyloidogenic pathway: α-secretases and γ-secretases

In the non-amyloidogenic pathway, APP is sequentially processed by α-secretases and γ-secretases. The α-secretase cleavage site is located within the Aβ domain, and thus precludes Aβ generation (Sisodia, 1992; Spies et al., 2012). Following processing, a large soluble ectodomain called sAPPα is generated, which has an important role in neuronal plasticity and survival and has a protective function against neurotoxicity (Furukawa et al., 1996; Mattson, 1997), as well as in the regulation of neural stem cell proliferation (Caillé et al., 2004). Alongside the sAPPα fragment, a C-terminal fragment of 83 amino acids, α-CTF, that remains bound to the membrane is also generated. This α-CTF is further processed by γ-secretase, releasing a soluble intracellular fragment, the so-called APP Intra-Cellular Domain (AICD) and a small extracellular non-amyloidogenic fragment known as P3, which is rapidly degraded and does not appear to have any significant biological role.

α-secretase activity mainly resides with several members of the ADAM (A Disintegrin And Metalloproteinase) family, especially ADAM10, but also ADAM17 (Lichtenthaler et al., 2021). Overexpression of ADAM10 increases α-cleavage of APP in several cell lines (Kuhn et al., 2010), whereas ADAM10 conditional knock-out nearly abolishes sAPPα generation (Jorissen et al., 2010). It has been demonstrated that activation of ADAM10 by the synthetic retinoid acitretin is viable *in vitro* and in patients with AD, and this activation induces an increase of the levels of sAPPα in the cerebrospinal fluid (CSF) (Endres et al., 2014). Furthermore, in AD patients, reduced ADAM10 protein levels in platelets have been associated to significantly reduced sAPPα levels in platelets and in the CSF (Colciaghi et al., 2002), and reduced α-secretase activity has been detected in the temporal cortex of affected patients (Tyler et al., 2002). Indeed, ADAM10 is detectable in the CSF and the levels of the mature full-length species and fragments of ADAM10 seem to be significantly reduced in AD CSF samples (Sogorb-Esteve et al., 2018).

The γ-secretase activity resides in a complex of high molecular mass consisting of four components, all of which are necessary for enzymatic activity (Kimberly et al., 2003; Takasugi et al., 2003):

- Presenilin (PS), present as two distinct homologs, PS1 and PS2, that act as catalytic components of the γ-secretase (Ahn et al., 2010).
- Nicastrin, which is a large glycoprotein that acts as a scaffolding protein within the complex (Arakawa et al., 2002)
- Anterior pharynx-defective-1 (APH-1), which is required for the cell-surface localization of nicastrin (Goutte et al., 2002).
- Presenilin-enhancer-2 (PEN-2), which is necessary for the expression of PS and the maturation of nicastrin (Steiner et al., 2002).

APP amyloidogenic pathway: β-secretases and γ-secretases

The amyloidogenic pathway consists in the sequential processing of APP through β-secretases that are exclusive to this processing pathway, and γ-secretases, which are shared between the two pathways. BACE1 (Beta-site Amyloid precursor protein Cleaving Enzyme 1) is the main β-secretase in the central nervous system (CNS) (Sinha et al., 1999; Hampel et al., 2021). BACE1 has been proven to be directly involved in Aβ production in several transgenic mouse models (Luo et al., 2001; Domínguez et al., 2005), as BACE1 knock-out mice do not produce detectable levels of Aβ and are rescued from neuronal loss and memory deficits (Ohno et al., 2004; Ohno et al., 2006). Studies in human brains have detected that BACE1 protein and activity levels are elevated in regions affected by AD (Yang et al., 2003; Johnston et al., 2005). In the CSF of AD patients, various different BACE1 species co-exist, yet the mature full-length species is the only one presenting higher levels (López-Font et al., 2019). Since cleavage of APP by BACE1 is the rate-limiting step in Aβ production, the viability of BACE1 as a therapeutic target in AD has been extensively studied (Egan et al., 2018; Henley et al., 2019).

As a result of the β-cleavage, the APP ectodomain is released as a soluble fragment: sAPPβ. sAPPβ is shorter than sAPPα, given that it does not contain any part of the Aβ peptide (amino acids 1-16), unlike sAPPα, and has a role in mediating axonal pruning and neuronal cell death (Nikolaev et al., 2009). The

APP domain that remains inserted in the membrane, β-CTF, is also further processed by γ-secretase, thus finally producing extracellular Aβ and intracellular AICD fragments (Zhang et al., 2017). γ-secretase cleavage takes place within the transmembrane domain and can yield Aβ species of varying length, of which the most relevant *in vivo* species are Aβ40 (containing 40 amino acids), the most common species, and Aβ42 (containing 42 amino acids), the most amyloidogenic species associated to AD pathology (Zhao et al., 2007; Kandalepas et al., 2013; Sadleir et al., 2016).

Alternative APP secretases, including δ- and η-secretases, as well as alternative β-secretases, have been discovered recently and appear to be linked to AD (discussed in Andrew et al., 2016). Therefore, many APP proteolytic pathways co-exist.

Monomeric Aβ is released under physiological conditions and regulates synaptic functions, amongst others, such as promoting brain recovery after injury and fixing leaks in the blood-brain barrier (BBB) (Jeong et al., 2022). The levels of the Aβ peptide are physiologically controlled through a balance of its production and clearance, but the peptide, particularly the Aβ42 species, has a natural tendency to self-associate into dimers and soluble oligomers. In AD, abnormally folded amyloid peptides form insoluble and toxic amyloid fibrils that accumulate in extracellular plaques (Lane et al., 2018). Accordingly, high levels of amyloid deposits in the brain are associated to low CSF Aβ levels, thus indicating a decline in the solubility of the peptides alongside a reduced rate of clearance (Grimmer et al., 2009; Strozyk et al., 2003). Further studies associate the reduction in CSF Aβ levels to AD progression (Wahlund & Blennow, 2003), and for this reason the measurement of decreased CSF Aβ levels is a diagnostic biomarker used nowadays (Blennow & Zetterberg, 2018), which will be discussed at a later point.

The accumulation of Aβ in SPs led to the belief that the production of Aβ fibrils was the triggering factor responsible for AD progression, referred to as the amyloid cascade hypothesis (Hardy & Higgins, 1992). Nonetheless, recent studies reported toxic effects for Aβ oligomers, in addition to fibrils, indicating that Aβ oligomers, rather than SPs, are the leading effectors of AD (Selkoe & Hardy, 2016; Cline et al., 2018). Thus, Aβ plays a major role in neurotoxicity in key areas

such as the hippocampus and cerebral cortex, leading to cognitive impairment, as well as causing damage to astrocytes, microglia and neurons, and influencing NFT formation (Chen et al., 2017). Aβ can also become toxic by promoting oxidative stress and alterations in calcium metabolism and membrane potentials (Reiss et al., 2017; Soria Lopez et al., 2019).
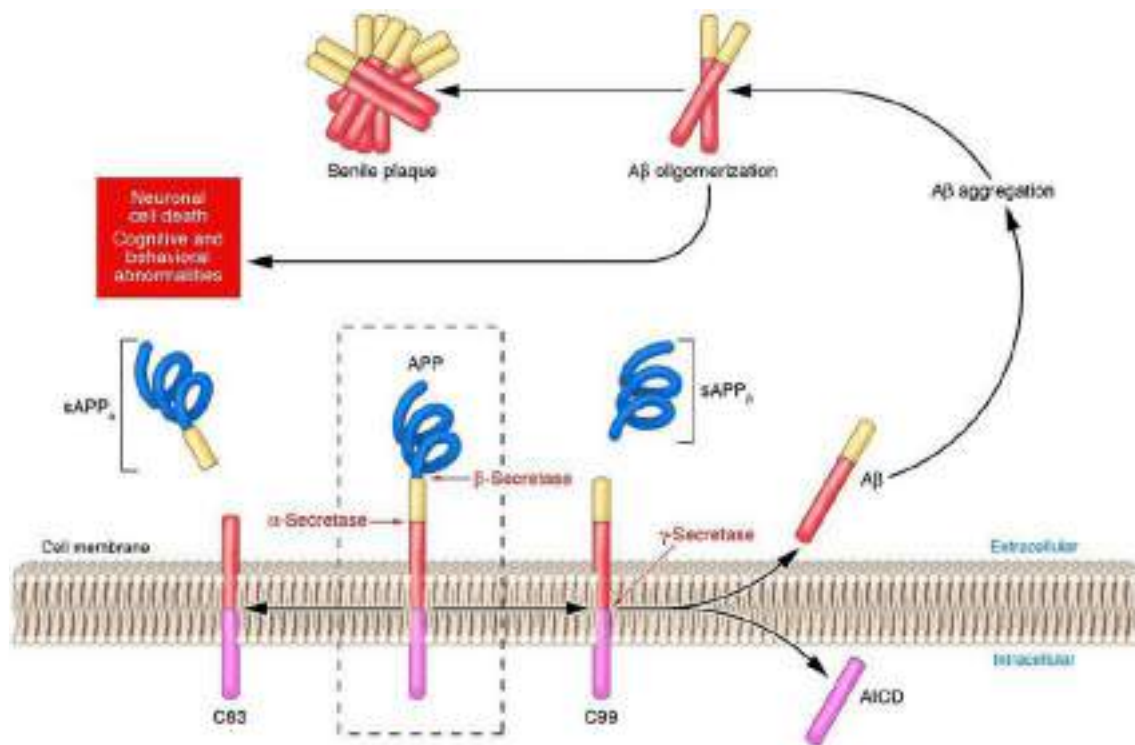

Figure 2. **APP processing pathways**. APP can be processed by the non-amyloidogenic pathway (left) or the amyloidogenic pathway (right). APP is first cleaved by α- or β-secretase into large soluble fragments (sAPPα and sAPPβ, respectively) and a membrane-bound C-terminal fragment (C83 and C99, respectively). These CTFs are further processed by γ-secretase, yielding an APP intracellular domain (AICD) common to both pathways, and a soluble fragment, which is Aβ in the case of the amyloidogenic pathway. Aβ then aggregates and can form soluble oligomers, or insoluble senile plaques in the extracellular space. Extracted from Spies et al., 2012.

Tau: Formation of NFTs

Tau is a microtubule associated protein expressed mainly in neurons (Grundke-Iqbal et al., 1989; Wood et al., 1986) that is encoded by the *MAPT* gene. Tau plays a key role in the maintenance of neuronal morphology, the axonal transport of organelles and synaptic plasticity (Robbins et al., 2021), and these functions are modulated by site-specific phosphorylation, regulated by kinases and

phosphatases (Mandelkow & Mandelkow, 2012). There is significant evidence supporting the notion that a disruption of normal phosphorylation events results in tau dysfunction in neurodegenerative diseases, including AD, but also others such as Pick's disease, progressive supranuclear palsy, corticobasal degeneration, argyrophilic grain disease and other primary age-related tauopathies (Kovacs, 2017). In AD, the tau protein is hyperphosphorylated and incapable of performing its biological roles adequately, consequently affecting long-term potentiation and synaptic plasticity (Boekhoorn et al., 2006; Shentu et al., 2018). In fact, since tau plays an important role in maintaining synaptic function and neuronal projections, a loss of tau function in key areas such as the hippocampus could be responsible for the memory deficits present in AD (Selkoe, 2002).

Abnormal modifications and truncations of tau, alongside the accumulation of hyperphosphorylated tau (P-tau), results in its self-aggregation within neurons into loosely intertwined paired helical filaments (PHFs) and tightly wrapped straight filaments, which then lead to the formation of NFTs (Sinsky et al., 2021), finally leading to neuronal collapse and cell death (Goedert et al., 1992). The formation of NFTs is illustrated in **Figure 3**. The accumulation of NFTs starts in specific regions of the cortex, before expanding to the majority of cortical structures in the latter stages of the disease. Despite the distinct spatial distribution of NFTs (intracellular) and SPs (extracellular), studies in mouse models have shown that Aβ can enhance tau aggregation (He et al., 2017); similarly, other factors, such as cleavage by proteases, may also promote tau aggregation (Zhang et al., 2017). Tau also accumulates in the AD brain as neuropil filaments, which occurs in areas of the brain lacking cell bodies (Braak & Braak, 1988).
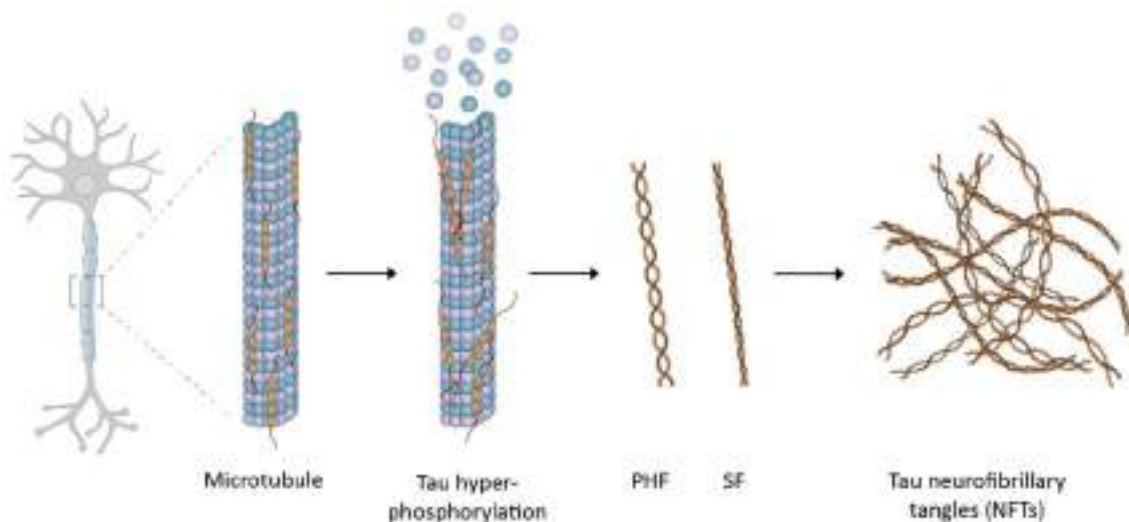
Figure 3. NFT formation. The hyperphosphorylation of microtubule-associated tau protein leads to its self-aggregation and the accumulation of intracellular loosely intertwined paired helical filaments (PHF) and tightly wrapped straight filaments (SF). These PHFs and SFs then lead to the accumulation of NFTs. Extracted from Jie et al., 2021.

Other characteristics of AD

Alongside the key hallmarks mentioned beforehand, AD is also characterized by other factors:

- **Synaptic deficits**: The loss of synaptic plasticity is at the centre of the clinical manifestations of AD, as the loss of synapses and synaptic receptors correlates with the cognitive decline presented throughout the disease (Boros et al., 2017). The progressive deposition of Aβ into plaques, which slowly grow in size, is believed to be responsible for the damage to synapses and the subsequent reduction in glutamatergic transmission (Wu et al., 2010; Burgold et al., 2011). However, there is much evidence that implicates soluble oligomeric Aβ as the primary noxious form leading to synaptic loss (reviewed in Reiss et al., 2018). As the harmful effects of Aβ spread to other brain areas, the damage becomes more severe and can also promote the phosphorylation of tau, its dissociation from microtubules, and the formation of NFTs, which directly cause neurodegeneration (Jack et al., 2018). Therefore, it is possible that β-amyloid-induced synaptic deficits are responsible for the early stages of the disease, whereas the tau-associated axonal damage

characterizes the latter stages of synaptic degradation in AD (Pereira et al., 2021), however alternative hypotheses have also been proposed (reviewed in Ferrer et al., 2022).

- **Neuroinflammation**: Astrocytes and microglia are the main cell types in the central nervous system responsible for the inflammatory response, and prolonged neuroinflammation plays a key role in several neurodegenerative diseases, although its precise role has yet to be determined (Calsolaro & Edison, 2016, Parkhizar & Holtzman, 2022). Activated microglia and reactive astrocytes have been detected in the brains of AD patients, and microglial cells have been observed surrounding amyloid plaques (Sastre et al., 2006). Microglia and astrocytes can play a key role in AD through the release of high levels of pro-inflammatory cytokines (Morales et al., 2014) or by promoting Aβ deposition (Guo et al., 2002). Furthermore, astrocytes and microglia can up-regulate β-secretase protein levels and enzymatic activity, thus increasing the production of Aβ (Sastre et al., 2003). Finally, these glial cell types may also contribute to the progression of the disease by enhancing oxidative and endoplasmic reticulum stress (Chen et al., 2014; Li et al., 2015; Lennol et al., 2021).

- **Lipids**: The brain is one of the most lipid-rich organs in the body, as lipids constitute the basic structural component of neuronal cell membranes. The disruption of lipid homeostasis is linked to neurological disorders including AD, and as such, variations of fatty acids in lipid rafts and cerebral lipid peroxidation are detected in the early stages of the disease (Kao et al., 2020). The most abundant lipid in the brain is cholesterol, where it is formed *de novo*, given that the blood-brain barrier prevents lipids entering the brain (Vance et al., 2005). Cholesterol plays an important role in amyloidogenesis (Di Paolo & Kim, 2011), as demonstrated by studies showing that increased levels of cholesterol seem to be responsible for Aβ formation in the early stages of AD (Kojro et al., 2001). Cholesterol influences APP processing by affecting the activity of all the secretases involved (α-, β- and γ-secretases), and mediates Aβ metabolism, as increased cholesterol levels are associated

to increased Aβ levels (Puglielli et al., 2003). Cholesterol metabolites also appear to play a key role in AD, as high levels of 27-hydroxycholesterol have been detected in the brain and CSF of AD patients (Testa et al., 2016). Furthermore, many of the genetic risk factors for AD are involved in lipid homeostasis (Harold et al., 2009).

Genetics

As mentioned, two different variants of AD exist: sporadic AD (sAD), also known as late-onset AD, associated to an increased risk in the older population; and early-onset AD, which is usually linked to several genetic mutations in key elements of the disease that lead to an early development of symptoms, in which case it is also referred to as familial AD (fAD). sAD is the most common form of the disease and is responsible for 95-98% of cases (van Cauwenberghe et al., 2016).

fAD is an autosomal dominant condition caused by the mutation in one (or more) of the following three genes: *APP* (on chromosome 21, encoding the amyloid precursor protein, APP) (Goate et al., 1991), *PSEN1* (on chromosome 14, encoding the γ-secretase catalytic subunit presenilin 1, PS1) (Sherrington et al., 1995) or its homologous *PSEN2* (on chromosome 1, encoding presenilin 2, PS2, which can substitute PS1 in the γ-secretase complex) (Levy-Lahad et al., 1995; Canavelli et al., 2014). More than 200 mutations for these genes have been described (Cruts et al., 2012) that are believed to cause this early form of AD, either by enhancing the production and deposition of Aβ through the increase of APP levels and its amyloidogenic processing, or by the generation of an imbalance between Aβ42 and Aβ40 species (Selkoe, 1997; Walker et al., 2005). The heritability of this presentation of the disease ranges between 92 and 100% (Cacace et al., 2016). Nonetheless, uncertainties arise regarding the heritability of the illness due to the appearance of rare variants (Ayodele et al., 2021) associated to mutations in genes such as *SORL1* (Andersen et al., 2016) and *TREM2* (Bellenguez et al., 2017). Thus, it is plausible that some early-onset AD forms are not caused by an inherited change in one of these three deterministic genes, and may rather be a consequence of a combination of other genes that

do not cause the disease directly but drastically increase the risk of developing AD.

Regarding the genetic risk factors of the most common variant of the disease, sAD, many different genes involved in different processes have been linked to the disease, such as genes related to inflammatory processes (*TREM2*) (Guerreiro et al., 2012, Jonsson et al., 2013), membrane trafficking (*SORL1, PICALM*) (Harold et al., 2009, Pottier et al., 2012), and lipid metabolism *(CLU, ABCA7)* (Harold et al., 2009; Naj et al., 2011). Recent studies have also discovered a novel mutation in the *ADAM10* gene linked to an increased likelihood of developing the disease (Agüero et al., 2020). However, the most important risk factor for sAD is the *APOE* gene (Corder et al., 1993), encoding the apolipoprotein E protein, which will be analysed in depth throughout the following sections.

sAD is likely to be caused by an interplay between various genetic and environmental factors. Epidemiological evidence indicates that hypertension and obesity increase the risk of developing sAD (Xu et al., 2015; Qizilbash et al., 2015), as well as high cholesterol, diabetes, smoking, depression, physical and mental inactivity, and a poor diet (Barnes & Yaffe, 2011; Nordestgaard et al., 2022). On the other hand, healthy activities such as physical exercise (de la Rosa et al., 2020), a healthy diet (Petersson & Philippou, 2016) and increasing cognitive reserve (Stern, 2012) all reduce the risk of developing AD, or, at least, delay the onset of the disease (reviewed in Livingston et al., 2020).

APOLIPOPROTEIN E

Basic functions and characteristics

Apolipoprotein E (apoE) is a glycoprotein of approximately 34 kDa in molecular mass that is composed of 299 amino acids. It is present ubiquitously throughout the body, although its production is tissue-specific and can be regulated by various factors, such as lipids, hormones or transcription factors (Kockx et al., 2018). In the peripheral system, apoE is produced mainly by the liver and plays an essential role in cholesterol metabolism.

In the CNS, apoE is mainly produced by astrocytes (Boyles et al., 1985), although under stress conditions it can also be produced by microglia, oligodendrocytes, choroidal epithelial cells of the choroid plexus, and even neurons (Bruinsma et al., 2010; Buttini et al., 2010). The protein is synthesized in the endoplasmic reticulum (ER), post-translationally glycosylated in the Golgi network, where it is O-glycosylated and sialylated, and then transported to the plasma membrane and secreted (Kockx et al., 2007). O-glycosylation, alongside N-glycosylation, are the main protein glycosylation mechanisms. N-glycosylation can take place in the ER and Golgi apparatus, and consists in the addition of a N-acetylglucosamine (GlcNAc) to an Asparagine (Asn) residue; O-glycosylation, on the other hand, is a more diverse form of glycosylation that occurs exclusively in the Golgi apparatus and consists in the covalent linkage of glycans to a Ser/Thr residue (Haukedal & Freude, 2020).

ApoE is the most important protein involved in lipid transport and cholesterol metabolism in the brain, which, indeed, is the most cholesterol-rich organ in the body. ApoE provides cholesterol to neurons and carries out the clearance if excessive levels are present (Mahley, 2016). In this manner, apoE participates in many different functions, such as cell membrane support and repair after injury (Lane-Donovan et al., 2016; Tensaouti et al., 2020). In order to correctly perform most of these functions, apoE needs to be secreted and lipidated.

ApoE lipidation is mediated by the ATP binding cassette transporter A1 (ABCA1) and ATP binding cassette subfamily G member 1 (ABCG1), both of which control cholesterol efflux to apoE (Vance & Hayashi, 2010). ABCA1 is one

of the key transporters regulating cholesterol efflux through lipoproteins, and thus plays a key role in forming high-density lipoproteins (HDL) (Jacobo-Albavera et al., 2021). Lipoproteins are biochemical structures responsible for the transport of insoluble lipids through extracellular fluids, and apoE binds to these structures to stabilise them and guide their function and transport (Feingold, 2022).

Astrocytic production and secretion of apoE are regulated by the liver X receptor (LXR) and the retinoid X receptor (RXR), which are nuclear receptors of transcription factors implicated in cholesterol metabolism (Fernández-Calle et al., 2022). These receptors are involved in the transcriptional regulation of *APOE* (Hong & Tontonoz, 2014), and LXR also regulates ABCA1 transcription (Koldamova et al., 2007).

The *APOE* gene is the most important genetic risk factor for sAD and is located on chromosome 19q13.32. *APOE* presents three distinct variants: *APOE* ε2, ε3 and ε4, which encode the apoE2, apoE3 and apoE4 isoforms, respectively. Given these allelic variations, six different *APOE* genotypes arise: three homozygous (*APOE* ε2/ε2, ε3/ε3 and ε4/ε4) and three heterozygous (*APOE* ε2/ε3, ε2/ε4 and ε3/ε4). The ε3 allele is by far the most common, as it presents an allele frequency of 75-78%, and is considered to be risk neutral for AD. The *APOE* ε2 allele has been reported to be protective against AD (Li et al., 2020), and is the least frequent, present in 5-8% of the population. The ε4 allele is present in ~14% of the population (Eisenberg et al., 2010; Husain et al., 2021), and has been associated to an increased risk of developing AD. Expressing one copy of the ε4 allele increases the risk of AD threefold, whereas expressing two copies of the ε4 allele can increase the risk 9- to 15-fold compared to the expression of the ε3 allele (Sando et al., 2008; Yamazaki et al., 2019); furthermore, expressing ε4 alleles also considerably reduces the age of onset of AD (Roses et al., 1996). It is important to note that, within the population of AD individuals, the presence of the ε4 allele is considerably higher and is present in approximately 37% of cases (Farrer et al., 1997; Belloy et al., 2019).

ApoE forms differ in their relative abundance in the CSF and plasma. In the latter, apoE concentrations are isoform-dependent, with apoE2 presenting the highest concentration, and apoE4 the lowest (Rasmussen et al., 2015). In the CSF, contradictory results have been observed, depending on the quantification

method used: ELISA studies showed isoform-dependent differences in apoE levels (Shinohara et al., 2016), whereas mass spectrometry studies found no such differences (Wildsmith et al., 2012). Other studies found reduced levels of apoE in *APOE* ε3/ε4 and ε4/ε4 cases compared to apoE from *APOE* ε2/ε3 cases (Cruchaga et al., 2012). In induced pluripotent stem cell (iPSC)-derived astrocyte studies, apoE4 was associated to decreased protein and mRNA levels compared to apoE3 (Lin et al., 2018), but this result was not replicated in iPSC-derived cerebral organoids (Zhao et al., 2020). Nonetheless, apoE4 is normally associated to lower protein levels than apoE3 in the CNS (Sullivan et al., 2011).

The allelic variations of apoE also affect the lipid particle size and the type of lipids apoE binds to. In AD brains, apoE-containing particles from *APOE* ε4/ε4 subjects are significantly larger than those derived from *APOE* ε3/ε3 subjects (Garcia et al., 2021). ApoE4 presents preferential binding for very low-density lipoproteins (VLDLs) and low-density lipoproteins (LDLs), whereas the preference is for HDLs in the case of apoE3 (Li et al., 2013).

Biochemical features

ApoE protein presents three distinct regions: an N-terminal domain (residues 1-167), which contains the receptor-binding region (residues 136-150), a C-terminal domain (residues 206-299) containing the lipid-binding region (residues 244-272), and a flexible hinge region (residues 168-205) that joins the two domains (Weisgraber, 1994; Frieden & Garai, 2013; Chen et al., 2021). The isoforms derived from the genotypes differ from one another in the amino acids at positions 112 and 158: apoE2 possesses cysteine at both positions 112 and 158 (Cys112/Cys158), apoE3 possesses a cysteine at position 112 and an arginine residue at position 158 (Cys112/Arg158), and apoE4 possesses arginine at both positions (Arg112/Arg158). The amino acid substitution at position 112 significantly alters the structure of apoE4, as the presence of an arginine at this position enables the formation of a salt bridge between the N-terminal and C-terminal domains of apoE4, which are otherwise separated in apoE2 and apoE3 (Yu et al., 2014). Moreover, the presence of a cysteine at position 112 enables apoE2 and apoE3 isoforms, but not apoE4, to form disulphide-linked dimers in

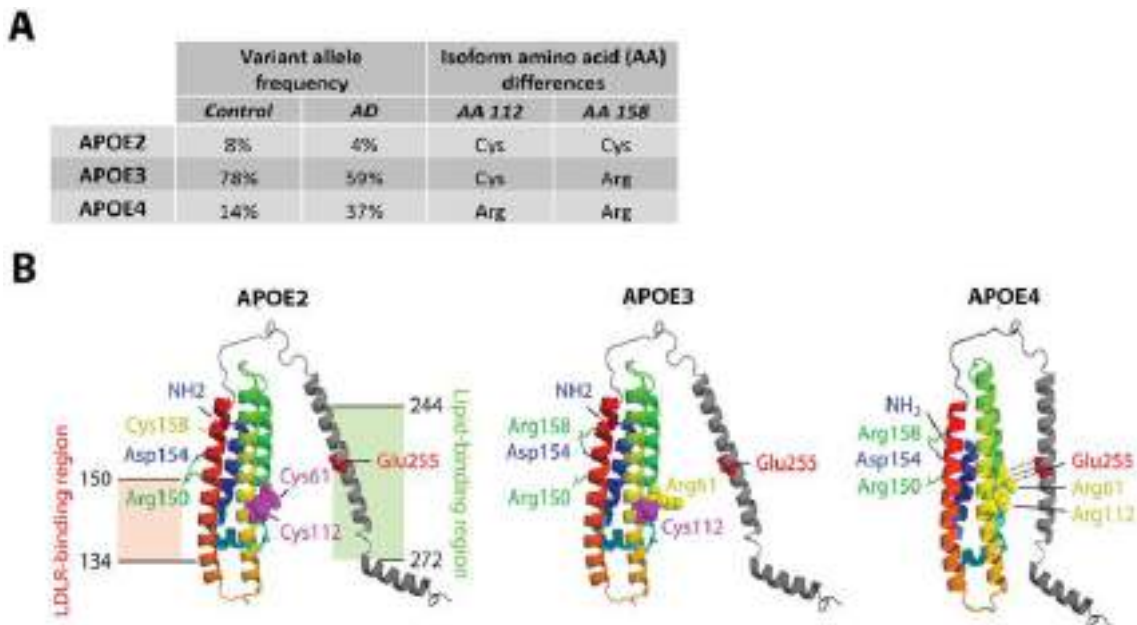the brain (Elliott et al., 2010). The structure of the different apoE isoforms is represented in **Figure 4**.

Figure 4. ApoE structure and isoforms. A: Variant frequency of each apoE isoform in control and AD subjects, and the amino acid substitutions. **B**: Visualization of the structure of the different apoE isoforms. Extracted from Belloy et al., 2019.

The amino acid composition of the different apoE isoforms influences their receptor and lipid binding abilities (Weisgraber et al., 1982) but also their lipidation levels, being apoE4 the least lipidated isoform, and apoE2 the most lipidated (Hubin et al., 2019).

Aside from the three basic allelic forms, rare variants of *APOE* have also been described, which modulate the influence of the *APOE* genotype on the risk of developing AD. The most relevant is the Christchurch mutation found in *APOE* ε3 (R136S), consisting in a substitution of Arg136 for Ser within the receptor binding region of apoE3 (Wardell et al., 1987). This mutation protected against fAD in a woman that carried two copies of *APOE* ε3 (R136S) and the *PSEN1* E280A mutation (Arboleda-Velasquez et al., 2019). Interestingly, heterozygous carriers of the R136S mutation do not appear to benefit from its protective effects (Hernandez et al., 2021). Other mutations have been recently described in the C-terminal region of apoE, including the V236E (known as the Jacksonville mutation, Valine → Glutamic acid) in *APOE* ε3, which reduces apoE aggregation,

and the R251G mutation (Arginine → Glycine) in *APOE* ε4, and both may have protective effects against the risk of developing AD (Le Guen et al., 2022).

ApoE protein is characterized by a series of post-translational modifications that affect its structure and dynamics, including phosphorylation (Jaros et al., 2012), oxidation (Jolivalt et al., 1996) and the binding of sugars either by a non-enzymatic process (glycation) (Shuvaev et al., 1999) or by enzymatic mechanisms, the most important of which is glycosylation (Ke et al., 2020). The O-glycosylation of apoE confers it the required flexibility to alter its conformation in order to bind lipoproteins. Eight different O-glycosylation sites have been identified throughout the entirety of the structure of apoE, presenting sites in the N-terminal domain (Thr8, Thr18, Ser94), the hinge region (Thr194 and Ser197), and the C-terminal region (Thr289, Thr290, Ser296) (Martens, 2022). The glycans held by apoE are mainly monosialylated (Neu5Acα2–3Galβ1–3GalNAcα1-) and disialylated (Neu5Acα2–3Galβ1–3(Neu5Acα2–6)GalNAcα1-) core 1 O-glycan structures (Flowers et al., 2020). Interestingly, apoE derived from the plasma and CSF differ in their glycosylation patterns, as CSF-derived apoE is more heavily glycosylated. Specifically, CSF-derived apoE presents much more C-terminal O-glycosylation but less N-terminal O-glycosylation than plasma apoE, with similar levels in the hinge region (Flowers et al., 2020). Moreover, apoE found within the cell appears to be more heavily glycosylated than the secreted forms (Lee et al., 2010). Furthermore, apoE glycosylation and secretion appears to depend on the cellular source: astrocytes secrete two differently glycosylated forms of apoE, whilst microglia secrete only one form of apoE but possess two intracellular forms, all of which are glycosylated (Lanfranco et al., 2021).

ApoE signalling pathway

ApoE is internalized by apoE receptors that belong to the low-density lipoprotein receptor (LDLR) family (Holtzman et al., 2012). The members of this family are seven structurally related transmembrane proteins (May et al., 2007), although recently other LDLR members have been discovered (Holtzman et al., 2012). Adequate apoE binding to these receptors is dependent on lipoprotein-binding:

when apoE binds to a lipoprotein it undergoes a conformational change that separates its N- and C- terminal regions, and this exposes the previously buried receptor-binding domain, which allows the interaction of the protein with its receptors (Chen et al., 2011). Among the LDLR family members, the receptor LDLR preferentially binds lipidated rather that non-lipidated apoE particles (Bu, 2009), whereas low density lipoprotein receptor-related protein 1 (LRP1) has a preference for binding recombinant rather than physiological apoE, HDL derived from the CSF, and lipoproteins enriched for apoE (Zhao et al., 2018). Accumulating evidence indicates that LRP1 is a key regulator of APP/Aβ metabolism (reviewed in: Shinohara et al., 2017). The allelic variations of *APOE* also affect receptor preference, as apoE4 has been observed to present a higher affinity to LRP1 than apoE3 (Cooper et al., 2021).

The sortilin-related receptor SorlA, encoded by the AD risk factor gene *SORL1* (Campion et al., 2019), preferentially binds apoE4 (Yajima et al., 2015). Furthermore, SorlA also acts as a neuronal receptor for APP and participates in the regulation of the amyloidogenic processing pathway (Spoelgen et al., 2006).

ApoE also binds proteoglycans, such as heparin sulphate proteoglycans (HSPG), through its N-terminal domain (Saito et al., 2003). Interestingly, the *APOE* Christchurch mutation has been associated to strongly decreased apoE binding to both heparin and LDLR (Lalazar et al., 1988; Arboleda-Velasquez et al., 2018).

ApoE also binds to the receptors apoER2 (another member of the LRP family, also known as LRP8) and very low-density lipoprotein receptor (VLDLR); however, reelin protein appears as the principal ligand for both receptors (D'Arcangelo et al., 1999), which will be discussed further ahead. The binding of apoE to apoER2 leads to the internalization of APP and BACE1, which could subsequently lead to an increased production of Aβ (He et al., 2007). Nonetheless, apoE may simply interfere with reelin signalling by competing for binding to the receptor (Beffert et al., 2004; Hoe & Rebeck, 2005), likely as unlipidated apoE.

Recently, new members of the LRP family, such as low-density lipoprotein receptor-related protein 3 (LRP3), have been described and may also have a role to play in AD. LRP3 is smaller and presents a different structure compared to

other core members of the LRP family, and has been associated to roles in osteogenic and adipocytic differentiation (Elsafadi et al., 2017), although the precise functions of LRP3 in the CNS are yet undiscovered.

As mentioned above, apoE forms disulphide-linked homodimers and heterodimers with apoA-II via the Cys112 residue (Martens et al., 2022), and apoE homodimers could be the necessary form to efficiently bind to the apoE/reelin receptors (Dyer et al., 1991). The presence of Arg112 that characterizes apoE4 affects its ability to form dimers, as evidenced by the lack of dimers in *APOE* ε4/ε4 subjects, and the lower levels in ε3/ε4 compared to ε3/ε3 subjects (Rebeck et al., 1998). This inability to form dimers may thus affect the interaction with apoER2 and some of the biological roles of apoE, and may be responsible, at least in part, for the increased risk of developing AD associated to the *APOE* ε4 isoform (Minagawa et al., 2009).

Reelin

Reelin is a large extracellular glycoprotein composed of 3461 amino acids with a molecular mass of approximately 430 kDa, produced by Cajal-Retzius neurons in the embryonic brain (DeSilva et al., 1997). In the adult brain, the main source of reelin is no longer the Cajal-Retzius cells, but a subpopulation of GABAergic interneurons (Alcantara et al., 1998).

Reelin is the main ligand for apoER2. In the embryonic brain reelin activates a signalling pathway that drives neuronal migration and establishes laminated structures (Frotshcer, 2010); whereas in the adult brain it is involved in regulating learning and dendritic growth, and consequentially synaptic plasticity (Jossin et al., 2020). Furthermore, in the adult brain reelin can also contribute to synapse formation and modulate synaptic transmission and plasticity by regulating Ca^{2+} entry through the interaction of apoER2 with the N-methyl-D-aspartate receptor (NMDAR) (Ventruti et al., 2011), therefore affecting learning and memory (Knuesel, 2010).

Secreted reelin forms homodimers (Kubo et al., 2002), which are likely the species that binds to receptors. Its signalling is regulated by proteolytic cleavage by metalloproteinases (namely ADAMTS-4 and ADAMTS-5) at three sites (Krstic

et al., 2012): the so-called C-terminal and N-terminal cleavage sites, and a third recently described cleavage site within the C-terminal region (Kohno et al., 2015), leading to the production of various different fragments that differ in their relative abundance and can interfere in reelin binding to apoER2 (Smalheiser et al., 2000). The proteolytic cleavage of reelin follows receptor binding, however it can also occur independently of its binding to receptors.

After reelin binds to apoER2, the receptor is sequentially processed by α- and γ-secretase (May et al., 2003; Hoe et al., 2006), and the secreted fragment of apoER2 can act as a dominant-negative receptor and inhibit reelin signalling (Koch et al., 2002). The main α-secretase responsible for this cleavage is ADAM10, in a similar fashion to APP (Chow et al., 2010), and following this α-secretase cleavage, the remaining C-terminal fragment of apoER2 is processed by γ-secretase, releasing the soluble intracellular domain (ICD), which can translocate to the nucleus and bind to the reelin promoter, leading to a decrease of reelin expression (Balmaceda et al., 2014). Thus, in addition to the interference of reelin and apoER2 extracellular fragments in subsequent reelin binding to the receptor, the ICD of apoER2 establishes a negative feedback loop between reelin binding to apoER2 and reelin expression.

The reelin signal is transduced, after binding to apoER2, beginning with the tyrosine phosphorylation of the intracellular adaptor Disabled-1 (Dab1) (Howell et al., 1999), which binds to the cytoplasmic region of apoER2. Reelin-dependent Dab1 phosphorylation leads to a kinase cascade, first by the activation of PI3K (phosphoinositide 3-kinase) (Bock et al., 2003), which in turn activates the serine-threonine protein kinase Akt (also known as protein kinase B), also by phosphorylation (Jossin & Goffinet, 2007). Activated Akt then inhibits GSK3β (glycogen synthase kinase beta) (Beffert et al., 2002), which has a key role in tau phosphorylation state (Ávila et al., 2012). In summary, reelin binding to apoER2 activates a signalling pathway that ultimately inhibits tau phosphorylation, as seen in **Figure 5**. Therefore, through its effects on tau, reelin appears to play a direct role in regulating microtubule assembly (Meseke et al., 2013), and a dysregulation of its signalling pathway could affect adequate repair of damaged neurons in AD (Krstic & Knuesel, 2013).

Reelin and Dab1 can interact with APP (Trommsdorff et al., 1998; Hoe et al., 2009), ultimately leading to a reduction in Aβ production, (Hoe et al., 2006). Furthermore, apoER2 can cluster together with APP and lead to an increase in non-amyloidogenic processing, thus also decreasing the production of Aβ (Hoe et al., 2005), leading to a complex picture in the crosstalk between reelin signalling and APP processing.

These interactions show a map of links between reelin, apoER2, APP processing (and subsequent Aβ secretion) and tau phosphorylation, the key pathological effectors in AD, and, as such, impaired reelin signalling could play an important role in the pathogenesis of the disease (Deutsch et al., 2006).
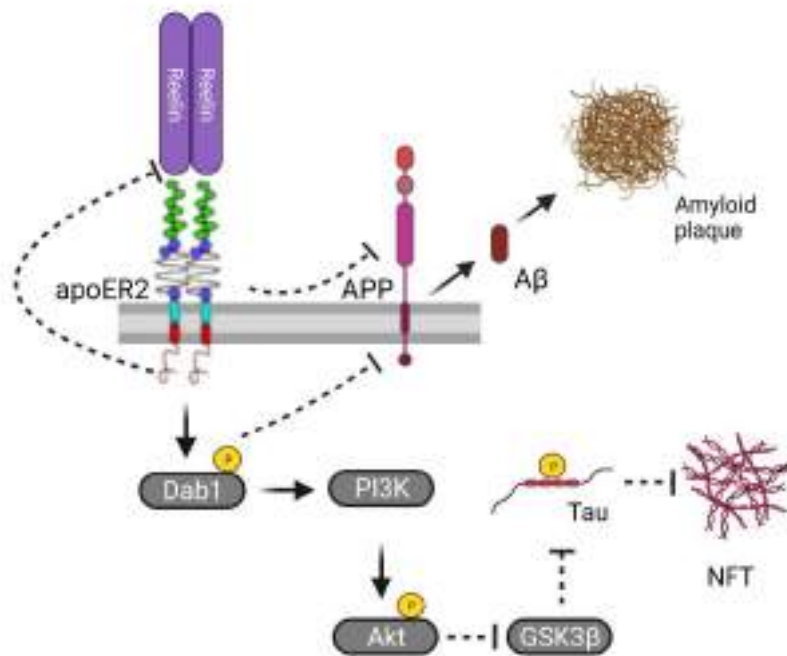

Figure 5. Reelin signalling pathway. Reelin binds to apoER2, which phosphorylates Dab1. Dab1 phosphorylation then activates PI3K, phosphorylating Akt, which inhibits GSK3β, ultimately leading to a reduction in tau phosphorylation and protecting against the formation of NFTs. ApoER2 can cluster with APP, and Dab1 can also interact with the receptor, leading to a reduced production of Aβ and subsequent SPs. Created with BioRender.com

THE ROLE OF APOE AND REELIN IN AD

ApoE in the pathogenesis of AD

Since the discovery of *APOE* ε4 as the most important genetic risk factor for AD, numerous studies have attempted to determine the exact role apoE plays in AD pathogenesis, with a special focus on the effects of the different *APOE* variants. In the normal brain, apoE is involved in the inhibition of inflammation, the clearance of debris for homeostasis, and the promotion of neuronal network resilience, all of which could play a part in the progression of AD (Flowers & Rebeck, 2020). As introduced briefly in the previous section, roles for apoE have been described for practically every aspect of the disease, including Aβ aggregation, tau phosphorylation, and synaptic deficits; however, much of the evidence is contradictory, given the conflicting results obtained from different studies depending, at least in part, on the approach used. Therefore, the precise role of the protein in AD has yet to be determined.

ApoE and Aβ: Binding, aggregation, and clearance

A vast number of studies regarding the role of apoE in Aβ accumulation, aggregation, seeding and clearance have been performed; and mouse models are frequently employed to this means. It is worth noting that apoE in mice (and other mammals) is present as the ancestral form: a single isoform that presents an Arg residue at position 112, and thus resembles the human apoE4 variant (McIntosh et al., 2012), and that the promoter regions of human and mouse apoE (*mouse-apoE*) share less than 40% homology (Maloney et al., 2007).

In AD mouse models, the expression of murine or human apoE affects the role of the protein regarding many different AD processes, such as neuroinflammation, synaptic integrity and Aβ clearance (Liao et al., 2015): in comparison to *mouse-apoE*, expression of human *APOE* isoforms reduces plaque deposition and onset, where *APOE* ε2 shows the strongest effect (Fryer et al., 2005). As human and mouse apoE differ so greatly in functions associated to AD, the development of human *APOE* knock-in transgenic murine models that

replicate AD is crucial to understand the increased risk associated to expressing the ε4 allelic variant of *APOE* (Lewandowski et al., 2020).

Many studies have reported a direct interaction between apoE and Aβ. Poorly lipidated apoE co-deposits with Aβ in amyloid plaques (Namba et al., 1991), and synthetic Aβ can bind *in vitro* to apoE derived from cells (LaDu et al., 1994), human CSF (Wisniewski et al., 1993), or human plasma (Strittmatter et al., 1993). Aβ can interact with both the N-terminal receptor binding domain and the C-terminal lipid binding domain of apoE (Wisniewski & Drummond, 2020); interestingly, heparin also interacts with both these binding sites, as well as a site on Aβ that binds apoE, and thus HSPGs could promote Aβ oligomerization and aggregation by facilitating interactions between Aβ and apoE (Brunden et al. 1993). Given the ability of Aβ to bind to the lipid binding domain of apoE, it may compete with lipids for apoE binding, and the lipidation state of apoE could determine the binding site. As such, *in vitro* studies have shown that lipid-free apoE interacts with Aβ with a higher affinity than lipidated apoE; furthermore, the incubation of apoE with Aβ oligomers hinders the ability of apoE to bind lipids and may therefore interfere with its physiological function (Verghese et al., 2013).

In addition to being dependent on the lipidation state, apoE binding to Aβ is also isoform dependent. ApoE3 has been seen to form more abundant SDS-stable complexes with Aβ than apoE4 (LaDu et al., 1995), which may indicate a better capacity of apoE3 to transport Aβ for clearance or to prevent aggregation (Petrlova et al., 2011). ApoE4 complexes with Aβ are less stable and fewer in number than those formed with apoE2 and apoE3 in the CSF of AD patients, which may be due to the poorer lipidation state of apoE4 (Tai et al., 2013). Nonetheless, conflicting results have also been found that question the interactions between apoE and Aβ. A recent study showed that soluble Aβ is a poor binding partner of apoE, and that the influence of apoE on Aβ metabolism and clearance may not require direct binding of the two proteins, and may depend instead on other mechanisms, such as LRP1 (Verghese et al., 2013).

Direct effects of apoE on Aβ, prior to plaque formation, have also been reported. Aβ accumulates in vulnerable neurons (Gouras et al., 2000), and this intracellular accumulation in late endosomal and lysosomal compartments in mice is increased by the presence of apoE4 (Zhao et al., 2014). ApoE4 can also

increase the rate of Aβ production to a greater extent than apoE2 and apoE3 when binding to apoER2, which triggers APP and BACE1 endocytosis and enhances the rate of intracellular Aβ generation (He et al., 2007). Furthermore, an *APOE* isoform dependent effect on APP transcription and subsequent Aβ production has also been reported, in which apoE4 induces the largest increase (Huang et al., 2017).

Different studies have reported an effect for *APOE* on amyloid deposition and plaque formation. *APOE* ε4-carriers present an increased plaque load and density compared to non-carriers (Tiraboschi et al., 2004), as well as the highest levels of plaque deposition, whereas *APOE* ε2-carriers present the lowest levels (Fagan et al., 2002). Moreover, mice expressing human apoE4 have higher amounts of Aβ deposition and plaques than those expressing other human apoE isoforms (Holtzman et al., 2000). The increase of Aβ in the brain coincides with a reduction in CSF Aβ42 levels, an indicator of AD, further supporting the notion that apoE4 promotes deposition (Morris et al., 2010). There is also an isoform-dependent effect of *APOE* on Aβ oligomerization, in which apoE4 increases the levels of Aβ oligomers (Hashimoto et al., 2012) and stabilizes them to a larger extent than apoE2 and apoE3 (Cerf et al., 2011).

During Aβ aggregation, the peptides change their conformation into a β-sheet structure that accelerates fibrillogenesis to form insoluble fibrils in a process known as seeding (Harper & Lansbury, 1997). A critical role for apoE4 in amyloid plaque seeding has been described, as expression of apoE4, but not apoE3, during the seeding stage enhanced amyloid deposition and neuritic dystrophy (Liu et al., 2017).

Human apoE4 may also enhance Aβ fibril formation *in vitro* (Castano et al., 1995), although results showing that apoE decreases Aβ aggregation *in vitro* have also been reported (Wood & Wetzel, 1996). As apoE3 interacts more with Aβ than apoE4, it is possible that apoE4 could be less effective in inhibiting Aβ fibrillization. This discrepancy could be explained by the differences in apoE/Aβ preparations in the different studies, as many factors, such as apoE lipidation, can play an important role. For example, the reduction of apoE lipidation (by ABCA1 depletion) increases amyloid deposition in AD transgenic mouse models (Wahrle et al., 2005).

APOE knock-out studies in mouse AD models have presented interesting results, as the knock-out led to a reduction of Aβ42 deposition in models overexpressing only human *APP* (Bales et al., 1999), whereas it led to an overall increase in plaque size in more aggressive models overexpressing both *APP* and *PSEN1* (Ulrich et al., 2018). On the other hand, the suppression of *APOE* expression in a humanized *APOE4/APP/PSEN1* mouse model led to a reduction in plaque load when performed before plaque onset, yet the reduction was not observed when performed after plaque formation onset (Huynh et al., 2017), thus supporting a role for *APOE* in plaque seeding, but not plaque growth.

Aside from the roles mentioned up to this point, many studies have also shown apoE-dependent effects on Aβ clearance. Aβ can be cleared through a plethora of mechanisms (Tarasoff-Conway et al., 2015), and apoE4 is associated to a reduced rate of clearance in all of them (Kanekiyo et al., 2014), as demonstrated in *in vivo* studies that showed a reduced rate of Aβ clearance in apoE4-TR (targeted replacement) mice when compared to apoE3-TR mice (Castellano et al., 2011).

One of the key mechanisms in the brain is Aβ degradation through the enzymatic activity of proteases, such as neprilysin and insulin-degrading enzyme (IDE), which can also degrade apoE in both intracellular compartments and in the extracellular space (Saido & Leissring, 2012). ApoE enhances the enzymatic clearance of Aβ, especially when highly lipidated (Jiang et al., 2008), however reduced neprilysin and IDE expression levels have been demonstrated in *APOE* ε4-carriers (Miners et al., 2006).

Aβ can also be cleared through the blood-brain barrier (BBB), and this clearance could be modulated by apoE (Ma et al., 2018). *APOE* ε4 is associated to BBB breakdown and a reduced rate of Aβ clearance (Montagne et al., 2020). ApoE receptors have also been implicated in Aβ clearance through the BBB, given that apoE2 and apoE3 are cleared at a faster rate through the BBB via LRP1 and VLDLR than apoE4, and the same differences in rate of clearance are present in apoE-Aβ complexes (Deane et al., 2008). Aβ can also be cleared through the interstitial fluid (ISF) via LRP1, however this pathway is complex, as some studies have seen an increased rate of clearance in *APOE*-KO mice (DeMattos et al., 2004).

A third mechanism of Aβ clearance is through intracellular lysosomal degradation in astrocytes, microglia, and neurons, and, once again, apoE4 is associated to a lower rate of clearance (Li et al., 2012). ApoE-Aβ complexes are internalized through LDLR and LRP1 to facilitate degradation (Carlo et al., 2013); however, apoE may also reduce the rate of Aβ internalization and degradation by competing for binding to receptors, such as LRP1 (Verghese et al., 2013), whereas other receptors also participate in Aβ degradation in an apoE-independent manner (Basak et al., 2012). Finally, apoE can also influence Aβ clearance through microglia and astrocytes by altering their expression profiles (Fernández et al., 2019).

In summary, many different roles for apoE in the amyloidogenic process have been described, supporting roles for apoE in the aggregation, deposition, oligomerization, and clearance of Aβ. These roles point towards a possible gain of toxic function of apoE4 by increasing the rate of amyloid deposition and aggregation, and enhancing plaque formation, or a loss of protective function compared to the other isoforms by hindering the rate of clearance or failing to protect against aggregation. The effects of apoE on Aβ are summarized in **Figure 6**.
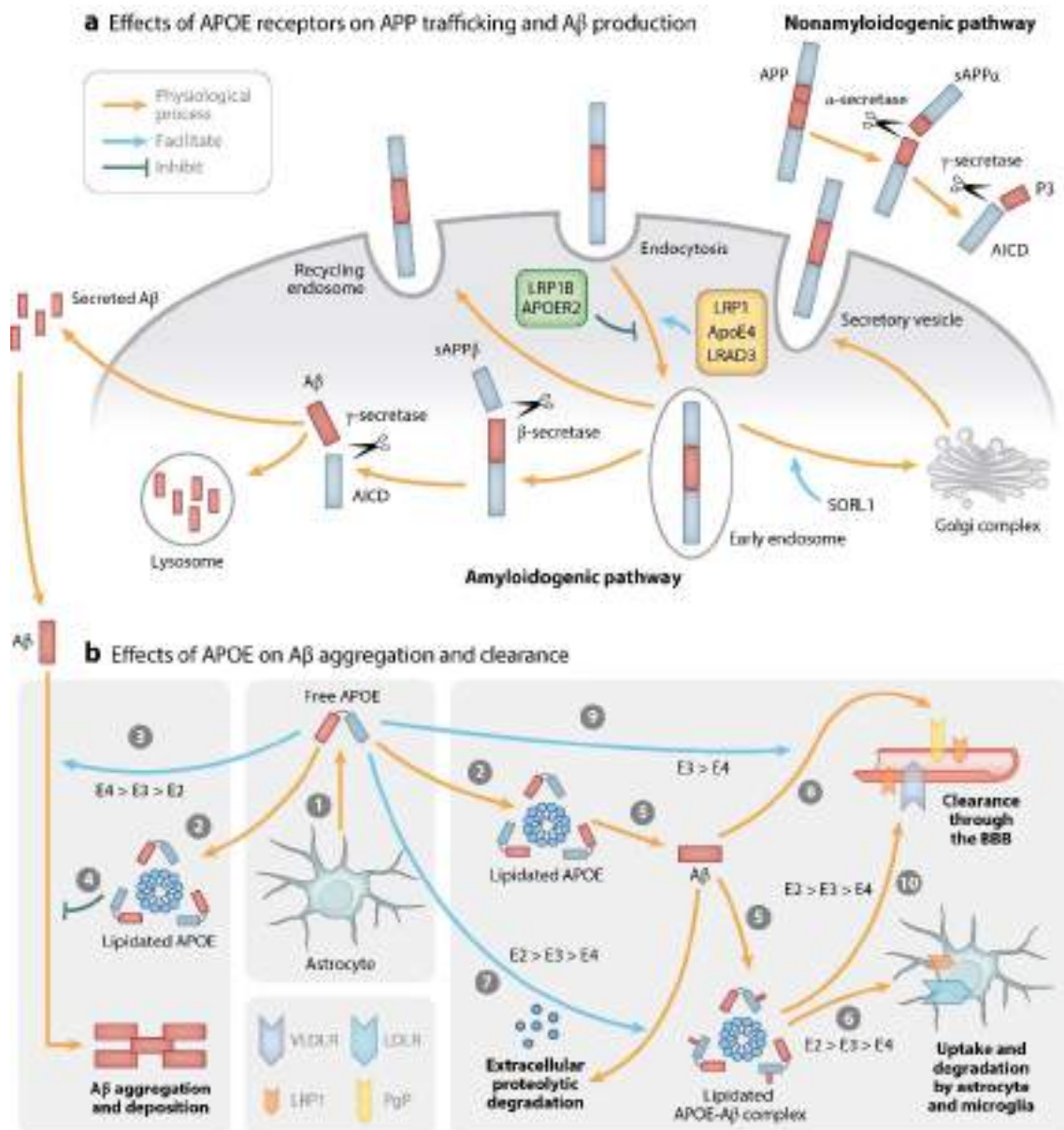
Figure 6. ApoE effects on Aβ. A: Effects of apoE on Aβ production. ApoE4 and LRP1 facilitate the endocytosis of APP, leading to an increased production of Aβ, whereas apoER2 inhibits this process. **B**: Effects of apoE on Aβ aggregation and clearance. ApoE4 facilitates Aβ aggregation and deposition, whereas lipidated apoE inhibits this process in an isoform-dependent manner (ε2>ε3>ε4). ApoE also facilitates Aβ clearance through the BBB and extracellular proteolytic degradation, also in an isoform-dependent manner (ε2>ε3>ε4). Lipidated apoE can form complexes with Aβ and participate in its intracellular degradation via LRP1 and LDLR, and, once again, apoE4 presents the lowest rate of clearance. Extracted from Yu et al., 2014.

ApoE and tau in AD

The hyperphosphorylation of tau and the subsequent formation of intracellular NFTs is one of the key hallmarks for AD that could result in a gain of toxic function of tau (Gendron & Petrucelli, 2009), and may drive the pathology (Benjanin et al., 2017). Histopathological studies have shown a link between *APOE* and NFTs in the AD brain (Rohn et al., 2012), as *APOE* ε4-carriers present a more severe temporal and medial spread of tau throughout the cortex, which follows the Braak staging described previously (Braak & Braak, 1991; Sanchez et al., 2021; Vogel et al., 2021). Interestingly, no protective effect for *APOE* ε2 on tau pathology has been described; in fact, *APOE* ε2 homozygosity enhances tau pathology and increases the risk of tauopathy (Robinson et al., 2020).

The *APOE* ε4 genotype has been associated to increased tau-associated pathogenesis, neurodegeneration and neuroinflammation (Wang et al., 2021), and apoE4 can enhance tau neurotoxicity through the inhibition of neurotransmitter transport into synaptic vesicles, consequently leading to the degeneration of the Locus Coeruleus (Kang et al., 2021). In mice tauopathy models, *APOE* ε4-expressing mice showed the highest amount of neurodegeneration compared to the other two isoforms, and *APOE* KO mice were protected from tau-induced tauopathy (Shi et al., 2017); furthermore, in the same tauopathy models, the reduction of apoE4 levels protected against tau pathology (Litvinchuk et al., 2021), and tau removal rescued the toxicity and deficits induced by apoE4, suggesting an underlying pathological mechanism in AD that requires both apoE and tau (Andrews-Zwilling et al., 2010).

Similar results have also been demonstrated in human iPSC-derived cell models, showing a link between apoE4 and tau pathology in glial cells and neurons (Wadhwani et al., 2019). iPSC-derived neurons from *APOE* ε4-carrier patients showed higher levels of P-tau and neuron degeneration than non-carriers (Wang et al., 2018), and CRISPR mutation from apoE3 to apoE4 has also been demonstrated to enhance P-tau levels (Lin et al., 2018).

Higher tau levels have been associated to increased cortical plasticity impairment and cognitive decline, and reduced astrocyte survival in the CSF of *APOE* ε4-carriers (Koch et al., 2017). Furthermore, apoE4 levels have been positively associated to total tau and P-tau levels in the CSF of AD patients

(Wattmo et al., 2020; Liu et al., 2021), although many contradictory findings have also been reported (Rodriguez-Vieitez & Nielsen, 2019).

APOE ε4-non-carriers present a tau uptake pattern that does not coincide with the Braak pattern, with less uptake in the entorhinal cortex and higher amounts in the neocortex (Whitwell et al., 2018). Tau can be internalized in neurons by HSPGs (Holmes et al., 2013), but also by LRP1, both of which are apoE receptors. Studies have shown that apoE may regulate tau uptake within cells using HSPGs (Jablonski et al., 2021), whereas others have shown that apoE inhibits the direct interaction between tau and LRP1, being apoE4 the least efficient isoform at inhibiting this interaction (Rauch et al., 2020). The reduced inhibition of tau interaction with LRP1 also leads to increased tau propagation (Rauch et al., 2020), thus supporting a role for apoE receptors in tau spreading. In this manner, LRP1 knockdown leads to reduced tau propagation, whereas LDLR appears to have an opposing effect, as its overexpression also leads to reduced tau propagation (Shi et al., 2021).

As apoE is secreted and tau is usually located within the cell, no link between these two factors comparable to the one between apoE and Aβ has been described, and furthermore, the effects of apoE on tau pathology may be mediated by its effects on Aβ pathology. In fact, immunotherapy studies targeting the apoE present in amyloid plaques appear to reduce Aβ-mediated tau seeding and spreading (Gratuze et al., 2022), although other studies have reported Aβ-independent effects (Baek et al., 2020; Therriault et al., 2020).

Therefore, the precise mechanism by which *APOE* affects tau pathology has yet to be fully understood.

ApoE and AD-related synaptic deficits

Some of the earliest damage present in AD is localized at the synapses, and synapse loss correlates with cognitive impairment in AD (Scheff et al., 2006). Synapses are affected at both presynaptic and postsynaptic levels (Reddy et al., 2005), and Aβ oligomers, rather than amyloid plaques, appear be responsible for the damage by causing synaptic toxicity, thus affecting synaptic plasticity and leading to synaptic dysfunction and loss (Tu et al., 2014). Aβ oligomer localization

at synaptic terminals can occur before plaque formation, which may indicate an early effect of Aβ on synapses (Klementieva et al., 2017).

As apoE is the main cholesterol transporter in the brain, it plays a crucial role in the maintenance of synaptic membranes (Liu et al., 2013) and neuronal repair (Mahley & Huang, 2012); and, therefore, apoE dysfunction has been linked to the synaptic deficits present in AD (Perdigão et al., 2020). *APOE* ε4 has been associated to reduced neuronal outgrowth (Wang et al., 2005) and synaptic density compared to *APOE* ε3 (Dumanis et al., 2009), and *APOE* ε4 also affects the architecture of neurons by reducing dendritic length and arborization, and by decreasing the density of dendritic spines (Jain et al., 2013). In iPSC-derived organoids, apoE4 exacerbated synaptic loss by decreasing presynaptic and postsynaptic proteins (Lin et al., 2018). *APOE* ε4 has also been associated to decreased long-term potentiation (LTP) (Trommer et al., 2004), through a NMDAR-dependent mechanism (Korwek et al., 2009), and, furthermore, the presence of apoE4 has also been linked to poor learning and memory (Rodríguez et al., 2013).

The exact mechanism by which apoE4 hinders synapses has yet to be elucidated. ApoE4 may affect synaptic integrity acting as a cofactor by directing toxic Aβ oligomers to synapses (Koffie et al., 2012), or through the impairment of endosome recycling (Xian et al., 2018), as apoE4 has been linked to a reduced rate of recycling and an increased intracellular accumulation of apoE (Heeren et al., 2004). This impairment could trap apoE alongside glutamatergic receptors such as NMDAR and AMPA receptor, which would in turn impair synaptic regulation (Chen et al., 2010), an effect which may be dependent on apoE4 interaction with apoER2. Additionally, apoER2 may also be trapped in endosomes, leading to reduced receptor binding by reelin and subsequent synaptic dysregulation (Weeber et al., 2002).

ApoE and glial cells in AD: a role in neuroinflammation

Neuroinflammation has been referred to as the third pathological hallmark of AD (Guzman-Martinez et al., 2019). Microglial cells and astrocytes mediate the neuroinflammatory response by triggering several signalling pathways through

the release of pro-inflammatory cytokines (Shabab et al., 2017). *APOE* can play an important role in modulating the inflammatory response by impacting synaptic function and glial activation (Cudaback et al., 2011). For example, *APOE* ε4 knock-in mice presented an exacerbated loss of synaptic proteins, alongside increased glial activation and production of pro-inflammatory cytokines following lipopolysaccharide (LPS, a widely known activator of the inflammatory response (Ngkelo et al., 2012)) insult, compared to *APOE* ε2 and ε3 mice (Cudaback et al., 2011).

Inflammatory responses can also influence apoE secretion and expression. In primary cell cultures, following LPS insult, microglia of *APOE* ε2 or ε3 knock-in mice showed increased secretion of apoE, whereas no comparable effect was observed in *APOE* ε4 knock-in mouse microglia. On the other hand, astrocytes from *APOE* ε4 knock-in mice presented a reduced level of apoE expression and secretion following TNF-α (tumour necrosis factor α; a cytokine that act as a major regulator of the inflammatory response) treatment, and no change after LPS treatment. Taken together, these results indicate dysfunctional responses of *APOE* ε4-expressing microglia and astrocytes towards stimuli that activate the inflammatory pathway (Lanfranco et al., 2021).

Regarding microglia, apoE may exert its influence on the inflammatory response through receptors such as TREM2 (triggering receptor expressed on myeloid cells 2), whose encoding gene is one of the recently described genetic risk factors for AD (Carmona et al., 2018). TREM2 has many ligands, including glycolipids, clusterin, apoE and Aβ (Gratuze et al., 2018) and is expressed in the brain mainly by microglia (Ulland & Colonna, 2018). Upregulated TREM2 mRNA levels have been detected in microglial cells obtained from AD patients (Gosselin et al., 2017). The precise role of TREM2 in AD is unknown, but studies regarding TREM2 absence reported increased neuritic dystrophies associated to Aβ plaques (Zhong et al., 2017), and either a reduction (Leyns et al., 2017) or exacerbation (Bemiller et al., 2017) of tau pathology. Other studies described an important role for TREM2 in Aβ and tau seeding and spreading (Leyns et al., 2019; Parhizkar et al., 2019). The interaction between apoE and TREM2 is unclear, as TREM2 loss-of-function has been associated to reduced levels of apoE in amyloid plaques (Parhizkar et al., 2019) and aberrant lipid metabolism,

which could influence apoE (Andreone et al., 2020), whereas *TREM2* deletion impairs microglial phagocytosis of apoE (McQuade et al., 2020). The exact role of the interaction between apoE and TREM2 on neuroinflammation, thus, requires further investigation.

ApoE may also influence microglial response through its interaction with toll-like receptors (TLR), whose activation primes microglia and constitutes the first step in the inflammatory response (Shen et al., 2018). Specifically, a TLR4-dependent pathway has been associated with apoE, and as such apoE3 can inhibit the microglial activation promoted by TLR4 (Zhu et al., 2010), whereas the *APOE* ε4 genotype is linked to a deleterious effect in AD through this receptor (Krasemann et al., 2017). 25-hydrocholesterol, an important inflammatory mediator produced by microglia, promotes neuroinflammation in an *APOE* isoform-dependent manner (ε4 > ε3/ε2) and is produced in larger quantities in *APOE* ε4 microglia (Wong et al., 2020).

LRP1 is also highly expressed in microglia and conflicting results have associated the activation of the receptor with a suppression in microglial activity (Chuang et al., 2016), but also with an amplified inflammatory response and increased microglia activation following LPS insult (Brifault et al., 2019); in addition, LRP1 silencing has been shown to enhance the inflammatory response (He et al., 2020). Therefore, given its importance in this mechanism, LRP1 may modulate the effect of apoE on microglial inflammation (Pocivavsek et al., 2009).

How apoE affects the microglial inflammatory response is still under debate, as various potential mediatory mechanisms exist. Nonetheless, the evidence points towards a deleterious effect of the *APOE* ε4 genotype that enhances the inflammatory response and may lead to an exacerbation of subsequent neurodegeneration.

The *APOE* genotype can also influence astrocytic functions. Astrocytes play an important role in maintaining brain energy homeostasis, and astrocytes expressing *APOE* ε4 present reduced mitochondrial function (Schmukler et al., 2020) and aberrant glucose utilization (Farmer et al., 2021). Therefore, an *APOE* ε4 genotype may lead to an exacerbation of neurodegeneration in AD through dysfunctional brain energy homeostasis maintenance and altered responses to inflammatory stimuli, ultimately leading to neurotoxicity.

The role of apoE and lipids in AD

As commented through the text, the key role for apoE in the CNS is to transport cholesterol to maintain adequate neuronal function (Zhang & Liu, 2015). ApoE derived from *APOE* ε4 individuals is produced at lower levels and is poorly lipidated in comparison to *APOE* ε3-derived apoE, thus apoE4 may be less efficient at transporting cholesterol (Gong et al., 2002; Zhao et al., 2017), and the lower lipidation likely results in impaired cholesterol metabolism in astrocytes. Nonetheless, iPSC-derived *APOE* ε4 astrocytes appeared to present increased secretion and intracellular levels of cholesterol (TCW et al., 2022), therefore the precise cause behind the poorer lipidation of apoE is yet unknown. A potential mechanism lies in the higher tendency of apoE4 to self-aggregate and misfold, which can in turn increase ABCA1 aggregation and decrease membrane-recycling, thus lowering the lipidation of apoE4 (Rawat et al., 2019).

The different *APOE* isoforms vary in their lipid-binding preference: apoE2 and apoE3 both preferentially bind to small HDLs, whereas apoE4 binds to large VLDLs and LDLs (Li et al., 2013). Furthermore, apoE2 decreases the levels of cholesterol in plasma, in contrast to apoE4 which increases them (Kao et al., 2020), as seen in other studies demonstrating that apoE4 homozygosity is linked to elevated plasma cholesterol levels and CSF levels of 24S-hydroxycholesterol (Papassotiropoulos et al., 2002), which acts as a counterbalancing mechanism in cholesterol homeostasis.

ApoE may exert its influence through lipid rafts, structures within cell membranes that play crucial roles in signal transduction, cell adhesion and lipid and protein sorting. They serve as a platform for apoE interaction with Aβ and tau to promote their aggregation and hyperphosphorylation, respectively (Kawarabayashi et al., 2004). AD-related proteins can also be found in lipid rafts, such as APP, BACE1, γ-secretase, and neprilysin (El Gaamouch et al., 2016); consequently, Aβ generation and degradation are associated to the composition of lipid rafts (Schengrund, 2010). Interestingly, cholesterol appears to be an essential component in the lipid raft triggering of Aβ fibrillization (Okada et al., 2008).

The cholesterol transporters responsible for the lipidation of apoE may mediate its influence on lipids in AD. As mentioned beforehand, ABCA1 is the

main mechanism responsible for lipid efflux and apoE lipidation, and loss-of-function mutations in ABCA1 are associated to increased AD risk (Nordestgaard et al., 2015). ABCA1 overexpression inhibits amyloid deposition (Wahrle et al., 2008), whereas lower levels of expression impair Aβ clearance (Wahrle et al., 2004), and *APOE* isoforms may have a role in this function, as ABCA1 deficiency led to increased Aβ aggregation in *APOE* ε4-expressing mice, but not when mice expressed *APOE* ε3 (Fitz et al., 2012). Other members of the ABC family also participate in APP processing and Aβ production and aggregation, such as ABCA2 and ABCA7, although no evidence regarding a modulatory effect of apoE has been reported as of yet.

Lipid metabolism in the brain, although normally directed from astrocytes to neurons, can also involve an inverted mechanism, by which fatty acids, specifically unsaturated triglycerides stored in the form of toxic lipid droplets, are transferred, via apoE, from neurons to astrocytes for neutralization (Liu et al., 2017), due to very limited capacity of neurons to store or catabolize fatty acids compared to astrocytes (Schönfeld et al., 2013; Ioannou et al., 2019). Excessive fatty acids can lead to toxicity, lipid peroxidation and, ultimately, neurodegeneration (Nguyen et al.,2017); as such, apoE4 appears to be less efficient at transporting these fatty acids from neurons to astrocytes (Qi et al., 2021) and at neutralizing these toxic lipid droplets (Sienski et al., 2021), leading to enhanced neurodegeneration.

Altered glycosylation in AD

Aside from the key aspects mentioned up to this point, new characteristics of apoE are being progressively implicated in AD pathogenesis, such as apoE glycosylation. Recent evidence has demonstrated that the glycosylation pattern of various AD-related proteins is altered during the pathological progression of the disease (Haukedal & Freude, 2021), including APP (Boix et al., 2020) and tau (Almansoub et al., 2019). Glycosylation differences within the brains of AD patients have been reported in O-GlcNAcylation and N-/O-glycosylation (Frenkel-Pinter et al., 2017). ApoE glycosylation differs in a tissue-specific manner, and the cellular source of apoE in the CNS affects its glycosylation pattern, as

astrocyte-derived apoE is more heavily sialylated and glycosylated (Flowers et al., 2020). Correct apoE glycosylation is essential for its correct functioning and modulates its lipid receptor affinity, lipid transportation and metabolic functions (Kacperczyk et al., 2021), as well as protecting against self-association and aggregation (Lee et al., 2010). An altered glycosylation pattern for apoE has been previously described in a Niemann-Pick Type C model, which shares some pathological mechanisms with AD including Aβ deposition, in which changes in apoE glycosylation led to increased levels of Aβ42 (Chua et al., 2010) due to a lower rate of binding between the proteins; and, thus, a role for a specific sialic moiety of apoE on its interaction was suggested (Sugano et al., 2008). In sum, there is evidence to support a role for apoE glycosylation in AD.

ApoE dimerization in AD

ApoE2 and apoE3 are able to form disulphide-linked hetero- and homodimers through the presence of Cys at position 112; whereas apoE4 lacks this ability as it presents Arg at position 112. In human CSF studies, no differences in apoE dimer levels between control and AD subjects were found (Montine et al., 1998); however, a recent report showed lower plasma levels of dimers in AD *APOE* ε3-carrier subjects compared to controls (Patra et al., 2019). Despite the natural inability to form disulphide-linked dimers, apoE4 SDS-resistant dimers with Aβ have been described *in vitro* (Martel et al., 1997), in non-pathological human CSF (LaDu et al., 2012), and in the AD brain (Permanne et al., 1997), and these species have been implicated in Aβ clearance and fibrillization (Deroo et al., 2015). Therefore, the capacity of dimerization of apoE could play an important role in Aβ toxicity in AD, and the interaction of apoE with Aβ could lead to the appearance of complexes, regardless of the *APOE* genotype.

ApoE and myelination in AD

AD is characterized by a progressive and generalized loss of white matter, due to demyelination and cell death (Safaiyan et al., 2021), that is closely related to motor deficits and cognitive dysfunction (Ji et al., 2019). *APOE* ε4 may fail to properly modulate white matter integrity (Heise et al., 2010) and has been linked

to an increase in MRI-detected white matter hyperintensities, which are risk factors for cognitive impairment, in AD patients (Mirza et al., 2019).

ApoE in the endocytic/autophagic pathway in AD

Alterations in cellular trafficking and recycling have been implied in AD, including endocytosis (recycling and internalization of molecules from the plasma membrane), autophagy (removal of intracellular sources and organelles) and phagocytosis (degradation of extracellular materials). Endo-lysosomal trafficking and autophagy plays key roles in the formation of Aβ (van Acker et al., 2019), APP degradation (Xiao et al., 2015), and clearance of Aβ (Cho et al., 2014). Failures in this system are detected early in AD pathology, leading to Aβ accumulation (Nixon, 2017) that could in turn affect other aspects of AD, including neuroinflammation (François et al., 2013).

The *APOE* ε4 genotype has been associated to the endocytic/autophagic pathway (Lambert et al., 2013) given its role in Aβ internalization, and, as such, *APOE* ε4 astrocytes appear to possess a lower capacity to clear Aβ through autophagic routes (Simonovitch et al., 2016). In transgenic mice, *APOE* ε4 has been associated to a dysregulation of the endosomal-lysosomal pathway (Nuriel et al., 2017) and decreased autophagy in the hippocampus (Simonovitch et al., 2019). In the human brain, *APOE* ε4-carriers showed lower mRNA transcripts of proteins associated to autophagy (Parcon et al., 2018). These studies indicate that there is an *APOE* ε4-associated alteration in autophagy.

To summarize, a pathological role for *APOE* has been described in diverse aspects of AD, ranging from increments in Aβ aggregation and tau phosphorylation to the induction of neuroinflammation and synaptic and autophagic deficits, and *APOE* ε4 has been linked to an exacerbation of all aspects of the pathology (reviewed in Tzioras et al., 2018 and Fernández-Calle et al., 2022). All the proposed roles for apoE in AD are summarized in **Figure 7**. Key characteristics of the protein, such as its lipid-binding capacity, stabilization into complexes, and glycosylation have all been implicated in the disease process to some description, and in all these processes, the risk-associated ε4 allele has

been reported to exacerbate AD pathology, leading to a general negative impact on the clinical outcome and progression of the disease.
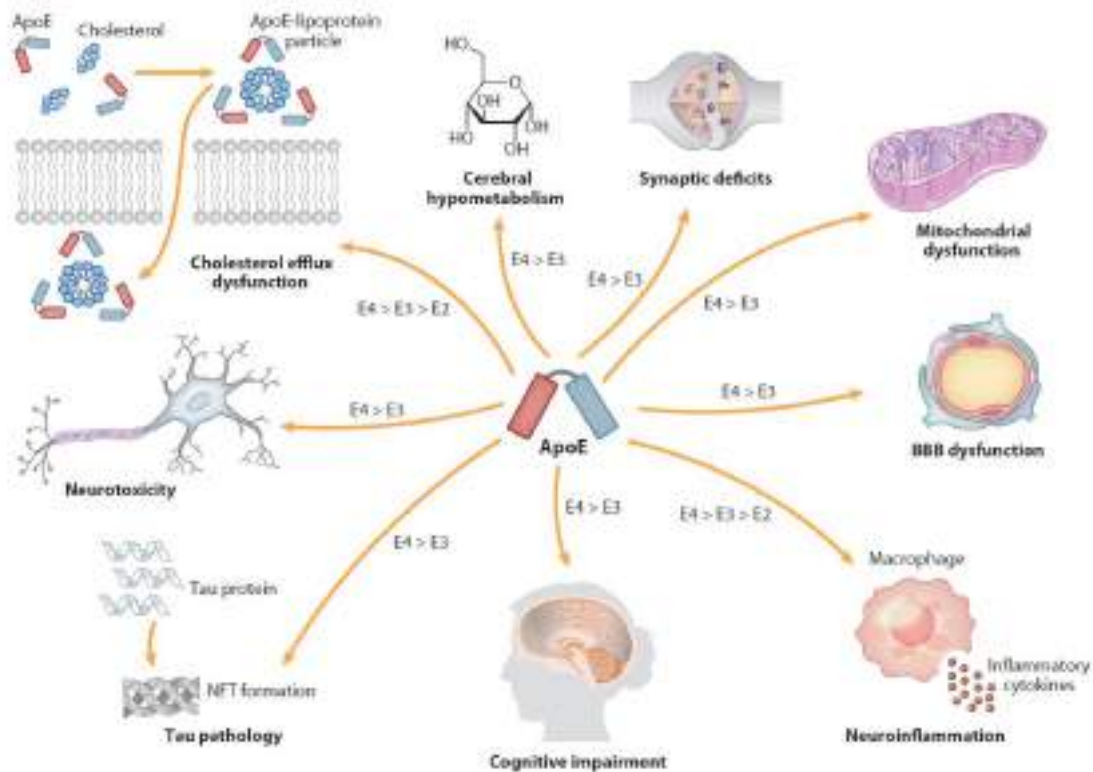

Figure 7. Proposed roles for apoE in AD. ApoE participates in many different aspects of AD, and the *APOE* ε4 isoform has been associated to an exacerbation of the disease regarding every role described. Obtained from Yu et al., 2014.

Impaired reelin signalling in the pathogenesis of AD

Reelin is a large glycoprotein that binds to apoER2. Despite the potential influence of reelin signalling on Aβ secretion and tau phosphorylation, the number of studies regarding the role of this protein is nowhere near comparable to the amount of research regarding the role of apoE in AD. Nonetheless, the studies performed have shown an affectation of the reelin signalling pathway in AD, and it is therefore plausible to consider a key role for reelin from the early stages of AD and throughout the progression of the disease (Krstic et al., 2013).

Reelin signalling antagonizes AD-related pathways by binding to apoER2, which can ultimately lead to the inhibition of tau phosphorylation (Ohkubo et al., 2003; Beffert et al., 2004) and a reduced secretion of Aβ through its effects on

Dab1 (Hoe & Rebeck, 2008). A protective effect for reelin on synapse dysfunction has also been reported, in which reelin can prevent LTP and NMDAR suppression until the amyloid burden becomes excessive (Durakoglugil et al., 2009). Reelin may maintain synaptic plasticity by competing with apoE to prevent it from sequestering NMDAR and apoER2, which occurs more frequently in the presence of apoE4 (Chen et al., 2010). In fact, reelin KO and *APOE* ε4 knock-in mice models both show similar effects on increased tau phosphorylation (Kobayashi et al., 2003).

Reelin protein levels appear to be depleted in the entorhinal cortex of AD patients (Chin et al., 2007), and this depletion can also be observed in the human frontal cortex in the preclinical stage of AD and in the murine hippocampus before the onset of amyloid pathology (Herring et al., 2012); nonetheless, other studies reported higher levels of reelin mRNA and protein levels in the brain of AD patients (Botella-López et al., 2006). Increased reelin fragment levels have also been reported in the CSF of AD patients (Sáez-Valero et al., 2003; Botella-López et al., 2006), and the deposition of C-terminal and N-terminal reelin fragments associated to dementia status have been detected in the human hippocampus (Notter & Knuesel, 2013). On the other hand, studies of reelin mRNA levels have demonstrated an up-regulation in the frontal cortex in the latter stages of AD (Botella-López et al., 2006), although a reduction in the hippocampus has also been reported (Knuesel et al., 2009).

Anyhow, regardless of the variations in reelin mRNA expression and protein levels, it is likely that reelin signalling is impaired in AD, given the specific alterations detected in the protein that affect its correct functioning, such as aberrant glycosylation (Botella-López et al., 2006), which could hinder its protective effects (Cuchillo-Ibáñez et al., 2016). Increased reelin expression has been described in parallel to decreased apoER2-CTFs, thus indicating dysfunctional reelin signalling through this receptor (Mata-Balaguer et al., 2018). Reelin co-localizes with Aβ (Doehner et al., 2010), and consequently Aβ may interfere with the reelin signalling pathway and compromise its function by aggregating and trapping reelin (Cuchillo-Ibáñez et al., 2016). Progressive reelin aggregation over time may also hinder the signalling pathway and increase synaptic vulnerability to Aβ deposition (Kocherhans et al., 2010). Furthermore,

treatment of SH-SY5Y neuroblastoma cells with Aβ42 led to increased reelin levels and an altered glycosylation pattern (Botella-López et al., 2010).

Genetic variations in components of the reelin signalling pathway have also been linked to AD pathogenicity, such as polymorphisms of *APOER2* and *VLDLR*, which have been related to an increased risk of developing AD (Helbecque et al., 2009). ApoER2 proteolytic processing and Dab1 phosphorylation, both regulated by ligand-receptor binding, appear to be reduced in AD (Cuchillo-Ibáñez et al., 2016). Nonetheless, Dab1 mRNA expression is up-regulated in the brain of AD patients, which has been associated to a disruption of the cellular proteome (Müller et al., 2011), leading to increased expression and processing of key proteins such as APP (Parisiadou & Efthimiopoulos. 2006). Therefore, Dab1 expression in early stages of the pathology may be beneficial in preventing AD, given its key role in the reelin/apoER2 signalling pathway, however at later stages it could play an important role in the exacerbation of the pathology (Gao et al., 2015).

In conclusion, reelin initially appears to have a protective role in AD by inhibiting tau phosphorylation and Aβ secretion. However, as the pathology progresses and the amyloid burden increases, the signalling pathway appears to present a loss of protective function characterized by increased levels of reelin expression and protein, but an ineffective activation of the signalling pathway due to altered glycosylation and aggregation of reelin through the effects of Aβ. This inefficient apoER2 activation could ultimately convert the beneficial effect of the pathway into an exacerbation of the AD pathology.

AD biomarkers: apoE and reelin as potential targets

ApoE and reelin both appear to play important roles in AD by participating in many key aspects of the pathology. Moreover, both apoE and reelin are secreted proteins present in the human CSF and could theoretically have diagnostic potential. Therefore, it comes as no surprise that both proteins have been proposed as biomarkers to measure AD pathology progression. A precise diagnosis of AD can only be performed in the post-mortem human cortex, as a clinical diagnosis of AD is unreliable due to the heterogeneity of AD symptoms

(Beach et al., 2010). As AD pathophysiology occurs long before the onset of clinical symptoms, the development of tools to assist early diagnosis is crucial, and recent studies have attempted to find diagnostic tools in accessible bodily fluids, such as the CSF and blood. CSF biomarkers present an advantage over those derived from the blood due to the proximity to the brain parenchyma, as brain proteins are secreted to the CSF (Blennow et al., 2010).

In the context of potential CSF biomarkers for AD, and in recent years, clinical evidence has supported that the key hallmarks of AD, Aβ and tau, can serve as consistent biomarkers for AD, with the first studies quantifying these proteins in human CSF having been published approximately 20 years ago (Blennow et al., 1995; Andreasen et al., 1999).

Early studies demonstrated that Aβ is secreted to the CSF (Seubert et al., 1992), and quantification of Aβ42 showed an important decrease in AD patients across many studies (Olsson et al., 2017), a paradoxical change, since its generation is increased in the AD brain, which is probably due to the accumulation of Aβ into plaques (Strozyk et al., 2003). In this manner, a high concordance between decreased CSF Aβ42 levels and amyloid status detected by positron emission tomography (PET) scans has been demonstrated (Blennow et al., 2015). Another Aβ species, the more abundant Aβ40 peptide, can also be detected in the CSF and also appears to decrease, but to a lesser extent than Aβ42; as such, various studies have demonstrated that a CSF ratio of Aβ42/Aβ40 performed better than Aβ42 alone (Hansson et al., 2007), and presented a higher concordance with PET amyloid positivity (Lewczuk et al., 2017), thus improving the diagnostic accuracy of Aβ as a biomarker (Shoji et al., 1998). This improved accuracy may be due to Aβ40 reflecting "total" Aβ levels, and therefore Aβ42 levels are interpreted in a more subject-dependent level based on the production of Aβ of each individual (Lewczuk et al., 2015).

Both total tau (T-tau) and phosphorylated tau (P-tau) can also be detected in CSF, despite being cytoskeletal proteins, and many studies have consistently found a significant increase in total tau (T-tau) levels in AD patients (Olsson et al., 2017). CSF T-tau levels reflect the intensity of neurodegeneration or neuronal damage in the brain (Blennow & Hampel, 2003), as observed in individuals after acute brain damage (Zetterberg et al., 2006). As such, higher T-tau levels in AD

are indicative of rapid disease progression (Buchhave et al., 2012). In a similar fashion, increased P-tau levels have been associated to AD progression (Wallin et al., 2010). However, unlike T-tau levels, CSF P-tau levels remain normal or only marginally increased in individuals with neurodegenerative diseases without NFTs or following acute damage (Skillbäck et al., 2014); therefore, P-tau measurements appear to reflect current tau phosphorylation rather than neuronal damage and seem to be more characteristic of AD.

Unlike Aβ, both tau biomarkers show low concordance with PET visualization of tau pathology (Gordon et al., 2016), due to the fact that T-tau and P-tau levels are elevated at earlier stages of the pathology, before tau aggregates can be detected by PET. Therefore, T-tau and P-tau likely represent neurodegeneration and tau phosphorylation state, respectively, whereas tau PET scans correlate with the stage of cerebral atrophy and the severity of cognitive deficits (Blennow & Zetterberg, 2018).

A combination of low Aβ42 and high T-tau/P-tau levels present high sensitivity in predicting AD in the prodromal stage of the disease and efficiently differentiate between AD and MCI or other neurodegenerative disorders (Hansson et al., 2006). Nonetheless, low CSF Aβ42 levels can predict future cognitive decline, whereas T-tau changes cannot, and thus lowered CSF Aβ42 can be considered as a very early indicator of amyloidosis (Gustafson et al., 2007). The measurement of CSF tau and Aβ42 levels are now widely included in the diagnostic procedure for AD in several countries (Jack et al., 2016), however the quantification of these CSF biomarkers on fully automated machines is required to remove human error from the calculations (Blennow & Zetterberg, 2018).

Other proteins, aside from Aβ42 and T-tau/P-tau, may also be sensitive to changes in AD and could have diagnostic potential, including synaptic proteins such as neurogranin, high CSF levels of which are associated to AD (Kvartsberg et al., 2015) and to hippocampal atrophy (Portelius et al., 2015). Other CSF biomarkers, such as neurofilament light (NfL), glial fibrillary acidic protein (GFAP), or α-synuclein have also been proposed (Johnson et al., 2023), as well others (Blennow & Zetterberg, 2018).

The use of CSF biomarkers has two important setbacks: the obtention of CSF samples requires invasive methods (lumbar puncture), and the quantity of sample obtained is limited. For this reason, blood biomarkers have been proposed as an alternative, as blood samples are far more accessible than those from the CSF. However, difficulties arise in the development of blood biomarkers, as very few brain proteins enter the bloodstream compared to the CSF; additionally, blood is much richer in peripheral proteins, and plasma proteins, such as albumin and IgG, can interfere with the analytical methods (Blennow & Zetterberg, 2015). The potential new blood biomarkers for AD may be ubiquitous proteins, produced also by peripheral organs, thus making it difficult to detect specific brain changes. Furthermore, the brain proteins released into the bloodstream could very easily be degraded by proteases or cleared by the liver or kidneys (O'Bryant et al., 2015).

For blood biomarkers to be used, previous fractionation of proteins associated to exosomes originated in the CNS, or proteins that present CNS-exclusive isoforms, could be an advantage. Moreover, specialized and more precise techniques, such as ultrasensitive immunoassays and mass spectrometry, are needed (Andreasson et al., 2016).

In this context, measurements of Aβ42 levels derived from the brain in plasma present difficulties due to the contribution of peripheral tissues, leading to a lack of consistent correlations between CSF and plasma Aβ levels (Hansson et al., 2010). Nonetheless, recent innovative techniques have been capable of establishing weak correlations between CSF and plasma Aβ42 and Aβ42/Aβ40 levels, as well as a significantly reduced Aβ42/Aβ40 ratio in AD cases compared with controls (Janelidze et al., 2016).

By using ultrasensitive techniques, such as single-molecule arrays (Simoa), tau can be measured in blood samples, and increased levels are detected in AD samples (Zetterberg et al., 2013), although substantial overlap with controls is also found, which reduces its diagnostic potential (Mattson et al., 2016). Nonetheless, recent studies have shown that tau phosphorylation at Thr217 (P-tau217) adequately discriminates between AD and other neurodegenerative disorders, and thus has potential as a plasma biomarker for AD (Palmqvist et al., 2020).

Neurofilament light (NfL) is a recently discovered blood biomarker (Gaetani et al., 2019) that presents a high correlation between plasma and CSF levels (Gisslén et al., 2015). Plasma NfL levels are markedly increased in AD, with a sensitivity comparable to the core AD CSF biomarkers Aβ42 and T-tau/P-tau (Mattson et al., 2017). Furthermore, NfL levels are also elevated in symptomatic and pre-symptomatic fAD, meaning that Nfl could also detect neurodegeneration in the preclinical stage of AD (Weston et al., 2017). However, despite these promising results, it is important to note that increased plasma NfL levels are not an exclusive feature to AD, as this phenomenon is common to other neurodegenerative disorders such as frontotemporal dementia (Rohrer et al., 2016). As such, its potential may be limited to detecting generic neurodegeneration that would require further analyses to determine the exact nature of the damage.

Given the high accessibility of blood samples, further development of specialized techniques is essential to enhance the diagnostic power of these markers, although the use of blood biomarkers in the detection of AD is currently limited. Therefore, at this moment in time, the discovery of CSF biomarkers is still of great interest to improve the early detection of AD, even before the onset of clinical symptoms. Given the roles of reelin and, particularly, apoE in AD and their interactions with Aβ and tau, it is feasible to regard them as alternative biomarkers for AD.

ApoE studies performed in plasma samples found a general decrease of plasma apoE levels in AD compared to controls and a low correlation with CSF Aβ42 levels (Gupta et al., 2011). In addition, the balance of apoE isoforms in different *APOE* genotypes differs in the plasma: apoE4 protein levels are lower compared to the other isoforms, and as such a lower proportion of apoE4 compared to apoE3 is present in *APOE* ε3/ε4 subjects (Martínez-Morillo et al., 2014), which has been attributed to a faster catabolic rate of apoE4 compared with other isoforms (Gregg et al., 1986). It is worth noting that these proteins do not cross the BBB, and consequently a very low correlation between plasma and CSF apoE levels has been reported (Fukumoto et al., 2003). Therefore, although various studies have reported interesting (yet contradictory) results in the plasma, the focus should be focused on the CSF.

Studies of apoE protein levels in *APOE* knock-in mice found a genotype-dependent effect, with ε2 knock-in mice presenting the highest apoE protein levels in the brain, and ε4 knock-in mice the lowest (Ramaswamy et al., 2005). This suggests that in CSF studies of apoE content, the genotype could be an important variable to take into consideration. Initial human studies quantifying apoE protein levels presented mixed results, and in general failed to establish an association between CSF apoE protein levels and AD risk (Fukumoto et al., 2003).

Studies quantifying total CSF apoE protein levels have produced inconclusive findings. When taking the *APOE* genotype into account, *APOE* ε4-carriers presented the lowest levels of CSF apoE protein in some studies (Riddell et al., 2008), and the highest levels in others (Darreh-Shori et al., 2011). Unlike in the plasma, some studies indicated that the CSF isoform composition did not vary in *APOE* heterozygotes (Wahrle et al., 2007), although recent evidence points towards differences in apoE isoform composition in heterozygote subjects (Minta et al., 2020). A recent report suggested that the discrepancies regarding the balance of isoforms in the CSF may be related to differences in their Aβ clearance capacity (Honda et al., 2023). However, once again, no association between CSF apoE levels or its isoform composition were associated to Aβ status or disease progression. Whereas some CSF studies detected a strong correlation between CSF apoE levels with Aβ42 levels and with fibrillar Aβ brain deposition (Cruchaga et al., 2012), others found a correlation only in *APOE* ε4-carriers (Nielsen et al., 2017). The incongruencies detected amongst the studies are likely due to the sample size and analytic method used (Simon et al., 2012), and may also be related to the specific type of apoE species detected, given the different dimeric capabilities of the apoE isoforms as a consequence of the Cys112 substitution for Arg112 in apoE4.

The *APOE* genotype can affect CSF Aβ42 levels (Cruchaga et al., 2010) and amyloid PET scan results (Morris et al., 2010); as such, even in cognitively normal subjects, *APOE* ε4-carriers present increased PET amyloid positivity and reduced CSF Aβ42 levels (Reiman et al., 2009), and the affectation is more severe in homozygotes, suggesting a dose-dependent effect of *APOE* ε4.

The associations between CSF apoE levels and Aβ42 levels have been seen to vary across studies. In the same manner, associations have been found between apoE3 and apoE4 with T-tau and P-tau concentrations (Martínez-Morillo et al., 2014), but only in *APOE* ε4-carriers (Deming et al., 2017). Given the cellular localization of tau and apoE, there is a "physiological" difficulty for these proteins to interact, and as such the connection between them is more complex than the connection between apoE and Aβ.

Regarding the potential of reelin as a biomarker for AD, few studies have been performed. Reelin is present in the CSF as the full-length species and as C-terminally and N-terminally truncated fragments. Previous studies detected increased levels of the 180 kDa fragment in AD (Botella-López et al., 2006), the fragment generated following interaction with apoER2 (Hibi & Hattori, 2009); although significance was not achieved in other studies (Botella-López et al., 2010). Recent reports indicate that reelin fragments can be generated through the activity of extracellular matrix metalloproteinases regardless of receptor interaction (Hattori & Kohno, 2021). Further studies regarding the balance of reelin fragments are required to consider reelin protein levels as a potential biomarker for AD.

ApoER2 ectodomain fragments can be detected in the CSF and may also have potential as a biomarker for reelin signalling. These CSF apoER2 fragments correlate with reelin levels in control subjects, but not in AD, where these fragments appear to diminish (Cuchillo-Ibáñez et al., 2016), suggesting inefficient reelin signalling in the brain of AD patients.

In conclusion, despite the existence of studies regarding the potential of CSF levels of apoE and reelin as read-outs of impaired reelin/apoE signalling and AD progression, given the complex interactions of these proteins with key components of the AD pathology, and the plethora of variables that could lead to differences, more research is required to determine the exact potential of these proteins in detecting AD at the earliest stage possible.

HYPOTHESIS AND OBJECTIVES OF THE DOCTORAL THESIS

Throughout the Introduction section the importance of apoE in AD has been described thoroughly, and the implications of carrying an *APOE* ε4 allele have been illustrated. Despite the large amount of research published regarding the role of apoE in AD, the vast majority of studies have focused on the impact of expressing an *APOE* ε4 genotype instead of the alternative isoforms in various disease-related aspects. Many conflicting results have been reported regarding the role of apoE in the progression of the disease. This could be due to different variables that could potentially alter the interpretation of the findings, such as the apoE source, extraction method, apoE lipidation state, analytic method used, etc. The focus on *APOE* ε4 is understandable, given the associated increased risk of developing AD. Nonetheless, expressing an ε4 allele does not necessarily mean that AD will be developed, and, furthermore, most AD patients carry the much more common *APOE* ε3 allele.

Pathological alterations are likely present in all apoE isoforms, perhaps to a different extent in apoE4, due to the basal compromise in some physiological roles compared with apoE3 and apoE2; however, there is a gap in the knowledge regarding alterations in the structure of apoE, and how these changes can affect the pathophysiology of the disease. The evidence obtained does propose that important aspects, such as apoE glycosylation and its capacity to form dimers, could be related to AD development. The study of alterations in apoE structure could provide valuable information regarding the role apoE plays in AD and could contribute to its diagnostic potential. Nonetheless, few studies have dedicated their efforts to quantifying and characterizing the specific apoE species present in the CSF of AD individuals, and the reports performed up until now present incongruent findings.

The main hypothesis of this doctoral thesis is that apoE protein presents alterations associated to AD, regardless of the isoform, and that these apoE alterations are expected to be found in AD CSF and brain samples. Moreover, as apoE and reelin are both soluble glycoproteins that compete for binding to the same receptor, apoER2, we also hypothesize that similar alterations to apoE

could be found in reelin in AD samples. Alongside apoER2, other receptors from the LRP family, such as LRP3, may play yet undiscovered roles in AD. These alterations in apoE/reelin and apoE receptors could contribute to the progression of AD.

The objectives of the thesis are the following:
1. To characterize apoE species in the CSF of AD individuals with different *APOE* genotypes. Specifically, the aim is to perform a biochemical characterization of the protein, including glycosylation, oligomerization, and the analysis of specific species associated to the disease, in order to obtain a particular apoE profile in human AD CSF.
2. To obtain a similar apoE profile in different brain areas of AD individuals. Specifically, to analyse apoE in frontal and temporal brain regions.
3. To analyse reelin protein levels, including proteolytic fragments, in the CSF of AD individuals with different *APOE* genotypes, in order to evaluate a potential read-out of reelin impairment in AD, and to analyse whether the *APOE* genotype has any impact on reelin levels.
4. To characterize LRP3, a novel apoE receptor of the apoER2 family, in AD brain extracts and cellular models, to define its role in the pathology, and to study the potential influence of LRP3 on APP levels and/or proteolytic processing.

The main method employed to study these objectives was Sodium dodecyl-sulphate polyacrylamide gel electrophoresis (SDS-PAGE) and western blot, using samples from human CSF and brain extracts from control and AD subjects with different *APOE* genotypes, as well as samples from animal and cellular models. Western blotting is a method that allows the characterization and quantification of protein species that differ in molecular mass, as well as the discrimination between fragments of the same protein. Other techniques, such as native-PAGE or mass spectrometry, were also employed. Cellular models expressing specific proteins of interest, such as reelin or LRP3, allowed us to observe alterations induced by AD-triggering effectors. Immunoprecipitation

assays were frequently used to study the interaction between specific proteins, but also to assure the identity of the protein species under study.

The results obtained from the studies performed throughout the doctoral thesis led to three publications, all in Q1 journals, which can be found annexed following the Materials and Methods section.

SUMMARY OF MATERIALS AND METHODS

In this section the samples and methods used in our studies will be briefly described. For detailed information regarding methods employed in some studies, please refer to the corresponding research paper.

Samples

For our studies human CSF and brain samples with known *APOE* genotypes were used. All studies were approved by the ethics committee at the Miguel Hernández University and were carried out in accordance with the Helsinki declaration regarding research on humans.

The CSF samples were all de-identified aliquots from clinical routine analyses, following procedures approved by the ethics committees of the University of Gothenburg (Sweden) and the Hospital Sant Pau (Spain). The CSF samples were obtained by lumbar puncture and centrifuged ($2000\times g$, 10 min) and then immediately aliquoted and stored in ultrafreezers at -80ºC until analysis. The time between CSF acquisition and storage was less than 4 hours in all cases. Freeze-thaw cycles were avoided, and new aliquots were used for each independent analysis. AD core biomarker levels were obtained by standardized methods in each cohort, and specific cut-off points were determined. For information regarding the AD diagnosis and specific details of the cohorts used, please refer to the corresponding research articles (apoE and reelin studies) (Lennol et al., 2022; López-Font et al., 2022).

Brain samples from the frontal or temporal areas were obtained from the brain banks of the Institute of Neuropathology (Bellvitge University Hospital, Spain) and the University of Edinburgh (Scotland). Cases with AD were considered as those showing NFTs and/or senile plaques with the appropriate Braak staging at the post-mortem neuropathological examination. For information regarding the characteristics of the samples used, please refer to the corresponding research papers (LRP3 study and apoE annex) (Cuchillo-Ibáñez et al., 2021).

For the apoE CSF study, transgenic rat CSF samples were also used. Transgenic Tg344-AD rats expressing mutant human APP and presenilin-1 were bred in animal research facilities at the University of Barcelona with the approval

of the Experimental Animal ethical committee, and in compliance with European legislation. CSF samples were obtained at different time-points by cisternal puncture in the suboccipital region through the atlanto-occipital membrane, with a single incision into the subarachnoid space. For information regarding the characteristics of the samples, please refer to the apoE research paper.

Cell cultures

HEK-293T cells stably transfected with reelin were employed to study the effects on Aβ42 on cellular reelin levels (López-Font et al., 2022). Briefly, 2×10^6 cells/dish were grown in six-well plates in Dulbecco's modified Eagle's medium (DMEM) supplemented with 10% foetal bovine serum (FBS), penicillin/streptomycin and G418. After 24 hours the medium was changed to a modified Eagle's Minimum Essential Media (Opti-MEM), and cells were treated with 2.5 µM Aβ42 or a scrambled Aβ peptide for 2 consecutive days with no media change. The cell medium was then collected, filtered through 0.2 µm pores and concentrated with an Amicon Ultra 100 kDa size exclusion filter, and then conserved at -80ºC until analysis by western blot.

SH-SY5Y cells, a human neuroblastoma line, were differentiated to neural-like cells to assess the interaction of apoER2 with LRP3. Briefly, cells were seeded at a density of 1×10^5 cells/well in 6-well plates and cultured in DMEM supplemented with 1% FBS, penicillin and streptomycin. To neuro-differentiate cells, all-trans-retinoic acid (RA) was employed to enhance neuronal markers and the expression of reelin and apoER2. 10 µM of RA diluted in DMEM with 1% FBS was added every 2 days. After 6 days, some cells were treated with recombinant reelin (12 µg for 24 hours), whereas others were treated with Aβ42 or scrambled Aβ protein in DMEM with 1% FBS for 2 consecutive days without media change at a concentration of 500 nM, 1 µM or 5 µM.

Non-differentiated SH-SY5Y cells were transfected with Lipofectamine 3000 with a construct encoding full-length apoER2 and apoER2-ICD expressing only the cytoplasmic domain, or with GFP as a mock transfection, for 48 hours. CHO cells stably overexpressing wild-type human APP (CHO-PS70 cells) were grown in DMEM with 10% FBS, 0.1% puromycin and 0.2% G418. CHO-PS70

cells were transfected with full-length human LRP3 cDNA for 48 hours. After 24 hours post-transfection, some cells were treated with 10 µM chloroquine for 24 hours (Cuchillo-Ibáñez et al., 2021).

Western blotting

SDS-PAGE and Western blotting is a technique used in all the research papers included in this compendium. Samples of human brain or CSF (quantities dependent on the protein being studied) were denatured for 5 minutes (unless otherwise stated) and resolved by sodium dodecyl sulphate-polyacrylamide gel electrophoresis (SDS-PAGE) under reducing conditions (unless otherwise stated). Premade or homemade gels of varying acrylamide percentage were used accordingly. In all studies, samples were analysed at least in duplicate (in separate gels) and distributed in the gels to ensure the comparison across different conditions. The distribution of samples and the experiments were performed by different research team members, to ensure no experimenter bias was involved.

Following electrophoresis, proteins were blotted onto 0.45 µM nitrocellulose membranes, and immunoreactive bands were detected using the corresponding antibody (see **Table 2**). Blots were then probed with the appropriate conjugated secondary antibodies and imaged on an Odyssey CLx Infrared Imaging System. Band intensities were analysed using LI-COR software. When required, loading reference controls were included to allow normalisation across blots (Cuchillo-Ibáñez et al., 2021; Lennol et al., 2022; López-Font et al., 2022).

Antibodies	Protein detected	Concentration	Study
AB178479	apoE (all isoforms)	1:1500	apoE and annex
AB947	apoE (all isoforms)	1:1000	apoE
NBP1-49529	apoE (apoE4)	1:1000	apoE
MAB5366	reelin (N-terminal)	1:1000	reelin
Ab139691	reelin (C-terminal)	1:1000	reelin
Y186	apoER2 (N-terminal)	1:4000	reelin
SAB1402255	LRP3 (C-terminal)	1:100	LRP3
SAB4501786	LRP3 (N-terminal)	1:100	LRP3
F1804	Flag	1:1000	LRP3
ZRB1176	LDLR (C-terminal)	1:200	LRP3
SAB1306331	apoER2 (C-terminal)	1:2000	LRP3
A8717	APP (C-terminal)	1:2000	LRP3
A8967	APP (N-terminal)	1:2000	LRP3
11088	sAPPα	1:1000	LRP3
18957	sAPPβ	1:1000	LRP3
Ab63817	LC3B	1:2000	LRP3
T6199	α-tubulin	1:4000	LRP3

Table 2. Antibodies used in studies.

Immunoprecipitation

CSF or brain samples were incubated on a roller overnight with PureProteome FlexiBind Magnetic Beads coupled with the corresponding antibody. The supernatant was removed (unbound fraction) and the beads were washed and then resuspended and boiled at 98°C for 5 min (unless otherwise stated) in SDS-PAGE sample buffer and analysed by western blot with the appropriate antibody. Control immunoprecipitations were performed (Cuchillo-Ibáñez et al., 2021; Lennol et al., 2022).

Native-PAGE

For blue-native gel electrophoresis, CSF samples were not heated (native conditions) and were loaded with LDS 4x sample buffer into native-PAGE 4-16% gels. Buffers were prepared using native-PAGE running buffer and native-PAGE cathode buffer additive. Immunoreactivity was detected using the AB178479 antibody and HRP anti-goat secondary antibody. The signal was visualized by ECL and analysed using ImageStudio software (Lennol et al., 2022).

Enzymatic deglycosylation

CSF samples were deglycosylated using an Agilent Enzymatic Deglycosylation Kit. Briefly, 30 μL of control or AD CSF was mixed with 10 μl incubation buffer and 2.5 μL denaturing buffer and heated at 100°C for 5 min. The samples were then cooled down to room temperature, and 2.5 μL of detergent (15% NP-40) was added while mixing gently. O-linked (1 μL sialidase and 1 μL O-glycanase) or N-linked (1 μL N-glycanase) deglycosylating enzymes were then added according to each different condition (O-linked, N-linked, or O- and N-linked deglycosylation) and samples were heated at 37°C for 3 hours. Control deglycosylation was performed by exposing samples to the same heating conditions in absence of deglycosylating enzymes. Samples were analysed by western blot (Lennol et al., 2022).

In-gel digestion and mass spectrometry

1 mL of CSF pooled from several AD patients was immunoprecipitated with AB178479 antibody and loaded into an SDS-polyacrylamide gel under reducing conditions. Recombinant apoE was included as a reference. Upon electrophoresis, the gel was divided into 2 pieces, one for protein visualization by SimplyBlue™ SafeStain Coomassie and one for blotting with the AB947 antibody to confirm band presence and location. Bands of interest were cut-out from the AD CSF and recombinant lanes and destained. Gel pieces were then dehydrated, reduced and alkylated. Gel pieces were then washed, dehydrated and dried once more, and digested overnight with trypsin enzyme. Digestion was stopped and peptides were collected. Pooled extracts were dried and stored until MS analysis.

For MS analysis samples were reconstituted and analysed with a Dionex 3000 nanoflow liquid chromatography system coupled to a Q Exactive. Mass spectra were acquired in positive ion mode and in a data-dependent manner. Fragmentation was obtained by higher energy collision-induced dissociation. Database searches were made using PEAKS Studio XPRO (Lennol et al., 2022).

Brain membrane enriched-fractions

Brain cortex samples were homogenized using a polytron Heidolph RZR-1 at 600-800 rpm in a glass potter applying 10-15 pulses in buffer at 10% (w/v). The homogenate was centrifuged at 1000×g for 20 min at 4ºC. The supernatant (post-nuclear fraction) was centrifuged at 13000xg for 15 min at 4ºC, and then the supernatant (cytosolic fraction) was aliquoted, and the resulting pellet (membrane-enriched fraction) was resuspended in buffer.

Differential centrifugation was performed in some CHO-PS70 cells. After homogenization of cell extracts in sucrose buffer, the homogenate was centrifuged at 1000×g for 10 min, and the supernatant was then centrifuged at 15000×g for 15 min. The resultant supernatant (fraction containing the plasma membrane and soluble proteins from the cytosol) and the pellet (containing membranes from the endoplasmic reticulum, mitochondria, lysosomes, peroxisomes and endosomes) were quantified and stored for subsequent analysis (Cuchillo-Ibáñez et al., 2021).

Microarray analysis

Gene expression was analysed in SH-SY5Y cells 48 hours after transfection with apoER2 using microarrays SurePrint G3 Human Microarrays, and performed by Bioarray SL. RNA concentration and purity was determined by a NanoDrop spectrophotometer, and RNA quality was determined with the R6K Screen Tape kit, and RNA integrity ranged between 9.5 and 9.7. Each sample was labelled with Cy3 using the Ono-Color Microarray-Based Gene Expression Microarrays Analysis v6.6 and data were imported to linear models for microarray data Bioconductor software. Raw data were subjected to background subtraction, then to within-array loess normalization. Across-array normalization was then

performed. Normalized data were fitted to a linear model, and the significance of gene expression changes was analysed to the adjusted *p* value (Cuchillo-Ibáñez et al., 2021).

qRT-PCR analysis

RNA was extracted from human brains, SH-SY5Y cells or CHO-PS70 cells using TRIzol® Reagent in the PureLink™ Micro-to-Midi Total RNA Purification System. SuperScript™ III Reverse Transcriptase was used to synthesize cDNAs from this total RNA (2 µg) using random primers. Quantitative PCR amplification was performed on a StepOne™ Real-Time PCR System with TaqMan probes specific for human *LRP3* (assay ID: HS01041220_m1), *LDLR* (assay ID: HS00181192_m1), and human *18S* as a housekeeping gene for the human brain and SH-SY5Y cell samples. In CHO-PS70 cells, mRNA expression was measured with primers for human *APP* (forward: AACCAGTGACCATCCAGAAC; reverse: ACTTGTCAGGAACGAGAAGG) and for *GAPDH* (GAPDH, forward: AGAAGGTGGTGAAGCAGGCAT; reverse: AGGTCCACCACTCTGTTGCTGT) to normalize the expression levels of the target genes by the ΔCt method curves (Cuchillo-Ibáñez et al., 2021).

Immunofluorescence and confocal microscopy

CHO-PS70 cells overexpressing LRP3-flag were washed with cold Hank-buffered salt solution and fixed with 4% paraformaldehyde and 0.1 M EGTA for 10 min. To stain the plasma membrane, cells were incubated with WGA-FITC (WGA: lectin from *Triticum vulgaris*, FITC (fluorescin) conjugate) for 15 min at room temperature, and the nonspecific sites were blocked with 10% (w/v) bovine serum albumin for 30 min. No permeabilization steps were included before or during the incubation with the primary antibodies. Cells were incubated with primary antibody for Flag (1:200) for 1 hour, followed by secondary antibody (1:200, Cy5 anti-mouse) for 1 hour. After washes with PBS, cells were incubated briefly with Hoechst dye to label nuclei. Pictures were obtained in a Leica SPEII upright TCL-SL confocal microscope using an oil-immersion 40× objective.

The frontal cortex and hippocampus of 14 cases with different pathology stages were used in the fluorescence study. Formalin-fixed, paraffin-embedded-de-waxed sections, 4 μm in thickness, were stained with a saturated solution of Sudan black B for 15 min to block autofluorescence of lipofuscin granules present in cell bodies and then rinsed in 70% ethanol and washed in distilled water. The sections were boiled in citrate buffer to enhance antigenicity and blocked for 30 min at room temperature with 10% FBS diluted in PBS. Then, the sections were incubated at 4ºC overnight with combinations of primary antibodies: LRP3 C-terminal (1:50) and apoER2 (1:50). After washing, the sections were incubated with fluorescent secondary antibodies against the corresponding host species. Nuclei were stained with DRAQ5™ (1:2000). After washing, sections were mounted in an Immuno-Fluore medium, sealed, and dried overnight. Sections were examined with a Leica TCS-SL confocal microscope (Cuchillo-Ibáñez et al., 2021).

Statistical analyses

Data analyses were performed using GraphPad Prism (version 7). The distribution of data was tested for normality using D'Agostino-Pearson tests. ANOVA was performed for parametric variables and Kruskal-Wallis test for non-parametric variables to compare between groups. To compare two specific groups and determine exact p values Student's t-test for parametric variables and Mann-Whitney U tests for non-parametric variables were performed. For correlations, Pearson and Spearman tests were used. p value < 0.05 was considered significant.

PUBLICATIONS

ARTICLE #1: APOLIPROTEIN E IMABALANCE IN THE CEREBROSPINAL FLUID OF ALZHEIMER'S DISEASE PATIENTS

Matthew Paul Lennol, Irene Sánchez-Domínguez, Inmaculada Cuchillo-Ibáñez, Elena Camporesi, Gunnar Brinkmalm, Daniel Alcolea, Juan Fortea, Alberto Lleó, Guadalupe Soria, Fernando Aguado, Henrik Zetterberg, Kaj Blennow & Javier Sáez-Valero

RESEARCH

Apolipoprotein E imbalance in the cerebrospinal fluid of Alzheimer's disease patients

Matthew Paul Lennol[1,2], Irene Sánchez-Domínguez[3,4], Inmaculada Cuchillo-Ibañez[1,2,5], Elena Camporesi[6], Gunnar Brinkmalm[6], Daniel Alcolea[2,7], Juan Fortea[2,7,8], Alberto Lleó[2,7], Guadalupe Soria[4,9], Fernando Aguado[3,4], Henrik Zetterberg[6,10,11,12,13], Kaj Blennow[6,10] and Javier Sáez-Valero[1,2,5*]

Abstract

Objective: The purpose of this study was to examine the levels of cerebrospinal fluid (CSF) apolipoprotein E (apoE) species in Alzheimer's disease (AD) patients.

Methods: We analyzed two CSF cohorts of AD and control individuals expressing different *APOE* genotypes. Moreover, CSF samples from the TgF344-AD rat model were included. Samples were run in native- and SDS-PAGE under reducing or non-reducing conditions (with or without β-mercaptoethanol). Immunoprecipitation combined with mass spectrometry or western blotting analyses served to assess the identity of apoE complexes.

Results: In TgF344-AD rats expressing a unique apoE variant resembling human apoE4, a ~35-kDa apoE monomer was identified, increasing at 16.5 months compared with wild-types. In humans, apoE isoforms form disulfide-linked dimers in CSF, except apoE4, which lacks a cysteine residue. Thus, controls showed a decrease in the apoE dimer/monomer quotient in the *APOE* ε3/ε4 group compared with ε3/ε3 by native electrophoresis. A major contribution of dimers was found in *APOE* ε3/ε4 AD cases, and, unexpectedly, dimers were also found in ε4/ε4 AD cases. Under reducing conditions, two apoE monomeric glycoforms at 36 kDa and at 34 kDa were found in all human samples. In AD patients, the amount of the 34-kDa species increased, while the 36-kDa/34-kDa quotient was lower compared with controls. Interestingly, under reducing conditions, a ~100-kDa apoE complex, the identity of which was confirmed by mass spectrometry, also appeared in human AD individuals across all *APOE* genotypes, suggesting the occurrence of aberrantly resistant apoE aggregates. A second independent cohort of CSF samples validated these results.

Conclusion: These results indicate that despite the increase in total apoE content the apoE protein is altered in AD CSF, suggesting that function may be compromised.

Keywords: Alzheimer's disease, apoE, Biomarker, Aberrant complexes, Cerebrospinal fluid, Glycoform imbalance

Background

An important breakthrough in our understanding of Alzheimer's disease (AD) was the identification of the apolipoprotein E *APOE*-ε4 allele as a risk factor [1]. Apolipoprotein E (apoE) protein is a component of lipoprotein particles in the plasma, as well as in the cerebrospinal fluid (CSF) [2]. ApoE regulates important signaling pathways by interacting with receptors and is present

*Correspondence: j.saez@umh.es

[1] Instituto de Neurociencias de Alicante, Universidad Miguel Hernández-CSIC, Av. Ramón y Cajal s/n, E-03550 Sant Joan d'Alacant, Spain
Full list of author information is available at the end of the article

as sialylated glycoforms [3]. Human apoE lacks the consensus sequence necessary for N-linked glycosylation; thus, O-linked carbohydrates probably account for glycosylation [4]. The impact of apoE glycosylation remains unclear, but evidence indicates that glycosylation acts as an important post-translational mechanism for fine-tuning apoE interaction with receptors and proteins [5].

In humans, three versions of the *APOE* gene exist, ε2 (apoE2), ε3 (apoE3), and ε4 (apoE4) alleles, while other mammals only have one version of the *APOE* gene, resembling ancestral apoE4 [6]. *APOE*-ε3 is the most common allele (~75%), followed by ε4 (15–20%) and ε2 (4–8%) [7]. Compared to the most common *APOE* ε3/ε3 genotype, each additional copy of the *APOE*-ε4 allele is associated with a higher risk of AD and a younger mean age of dementia onset. Thus, in individuals with one copy of the *APOE*-ε4 allele, the risk of AD increases 2–3 times and 8–12 times in individuals with two copies [8]. Experimental evidence shows the deleterious effect of the apoE4 variant for AD, while the lack of apoE4 appears to be protective [9]. In contrast, the presence of one or two copies of the *APOE*-ε2 allele is associated with a lower risk of AD and an older mean age of dementia onset [10]; therefore, it has been hypothesized that the apoE2 protein could be protective against AD [11]. Indeed, *APOE*-ε2 homozygotes present an exceptionally low likelihood of developing AD [12]. The reported effects of different *APOE* genotypes on AD risk vary widely with demographic factors such as gender and ethnicity [7]. Moreover, the percentage of *APOE* genotypes in cognitively unimpaired people with neuropathological or biomarker evidence of preclinical AD, or the percentage of people who meet the criteria for mild cognitive impairment with or without biomarker evidence of AD, is not well established (discussed in [12]). Anyhow, despite the 2–3-fold increase in AD prevalence in *APOE*-ε4 subjects compared to the general population, most of the individuals with AD are *APOE*-ε3 homozygotes [13].

Nonetheless, given the important physiological functions of apoE, a malfunctioning of the apoE protein may also contribute to AD pathology in ε4 non-carriers [14]. The differences in the structure of apoE isoforms influence their ability to bind lipids, receptors, and amyloid-β (Aβ), which aggregates in plaques within the brain of AD patients [14].

Interestingly, apoE forms disulfide-linked homodimers and heterodimers with the apoA-II apolipoprotein involving the cysteine (Cys) at position 112 [7, 14]. Indeed, these apoE homodimers linked by disulfide bonds could be the native form able to bind to receptors [15]. The three human apoE isoforms differ in the presence of Cys/arginine (Arg) at positions 112 and 158 within the receptor binding domain, as apoE4 lacks Cys

residues at both these positions [4]. The amino acid substitution of Cys-112 by Arg in apoE4 explains the lower number of disulfide-linked dimers in the CSF of *APOE* ε3/ε4 subjects compared with *APOE* ε3/3 subjects, and their absence in *APOE* ε4/ε4 subjects [16, 17], but may also explain the reduced ability of apoE4 to mediate some of its biological roles, compared with apoE2 or apoE3 [18].

The mature apoE protein has 299 amino acids and a molecular mass of ~35 kDa. However, previous studies performed in the brain [19] and CSF [17] reported a ~100-kDa apoE band in non-reducing conditions, as opposed to the predicted ~70 kDa, which was referred to as an apoE homodimer.

Previous studies that considered total CSF apoE levels failed to demonstrate consistent changes when the *APOE* genotype was included as a covariate in the models [20–22]. However, other studies associated high CSF apoE concentrations with an increased risk of impaired cognitive progression in non-apoE4 carriers [23].

Anyhow, in order to consider the estimation of apoE levels in CSF as a read-out of AD occurrence or progression, in addition to the *APOE* genotype, the studies should also consider changes in the protein conformation/structure that can compromise the biological function of the apoE protein. In this study, we aimed to characterize the occurrence of different apoE species in AD CSF from individuals with different *APOE* genotypes, while considering changes in the balance of apoE glycoforms and the occurrence of aberrant apoE dimers that could indicate a compromise of apoE function in the brain.

Materials and methods
Patients
CSF samples from individuals with known *APOE* genotypes were obtained from two independent cohorts. The CSF samples from both cohorts used for this study were de-identified aliquots from clinical routine analyses, following procedures approved by the Ethics Committees at the University of Gothenburg and the Hospital Sant Pau, respectively. Additionally, this study was approved by the ethics committee at the Miguel Hernandez University, and was carried out in accordance with the Helsinki Declaration regarding research on humans.

The CSF samples were obtained by lumbar puncture and centrifuged (2000×g, 10 min) and then immediately aliquoted and stored in ultrafreezers and kept at −80°C until analysis. The time between CSF acquisition and storage was less than 4 h in all cases. The handling of the samples was performed following recommended

operating procedures [24]. Freeze-thaw cycles were avoided and new aliquots were used for each independent analysis.

The first cohort was from the longitudinal geriatric population study in Piteå, Sweden [25], the Piteå Dementia Project. The diagnostic evaluation included a clinical examination (detailed medical history and somatic, neuropsychiatric, and neurological status), a neuropsychological test battery, routine blood and CSF tests, and a CT scan to exclude secondary dementias [26]. All clinical diagnoses and evaluations were made without knowledge of the results of the biochemical analyses and vice versa. The cohort consisted of 45 patients with AD (fourteen men and thirty-one women, mean age 77±1 years) and was selected based on the APOE-ε4 status, so that fifteen each had APOE ε3/ε3, APOE ε3/ε4, or APOE ε4/ε4. In addition, fourteen non-AD controls [seven men and seven women, mean age (67 ± 3 years); APOE ε3/ε3: 9, APOE ε3/ε4: 5] were included. APOE genotype was determined by the solid-phase mini-sequencing method as previously described [27]. For this study, patients who were designated as AD or controls also had typical core CSF biomarker levels [Aβ42 and total tau (T-tau)] using cut-offs that are >90% specific for AD [28], but except for CSF Aβ42 and T-tau, all biochemical analyses were made without knowledge of the clinical data. The ethics committees in Umeå University and University of Gothenburg approved the study.

The second cohort was obtained from the Sant Pau Initiative on Neurodegeneration (SPIN cohort) [29] from Hospital Sant Pau (Barcelona, Spain). We included samples from 29 AD patients (thirteen men and sixteen women, mean age 73±1 years; APOE: 10 ε3/ε3, 10 ε3/ε4, 9 ε4/ε4) and ten controls (seven men and three women, mean age 69±2 years; APOE: 5 ε3/ε3, 5 ε3/ε4). Typically, these are patients who present cognitive complaints and are referred to the specialized memory unit from their primary care physician. All patients undergo a full neuropsychological evaluation that demonstrates objective cognitive impairment. Patients were included in the cohort when they presented supportive biomarkers of the AD pathophysiological process. Cognitively normal participants were volunteers without cognitive complaints and normal neuropsychological evaluation. More details about inclusion/exclusion criteria and neuropsychological tests in this cohort are detailed elsewhere [29].

In this cohort, the APOE genotype was determined by direct DNA sequencing and visual analysis of the resulting electropherogram performed to identify the two coding polymorphisms that encode the three possible apoE variants [29].

Each center applied their own internally validated cut-offs, according to their preanalytical and analytical particularities. More details about the cut-offs applied are indicated below. Samples were retrospectively selected from large cohorts to balance age, sex, and APOE status. Most of the selected cases (92%, 43 of 45 from

Table 1 Demographic and biomarker information from the CSF samples obtained from the Gothenburg (Sweden) and Barcelona (Spain) cohorts

Cohort: Gothenburg (Sweden)

	Control			Alzheimer's disease			
APOE	ε3/ε3	ε3/ε4	All	ε3/ε3	ε3/ε4	ε4/ε4	All
N	9	5	14	15	15	15	45
Age (years)	69±2	62±5	67±3	79±2	78±1	73±1	77±1*
Age (range)	60–81	44–75	44–81	62–88	69–84	63–83	62–88
Female/male	5/4	2/3	7/7	11/4	11/4	9/6	31/14
CSF Aβ42 (pg/mL)	845±96	746±121	804±74	470±13*	480±8*	419±21	457±10*
CSF tau (pg/mL)	317±53	303±34	312±35	816±88*	917±112*	731±53	840±52*

Cohort: Barcelona (Spain)

	Control			Alzheimer's disease			
APOE	ε3/ε3	ε3/ε4	All	ε3/ε3	ε3/ε4	ε4/ε4	All
N	5	5	10	10	10	9	29
Age (years)	71±2	67±52	69±2	75±2	73±2	72±2	73±1*
Age (range)	66–76	60–72	60–76	64–84	64–83	61–85	61–85
Female/male	1/4	2/3	3/7	7/3	2/8	7/2	16/13
CSF Aβ42 (pg/mL)	1139±248	1010±116	1075±131	607±60*	543±37*	493±62	549±31*
CSF tau (pg/mL)	295±49	261±23	278±26	778±94*	624±62*	908±81	765±50*

Values are represented as mean ± SEM. *Significantly different (T-test, p< 0.05) from the control group with the same APOE genotype or regardless of the genotype ("All" columns)

Gothenburg and 25 of 29 from Barcelona) were categorized A+T+ according to [30]; thus, subgrouping by the AT(N) system for analysis was impractical. For full details about the collections, see Table 1.

Determination of AD core biomarkers by ELISA and definition of cut-offs

In the cohort from Gothenburg, the levels of the AD core biomarkers T-tau, P-tau, and Aβ42 were measured in the CSF using INNOTEST ELISAs (Fujirebio-Europe, Gent, Belgium). Patients were designated as AD or controls according to CSF biomarker levels using cut-offs that are >90% specific for AD: Aβ42 <550 pg/mL and total tau (T-tau) >400 pg/mL [20].

For the cohort from Barcelona, cut-offs for AD biomarkers measured in the Lumipulse automated platform (Fujirebio-Europe) were T-tau > 400 pg/mL, P-tau > 63 pg/mL, and 0.062 for the Aβ42/Aβ40 ratio [29].

All samples were analyzed as part of a clinical routine by board-certified laboratory technicians following strict procedures for batch-bridging, analyses, and quality control of individual ELISA plates.

Transgenic rat CSF

The experiments were carried out using a cohort of 107 rats (53 males and 54 females), including transgenic TgF344-AD rats ($n = 52$) expressing mutant human APP (APPsw) and presenilin-1 (PS1ΔE9) genes [31] and wild-type Fischer rats ($n = 55$). Rats were bred in the animal research facilities at the University of Barcelona. Animals were provided with food and water ad libitum and maintained in a temperature-controlled environment in a 12/12-h light-dark cycle. CSF samples (50–100 μL) were collected from ketamine/xylazine-anesthetized animals by cisternal puncture with a glass capillary in the suboccipital region through the atlanto-occipital membrane, with a single incision into the subarachnoid space [32]. CSF aliquots from different time points [4 months: 16 wild-type (8 male, 8 female) and 16 TgF344-AD animals (8 male, 8 female); 10.5 months: 17 wild-type (8 male, 9 female) and 16 TgF344-AD animals (8 male, 8 female); 16.5 months: 22 wild-type (12 male, 10 female) and 20 TgF344-AD animals (9 male, 11 female)] were analyzed. This study was part of a large project assessing various different proteins that included brain analysis at each stage; thus, it was not possible to perform longitudinal measurements in the same animal (repeat sampling) to reduce the number of animals. Animal work was performed in accordance with the local legislation, with the approval of the Experimental Animal Ethical Committee of the University of Barcelona, and in compliance with European legislation.

Western blotting

Samples of human or rat CSF (10 μL) were denatured at 98°C for 5 min and resolved by sodium dodecyl sulfate-polyacrylamide gel electrophoresis (SDS-PAGE) under reducing or non-reducing conditions (determined by the presence or absence of β-mercaptoethanol in the sample buffer, respectively). Unless specified, the studies presented in the text were performed under reducing conditions. For this study, we used 12% precast gels (Bio-Rad Laboratories, GmbH, Munich, Germany; #4561046). All the samples were analyzed at least in duplicate (duplicates in separate gels) and distributed in the gels to ensure the comparison by disease condition and APOE genotype. The distribution of the samples in the gels was performed by a member of the team and the experiments were performed by another, the experimenter, in a blind way.

Following electrophoresis, proteins were blotted onto 0.45-μm nitrocellulose membranes (Bio-Rad Laboratories, GmbH, Munich, Germany). Bands of apoE immunoreactivity were detected using either the antibody AB178479 (goat polyclonal; Merck Millipore) or the antibody AB947 (goat polyclonal; Merck Millipore), both common to all apoE isoforms, or alternatively by an antibody specific to the apoE4 isoform (recognizes an internal domain comprising the Arg112 residue present exclusively in apoE4 species; mouse monoclonal, Novus Biologicals; NBP1-49529). Blots were then probed with the appropriate conjugated secondary antibodies (IRDye secondary antibodies, LI-COR Biosciences, Lincoln, NE, USA) and imaged on an Odyssey CLx Infrared Imaging System (LI-COR Biosciences). Band intensities were analyzed using LI-COR software (ImageStudio Lite). The boxes selected with the ImageQuant Studio software for quantification, as well as the completed blots, are shown as supplementary figures. Recombinant apoE3 (Peprotech, ThermoFisher Scientific# 350-02) was included into each blot to serve as a loading reference and for normalizing the immunoreactivity signal between blots. Specifically, the same amount of recombinant apoE3 was always included, and the immunoreactivity of the apoE bands from each blot was referred to (divided by) the immunoreactivity of recombinant apoE3, thus correcting inter-blot differences and allowing for comparisons across assays.

For blue-native gel electrophoresis, the CSF samples were not heated (native conditions) and were loaded with NuPage LDS 4× Sample Buffer (ThermoFisher Scientific, NP007) into native-PAGE 4–16% gels (ThermoFisher Scientific, BN1002BOX). Buffers were prepared using native-PAGE Running Buffer (ThermoFisher Scientific, BN2001) and native-PAGE Cathode Buffer Additive (ThermoFisher Scientific, BN2002). Immunoreactivity

was detected using the AB178479 antibody and HRP anti-goat secondary antibody (ThermoFisher). The signal was visualized by ECL (GE Healthcare Life Science) and analyzed using ImageStudio Lite.

ApoE immunoprecipitation

CSF samples (50 µL) were incubated on a roller overnight with 100 µL PureProteome FlexiBind Magnetic Beads (Merck Millipore, LSKMAGN04) coupled with the AB178479 apoE antibody (Merck Millipore). The supernatant was removed, and the beads were washed and then resuspended and boiled at 98 °C for 5 min in SDS-PAGE sample buffer and analyzed by western blot with the AB947 antibody (Merck Millipore) or anti-apoE4 antibody (Novus Biologicals, NBP1-49529). For a control immunoprecipitation, beads were coupled with horse serum and then incubated with CSF samples.

Enzymatic deglycosylation

Enzymatic deglycosylation was performed using an Agilent Enzymatic Deglycosylation Kit (Agilent Technologies, GK80110) following the manufacturer's instructions. Briefly, for each condition, 30 µL of control or AD CSF was mixed with 10-µl incubation buffer and 2.5-µL denaturing buffer and heated at 100 °C for 5 min. The samples were then cooled down to room temperature, and 2.5 µL of detergent (15% NP-40) was added while mixing gently. O- (1 µL sialidase and 1 µL O-glycanase) or N-linked (1 µL N-glycanase) deglycosylating enzymes were then added according to each different condition (O-linked, N-linked, or O- and N-linked deglycosylation) and samples were heated at 37 °C for 3 h. Samples were then analyzed by western blot. As for control of the deglycosylation process, samples exposed to the same heating conditions but without deglycosylating enzymes were included.

In-gel digestion

In-gel digestion was performed as previously described [33] in order to investigate the content of western blot immunoreactive bands of interest using an antibody-free method. Briefly, 1 mL of a pool of AD CSF (*APOE* ε3/ε4 and *APOE* ε3/ε4 cases) was immunoprecipitated with AB178479 antibody and loaded into SDS-polyacrylamide gel under reducing conditions, as described above. ApoE3 and apoE4 recombinant proteins (Peprotech, ThermoFisher Scientific# 350-02 and 350-04) were also loaded in the gel (10 pmol) and used as a reference for band excising and positive control. Upon electrophoresis, the gel was divided into two parts, one for protein visualization by SimplyBlue™ SafeStain Coomassie (ThermoFisher Scientific, cat# LC6060) and one for blotting with the AB947 antibody as confirmation of band presence and location. Bands of interest were cut-out from the AD CSF gel lane and recombinant protein lanes and destained using a 1:1 mixture of acetonitrile and 50 mM ammonium bicarbonate solution twice for 15 min. Furthermore, gel pieces were de-hydrated with 100% acetonitrile and dried using a vacuum centrifuge. Samples were subsequently reduced with 10 mM dithiothreitol (DTT) for 1 h at 56 °C and alkylated with 25 mM iodoacetamide (IAA) for 45 min at room temperature in the dark. Gel pieces were further washed with 25mM ammonium bicarbonate, de-hydrated with 100% acetonitrile, and dried using a vacuum centrifuge once more. Samples were digested overnight at 37°C using 100 ng/µL trypsin enzyme (Sequencing Grade Modified Trypsin, #V511A, Promega). The next day, digestion was stopped by the addition of 2% trifluoroacetic acid and 75% acetonitrile solution, and peptides were collected into a new tube (Costar, #3207). Gel pieces were further extracted with the addition of 50% acetonitrile and 0.2% trifluoroacetic acid solution shaking for 30 min. The supernatant containing the peptides was transferred to the collection tube. Pooled extracts for each gel piece were dried through vacuum centrifugation and stored at −80 °C pending mass spectrometry (MS) analysis.

Mass spectrometry data analysis

Dried in-gel digested samples were reconstituted in 7 µL 8% acetonitrile/8% formic acid solution and shaken for 30 min. A total of 6 µL of each sample was investigated using mass spectrometry (MS) analysis performed with a Dionex 3000 nanoflow liquid chromatography system coupled to a Q Exactive (both Thermo Fisher Scientific). Briefly, a reversed phase Acclaim PepMap C18 (100 Å pore size, 3 µm particle size, 20 mm length, 75 µm i.d., Thermo Fisher Scientific) trap column was used for online desalting and sample clean-up. Separation was performed with a reversed phase Acclaim PepMap RSLC C18 (100 Å pore size, 2 µm particle size, 75 µm i.d., 150 mm length, Thermo Fisher Scientific) column at a flow rate of 300 nL/min by applying a linear gradient of 0–40% B for 50 min. Mobile phase A was 0.1% formic acid in water (v/v) and mobile phase B was 0.1% formic acid and 84% acetonitrile in water (v/v/v).

Mass spectra were acquired in positive ion mode and in a data-dependent manner with a resolution setting of 70,000 for precursor and 17,500 for fragment ion acquisitions. Fragmentation was obtained by higher energy collision-induced dissociation (HCD) using a normalized collision energy (NCE) setting of 28. Database searches were made using PEAKS Studio XPRO (Bioinformatic Solutions, Inc., Waterloo, Canada).
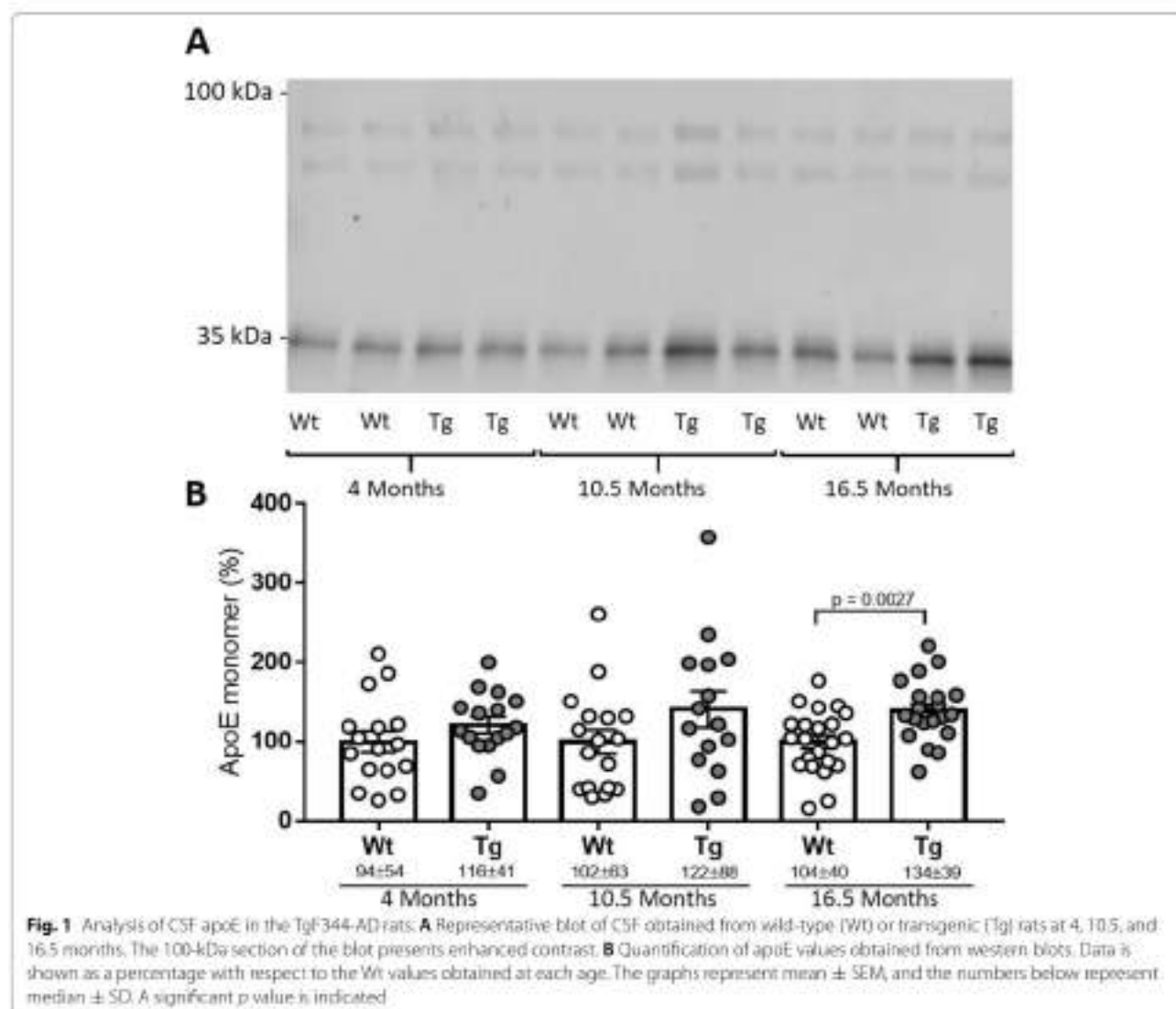
Statistical analysis

All the data was analyzed using GraphPad Prism (version 7; GraphPad software, San Diego, CA, USA). The test was used to analyze the distribution of each variable. Firstly, multiple comparisons were performed between groups. ANOVA was used for parametric variables, and the Kruskal-Wallis test for non-parametric variables. A Student's t-test for parametric variables and a Mann-Whitney U test for non-parametric variables were employed for comparison between two groups and for determining precise p values. For correlations, the Pearson and Spearman tests were used. The results are shown as means ± SEM; the standard deviation (SD) and median values are also displayed as indicated in the figure legends.

Results

CSF apoE in Tg344-AD rats

To determine whether altered CSF apoE levels could be indicative of pathology-associated changes, we initially examined them in a rat transgenic AD model. The TgF344-AD rat expresses human *APP* with the Swedish mutation and human *PSEN1* with the Δ exon 9 mutation. As mentioned above, while humans have three versions of the *APOE* gene, other mammals such as rats only have one isoform of the apoE protein, which presents Arg at position 112 (https://web.expasy.org/variant_pages/VAR_000652.html) and thus shares the inability to form disulfide-linked dimers with human apoE4. We examined apoE levels in the CSF of 4-, 10.5-, and 16.5-month-old transgenic rats and wild-type littermates by SDS-PAGE

Fig. 1 Analysis of CSF apoE in the TgF344-AD rats. **A** Representative blot of CSF obtained from wild-type (Wt) or transgenic (Tg) rats at 4, 10.5, and 16.5 months. The 100-kDa section of the blot presents enhanced contrast. **B** Quantification of apoE values obtained from western blots. Data is shown as a percentage with respect to the Wt values obtained at each age. The graphs represent mean ± SEM, and the numbers below represent median ± SD. A significant p value is indicated

80

using the AB178479 antibody. In all the animals and at all ages, apoE appeared as a single ~35-kDa band (Fig. 1A) and no differences were found between males and females ($p > 0.05$ for the comparison at every age). We did not find different glycoforms. Although no differences were found at 4 and 10.5 months between wild-type and TgF344-AD rats, a trend of apoE increment was observed. At 16.5 months of age, apoE levels were 50% higher in TgF344-AD animals than in wild-types ($p = 0.003$, Fig. 1B). The significant differences for CSF apoE levels detected between TgF344-AD and controls at 16.5 months of age were maintained when the animals were subgrouped by gender (male: control vs TgF344: $p = 0.019$; female: control vs TgF344: $p = 0.048$).

Characterization of apoE in human CSF

We examined the presence of apoE species in CSF samples by SDS-PAGE and western blot under reducing conditions (in presence of the reducing agent β-mercaptoethanol that breaks disulfide bonds) from a cohort of control and AD patients from Gothenburg (Sweden; see Table 1) expressing different *APOE* genotypes.

In all CSF samples, using the AB178479 antibody, apoE appeared as two distinct immunoreactive bands of ~34 and ~36 kDa (Fig. 2A). Immunoprecipitation with this antibody and subsequent immunoblotting with an alternative apoE antibody, AB947, confirmed the characterization of both apoE monomeric species in *APOE* ε3/ε3 samples (Fig. 2B). The same occurred when using an anti-apoE4 antibody in *APOE* ε3/ε4 samples (Fig. 2C). An apoE band of ~100 kDa was also observed, almost exclusively in the AD CSF samples, and this band was immunoprecipitated similarly to monomers (Fig. 2A–C). ApoE3 and apoE2 isoforms form disulfide-linked dimers in CSF, but these dimers should be sensitive to the reducing agent β-mercaptoethanol. Additional bands between the monomers and the 100-kDa bands did not appear to follow any specific pattern related with the pathology condition or the *APOE* genotype and were not consistently represented in the immunoprecipitated fraction; therefore, they were not considered for further investigations. Immunoprecipitated complexes of 100 kDa, using the AB178479 antibody, were dissected after electrophoresis and examined by MS analysis identifying 14 tryptic peptides spanning throughout the sequence of human apoE (Uniprot entry P02649_HUMAN), and both apoE3 and apoE4 isoforms were detected. Matching sequences are displayed in Table 2.

We first aimed to understand why the monomers appeared as two distinct bands with different molecular masses. We hypothesized that the bands likely represent
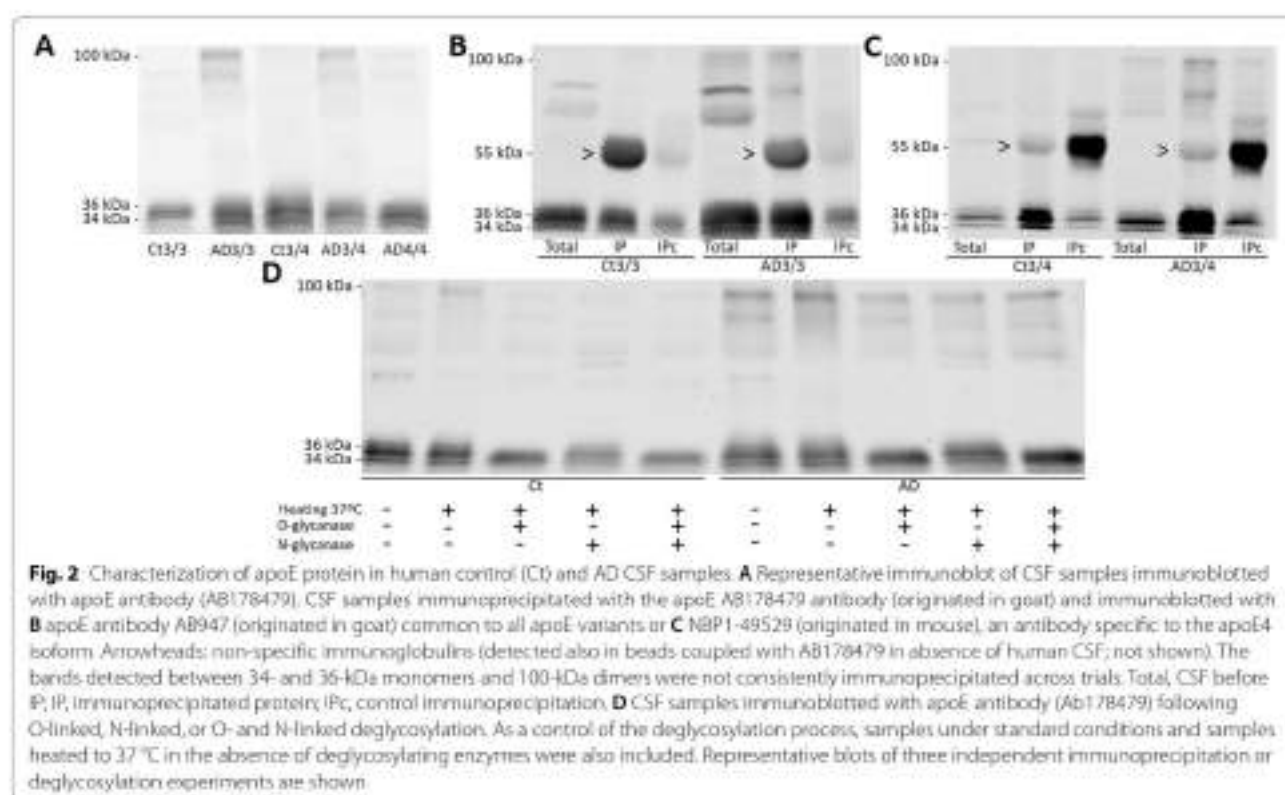

Fig. 2 Characterization of apoE protein in human control (Ct) and AD CSF samples. A Representative immunoblot of CSF samples immunoblotted with apoE antibody (AB178479). CSF samples immunoprecipitated with the apoE AB178479 antibody (originated in goat) and immunoblotted with B apoE antibody AB947 (originated in goat) common to all apoE variants or C NBP1-49529 (originated in mouse), an antibody specific to the apoE4 isoform. Arrowheads: non-specific immunoglobulins (detected also in beads coupled with AB178479 in absence of human CSF; not shown). The bands detected between 34- and 36-kDa monomers and 100-kDa dimers were not consistently immunoprecipitated across trials. Total, CSF before IP; IP, immunoprecipitated protein; IPc, control immunoprecipitation. D CSF samples immunoblotted with apoE antibody (Ab178479) following O-linked, N-linked, or O- and N-linked deglycosylation. As a control of the deglycosylation process, samples under standard conditions and samples heated to 37 °C in the absence of deglycosylating enzymes were also included. Representative blots of three independent immunoprecipitation or deglycosylation experiments are shown

Lennol et al. Alzheimer's Research & Therapy   (2022) 14:161

Page 8 of 19

Table 2 Identified peptides from apoE species of human CSF by MS

A

```
                1
    HKVLHALLV  TTLKGGAEV  EQAVETEPEP  ELRQQTEWQS  GQRWELALGR
33  FWDYLRWVQT  LSEQVQEELL  SSQVTQELRA  LMDETMKELS  AYKSELEEQL
83  TPVAEETRAR  LSKELQAAQA  RLGADMEDVC  GRLVQYRGEV  QAMLGQSTEE
133 LRVRLASHLR  KLRKRLLRDA  DDLQKRLAVY  QAGAREGAER  GLSAIRERLG
183 PLVEQGRVRA  ATVGSLAGQP  LQERAQAWGE  RLRARMEEMG  SRTRDRLDEV
233 KEQVAEVRAK  LEEQAQQIRL  QAEAFQARLK  SWFEPLVEDM  QRQWAGLVEK
283 VQAAVGTSAA  PVPSDNH
                299
```

B

```
                1
    HKVLHALLV  TTLKGGAEV  EQAVETEPEP  ELRQQTEWQS  GQRWELALGR
33  FWDYLRWVQT  LSEQVQEELL  SSQVTQELRA  LMDETMKELS  AYKSELEEQL
83  TPVAEETRAR  LSKELQAAQA  RLGADMEDVC  GRLVQYRGEV  QAMLGQSTEE
133 LRVRLASHLR  KLRKRLLRDA  DDLQKRLAVY  QAGAREGAER  GLSAIRERLG
183 PLVEQGRVRA  ATVGSLAGQP  LQERAQAWGE  RLRARMEEMG  SRTRDRLDEV
233 KEQVAEVRAK  LEEQAQQIRL  QAEAFQARLK  SWFEPLVEDM  QRQWAGLVEK
283 VQAAVGTSAA  PVPSDNH
                299
```

C

Peptide	E3/E4	Start[a]	End[a]	PTM	Mass [Da]	Score[b]	Δmass [ppm]	Area 35 kDa	Area 100 kDa
K.VEQAVETEPEPELR.Q		2	15		1624.7944	140.9	0.3	1.1E+08	3.7E+06
R.QQTEWQSGQR.W		16	25		1246.5691	60.27	-0.1	2.8E+05	
R.WELALGR.F		26	32		843.4603	72.33	-0.5	1.0E+09	1.6E+08
R.WVQTLSEQVQEELLSSQVTQELR.A		39	61		2729.3872	200	0.2	4.2E+08	6.9E+07
R.ALMDETMK.E		62	69		937.4249	89.9	0.2	1.7E+08	4.6E+07
R.ALMDETmK.E		62	69	Oxidation (M7)	953.4198	62.96	-0.1	6.3E+07	0.0E+00
R.ALmDETMK.E		62	69	Oxidation (M3)	953.4198	82.28	-0.1	6.3E+07	5.2E+06
R.ALmDETmK.E		62	69	2x Oxidation (M3, M7)	969.4147	68.11	-0.7	1.6E+06	
K.SELEEQLTPVAEETR.A		76	90		1729.8369	153.29	2.6	5.4E+09	1.5E+08
K.ELQAAQAR.L		96	103		885.4668	77.08	-0.4	4.9E+06	
R.LGADMEDVcGR.L	E3	104	114	Carbamidomethylation [C9]	1221.5118	120.62	2.0	1.9E+08	3.3E+07
R.LGADmEDVcGR.L	E3	104	114	Oxidation (M5); Carbamidomethylation [C9]	1237.5067	111.45	0.1	1.1E+07	4.5E+06
R.LGADMEDVR.G	E4	104	112		1004.4597	93.38	-0.8	3.8E+08	6.8E+07
R.LGADmEDVR.G	E4	104	112	Oxidation (M5)	1020.4546	83.95	-0.5	4.7E+07	5.0E+06
R.GEVQAMLGQSTEELR.V		120	134		1646.7933	136.25	3.1	8.7E+08	1.3E+08
R.GEVQAmLGQSTEELR.V		120	134	Oxidation (M6)	1662.7883	124.7	1.2	7.4E+08	4.5E+07
R.DADDLQK.R		151	157		803.3661	47.3	-2.2	2.3E+06	
R.LAVYQAGAR.E		159	167		947.5188	88.07	2.4	6.4E+09	1.6E+08
R.LGPLVEQGR.V		181	189		967.545	87.5	-0.7	5.4E+09	2.5E+08
R.AATVGSLAGQPLQER.A		192	206		1496.7947	122.03	2.4	4.1E+09	1.6E+08
R.AQAWGER.L		207	213		816.3878	58.47	-0.4	2.5E+05	
K.EQVAEVR.A		234	240		829.4293	54.21	-1.8	3.7E+06	
K.LEEQAQQIR.L		243	251		1113.5778	84.72	-0.1	9.2E+06	
R.LQAEAFQAR.L		252	260		1032.5352	74.31	0.3	5.1E+09	2.5E+08
K.SWFEPLVEDMQR.Q		263	274		1535.7079	133.05	-0.8	7.5E+07	2.0E+07
K.SWFEPLVEDmQR.Q		263	274	Oxidation (M10)	1551.7028	120.14	-0.9	5.8E+07	2.2E+07
R.QWAGLVEK.V		275	282		929.4971	56.77	0.0	4.8E+08	1.1E+08
K.VQAAVGTSAAPVPSDNH.-		283	299		1610.7003	158.69	-0.3	1.9E+09	6.9E+07

A, B: ApoE peptide chains assessed in monomeric (A) and the 100-kDa (B) species. The 18 aa signal peptide is shown in light gray; numbering is according to the mature protein, and X (marked in green) at position 112 denotes C (Cys) for e3 and R (Arg) for e4 isoforms, respectively. C: Data obtained from MS analysis. [a]Start and end positions refer to the mature protein without signal peptide. [b]Score as calculated by PEAKS Studio = −10 lg(P), where P is the probability for a false positive as determined by the software. PTM post-translational modifications, ppm mass error of the measured peptide in parts per million
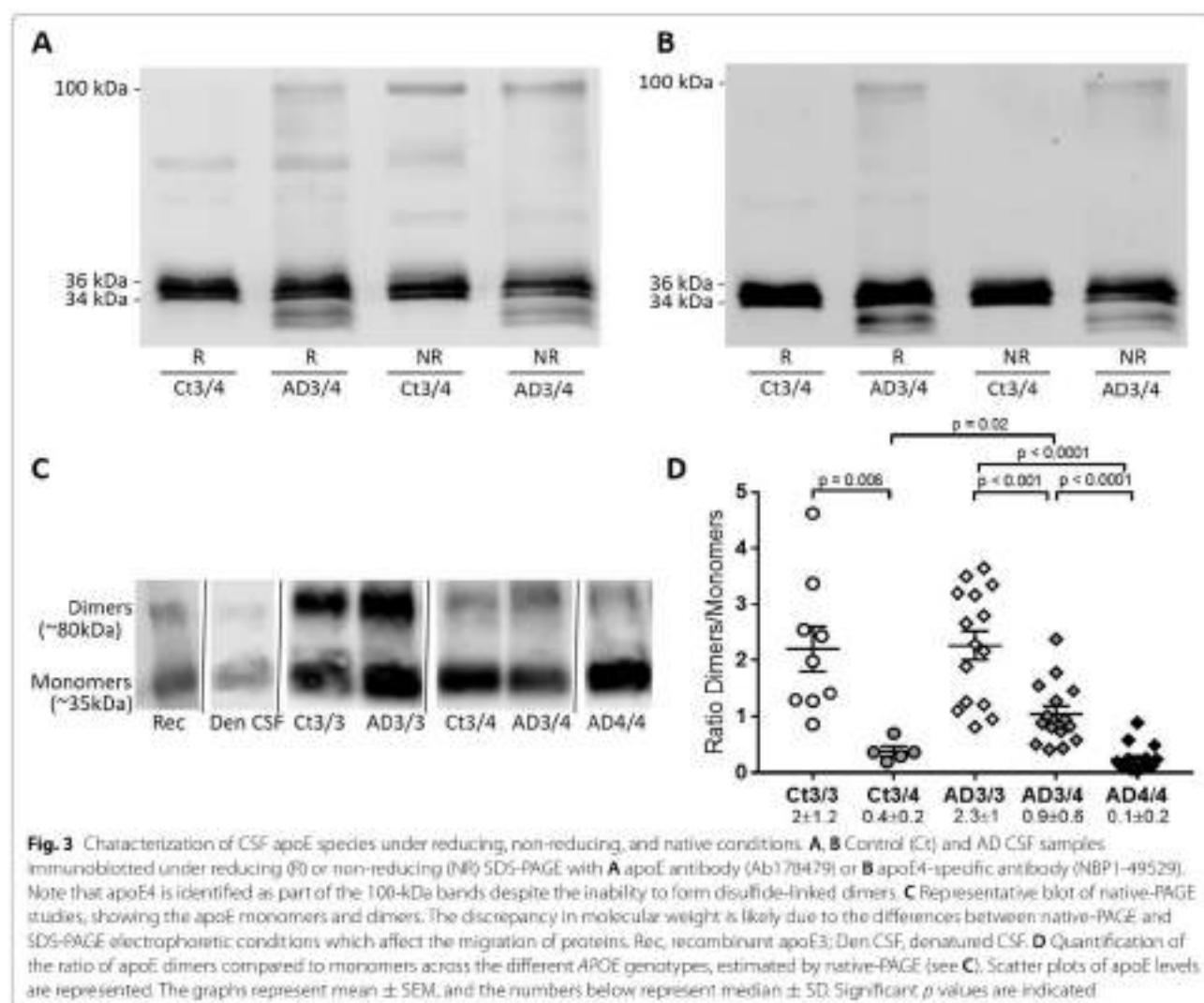
different glycoforms of the protein and, thus, an enzymatic deglycosylation assay was performed. While, as expected, N-deglycosylation did not alter the apoE band pattern, O-deglycosylation simplified the apoE pattern to a single immunoreactive band, suggesting that O-glycosylation could account for the differences in the molecular mass between the 36- and 34-kDa apoE species (Fig. 2D). The small differences in the electrophoretic mobility between glycosylated and deglycosylated apoE monomers are probably related to the slight carbohydrate

mass associated to O-glycosylation, but also to changes in protein shape that affect their electrophoretic migration. Glycosylated proteins are normally more globular than non-glycosylated proteins, because the carbohydrate chains are not linear, even in reducing conditions. The apparent levels of the 100-kDa apoE band were not significantly modified following enzymatic deglycosylation, suggesting that these species are resistant to enzymatic deglycosylation (Fig. 2D). We observed the occurrence of apoE dimers in the recombinant protein (a non-glycosylated species since it is produced in bacteria), suggesting that sugar residues are not relevant epitopes for disulfide-linked dimer formation.

As previously mentioned, the ~100-kDa apoE band was observed almost exclusively in AD CSF samples, including APOE ε4/ε4 samples (Fig. 2A). To further characterize this apoE species, we performed SDS-PAGE studies in non-reducing conditions to preserve the disulfide bonds (absence of β-mercaptoethanol). The 100-kDa apoE band in AD samples appeared to be indistinguishable from the one observed in reducing conditions, and remarkably, this band appeared in the control samples in non-reducing conditions, probably representing apoE dimers linked by disulfide bonds (Fig. 3A). When a specific antibody for apoE4 was used, NBP1-49529, the 100-kDa immunoreactivity was also detected in samples from APOE ε3/ε4 AD subjects under both reducing and non-reducing conditions, while no immunoreactivity was detected in APOE ε3/ε4 control samples under non-reducing conditions (Fig. 3B). This could corroborate that apoE4 in AD samples participates in complexes to form 100-kDa stable species, in both apoE3/4 or apoE4/4 subjects, that do not rely on disulfide bonds, due to its lack of Cys112, thus representing aberrant/anomalous apoE aggregates.

Fig. 3 Characterization of CSF apoE species under reducing, non-reducing, and native conditions. A, B Control (Ct) and AD CSF samples immunoblotted under reducing (R) or non-reducing (NR) SDS-PAGE with A apoE antibody (Ab178479) or B apoE4-specific antibody (NBP1-49529). Note that apoE4 is identified as part of the 100-kDa bands despite the inability to form disulfide-linked dimers. C Representative blot of native-PAGE studies, showing the apoE monomers and dimers. The discrepancy in molecular weight is likely due to the differences between native-PAGE and SDS-PAGE electrophoretic conditions which affect the migration of proteins. Rec, recombinant apoE3; Den CSF, denatured CSF. D Quantification of the ratio of apoE dimers compared to monomers across the different APOE genotypes, estimated by native-PAGE (see C). Scatter plots of apoE levels are represented. The graphs represent mean ± SEM, and the numbers below represent median ± SD. Significant p values are indicated

In *APOE* ε3/ε4 control subjects, however, apoE4 does not participate in the 100-kDa species observed under non-reducing conditions, given its complete reliance on disulfide bonds to form functional dimers.

To determine the different contributions of the apoE 100-kDa species in AD and control cases, we first estimated the apoE dimer/monomer balance by native-PAGE electrophoresis. We included a CSF control sample under fully reducing and denaturing conditions, as well as an apoE3 recombinant protein under native conditions, which served to identify the monomeric and dimeric apoE bands. Two immunoreactive apoE bands were observed, likely representing apoE monomers and dimers (Fig. 3C). An immunoreactive band compatible with dimeric complexes was detected in CSF from AD *APOE* ε4/ε4 cases, whose lack of Cys112 should eliminate their ability to form disulfide-bond-dependent complexes. Given the difficulty of finding age-matched *APOE* ε4/ε4 control subjects (low prevalence of this genotype in the general and healthy population), we cannot compare AD *APOE* ε4/ε4 with control ε4/ε4 cases. We compared the apoE dimer/monomer quotient (ratio D/M) between AD CSF samples and controls, subgrouping the samples by *APOE* genotype (Fig. 3D). In the control group, the dimer/monomer quotient was significantly lower in the *APOE* ε3/ε4 group (ratio D/M = 0.38) compared to that of the ε3/ε3 group (ratio D/M = 2.20; p = 0.006), associated to the inability of the apoE4 isoform to form disulfide-linked dimers. The same situation was found in the AD group, where the dimer/monomer ratio decreased as the ε4 allele was present (ε3/ε3: ratio D/M = 2.27; ε3/ε4: ratio D/M = 1.04; ε4/ε4: ratio D/M = 0.24). For *APOE* ε3/ε3 subjects, the dimer/monomer ratio in controls was not significantly different to that found in AD subjects; however, for *APOE* ε3/ε4 subjects, the quotient was higher in the AD group compared with controls (p = 0.02; Fig. 3D). This may be reflecting the accumulation of aberrant aggregates in the AD samples expressing apoE4, in addition to the physiological disulfide-bound dimers present in controls.

Levels of CSF apoE species in AD

Given the differences in CSF apoE aggregates found under native conditions between AD and controls, we evaluated the levels of the 34-kDa, 36-kDa, and 100-kDa apoE species by SDS-PAGE in reducing conditions and western blotting, using the AB178479 antibody (Fig. 4A). The 34-kDa apoE band was significantly increased in AD compared with controls (p = 0.003; Fig. 4B). When discriminating by *APOE* genotype, only the *APOE* ε3/ε3 genotype was significantly elevated in AD compared with control samples (p = 0.02; Fig. 4C). The same analysis within the *APOE* ε3/ε4 genotype exhibited less statistical power because the size of the control group is small; nonetheless, we observed a trend of 34-kDa apoE increment in ε3/ε4 genotype AD samples with respect to controls (p = 0.09; Fig. 4C). The 36-kDa apoE appeared significantly increased in AD compared with controls overall (p = 0.002; Fig. 4D), but not among *APOE* genotypes (Fig. 4E).

As expected, when we considered the sum of the apoE immunoreactivity for the 34- and 36-kDa bands, increased levels were seen in AD patients (27 ± 5%), as compared with controls (p = 0.005). Despite the fact that these results indicate a net increase of CSF apoE in AD samples, when defining a quotient between the apoE monomeric glycoforms (ratio 36 kDa/34 kDa) we detected an imbalance in the AD samples, which displayed a decreased 36-kDa/34-kDa ratio compared with controls (p = 0.007; Fig. 4F). These differences were maintained when the samples were separated by *APOE* genotype (ε3/ε3 control: ratio 36 kDa/34 kDa = 1.61 vs ε3/ε3 AD: ratio 36 kDa/34 kDa = 1.46, p = 0.01; ε3/ε4 control: ratio 36 kDa/34 kDa = 1.67 vs ε3/ε4 AD: ratio = 1.38, p = 0.001; Fig. 4G). Within the AD group, we also observed significant differences between the genotypes, as the 36-kDa/34-kDa ratio was significantly lower in *APOE* ε3/ε3 (p < 0.0001) and ε3/ε4 (p < 0.0001) samples when compared with ε4/ε4 AD samples (ratio 36 kDa/34 kDa = 1.64). In each group, CSF apoE levels appeared unaltered when subgrouping between males and females (p > 0.05 for all the subgroups). There were no clear correlations between the level of the 34- or 36-kDa apoE or the 36-kDa/34-kDa ratio with the age of the subjects, in either of the groups considered individually.

The immunoreactivity of the 100-kDa apoE species was quite faint in control samples, and accordingly, substantial differences were found between AD samples and controls (p < 0.0001; Fig. 4H, I). In the AD group, the 100-kDa apoE species levels were significantly lower in

Fig. 4 Analysis of CSF apoE species from the Gothenburg cohort. Control (Ct) and AD CSF samples analyzed by SDS-PAGE. Each individual band was quantified and normalized to the reference value (recombinant apoE). **A** Representative immunoblot of CSF samples with apoE antibody and legend for graphs. The 100-kDa section of the blot presents enhanced contrast. **B, C** Statistical analysis of the 34-kDa apoE immunoreactive band in **B** control and AD and by **C** *APOE* genotype. **D, E** Statistical analysis of the 36-kDa apoE immunoreactive band in **D** control and AD and by **E** *APOE* genotype. **F, G** Statistical analysis of the ratio of 36-kDa/34-kDa immunoreactive bands in **F** control and AD and by **G** *APOE* genotype. **H, I** Statistical analysis of the 100-kDa apoE immunoreactive band in **H** control and AD and by **I** *APOE* genotype. The graphs represent mean ± SEM, and the numbers below represent median ± SD. Significant p values are indicated
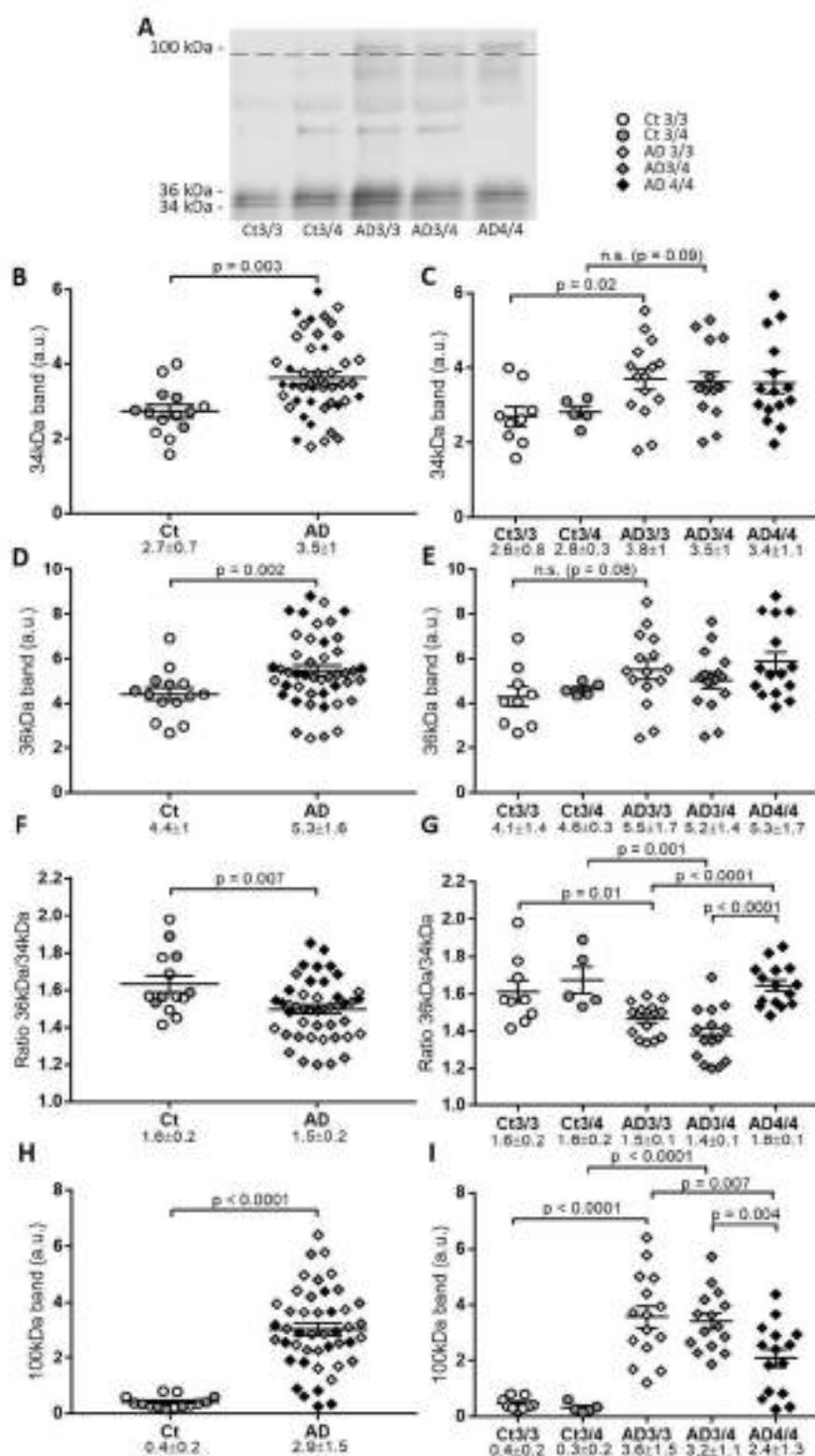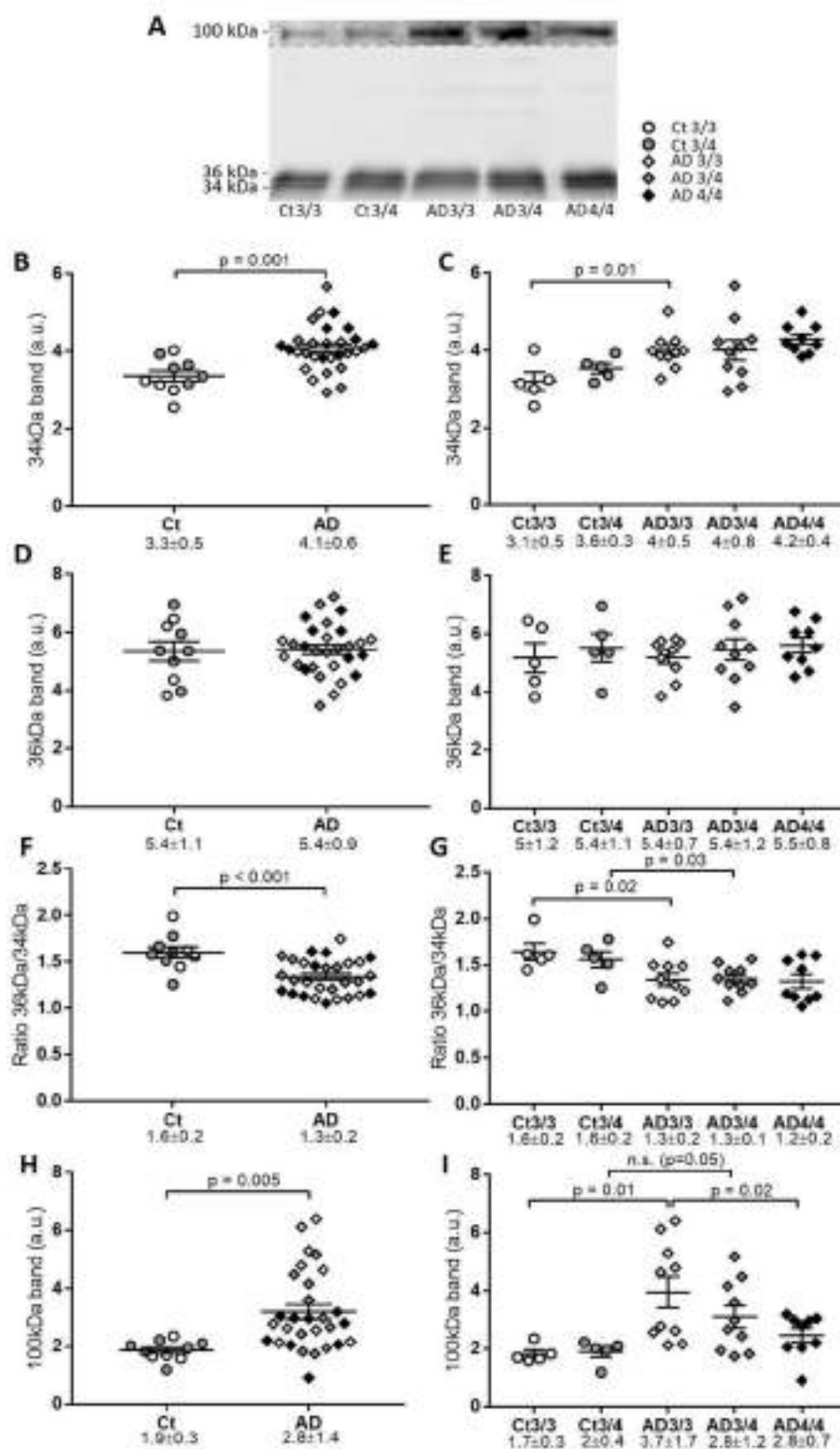
Fig. 4 (See legend on previous page.)

85

Lennol et al. Alzheimer's Research & Therapy   (2022) 14:161

Page 12 of 19

the *APOE* ε4/ε4 group when compared to both ε3/ε3 (p < 0.0001) and ε3/ε4 (p < 0.0001) groups. Interestingly, in the *APOE* ε4/ε4 AD cases, the samples with the lowest 100-kDa apoE immunoreactivity belonged to the youngest subjects ($n = 5$, 68±2 years), as compared to the other cases ($n = 10$, 76±1 years; $p=0.002$). Within the AD *APOE* ε4/ε4 subgroup, we also observed a statistically significant positive correlation between the age of participants and the immunoreactivity of the 100-kDa apoE band ($r = 0.622$, $p = 0.013$). For the rest of the groups, we failed to determine a correlation between the 100-kDa band and age.

Interestingly, the quotient of 36 kDa/34 kDa monomeric glycoforms ($r = 0.40$, $p = 0.007$), as well as the levels of the 34-kDa species ($r = 0.32$, $p = 0.034$), correlated with Aβ42 in AD individuals. Meanwhile, the levels of the 100-kDa apoE complexes correlated with T-tau levels ($r = 0.33$, $p = 0.028$), yet failed to achieve significance with the Aβ42 levels ($r = 0.27$, $p = 0.070$).

Levels of CSF apoE species in AD in a second cohort

We attempted to validate our results in a second independent cohort of CSF samples from Barcelona (see Table 1, Fig. 5A). As in the first cohort, the analyses were performed by SDS-PAGE under reducing conditions. In this cohort, the 34-kDa apoE levels were significantly higher in AD compared with controls ($p=0.001$), and specifically only for those with *APOE* ε3/ε3 genotype ($p = 0.01$) (Fig. 5B, C). In contrast to the first cohort, no differences in the 36-kDa species were detected (Fig. 5D, E). The 36-kDa/34-kDa ratio was again lower in AD compared with control samples ($p < 0.001$, Fig. 5F), and this difference was maintained when the samples were separated by genotype (AD vs controls for *APOE* ε3/ε3, $p=0.02$, and for *APOE* ε3/ε4, $p=0.03$) (Fig. 5G). ApoE levels once again appeared to be unaltered when subgrouping between males and females (p> 0.05 for all comparisons). In this cohort, we also failed to correlate 34- or 36-kDa levels or the 36-kDa/34-kDa ratio with the age of the subjects.

As in the first cohort, the 100-kDa apoE levels were higher in AD than in controls ($p = 0.005$; Fig. 5H). When the samples were stratified by *APOE* genotype (Fig. 5I), the significant differences between AD and controls were maintained in the ε3/ε3 group ($p = 0.01$) and were in the

limit of statistical significance in the *APOE* ε3/ε4 group ($p = 0.050$) despite the small number of controls. Within the AD group, the *APOE* ε4/ε4 samples once again displayed significantly lower 100-kDa apoE levels compared with ε3/ε3 cases ($p = 0.02$). The results from this cohort corroborate that 100-kDa apoE is associated to AD and that apoE4 has a reduced capacity to form these complexes.

In this cohort, and exclusively in the AD group overall, we detected a significant correlation between the age of the subjects and the 100-kDa apoE species ($r =0.645$, $p= 0.0002$), indicating that the appearance of the aberrant apoE aggregates may be related to aging in AD. This association was maintained within the *APOE* ε3/ε3 ($r = 0.813$, $p= 0.004$) and the ε3/ε4 ($r = 0.799$, $p= 0.006$) AD groups.

In this cohort, only the levels of the 100-kDa apoE species correlated with Aβ42 levels ($r= 0.41$, $p= 0.027$). Thus, despite finding some correlations, none of these significant correlations resulted in consistency between the two cohorts.

Discussion

Typically, transgenic models produce pathological changes that partially replicate changes seen in human patients. In this study, firstly, we have found an increase in CSF apoE in the TgF344-AD rats, with the documented occurrence of amyloid pathology around 10 months of age [31, 34]. This result can be interpreted as a suggestive gain of function for apoE in AD. In fact, this increase in CSF apoE content is similar to the one observed in AD patients when considering total apoE content. Considering the summation of the apoE immunoreactivity for 34- and 36-kDa (not including the value for the 100-kDa band) species, in samples from AD patients, a significant overall increase in total CSF apoE was found in the Gothenburg cohort and a non-significant trend to increase was seen in the Barcelona cohort compared to controls. However, the biochemical discrimination of different human CSF apoE species and the altered balance of these species lead us to believe that, despite the increase in total CSF apoE levels determined in the AD transgenic model and AD patients, the imbalance between apoE species should be interpreted as indicative of a potential impairment in apoE function in the brain. Thus, higher

(See figure on next page.)
Fig. 5 Analysis of CSF apoE species from the Barcelona cohort. Control (Ct) and AD CSF samples analyzed by SDS-PAGE. Each individual band was quantified and normalized to the reference value (recombinant apoE). **A** Representative immunoblot of CSF samples with apoE antibody and legend for graphs. The 100-kDa section of the blot presents enhanced contrast. **B, C** Statistical analysis of the 34-kDa apoE immunoreactive band in **B** control and AD and by **C** *APOE* genotype. **D, E** Statistical analysis of the 36-kDa apoE immunoreactive band in **D** control and AD and by **E** *APOE* genotype. **F, G** Statistical analysis of the ratio of 36-kDa/34-kDa immunoreactive bands in **F** control and AD and by **G** *APOE* genotype. **H, I** Statistical analysis of the 100-kDa apoE immunoreactive band in **H** control and AD and by **I** *APOE* genotype. The graphs represent mean ± SEM, and the numbers below represent median ± SD. Significant p values are indicated

Fig. 5 (See legend on previous page.)

87

Lennol et al. Alzheimer's Research & Therapy   (2022) 14:161

Page 14 of 19

levels of apoE could paradoxically result in less functionality if the increase is represented by complexes and immature glycoforms.

Indeed, we have identified two monomeric apoE species in human CSF and demonstrated that the balance between these species in AD patients differs compared to that of controls. Some previous studies that did not distinguish the contribution of particular apoE species have indicated that CSF apoE levels in AD patients are increased [35], also at follow-up [36], but many studies addressing total CSF apoE levels are inconclusive and found no clear association with the AD condition or *APOE* genotype [20–22]. In addition to recurrent confounding factors such as the handling of the samples, and also considering differences in the diagnostic accuracy between cohorts, the inconsistencies found in these previous reports could be associated mostly with the determination method used, as some are based in MS [17, 18], while others use immunoassays [16], both of which fail to discriminate between apoE species. Even if an immunoassay is the most available and desirable approach for quantitative analysis of altered levels of a biomarker, this method does not easily detect subtle changes in specific species (imbalance in glycoforms) and/or does not detect particular species suffering conformational changes (aberrant dimers).

The 34- and 36-kDa species are likely different O-glycoforms, and the difference in electrophoretic mobility of the apoE glycoforms could be a consequence of its sialylation [37]. ApoE is exclusively O-glycosylated and can be capped with one or two sialic acids [5]. In CSF, the existence of two glycans per molecule of apoE has been demonstrated [38], and previous studies indicate that astrocytes secrete two differential glycoforms of apoE [39] and that the sialo and asialo forms of apoE can both be secreted into the medium [40]. Our results indicate that the 34-kDa apoE monomers, which appear to be less sialylated than 36-kDa apoE monomers [3], are present at a higher proportion in AD subjects compared with controls, in both independent cohorts. Whether or not these 34-kDa species can participate in disulfide-linked apoE dimers or pathological complexes, as described here, requires further study.

Moreover, the altered balance between apoE glycoforms should be validated in external cohorts. Here, most of the results obtained in the Gothenburg cohort were validated in a second independent cohort from Barcelona, despite the small size of the groups in this cohort. Nonetheless, some inconsistent results were observed between cohorts regarding the ratio of the 36-kDa/34-kDa species. In the Gothenburg cohort, this ratio was significantly higher in AD individuals with an *APOE* ε4/ε4 genotype compared with *APOE* ε3/

ε3 and ε3/ε4, while in the Barcelona cohort, the ratios were at a similar level among AD individuals with different *APOE* genotypes. Additional studies will serve to determine if the imbalance between apoE glycoforms is a common feature for AD *APOE*-ε4 homozygote subjects.

Indeed, the changes observed in this study are less obvious in ε4/ε4 samples. This discrepancy may be due to the fact that small changes in apoE levels for ε4/ε4 subjects could be more detrimental than in the rest of *APOE* genotypes, perhaps caused by the basal compromise in some of the biological functions of apoE in the brain related with the inability of the apoE4 isoform to form dimers.

APOE-ε4 is the strongest risk factor gene for AD, although inheriting *APOE*-ε4 does not mean a person will definitely develop the disease. Thus, the opportunity to analyze the subset of *APOE* ε3/ε4 control individuals with no AD-like symptoms is very interesting. As stated, all the cases were retrospectively selected from large cohorts and based on the determination of AD core biomarkers. The diagnostic uncertainty is inherent in this type of studies, but the control individuals with *APOE* ε3/ε4 genotype displayed similar apoE values as the ones obtained in *APOE* ε3/ε3 individuals.

Correct apoE glycosylation is fundamental for its function and lipoprotein binding capacity. ApoE glycosylation can modulate receptor affinity, lipid-binding ability, lipid transportation, and metabolic functions [41–43]. Furthermore, apoE deglycosylation reduces its binding to Aβ42 [44] and may induce Aβ42 accumulation [45]. Our results suggest that the imbalance between the different glycoforms of apoE monomers observed in AD may interfere with its biological function, contributing to the progression of the disease. Interestingly, apoE glycosylation also plays a key role in the protection against self-association and spontaneous aggregation [46].

As mentioned, the apoE isoforms encoded by *APOE* ε3 or ε2 are able to form disulfide-linked hetero- and homodimers through the Cys residue at position 112, while *APOE* ε4 (which presents Arg at position 112) and apoE from non-human mammals are unable to form these oligomeric species. However, in our studies, apoE4 isoforms were present in 100-kDa aggregates in *APOE* ε3/ε4 AD cases, and these aggregates were identified in most of the *APOE* ε4/ε4 AD patients. These 100-kDa complexes are compatible in molecular mass to disulfide-linked apoE dimers, which exist as a major portion of apoE in human CSF of *APOE* ε3 or ε2 carriers [16]. The existence of SDS-resistant dimers of apoE4 was suggested when studying the in vitro formation of SDS-resistant Aβ-apoE complexes [47]; but, to our knowledge, it has never been demonstrated in vitro or in vivo. The

88

definitive identity of the 100-kDa species was confirmed by the diverse immunoprecipitation analyses combining antibodies originated from diverse animal species and the MS studies. Rats express a unique apoE variant most closely related to the human ε4-type haplotype. However, in the transgenic rat model of AD, we were not able to observe the 100-kDa resistant apoE species that we observed in AD *APOE* ε4/4 cases. Likewise, the possibility that inactive monomers of apoE occur in this animal model requires further study; however, models in which the amyloid condition results in an increase of apoE expression should consider this possibility.

ApoE dimers or multimers may be the biologically important species, particularly in receptor binding [15]. In a previous study, the levels of apoE dimers in the CSF from AD subjects were not different from those in controls [48], although in this study they did not assess the nature of the aberrant β-mercaptoethanol resistant complexes. In our AD samples, the 100-kDa apoE complexes are aberrantly resistant to reducing conditions; thus, they may represent a different species compared to the biologically active disulfide-bound dimers. The relevance of an apoE dimer/monomer profile in AD was also addressed previously in plasma, with the identification of dimers only in *APOE*-e3 carrier subjects, the levels of which decreased in the demented group [49]. A recent report using two-dimensional gel electrophoresis indicated that plasma apoE is elevated in AD with respect to controls [50]. However, it is worth noting that apoE does not cross the blood-CSF barrier [51].

ApoE can form heteromeric complexes with other apolipoproteins [17] and with proteins such as the ciliary neurotrophic factor [52] or APP [53], among others, but principally with Aβ. Indeed, apoE can form in vitro SDS-stable complexes with Aβ [1, 54, 55], but the interaction with exogenous Aβ does not induce drastic changes to the overall size of the Aβ/apoE-containing lipoprotein particles [55]. The formation of noncovalent apoE/Aβ complexes (1:1) is implicated in both Aβ clearance and fibrillization, and the three isoforms of apoE are able to form these complexes [56]. Complexes of apoE and Aβ have been demonstrated in non-pathological human CSF [55] and in AD brain [57, 58]. Thus, Aβ may act as a triggering driver for the crosslinking and stabilization of aberrant apoE complexes. In the AD brain, the balance between soluble to insoluble apoE/Aβ aggregates has been associated with impaired apoE activity in Aβ clearance, as apoE is responsible for the accumulation and fibrillization of Aβ [59]. The effects of apoE on Aβ aggregation may be restricted to HDL-like particle-bound apoE [60]. Other studies have demonstrated that apoE influences Aβ clearance despite minimal interaction [61].

However, despite the fact that Aβ can contribute to the formation of stable apoE dimers as a crosslinking agent, the behavior of the resulting species may differ from other apoE/Aβ aggregates. We favor the hypothesis that the stable apoE complexes may have compromised biological activity, regardless of the presence of Aβ.

It is also interesting to note that apoE binds Aβ in an isoform-specific manner. Thus, monomeric apoE4 binds to Aβ peptide more rapidly than monomeric apoE3 or apoE2, and so it appears that the efficiency of binding correlates inversely with the risk of developing AD pathology [62]. Moreover, soluble SDS-stable complexes of apoE4/Aβ precipitate more rapidly than apoE3/Aβ complexes [63]. Whether these monomeric apoE/Aβ complexes trigger the formation of oligomeric complexes, and the potential compromise of the apoE peptides involved in these complexes on Aβ clearance in vivo, require analysis.

The aberrant apoE complexes may also influence the role of apoE on lipid metabolism and transport. It is assumed that unlipidated apoE monomers are the species that form disulfide-linked dimers; however, it is also believed that apoE must be properly lipidated to participate in cholesterol and lipid transport. Aberrant dimers are not linked by disulfide bonds, but we can only speculate whether these species are lipidated or not, and if the occurrence of these aberrant dimers could compromise the role of apoE regulating lipid homeostasis by mediating lipid metabolism and transport. ApoE4 is poorly lipidated compared with apoE2 and apoE3 [64], and reduced binding affinity of apoE4 for HDL results in a greater proportion of unlipidated apoE, hence forming aggregates that can be more toxic for neurons than apoE2 and apoE3 aggregates [65]. Since lipidation of apoE impedes aggregate formation [66], we presume that these aberrant dimers are not lipidated; nonetheless, this possibility should be tested.

Finally, we found a correlation between the 100-kDa apoE levels and age in AD samples, which suggests that during pathological aging, apoE could be more likely to form non-disulfide-bound aggregates in the CSF. In the TgF344 rats, only the older animals showed statistically significant high apoE levels; accordingly, these AD models show an age-dependent increase of the levels of Aβ40 and Aβ42 from 6 months of age [31].

The imbalance of apoE glycoforms and the existence of aberrant apoE aggregates in the CSF from AD individuals could be considered as a read-out of alterations of the biological activity of apoE in the brain of AD individuals. The possibility that CSF levels of apoE are under strong genetic influence by the *APOE* polymorphism is plausible; however, the relevance of these changes in CSF

apoE levels on AD pathology remains elusive. The net increase of apoE levels in the CSF from AD individuals could be favored by aging. This increment, mainly due to the 34-kDa glycoform of apoE, which is likely hyposialylated, and the appearance of a β-mercaptoethanol-resistant 100-kDa apoE species, could indicate that the ability of apoE in AD to achieve its biological functions may be compromised.

In conclusion, while apoE levels tend to increase in AD CSF, this increase is more noticeable in certain glycoforms of monomers and aberrant complexes that may hinder its biological activity. A specific description of how these species affect apoE signaling and Aβ clearance should improve our understanding of the role of apoE in the AD pathology.

Conclusions

The imbalance of apoE glycoforms and the existence of aberrant apoE aggregates in the CSF from AD individuals could be considered as a read-out of alterations of the biological activity of apoE in the brain of AD individuals. The possibility that CSF levels of apoE are under strong genetic influence by the *APOE* polymorphism is plausible; however, the relevance of these changes in CSF apoE levels on AD pathology remains elusive. The net increase of apoE levels in the CSF from AD individuals could be favored by aging. This increment, mainly due to the 34-kDa glycoform of apoE, which is likely hyposialylated, and the appearance of a β-mercaptoethanol-resistant 100-kDa apoE species, could indicate that the ability of apoE in AD to achieve its biological functions may be compromised.

In conclusion, while apoE levels tend to increase in AD CSF, this increase is more noticeable in certain glycoforms of monomers and aberrant complexes that may hinder its biological activity. A specific description of how these species affect apoE signaling and Aβ clearance should improve our understanding of the role of apoE in the AD pathology.

Abbreviations

Aβ: Amyloid-beta; AD: Alzheimer's disease; APP: Amyloid precursor protein; ApoE: Apolipoprotein E; CSF: Cerebrospinal fluid; CNS: Central nervous system; HDL: High-density lipoprotein; MS: Mass spectrometry; SDS: Sodium dodecyl sulfate; PAGE: Polyacrylamide gel electrophoresis; Tg: Transgenic; Wt: Wild-type.

Supplementary Information

The online version contains supplementary material available at https://doi.org/10.1186/s13195-022-01108-2.

Additional file 1. Images of complete blots from which figures were obtained, and also the boxes selected with the ImageQuant Studio software for quantification.

Declarations

Ethics approval and consent to participate

This study was approved by the ethics committee at the Miguel Hernandez University (ref# UMH.IN.IS.01.18), and it was carried out in accordance with the Helsinki Declaration regarding research on humans. The present assays were performed on de-identified left-over aliquots from clinical diagnostic CSF samples; thus, no consent for participation was required. The samples were obtained following procedures approved by the Ethics Committees at the University of Gothenburg and the Hospital Sant Pau, respectively. Animal work

was performed in accordance with the local legislation, with the approval of the Experimental Animal Ethical Committee of the University of Barcelona, and in compliance with European legislation.

Consent for publication
Not applicable.

Competing interests
HZ has served at scientific advisory boards and/or as a consultant for Abbvie, Alector, Annexon, Artery Therapeutics, AZTherapies, CogRx, Denali, Eisai, Nervgen, Novo Nordisk, Pinteon Therapeutics, Red Abbey Labs, Passage Bio, Roche, Samumed, Siemens Healthineers, Triplet Therapeutics, and Wave; has given lectures in symposia sponsored by Cellectricon, Fujirebio, Alzecure, Biogen, and Roche; and is a co-founder of Brain Biomarker Solutions in Gothenburg AB (BBS), which is a part of the GU Ventures Incubator Program (outside submitted work). KB has served as a consultant, at advisory boards, or at data monitoring committees for Abcam, Axon, Biogen, JOMDD/Shimadzu, Julius Clinical, Lilly, MagQu, Novartis, Prothena, Roche Diagnostics, and Siemens Healthineers and is a co-founder of Brain Biomarker Solutions in Gothenburg AB (BBS), which is a part of the GU Ventures Incubator Program, all unrelated to the work presented in this paper. JF has served as a consultant for Novartis and Lundbeck; has received honoraria for lectures from Roche, NovoNordisk, Nestle, Esteve, and Biogen; and served at advisory boards for AC Immune, Zambon, and Lundbeck. DA participated in advisory boards from Fujirebio-Europe and Roche Diagnostics and received speaker honoraria from Fujirebio-Europe, Roche Diagnostics, Nutricia, Krka Farmacéutica S.L., Zambon S.A.U., and Esteve Pharmaceuticals S.A. AL has served at scientific advisory boards from Fujirebio-Europe, Nutricia, Roche-Genentech, Biogen, Grifols, and Roche Diagnostics and has filed a patent application of synaptic markers in neurodegenerative diseases.

Author details
[1]Instituto de Neurociencias de Alicante, Universidad Miguel Hernández-CSIC, Av. Ramón y Cajal s/n, E-03550 Sant Joan d'Alacant, Spain. [2]Centro de Investigación Biomédica en Red sobre Enfermedades Neurodegenerativas (CIBERNED), Sant Joan d'Alacant, Spain. [3]Department of Cell Biology, Physiology and Immunology, Faculty of Biology, University of Barcelona, Barcelona, Spain. [4]Institute of Neurosciences, University of Barcelona, Barcelona, Spain. [5]Instituto de Investigación Sanitaria y Biomédica de Alicante (ISABIAL), Alicante, Spain. [6]Institute of Neuroscience and Physiology, Department of Psychiatry and Neurochemistry, the Sahlgrenska Academy at the University of Gothenburg, Mölndal, Sweden. [7]Sant Pau Memory Unit, Neurology Department, Hospital de la Santa Creu i Sant Pau, Biomedical Research Institute Sant Pau, Universitat Autònoma de Barcelona, Barcelona, Spain. [8]Barcelona Down Medical Center, Fundació Catalana Síndrome de Down, Barcelona, Spain. [9]Laboratory of Surgical Neuroanatomy, School of Medicine and Health Sciences, University of Barcelona, Barcelona, Spain. [10]Clinical Neurochemistry Laboratory, Sahlgrenska University Hospital, Mölndal, Sweden. [11]Department of Neurodegenerative Disease, Institute of Neurology, University College London, London, UK. [12]UK Dementia Research Institute at UCL, London, UK. [13]Hong Kong Center for Neurodegenerative Diseases, Hong Kong, China.

References
1. Strittmatter WJ, Weisgraber KH, Huang DY, Dong LM, Salvesen GS, Pericak-Vance M, et al. Binding of human apolipoprotein E to synthetic amyloid beta peptide: isoform-specific effects and implications for late-onset Alzheimer disease. Proc Natl Acad Sci U S A. 1993;90:8098–102 Available from: https://pubmed.ncbi.nlm.nih.gov/8367470/. [Cited 2022 Feb 22].

2. Husain MA, Laurent B, Plourde M. APOE and Alzheimer's disease: from lipid transport to physiopathology and therapeutics. Front Neurosci. 2021;15 Available from: https://pubmed.ncbi.nlm.nih.gov/33679311/. [Cited 2022 Feb 22].

3. Moon HJ, Haroutunian V, Zhao L. Human apolipoprotein E isoforms are differentially sialylated and the sialic acid moiety in ApoE2 attenuates ApoE2-Aβ interaction and Aβ fibrillation. Neurobiol Dis. 2022;164

4. Rall SC, Weisgraber KH, Innerarity TL, Mahley RW. Structural basis for receptor binding heterogeneity of apolipoprotein E from type III hyperlipoproteinemic subjects. Proc Natl Acad Sci U S A. 1982;79:4696–700 Available from: https://pubmed.ncbi.nlm.nih.gov/6289314/. [Cited 2022 Feb 22].

5. Koch M, Traini M, Kritharides L. Cell-specific production, secretion, and function of apolipoprotein E. J Mol Med (Berl). 2018;96:361–71 Available from: https://pubmed.ncbi.nlm.nih.gov/29516132/. [Cited 2022 Feb 22].

6. McIntosh AM, Bennett C, Dickson D, Anestis SF, Watts DP, Webster TH, et al. The apolipoprotein E (APOE) gene appears functionally monomorphic in chimpanzees (Pan troglodytes). PLoS One. 2012;7 Available from: https://pubmed.ncbi.nlm.nih.gov/23112842/. [Cited 2022 Feb 22].

7. Heffernan AL, Chidgey C, Peng P, Masters CL, Roberts BR. The neurobiology and age-related prevalence of the ε4 allele of apolipoprotein E in Alzheimer's disease cohorts. J Mol Neurosci. 2016;60:316–24 Available from: https://pubmed.ncbi.nlm.nih.gov/27469620/. [Cited 2022 Feb 22].

8. Roses AD. Apolipoprotein E alleles as risk factors in Alzheimer's disease. Annu Rev Med. 1996;47:387–400 Available from: https://pubmed.ncbi.nlm.nih.gov/8712790/. [Cited 2022 Feb 22].

9. Uddin MS, Kabir MT, Al Mamun A, Abdel-Daim MM, Barreto GE, Ashraf GM. APOE and Alzheimer's disease: evidence mounts that targeting APOE4 may combat Alzheimer's pathogenesis. Mol Neurobiol. 2019;56:2450–65.

10. Corder EH, Saunders AM, Risch NJ, Strittmatter WJ, Schmechel DE, Gaskell PC, et al. Protective effect of apolipoprotein E type 2 allele for late onset Alzheimer disease. Nat Genet. 1994;7:180–4.

11. Li Z, Shue F, Zhao N, Shinohara M, Bu G. APOE2: protective mechanism and therapeutic implications for Alzheimer's disease. Mol Neurodegener. 2020;15:63.

12. Reiman EM, Arboleda-Velasquez JF, Quiroz YT, Huentelman MJ, Beach TG, Caselli RJ, et al. Exceptionally low likelihood of Alzheimer's dementia in APOE2 homozygotes from a 5,000-person neuropathological study. Nat Commun. 2020;11:667.

13. Saddiki H, Fayosse A, Cognat E, Sabia S, Engelborghs S, Wallon D, et al. Age and the association between apolipoprotein E genotype and Alzheimer disease: a cerebrospinal fluid biomarker-based case-control study. PLoS Med. 2020;17 Available from: https://pubmed.ncbi.nlm.nih.gov/32817639/. [Cited 2022 Feb 22].

14. Martens YA, Zhao N, Liu C-C, Kanekiyo T, Yang AJ, Goate AM, et al. ApoE Cascade Hypothesis in the pathogenesis of Alzheimer's disease and related dementias. Neuron. 2022;110(8):1304–17.

15. Dyer CA, Smith RS, Curtiss LK. Only multimers of a synthetic peptide of human apolipoprotein E are biologically active. J Biol Chem. 1991;266:15009–15.

16. Weisgraber KH, Shinto LH. Identification of the disulfide-linked homodimer of apolipoprotein E3 in plasma. Impact on receptor binding activity. J Biol Chem. 1991;266:12029–34.

17. Rebeck GW, Alonzo NC, Berezovska O, Harr SD, Knowles RB, Growdon JH, et al. Structure and functions of human cerebrospinal fluid lipoproteins from individuals of different APOE genotypes. Exp Neurol. 1998;149:175–82 Available from: https://pubmed.ncbi.nlm.nih.gov/9454626/. [Cited 2022 Feb 22].

18. Minagawa H, Gong JS, Jung CG, Watanabe A, Lund-Katz S, Phillips MC, et al. Mechanism underlying apolipoprotein E (ApoE) isoform-dependent lipid efflux from neural cells in culture. J Neurosci Res. 2009;87:2498–508 Available from: https://pubmed.ncbi.nlm.nih.gov/19326444/. [Cited 2022 Feb 22].

19. Elliott DA, Halliday GM, Garner B. Apolipoprotein-E forms dimers in human frontal cortex and hippocampus. BMC Neurosci. 2010;11 Available from: https://pubmed.ncbi.nlm.nih.gov/20170526/. [Cited 2022 Feb 22].

20. Cruchaga C, Kauwe JSK, Nowotny P, Bales K, Pickering EH, Mayo K, et al. Cerebrospinal fluid APOE levels: an endophenotype for genetic studies for Alzheimer's disease. Hum Mol Genet. 2012;21:4558–71 Available from: https://pubmed.ncbi.nlm.nih.gov/22821396/. [Cited 2022 Feb 22].

21. Martínez-Morillo E, Hansson O, Atagi Y, Bu G, Minthon L, Diamandis EP, et al. Total apolipoprotein E levels and specific isoform composition in cerebrospinal fluid and plasma from Alzheimer's disease patients and

Available from: https://pubmed.ncbi.nlm.nih.gov/35041991/. [Cited 2022 Feb 22].

91

controls. Acta Neuropathol. 2014;127:633–45 Available from: https://pubmed.ncbi.nlm.nih.gov/24633805/. [Cited 2022 Feb 22].

22. Minta K, Brinkmalm G, Janelidze S, Sjödin S, Portelius E, Stomrud E, et al. Quantification of total apolipoprotein E and its isoforms in cerebrospinal fluid from patients with neurodegenerative diseases. Alzheimers Res Ther. 2020;12 Available from: https://pubmed.ncbi.nlm.nih.gov/32054532/. [Cited 2022 Feb 22].

23. van Harten AC, Jongbloed W, Teunissen CE, Scheltens P, Veerhuis R, van der Flier WM. CSF ApoE predicts clinical progression in nondemented APOEε4 carriers. Neurobiol Aging. 2017;57:186–94 Available from: https://pubmed.ncbi.nlm.nih.gov/28571653/. [Cited 2022 Feb 22].

24. del Campo M, Mollenhauer B, Bertolotto A, Engelborghs S, Hampel H, Simonsen AH, et al. Recommendations to standardize preanalytical confounding factors in Alzheimer's and Parkinson's disease cerebrospinal fluid biomarkers: an update. Biomark Med. 2012;6:419–30.

25. Andreasen N, Blennow K, Sjödin C, Winblad B, Svärdsudd K. Prevalence and incidence of clinically diagnosed memory impairments in a geographically defined general population in Sweden. The Piteå Dementia Project. Neuroepidemiology. 1999;18:144–55.

26. Andreasen N, Minthon L, Davidsson P, Vanmechelen E, Vanderstichele H, Winblad B, et al. Evaluation of CSF-tau and CSF-Abeta42 as diagnostic markers for Alzheimer disease in clinical practice. Arch Neurol. 2001;58:373–9.

27. Blennow K, Ricksten A, Prince JA, Brookes AJ, Emahazion T, Wasslavik C, et al. No association between the alpha2-macroglobulin (A2M) deletion and Alzheimer's disease, and no change in A2M mRNA, protein, or protein expression. J Neural Transm (Vienna). 2000;107:1065–79.

28. Hansson O, Zetterberg H, Buchhave P, Londos E, Blennow K, Minthon L. Association between CSF biomarkers and incipient Alzheimer's disease in patients with mild cognitive impairment: a follow-up study. Lancet Neurol. 2006;5(3):228–34. S1474442206/03556. http://doi.org/10.1016/S1474-4422(06)70355-6.

29. Alcolea D, Clarimón J, Carmona-Iragui M, Illán-Gala I, Morenas-Rodríguez E, Barroeta I, et al. The Sant Pau Initiative on Neurodegeneration (SPIN) cohort: a data set for biomarker discovery and validation in neurodegenerative disorders. Alzheimers Dement (N Y). 2019;5:597–609.

30. Jack CR, Bennett DA, Blennow K, Carrillo MC, Dunn B, Haeberlein SB, et al. NIA-AA Research Framework: toward a biological definition of Alzheimer's disease. Alzheimers Dement. 2018;14:535–62.

31. Cohen RM, Rezai-Zadeh K, Weitz TM, Rentsendorj A, Gate D, Spivak I, et al. A transgenic Alzheimer rat with plaques, tau pathology, behavioral impairment, oligomeric aβ, and frank neuronal loss. J Neurosci. 2013;33:6245–56 Available from: https://pubmed.ncbi.nlm.nih.gov/23575824/. [Cited 2022 Feb 22].

32. Sáez-Valero J, Pérez De Gracia JA, Lockridge O. Intraperitoneal administration of 340 kDa human plasma butyrylcholinesterase increases the level of the enzyme in the cerebrospinal fluid of rats. Neurosci Lett. 2005;383:93–8 Available from: https://pubmed.ncbi.nlm.nih.gov/15936518/. [Cited 2022 Feb 22].

33. Camporesi E, Lashley T, Gobom J, Lantero-Rodriguez J, Hansson O, Zetterberg H, et al. Neuroligin-1 in brain and CSF of neurodegenerative disorders: investigation for synaptic biomarkers. Acta Neuropathol Commun. 2021;9:19.

34. Chaney AM, Lopez-Picon FR, Serrière S, Wang R, Bochicchio D, Webb SD, et al. Prodromal neuroinflammatory, cholinergic and metabolite dysfunction detected by PET and MRS in the TgF344-AD transgenic rat model of AD: a collaborative multi-modal study. Theranostics. 2021;11:6644–67.

35. Heywood WE, Galimberti D, Bliss E, Sirka E, Paterson RW, Magdalinou NK, et al. Identification of novel CSF biomarkers for neurodegeneration and their validation by a high-throughput multiplexed targeted proteomic assay. Mol Neurodegener. 2015;10 Available from: https://pubmed.ncbi.nlm.nih.gov/26627638/. [Cited 2022 Feb 22].

36. Lindh M, Blomberg M, Jensen M, Basun H, Lannfelt L, Engvall B, et al. Cerebrospinal fluid apolipoprotein E (apoE) levels in Alzheimer's disease patients are increased at follow up and show a correlation with levels of tau protein. Neurosci Lett. 1997;229:85–8 Available from: https://pubmed.ncbi.nlm.nih.gov/9223597/. [Cited 2022 Feb 22].

37. Halim A, Rüetschi U, Larson G, Nilsson J. LC-MS/MS characterization of O-glycosylation sites and glycan structures of human cerebrospinal fluid glycoproteins. J Proteome Res. J Proteome Res. 2013;12:573–84 Available from: https://pubmed.ncbi.nlm.nih.gov/23234360/. [Cited 2022 Feb 22].

38. Hu Y, Meuret C, Go S, Yassine HN, Nedelkov D. Simple and fast assay for apolipoprotein E phenotyping and glycotyping: discovering isoform-specific glycosylation in plasma and cerebrospinal fluid. J Alzheimers Dis. 2020;76:883–93 Available from: https://pubmed.ncbi.nlm.nih.gov/32568201/. [Cited 2022 Feb 22].

39. Lanfranco MF, Sepulveda J, Kopetsky G, Rebeck GW. Expression and secretion of apoE isoforms in astrocytes and microglia during inflammation. Glia. 2021;69:1478–93 Available from: https://pubmed.ncbi.nlm.nih.gov/33556209/. [Cited 2022 Feb 22].

40. Wernette-Hammond ME, Lauer SJ, Corsini A, Walker D, Taylor JM, Rall SC. Glycosylation of human apolipoprotein E. The carbohydrate attachment site is threonine 194. J Biol Chem. 1989;264:9094–101.

41. Flowers SA, Grant OC, Woods RJ, Rebeck GW. O-glycosylation on cerebrospinal fluid and plasma apolipoprotein E differs in the lipid-binding domain. Glycobiology. 2020;30:74–85 Available from: https://pubmed.ncbi.nlm.nih.gov/31616924/. [Cited 2022 Feb 22].

42. Ke LY, Chan HC, Chen CC, Chang CF, Lu PL, Chu CS, et al. Increased APOE glycosylation plays a key role in the atherogenicity of L5 low-density lipoprotein. FASEB J. 2020;34:9802–13 Available from: https://pubmed.ncbi.nlm.nih.gov/32501643/. [Cited 2022 Feb 22].

43. Kacperczyk M, Kmiecik A, Kratz EM. The role of ApoE expression and variability of its glycosylation in human reproductive health in the light of current information. Int J Mol Sci. 2021;22 Available from: https://pubmed.ncbi.nlm.nih.gov/34281251/. [Cited 2022 Feb 22].

44. Sugano M, Yamauchi K, Kawasaki K, Tozuka M, Fujita K, Okumura N, et al. Sialic acid moiety of apolipoprotein E3 at Thr(194) affects its interaction with beta-amyloid(1-42) peptides. Clin Chim Acta. 2008;388:123–9 Available from: https://pubmed.ncbi.nlm.nih.gov/18023277/. [Cited 2022 Feb 22].

45. Chua CC, Lim ML, Wong BS. Altered apolipoprotein E glycosylation is associated with Abeta(42) accumulation in an animal model of Niemann-Pick Type C disease. J Neurochem. 2010;112:1619–26 Available from: https://pubmed.ncbi.nlm.nih.gov/20070866/. [Cited 2022 Feb 22].

46. Lee Y, Kockx M, Raftery MJ, Jessup W, Griffith R, Kritharides L. Glycosylation and sialylation of macrophage-derived human apolipoprotein E analyzed by SDS-PAGE and mass spectrometry: evidence for a novel site of glycosylation on Ser290. Mol Cell Proteomics. 2010;9:1968–81 Available from: https://pubmed.ncbi.nlm.nih.gov/20511397/. [Cited 2022 Feb 22].

47. Martel CL, Mackic JB, Matsubara E, Governale S, Miguel C, Miao W, et al. Isoform-specific effects of apolipoproteins E2, E3, and E4 on cerebral capillary sequestration and blood-brain barrier transport of circulating Alzheimer's amyloid beta. J Neurochem. 1997;69:1995–2004 Available from: https://pubmed.ncbi.nlm.nih.gov/9349544/. [Cited 2022 Feb 22].

48. Montine KS, Bassett CN, Ou JJ, Markesbery WR, Swift LL, Montine TJ. Apolipoprotein E allelic influence on human cerebrospinal fluid apolipoproteins. J Lipid Res. 1998;39:2443–51.

49. Patra K, Giannisis A, Edlund AK, Sando SB, Lauridsen C, Berge G, et al. Plasma apolipoprotein E monomer and dimer profile and relevance to Alzheimer's disease. J Alzheimers Dis. 2019;71:1217–31 Available from: https://pubmed.ncbi.nlm.nih.gov/31524156/. [Cited 2022 Feb 22].

50. Laffoon SB, Doecke JD, Roberts AM, Vance JA, Reeves BD, Pertile KK, et al. Analysis of plasma proteins using 2D gels and novel fluorescent probes: in search of blood based biomarkers for Alzheimer's disease. Proteome Sci. 2022;20:2 Available from: https://pubmed.ncbi.nlm.nih.gov/35081972/. [Cited 2022 Feb 22].

51. Liu M, Kuhel DG, Shen L, Hui DY, Woods SC. Apolipoprotein E does not cross the blood-cerebrospinal fluid barrier, as revealed by an improved technique for sampling CSF from mice. Am J Phys Regul Integr Comp Phys. 2012;303 Available from: https://pubmed.ncbi.nlm.nih.gov/22933021/. [Cited 2022 Feb 22].

52. Gutman CR, Strittmatter WJ, Weisgraber KH, Matthew WD. Apolipoprotein E binds to and potentiates the biological activity of ciliary neurotrophic factor. J Neurosci. 1997;17:6114–21 Available from: https://pubmed.ncbi.nlm.nih.gov/9236223/. [Cited 2022 Feb 22].

53. Haas C, Cazorla P, de Miguel C, Valdivieso F, Vázquez J. Apolipoprotein E forms stable complexes with recombinant Alzheimer's disease beta-amyloid precursor protein. Biochem J. 1997;325(Pt 1):169–75 Available from: https://pubmed.ncbi.nlm.nih.gov/9224643/. [Cited 2022 Feb 22].

54. Wisniewski T, Golabek A, Matsubara E, Ghiso J, Frangione B. Apolipoprotein E: binding to soluble Alzheimer's beta-amyloid. Biochem Biophys Res

Lennol et al. Alzheimer's Research & Therapy   (2022) 14:161

Page 19 of 19

Commun. 1993;192:359–63 Available from: https://pubmed.ncbi.nlm.nih.gov/8484748/. [Cited 2022 Feb 22].

55. Ladu MJ, Munson GW, Jungbauer L, Getz GS, Reardon CA, Tai LM, et al. Preferential interactions between ApoE-containing lipoproteins and Aβ revealed by a detection method that combines size exclusion chromatography with non-reducing gel-shift. Biochim Biophys Acta. 2012;1821:295–302 Available from: https://pubmed.ncbi.nlm.nih.gov/22138302/. [Cited 2022 Feb 22].

56. Deroo S, Stengel F, Mohammadi A, Henry N, Hubin E, Krammer EM, et al. Chemical cross-linking/mass spectrometry maps the amyloid β peptide binding region on both apolipoprotein E domains. ACS Chem Biol. 2015;10:1010–6 Available from: https://pubmed.ncbi.nlm.nih.gov/25546376/. [Cited 2022 Feb 22].

57. Näslund J, Thyberg J, Tjernberg LO, Wernstedt C, Karlström AR, Bogdanovic N, et al. Characterization of stable complexes involving apolipoprotein E and the amyloid beta peptide in Alzheimer's disease brain. Neuron. 1995;15:219–28 Available from: https://pubmed.ncbi.nlm.nih.gov/7619525/. [Cited 2022 Feb 22].

58. Permanne B, Perez C, Soto C, Frangione B, Wisniewski T. Detection of apolipoprotein E/dimeric soluble amyloid beta complexes in Alzheimer's disease brain supernatants. Biochem Biophys Res Commun. 1997;240:715–20 Available from: https://pubmed.ncbi.nlm.nih.gov/9398632/. [Cited 2022 Feb 22].

59. Russo C, Angelini G, Dapino D, Piccini A, Piombo G, Schettini G, et al. Opposite roles of apolipoprotein E in normal brains and in Alzheimer's disease. Proc Natl Acad Sci U S A. 1998;95:15598–602 Available from: https://pubmed.ncbi.nlm.nih.gov/9861015/. [Cited 2022 Feb 22].

60. Padayachee ER, Zetterberg H, Portelius E, Borén J, Molinuevo JL, Andreasen N, et al. Cerebrospinal fluid-induced retardation of amyloid β aggregation correlates with Alzheimer's disease and the APOE ε4 allele. Brain Res. 2016;1651:11–6 Available from: https://pubmed.ncbi.nlm.nih.gov/27663981/. [Cited 2022 Feb 22].

61. Verghese PB, Castellano JM, Garai K, Wang Y, Jiang H, Shah A, et al. ApoE influences amyloid-β (Aβ) clearance despite minimal apoE/Aβ association in physiological conditions. Proc Natl Acad Sci U S A. 2013;110 Available from: https://pubmed.ncbi.nlm.nih.gov/23620513/. [Cited 2022 Feb 22].

62. Aleshkov S, Abraham CR, Zannis VI. Interaction of nascent ApoE2, ApoE3, and ApoE4 isoforms expressed in mammalian cells with amyloid peptide beta (1-40). Relevance to Alzheimer's disease. Biochemistry. 1997;36:10571–80.

63. Sanan DA, Weisgraber KH, Russell SJ, Mahley RW, Huang D, Saunders A, et al. Apolipoprotein E associates with beta amyloid peptide of Alzheimer's disease to form novel monofibrils. Isoform apoE4 associates more efficiently than apoE3. J Clin Invest. 1994;94:860–9.

64. Kanekiyo T, Xu H, Bu G. ApoE and Aβ in Alzheimer's disease: accidental encounters or partners? Neuron. 2014;81:740–54.

65. Hatters DM, Peters-Libeu CA, Weisgraber KH. Apolipoprotein E structure: insights into function. Trends Biochem Sci. 2006;31:445–54.

66. Hubin E, Verghese PB, van Nuland N, Broersen K. Apolipoprotein E associated with reconstituted high-density lipoprotein-like particles is protected from aggregation. FEBS Lett. 2019;593:1144–53.

Publisher's Note

ANNEX: APOE IN THE AD BRAIN

After observing significant modifications of the apoE protein in AD CSF samples, we decided to study apoE in brain samples obtained from AD subjects. In AD, apoE plays important roles in the deposition of Aβ (Morris et al., 2010), and histopathological studies have detected apoE in amyloid plaques (Namba et al., 1991) and NFTs (Rohn et al., 2012). Therefore, an aberrant behaviour of the protein is likely present in the brain, and it is plausible that a relevant percentage of apoE is trapped in these proteinaceous deposits.

Before analysing apoE in brain samples, we decided to confirm that the 34 kDa species was indeed an intermediate species in the synthesis of the protein that is released as 36 kDa apoE when adequately glycosylated. As such, we transfected HEK-293 cells with apoE3 and apoE4. 2×10^6 cells/dish were grown in six-well plates in Dulbecco's modified Eagle's medium (DMEM) supplemented with 10% FBS, 100 μg/mL penicillin/streptomycin and 250 μg/mL G418. After 24 hours, the medium was changed to Eagle's Minimum Essential Media (Opti-MEM) and cells were transfected with Lipofectamine 3000 following manufacturer's instructions with constructs encoding apoE3 or apoE4 for 48 hours (Addgene, plasmids #87086 and #87087, respectively). Cell media were then obtained and kept at -80ºC until analysis. Cell extracts were obtained by scraping the plates in presence of solubilization buffer containing Tris-HCl (50 mM, pH 7.4), NaCl (150mM), EDTA (5 mM), Triton X-100 (0.5%w/v), Nonidet P-40 (1% w/v), fresh 0.5 mM PMSF, and a cocktail of protease inhibitors. Protein concentration was determined using the bicinchoninic acid (BCA) method (Pierce™ BCA Protein Assay Kit) and samples were conserved at -80ºC until analyses.

The samples were heated for 5 minutes with sample buffer and analysed by SDS-PAGE/western blot under reducing conditions in 12% gels. Our results showed that the 34 kDa apoE species is more abundant in the cellular extracts, whereas the 36 kDa is predominantly found in the cell media (see **Figure 8**). These results suggest that 34 kDa apoE is a transient species, mainly located within the cell which, once fully glycosylated, will be released into the medium.
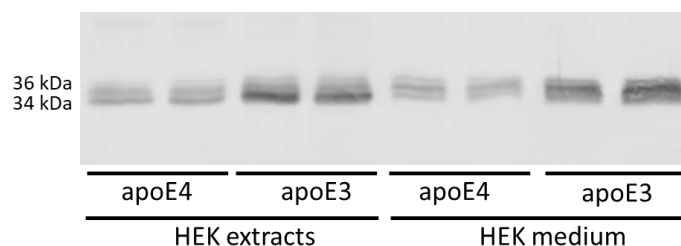
Figure 8. ApoE over-expressed in HEK cellular extracts and media. HEK cells were transfected with apoE3 and apoE4, and apoE protein species were analysed. The 34 kDa apoE is detected mainly in HEK extracts, whereas the 36 kDa species is more abundant in the media.

To study apoE in the brain we are using two well-characterized brain cohorts from the frontal or temporal cortex of subjects with known *APOE* genotypes (see **Table 1**). Small pieces of human cortex stored at -80ºC were thawed gradually at 4ºC and then homogenized (10% w/v) in ice-cold extraction buffer Tris-HCl (50 mM, pH 7.4), NaCl (150mM), EDTA (5 mM), Triton X-100 (0.5%w/v), Nonidet P-40 (1% w/v), fresh 0.5 mM PMSF, and a cocktail of protease inhibitors (Sáez-Valero et al., 1999). The samples were sonicated and centrifuged at 100000×*g* at 4ºC for 1 hour. The supernatant was then removed and conserved at -80ºC until analysis. Protein concentration was determined using the bicinchoninic acid (BCA) method (Pierce™ BCA Protein Assay Kit).

Brain extracts, 25 µg of each sample, were denatured at 98ºC for 5 minutes and resolved by SDS-PAGE (Tris-tricine 12% gels). Following electrophoresis, proteins were blotted onto 0.45 µm nitrocellulose membranes and bands of apoE immunoreactivity were detected using the AB178479 antibody (goat polyclonal; Merck Millipore) common to all apoE isoforms. Blots were probed with the appropriate secondary antibody (IRDye secondary antibody) and imaged on an Odyssey CLx Infrared Imaging System, as described in the methods section. Quantifications were performed using the ImageStudio software.

TABLE 1A: EDINBURGH (SCOTLAND)						
	CONTROL			ALZHEIMER'S DISEASE		
APOE	ε3/3	ε3/4	All	ε3/3	ε3/4	All
N	6	4	10	5	5	10
Average age (Years)	66	49.8	59.5	82.2	76.8	79.5
Age (Range)	53-78	34-59	34-78	65-87	57-90	57-90
Female/Male	2/4	1/3	3/7	2/3	0/5	2/8
Post-mortem (hours)	62.5	75	67.5	80.2	74.2	77.2
Braak stage (V/VI)	-	-	-	0/5	0/5	0/10

TABLE 1B: BARCELONA (SPAIN)				
	CONTROL	ALZHEIMER'S DISEASE		
APOE	ε3/3	ε3/3	ε3/4	All
N	6	6	4	10
Average age (Years)	51.8	79.5	74.3	77.4
Age (Range)	47-60	56-93	67-81	56-93
Female/Male	1/5	2/4	3/1	5/5
Post-mortem (hours)	8.9	11.8	8.5	10.5
Braak stage (V/VI)	-	4/2	3/1	7/3

Table 1. Demographic data of brain cohorts. Demographic data of the Edinburgh temporal cortex collection (Table 1A) and the Bellvitge frontal cortex collection (Table 1B).

Our initial studies were performed in a collection from the Edinburgh Brain Bank consisting in temporal cortex samples from control and AD samples (see **Table 1A**). Two distinct apoE glycoforms were present in control samples, with a similar molecular mass to the ones detected in CSF samples, with about 34 kDa and 36 kDa, thus probably representing immature and mature glycoforms. In the AD cases, however, only the 34 kDa apoE species were detected, as the 36 kDa species appeared to be mostly depleted (see **Figure 9**). No differences were observed between *APOE* genotypes, as all AD samples were affected to a similar extent in *APOE* ε4-carriers and non-carriers.

Due to the high affectation of the temporal cortex in AD from very early stages, we decided to corroborate the results obtained in another brain area that is affected later in AD, the frontal cortex, from another independent cohort (Brain Bank from the Hospital de Bellvitge/Universitat de Barcelona) (see **Table 1B**). Our initial studies showed that, in the frontal region, both apoE glycoforms of about 34 and 36 kDa were present in control and AD samples (see **Figure 9**).

Nonetheless, upon quantification, a lower 36/34 kDa glycoform ratio was detected in AD compared with controls ($p= 0.004$), and this quotient also reached significance when *APOE* ε3/ε3 cases ($p= 0.04$) and *APOE* ε3/ε4 cases ($p= 0.02$) were considered independently. No differences between AD cases with different *APOE* genotypes were detected.
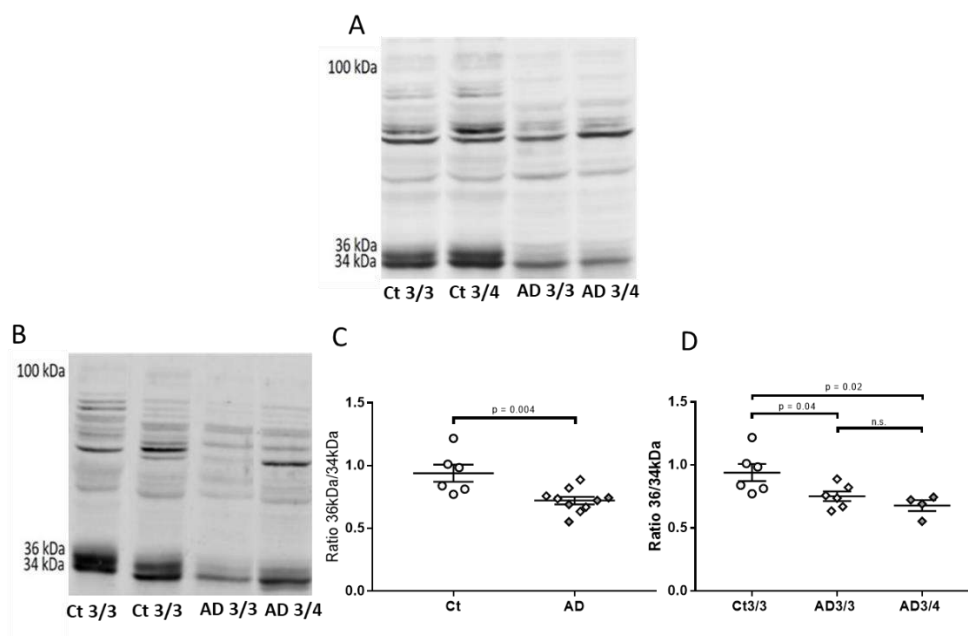

Figure 9. ApoE in brain samples. In SDS-PAGE/western blots, apoE is present in the brain as two glycoforms, in a similar manner to CSF. Samples from the temporal cortex (**A**) and frontal cortex (**B**) present an imbalance in immature and mature glycoforms. In the temporal cortex (Edinburgh cohort; see Table 1A), the 36 kDa species is practically absent in AD samples. In the frontal cortex (Bellvitge cohort; see Table 1B), the 36 kDa band appears to be less intense in AD cases (Braak stages V-VI) when compared with controls. The 36/34 kDa ratio from the frontal cortex collection is shown to the right (**C & D**), demonstrating a significant decrease in AD cases, considering all the AD cases (**C**) or when discriminating by *APOE* genotypes (**D**).

High molecular mass species immunoreactive to apoE were detected in all samples, including controls, however no apparent changes in their levels and no aberrant dimers comparable to the ones found in CSF samples were detected in AD samples.

Taken together, these results replicate the findings described in CSF samples regarding the imbalance of apoE glycoforms in AD. This imbalance favouring immature apoE glycoforms appears to be exacerbated in more affected regions at later stages of the disease.

We decided to characterize the 34 kDa glycoform in an attempt to detect further differences in this specific form associated to AD pathology. In non-pathological conditions, immature glycoforms should be attributable to transient species that are trafficking through the Golgi, a membrane compartment. We expected that the solubilisation of brain extracts using a saline buffer in absence of detergent (1 M NaCl, 50mM MgCl$_2$, 1 mM EGTA, 1 mg/ml bacitracin, 2 mM benzamidine, 0.1 mg/ml soybean trypsin inhibitor, 10 µg/ml pepstatin, 20 U/ml aprotinin, 20 µg/ml leupeptin, 10 mM Tris, pH 7.0) would be adequate to obtain the soluble apoE species, but would likely be less efficient for the solubilisation of transient apoE species from inside the Golgi and intracellular organelles. The protocol of sonication and centrifugation remained the same as the detergent-containing protocol. After centrifugation, the supernatant containing the soluble fraction was kept, and the remaining pellet was then re-solubilized in a buffer supplemented with detergent (Tris-HCl (50 mM, pH 7.4), NaCl (150mM), EDTA (5 mM), Triton X-100 (0.5%w/v), Nonidet P-40 (1% w/v), fresh 0.5 mM PMSF, with a cocktail of protease inhibitors). In this manner, we expected that the apoE species trafficking through organelles would be optimally released in the detergent fraction.

These studies are still in their early stages, so only preliminary results have been obtained. Nonetheless, our initial trials in controls have shown that a large proportion of 34 and 36 kDa apoE is obtained in the soluble fraction, although a proportion of both species is also detected in the detergent fraction. In AD samples, however, the 34 kDa species is only consistently released in the detergent fraction; as such, significantly less 34 kDa apoE is detected in the soluble fraction of AD samples compared to controls ($p < 0.0001$), as seen in **Figure 10**.
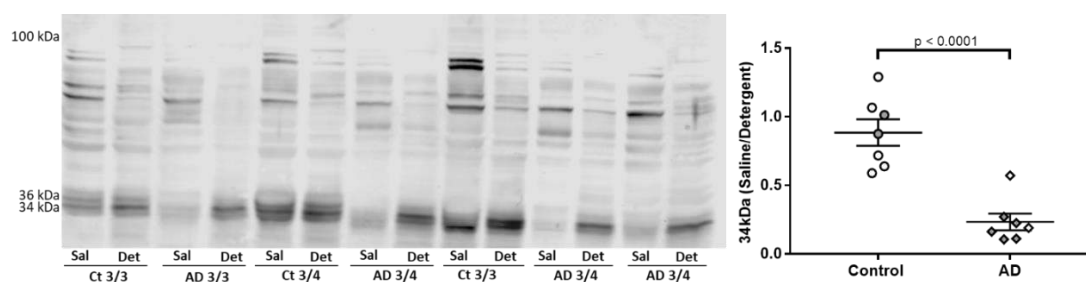
Figure 10. ApoE in soluble and detergent fractions from temporal cortex samples. ApoE was obtained from temporal cortex samples following solubilization with a saline buffer (Sal) to extract the soluble fraction, followed by a buffer containing detergent (Det) to extract the unreleased membrane-bound fraction. Note that both the 34 and 36 kDa species are visible following both saline and detergent solubilization in control cases, whereas the 34 kDa species is only present following solubilization with a detergent buffer in AD cases. The quantification of the 34 kDa apoE species obtained from each solubilization method is represented as a quotient (soluble/detergent fraction apoE).

Therefore, solubilization with the saline buffer alone is not sufficient to effectively release 34 kDa apoE in AD cases. This may indicate that, in AD, apoE may not be as readily secreted as in control cases, possibly due to it being retained within the organelles. Taking the predominant compartmentalization of 34 kDa apoE and the absence of 36 kDa apoE in AD into consideration, these findings could indicate that the functions of apoE may be seriously affected due to the increased presence of poorly glycosylated apoE that is not secreted adequately.

In conclusion, these preliminary results appear to corroborate the findings from our CSF studies regarding an imbalance in apoE immature glycoforms in AD. Despite the limitation that different areas also correspond to different cohorts, these changes appear to be exacerbated in brain areas that are more severely affected in AD. Therefore, although the levels of the 34 kDa species are maintained, the inability to generate 36 kDa species suggests that the normal glycosylation/secretion pathway for apoE is impaired in AD. In fact, as the 34 kDa immature apoE glycoform is not solubilized in absence of detergent with similar efficacy in AD as in control samples, these results suggest an alteration in the biosynthetic pathway of apoE in AD. Further studies are required to confirm these results, and to explore the functional implications of these apoE modifications.

Altogether, these findings suggest that the biological roles of apoE may be hindered due to aberrant post-translational modifications of the protein.

ARTICLE #2: ALTERED BALANCE OF REELIN PROTEOLYTIC FRAGMENTS IN THE CEREBROSPINAL FLUID OF ALZHEIMER'S DISEASE PATIENTS

Inmaculada López-Font †, **Matthew Paul Lennol** †, Guillermo Iborra-Lázaro, Henrik Zetterberg, Kaj Blennow & Javier Sáez-Valero

Article

Altered Balance of Reelin Proteolytic Fragments in the Cerebrospinal Fluid of Alzheimer's Disease Patients

Inmaculada Lopez-Font [1,2,3,*,†], Matthew P. Lennol [1,2,†], Guillermo Iborra-Lazaro [1,2], Henrik Zetterberg [4,5,6,7,8], Kaj Blennow [4,5] and Javier Sáez-Valero [1,2,3,*]

[1] Instituto de Neurociencias de Alicante, Universidad Miguel Hernández-CSIC, 03550 Sant Joan d'Alacant, Spain; mlennol@umh.es (M.P.L.); guillermo.iborra@uclm.es (G.I.-L.)
[2] Centro de Investigación Biomédica en Red sobre Enfermedades Neurodegenerativas (CIBERNED), 03550 Sant Joan d'Alacant, Spain
[3] Instituto de Investigación Sanitaria y Biomédica de Alicante (ISABIAL), 03010 Alicante, Spain
[4] Clinical Neurochemistry Laboratory, Sahlgrenska University Hospital, 413 45 Mölndal, Sweden; henrik.zetterberg@clinchem.gu.se (H.Z.); kaj.blennow@neuro.gu.se (K.B.)
[5] Department of Psychiatry and Neurochemistry, Institute of Neuroscience and Physiology, The Sahlgrenska Academy at the University of Gothenburg, 413 90 Mölndal, Sweden
[6] Department of Neurodegenerative Disease, Institute of Neurology, University College London, London WC1E 6BT, UK
[7] UK Dementia Research Institute at UCL, London WC1E 6BT, UK
[8] Hong Kong Center for Neurodegenerative Diseases, Hong Kong, China
* Correspondence: ilopez@umh.es (I.L.-F.); j.saez@umh.es (J.S.-V.); Tel.: +34-965919580 (J.S.-V.); Fax: +34-965919561 (J.S.-V.)
† These authors contributed equally to this work.

Abstract: Reelin binds to the apolipoprotein E receptor apoER2 to activate an intracellular signaling cascade. The proteolytic cleavage of reelin follows receptor binding but can also occur independently of its binding to receptors. This study assesses whether reelin proteolytic fragments are differentially affected in the cerebrospinal fluid (CSF) of Alzheimer's disease (AD) subjects. CSF reelin species were analyzed by Western blotting, employing antibodies against the N- and C-terminal domains. In AD patients, we found a decrease in the 420 kDa full-length reelin compared with controls. In these patients, we also found an increase in the N-terminal 310 kDa fragment resulting from the cleavage at the so-called C-t site, whereas the 180 kDa fragment originated from the N-t site remained unchanged. Regarding the C-terminal proteolytic fragments, the 100 kDa fragment resulting from the cleavage at the C-t site also displayed increased levels, whilst the one resulting from the N-t site, the 250 kDa fragment, decreased. We also detected the presence of an aberrant reelin species with a molecular mass of around 500 kDa present in AD samples (34 of 43 cases), while it was absent in the 14 control cases analyzed. These 500 kDa species were only immunoreactive to N-terminal antibodies. We validated the occurrence of these aberrant reelin species in an Aβ42-treated reelin-overexpressing cell model. When we compared the AD samples from *APOE* genotype subgroups, we only found minor differences in the levels of reelin fragments associated to the *APOE* genotype, but interestingly, the levels of fragments of apoER2 were lower in *APOE* ε4 carriers with regards to *APOE* ε3/ε3. The altered proportion of reelin/apoER2 fragments and the occurrence of reelin aberrant species suggest a complex regulation of the reelin signaling pathway, which results impaired in AD subjects.

Keywords: reelin; proteolytic fragment; aggregate; cerebrospinal fluid; biomarker; Alzheimer's disease

1. Introduction

The ever-growing prevalence of Alzheimer's disease (AD) is associated with the sporadic presentation of the disease [1,2]. Sporadic AD is a multifactorial disease with environmental contributing causes (mainly age); however, genetic risk factors are also

important [3–5]. Amongst the numerous genes implicated in AD pathogenesis, the most prominent genetic risk factor is the apolipoprotein E (apoE) encoding gene, *APOE*. The apoE protein is secreted mainly by glial cells in the central nervous system [6], and it participates in cholesterol and lipid transport in the brain [7,8], amongst other physiological functions, including signaling through receptor interactions [6]. Three major apoE isoforms, apoE2, apoE3, and apoE4, are encoded by different alleles of human *APOE*, where the *APOE ε3* allele (encoding apoE3) is the most common allele. The *APOE ε2* allele (encoding apoE2) is the most protective against AD; however, it is also the least common allele. The *APOE-ε4* allele (encoding apoE4), on the other hand, provides the highest risk of developing AD [9]. Interestingly, in humans, apoE isoforms form disulfide-linked homodimers that could be the native apoE form able to bind to receptors [10]. However, apoE4 is an exception, as it lacks a key cysteine residue.

Reelin is a large, secreted glycoprotein composed of 3461 amino acids [11] that competes with apoE for receptor binding [12,13]. Reelin and apoE bind to the LDL receptor (LDLR) family, particularly apoE receptor 2 (apoER2), and the very low-density lipoprotein receptor (VLDLR). ApoER2 is the main reelin receptor into the brain. Thus, reelin/apoE-mediated signaling transduction occurs after binding to its receptors [14,15]. By binding to these receptors, reelin/apoE plays a key role in synaptic plasticity of the adult brain, primarily by mediating reelin signaling [16].

Studies from our group have shown that reelin protein and mRNA levels are elevated in AD subjects [17–19]. However, we have also demonstrated impaired reelin signaling in AD due to Aβ-mediated interference [19,20]. Nonetheless, the influence of the *APOE* genotype on reelin levels and function are not yet fully understood.

Full-length reelin forms homodimers, which are the species that drive efficient signal transduction [12,21–23]. We reported that Aβ may disrupt reelin from binding to receptors by hindering its capacity to form homodimers, thereby compromising the signaling process [20]. After interaction with apoER2, both reelin and apoER2 undergo proteolytic cleavage by metalloproteinases and secretases, respectively [24–27]. Nonetheless, reelin can undergo proteolytic processing through the activity of extracellular matrix metalloproteinases independently of its interaction with receptors [28]. Interestingly, truncated forms of reelin can form larger complexes that bind to reelin receptors, but they do not induce the signaling cascade activation efficiently [21], nor does the reelin monomer [29]. ApoER2 fragments resulting from proteolysis during receptor activation can also inhibit signaling [30]. Therefore, reelin and apoER2 proteolytic fragments may finetune the signaling pathway.

We postulate that the quantification of reelin fragments in the cerebrospinal fluid (CSF) can give a credible read-out of altered proteolytic processing of reelin and signaling impairment in AD subjects. We also discover an aberrant reelin species present in most AD subjects, regardless of *APOE* genotype. We validate the occurrence of these aberrant reelin species in an Aβ42-treated reelin-overexpressing cell model. In the present study, we also examine the effect of *APOE* genotype on the soluble levels of apoER2 fragments from subjects suffering from AD. We find differences in the proportions of these fragments in AD CSF that are associated with *APOE* genotype.

2. Results

2.1. Characterization of Reelin Species in AD CSF

Reelin undergoes cleavage by metalloproteinases at two major sites, called N-t and C-t sites (Figure 1A), resulting in the production of fragments whose relative abundance differs among tissues and fluids [31]. A third processing site within the C-terminal region was recently demonstrated (CTR cleavage; Figure 1A) [32].
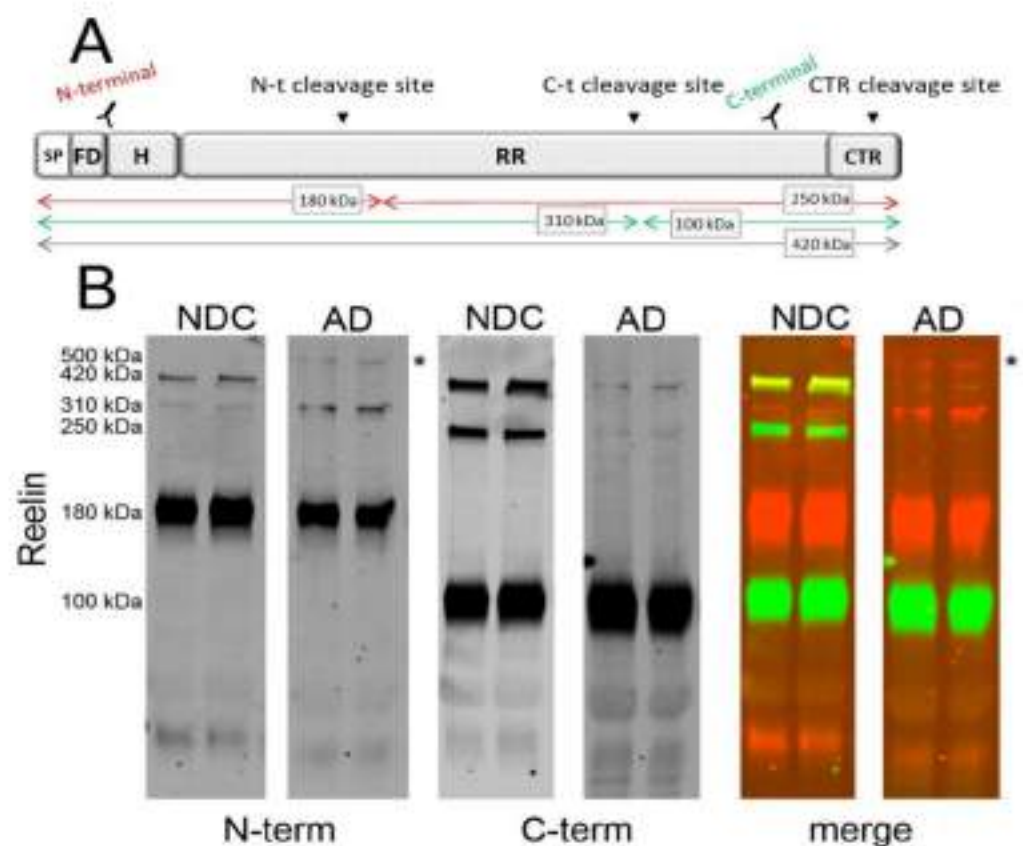
Figure 1. Reelin species present in human CSF. (**A**) Schematic representation of full-length reelin, the proteolytic cleavage site, and the epitope recognized by the antibodies used in the study. The reelin N-terminal region begins with a signal peptide (SP), an F-spondin-like domain (FD), and a hinge segment (H). This is followed by eight similar repeats (RR) separated by an EGF-like domain. The protein ends with a highly basic C-terminal region (CTR). Reelin cleavage at the N- and C-terminal regions leads to the formation of either 310 and 180 kDa N-terminal fragments of 100 kDa and 250 kDa C-terminal fragments, respectively. (**B**) The same human CSF samples from non-disease control (NDC) and AD subjects were simultaneously probed by Western blotting using multiplex fluorescence resolved with reelin N- and C-terminal antibodies. Representative blots of the N-terminal reelin bands (red) and C-terminal reelin bands (green) are shown, as well as simultaneous fluorescence (merge) demonstrating co-localization (yellow). * indicates ~500 kDa reelin immunoreactive band for N-terminal antibody present only in AD samples. The uncropped blot is included as Supplemental Figure S1.

Here, we analyzed CSF reelin species on 4–15% gradient SDS-PAGE with multiplex fluorescence using N- and C-terminal antibodies. In accordance with previous reports [17,18,24,33], a Western blot analysis of human CSF samples with an N-terminal antibody (mouse monoclonal) revealed full-length reelin (420 kDa), together with two proteolytic N-terminal fragments of 310 kDa (also known as NR6, a product of cleavage at the C-t site) and 180 kDa (also known as NR2, a product of cleavage at the N-t site) (Figure 1B). The C-terminal antibody (rabbit monoclonal) confirmed the identity of a 420 kDa full-length species, as well as fragments with the expected molecular mass [33], including a fragment of 100 kDa (also known as R7-8, a product of cleavage at the C-t site) and a less abundant 250 kDa fragment (also known as R3-8, a product of cleavage at the N-t site). Interestingly, while the N-terminal 180 kDa fragment was the most abundant, the correlative 250 kDa C-terminal fragment was the least abundant.

Intriguingly, we also detected the presence of an additional reelin immunoreactive band with a molecular mass around 500 kDa present exclusively in AD samples (Figure 1B). As far as we know, this 500 kDa reelin species has not been described previously. Moreover, this reelin species of 500 kDa was not immunoreactive to the C-terminal antibody, indicating that this species was not an alternative full-length isoform but, presumably, corresponded to SDS-stable complexes composed mainly of N-terminal fragments (Figure 1B). The higher sensitivity of the 420 kDa full-length reelin to proteolysis, including heating, limited the analysis of the complexes using alternative denaturing protocols since heating results in laddering [18,34].

2.2. Determination of Reelin Species in AD CSF

Next, we examined whether the levels of reelin fragments were altered in CSF samples from AD patients. Human CSF samples were from the Clinical Neurochemistry Laboratory (Mölndal, Sweden). All the AD patients fulfilled the NIAA-AA criteria for dementia [35] and were designated as AD according to CSF biomarker levels using cut-offs that were >90% specific for AD: $A\beta42 < 550ng/L$ and total tau (T-tau) > 400ng/L [36] (see Table 1). When immunoblotting with the N-terminal antibody, we distinguished a full-length 420 kDa band and two N-terminal fragments of 310 and 180 kDa in all the CSF samples analyzed (Figure 2A). Interestingly, the 420 kDa full-length reelin was seen to be decreased (40%, $p = 0.003$) in AD samples compared with NDCs, whereas the 310 kDa fragment levels were increased (120%, $p < 0.001$). However, no significant differences were detected between the AD and NDC samples in the relative levels of the more abundant reelin species, the 180 kDa fragment (Figure 2B). The different tendency of the N-terminal fragments determined in AD CSF samples resulted in significant differences of a 310 kDa/180 kDa quotient (Figure 2C, $p < 0.001$).

Table 1. Clinical and demographic data, as well as classic CSF biomarkers, for the samples used in this study. F, female; M, male. The data represent means ± SEM. Significant difference was * $p < 0.0001$, with respect to the NDC group.

	CSF Cohort						
	Control			Alzheimer's Disease			
APOE	ε3/3	ε3/4	All	ε3/3	ε3/4	ε4/4	All
N	9	5	14	15	13	15	43
Age (Years)	69 ± 2	62 ± 5	67 ± 3	79 ± 2	78 ± 1	73 ± 1	77 ± 1 *
Age (Range)	60–81	44–75	44–81	62–88	69–84	63–83	62–88
Female/Male	5/4	2/3	7/7	11/4	10/3	9/6	31/14
CSF Aβ42 (pg/mL)	845 ± 96	746 ± 121	804 ± 74	470 ± 13 *	484 ± 9 *	419 ± 21	457 ± 10 *
CSF Total Tau (pg/mL)	317 ± 53	303 ± 34	312 ± 35	816 ± 88 *	1004 ± 127 *	731 ± 53	840 ± 52 *

Regarding the comparison between CSF samples subgrouped by *APOE* genotype, the changes in reelin species immunoreactive to the N-terminal antibody were maintained when comparing *APOE* ε3/ε3 AD cases (420 kDa decrease: 74%, $p = 0.015$; 310 kDa increase: 200%; $p < 0.001$) with NDC ε3/ε3 subjects. Given the difficulty finding age-matched *APOE* ε4/ε4 control subjects (low prevalence of this genotype in the general and healthy population), we could not compare AD *APOE* ε4/ε4 with control ε4/ε4 cases, and the analysis within the *APOE* ε3/ε4 genotype exhibited less statistical power because the size of the control group was small. Regardless, in the *APOE* ε3/ε4 AD subgroup, the full-length 420 kDa reelin tended to decrease (50%, $p = 0.09$), and the 310 kDa fragment increased significantly (104%; $p = 0.019$). When AD cases were compared between different *APOE* genotype subgroups, only the 310 kDa reelin displayed significant changes, being significantly lower (29%, $p = 0.034$) in subjects with the *APOE* ε4/ε4 genotype when compared to *APOE* ε3/ε3 subjects.
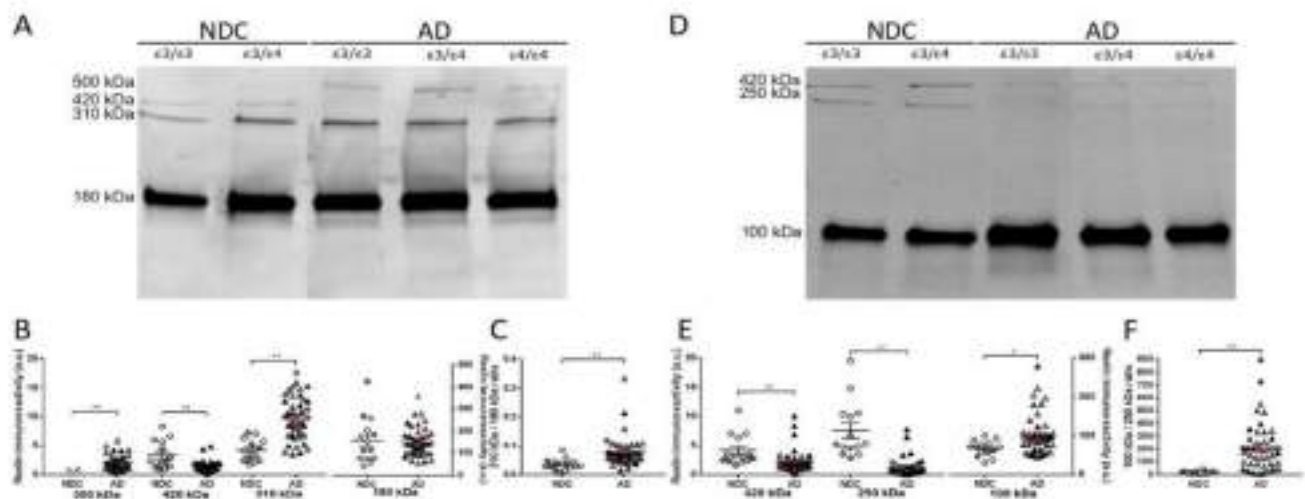
Figure 2. Characterization of reelin immunoreactive bands in CSF samples. (**A**) Representative blots of the reelin species detected in NDC and AD CSF samples using the N-terminal antibody. A species with a molecular mass of ~500 kDa was detected only in AD samples, together with the full-length species of 420 kDa and the 310 and 180 kDa proteolytic N-terminal fragments present in all the samples. (**B**) Densitometric quantification of the individual immunoreactivities of each reelin immunoreactive band detected with the N-terminal antibody. (**C**) Graph of the quotient obtained by dividing the level of immunoreactivity of the 310 kDa N-terminal fragment by the 180 kDa N-terminal fragment (310 kDa/180 kDa quotient). (**D**) Representative blot of reelin species immunoreactive to a C-terminal antibody in the CSF samples. (**E**) Densitometric quantification of reelin immunoreactivity from the 420 kDa full-length species and the 250 kDa and 100 kDa C-terminal fragments. (**F**) The ratio derived from the immunoreactivity for the 100 kDa C-terminal fragment with respect to the 250 kDa C-terminal fragment estimated in each sample (100 kDa/250 kDa quotient) is also shown. The samples are represented by the disease condition (NDC: circles; AD: triangles) and *APOE* genotype: *APOE* ε3/3 (white); *APOE* ε3/ε4 (grey); and *APOE* ε4/ε4 (black). There were 14 NDC subjects (9 *APOE* ε3 (7 *APOE* ε3/ε3 and 2 *APOE* ε3/ε2) and 5 *APOE* ε3/ε4) and 41 AD subjects (15 *APOE* ε3/ε3, 13 *APOE* ε3/ε4, and 15 *APOE* ε4/ε4). The data represent means ± SEM. * $p < 0.05$; ** $p < 0.001$; n.s. = nonsignificant; and n.d. = not detected. Graphs of comparisons between AD CSF samples subgrouped by *APOE* genotype are included as Supplemental Figures S2 and S3.

When immunoblotting with the C-terminal antibody (Figure 2D), the decreased levels of 420 kDa reelin were confirmed in the AD samples (Figure 2E; 51% decrease; $p < 0.001$). As expected, determination of the full-length reelin with the antibodies, both N- and C-terminal, displayed an effective correlation ($r = 0.77$, $p < 0.001$). The levels of the 100 kDa C-terminal fragment appeared increased in the AD samples (51%, $p = 0.014$) compared with NDC samples, whereas the 250 kDa fragment displayed a significant decrease (85%, $p < 0.001$). As a result, significant differences were also found for the 100 kDa/250 kDa quotient between the NDC and AD groups (Figure 2F; $p < 0.001$).

When the samples were subgrouped by *APOE* genotype, the changes in reelin species immunoreactive to the C-terminal antibody maintained their significance. Thus, in *APOE* ε3/ε3 subjects, the 420 kDa full-length reelin decreased in AD (51%, $p < 0.001$) compared to the NDC subgroup; the decrease was also significant when compared to *APOE* ε3/ε4 subjects (36%, $p = 0.002$). The increase in 100 kDa (58%, $p = 0.043$) and the decrease in 250 kDa (90%, $p < 0.001$) C-terminal fragments were still significant between the *APOE* ε3/ε3 AD and NDC subgroups. Similar changes were displayed in *APOE* ε3/ε4 subjects for the 250 kDa fragment (87% decrease in AD, $p = 0.002$), yet they failed to achieve significance for the 100 kDa fragment (68% increase in AD, $p = 0.07$). None of the C-terminal immunore-

109

active reelin species displayed significant changes between AD subjects subgrouped by *APOE* genotypes.

Furthermore, we confirmed the presence of the ~500 kDa reelin species (see Figure 1B) immunoreactive exclusively to the N-terminal antibody in AD cases in a total of 34 out of 43 CSF samples from AD patients across all the *APOE* genotypes, whilst the species was undetectable in the 14 NDC cases analyzed (Figure 2A).

Despite the fact that the AD subjects displayed differences in age compared with NDC subjects, the age of the subjects failed to correlate with the levels of the reelin species. Differences in reelin were not detected when the cases were subgrouped by gender.

There were no clear correlations between the levels of the reelin fragments with the levels of Aβ42 in either of the groups considered individually. Interestingly, in the NDC *APOE* ε3/ε3 subgroup, the levels of the major 180 kDa N-terminal fragment of reelin and T-tau correlated ($R = 0.73$, $p = 0.020$). This correlation was also significant in all the AD subjects subgrouped by *APOE* genotypes: ε3/ε3 ($R = 0.61$, $p = 0.016$), ε3/ε4 ($R = 0.85$, $p < 0.001$), and ε3/ε4 (T-tau with 180-kDa reelin: $R = 0.59$, $p = 0.025$). These results are in good agreement with a previous study also indicating that 180-kDa reelin levels correlated positively with T-tau protein in CSF [18].

2.3. Occurrence of the 500 kDa Reelin Species in Culture Media of Aβ42-Treated Cells

To validate the ~500 kDa reelin species and its association with the pathologic condition, we tested the potential occurrence of this species in a cellular model treated for 2 days with 2.5 μM Aβ42 or an Aβsc peptide, as described above. Culture media from HEK-293T cells over-expressing reelin were analyzed by Western blotting with an N-terminal reelin antibody. The characteristic N-terminal fragments were present in the culture media of cells over-expressing reelin, despite an important percentage of fragments being trapped with Aβ aggregates in pellets from the media of the cells, as described previously [19]. Interestingly, an immunoreactive reelin band of similar molecular mass to that of the ~500 kDa species identified in AD CSF samples appeared in cells treated with the amyloidogenic Aβ42 peptide, while the soluble reelin species present in the cells treated with the Aβsc peptide lacked the 500 kDa form (Figure 3).
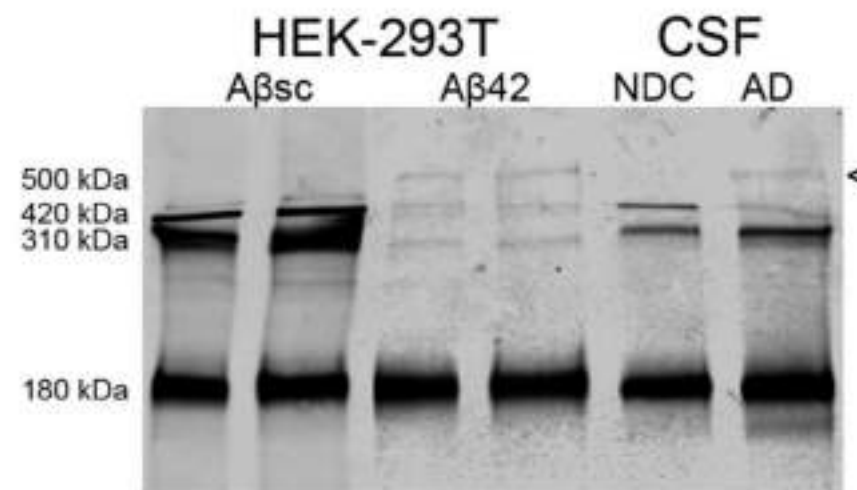
Figure 3. The 500 kDa reelin species was present in cell medium of HEK-293T treated with Aβ42. A representative blot showing the reelin immunoreactive bands detected with an N-terminal antibody from HEK-293T cells overexpressing reelin treated with Aβ42 or an Aβsc peptide. CSF samples from NDC and AD subjects were included to monitor the potential occurrence of the ~500 kDa species. When the cells were treated with Aβ42 peptide, a reelin immunoreactive band resembling the ~500 kDa band present in AD CSF was detected; this band was not present when the cells were treated with the Aβsc peptide. Arrowhead indicates the ~500 kDa band.

2.4. Determination of CSF apoER2 in AD Subjects Subgrouped by APOE Genotype

The full-length apoER2 receptor has not been described in CSF; however, soluble apoER2 fragments were seen in human and ovine CSF [19]. This soluble fragment is generated after reelin binds to a receptor and induces apoER2 proteolytic cleavage [30]. The anti-apoER2 Y186 antibody specifically recognizes the entire ligand-binding ectodomain of the apoER2 receptor [37] (Figure 4A).
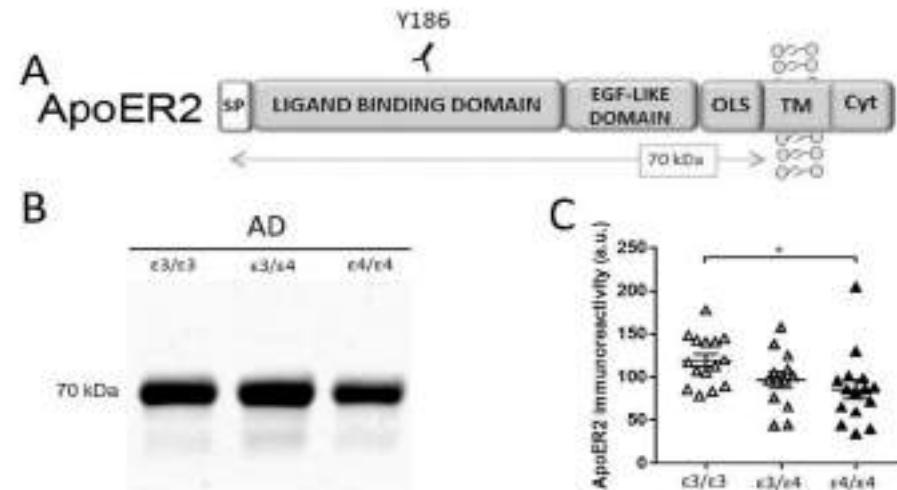

Figure 4. Characterization of apoER2 in CSF samples from AD. (**A**) Schematic representation of the apoER2 receptor and the epitope recognized by the Y186 antibody used in the study. ApoER2 is composed of a signal peptide (SP), followed by a ligand-binding domain containing an EGF-like region, an O-linked sugar domain (OLS), a transmembrane (TM) segment, and a cytoplasmic domain (Cyt). ApoER2 is processed by α-secretase upon ligand binding, generating a soluble ectodomain fragment (~70 kDa). (**B**) Representative blot of human CSF samples from AD subjects subgrouped by *APOE* genotype (15 *APOE* ε3/ε3, 13 *APOE* ε3/ε4, and 15 *APOE* ε4/ε4 subjects) and resolved with the indicated Y186 antibody. (**C**) Densitometric quantification and statistical analysis of the immunoreactivity and the 70 kDa ecto-apoER2 fragment. Samples are separated by *APOE* genotype: *APOE* ε3/3 (white), *APOE* ε3/ε4 (grey), and *APOE* ε4/ε4 (black). * $p < 0.05$.

This antibody confirmed the existence of a ~70 kDa apoER2-soluble fragment, ecto-apoER2, in all the CSF samples analyzed (Figure 4B). Due to limitations in the available CSF sample volumes, the study of ecto-apoER2 levels was restricted to the AD collections subgrouped by *APOE* genotype. A previous report from our group demonstrated lower levels of ecto-apoER2 in AD CSF compared to those in age-matched controls [38], but this study did not address the influence of *APOE* genotype.

Significantly higher levels of ecto-apoER2 were detected in AD *APOE* ε3/ε3 subjects compared to *APOE* ε4/ε4 samples (28% decrease, $p = 0.019$), whereas in the comparison with *APOE* ε3/ε4 subjects, the trend was maintained but significance was not achieved (19% decrease, $p = 0.073$) (Figure 4C).

3. Discussion

In this study, we analyzed different reelin species in the CSF of patients suffering from AD. The 420 kDa reelin band, attributable to the full-length species, was seen to be decreased in the CSF from AD patients, while the levels of reelin fragments displayed distinct changes. Intriguingly, a 500 kDa species not yet described in other studies was seen to be present exclusively in AD samples.

Previous studies from our group have demonstrated increases in reelin protein and mRNA levels in brain frontal cortex extracts from AD patients and individuals with dementia associated with Down syndrome [17–19,39,40]. Reelin levels have also appeared

to be increased in AD Tg2576 mutant mice and in cell cultures treated with amyloidogenic Aβ42 peptide [19,39]. Overall, our earlier studies have indicated that the more abundant 180 kDa reelin fragment appears to be slightly increased in the CSF of AD subjects, but this trend has not reached statistical significance in some reports [17,18,39]. In cells exposed to Aβ42 with increased cellular reelin protein levels, a reduced amount of soluble reelin was detectable in the culture media, probably because notable amounts of secreted reelin were "trapped" with the Aβ fibers [19]. Indeed, in the AD brain, considerable amounts of reelin appeared to be trapped in insoluble Aβ aggregates [40], and reelin immunostaining was observed in the amyloid plaques of APP/PS1 transgenic mice [41]. Thus, changes observed in the frontal cortex might not be reflected as clearly in the CSF from AD patients. It is worth mentioning that some studies have found contradictory results in which decreased reelin expression was associated with AD [42,43].

Several studies have indicated that dampened reelin signaling activity could contribute to the progression of AD (reviewed in [44]). Nonetheless, while reelin abundance could be elevated in the AD brain, we demonstrated that the interaction of reelin with Aβ hindered its biological activity [19]. A common feature in our previous studies has been the description of altered reelin glycosylation and oligomerization in the brain and CSF of AD subjects, which compromise the ability to transduce signals through the apoER2 receptor [18,20,39]. Thus, despite reelin levels being higher, the protein is inefficient in signal activation. The possibility that the generation of reelin and apoER2 proteolytic fragments after effective ligand-receptor interaction could also be affected has not been addressed until now.

In this context, the hypothesis of this study was that the analysis of reelin fragments in CSF could be informative of altered proteolytic processing and a subsequent impairment in signaling.

In previous studies addressing potential changes in the levels of reelin in AD CSF, the results have focused on the 180 kDa N-terminal fragment and the 100 kDa C-terminal fragment [17,18,33]. The full-length 420 kDa reelin and the less abundant 310 kDa fragment have been studied to a lesser extent due to difficulties in their detection due to weak staining. In this study, reelin species were detected with fluorescent-based imaging after SDS-PAGE and Western blotting. This technique provides a wider linear dynamic range than chemiluminescent detection [45], including a greater upper linear range of detection [46]. Moreover, all the analyses were performed on individual aliquots stored frozen at −80 °C, avoiding thawing–freezing cycles and limiting heating in the preparation of the samples for electrophoresis to 3 min since these pre-analytical and analytical factors can influence the measurement of reelin, particularly for full-length protein and large fragments [18,34]. Furthermore, in this study we optimized the resolution of the less abundant immunoreactive reelin bands of higher molecular mass by resolving the electrophoresis on 4-15% polyacrylamide-gradient gels (in previous analyses, 6% polyacrylamide gels have been used). These changes allowed us to enhance the resolution for a more reliable quantification of 420 kDa species and less abundant reelin fragments. We determined that the 420 kDa full-length reelin exhibited a pronounced reduction in the CSF of AD patients, whilst the 310 kDa N-terminal fragment presented a striking increase, suggesting a boosted rate of reelin proteolysis; however, the major N-terminal fragment of 180 kDa did not appear to be altered. Moreover, while the 100 kDa C-terminal fragment also increased, the 250 kDa fragment appeared clearly reduced in CSF samples from AD patients. Given that multiple proteolytic events allow the release of reelin fragments, the interpretation of these results is complex.

Experimental evidence has demonstrated that reelin is internalized following receptor binding [12] and subsequently suffers proteolytic processing [26], but little is known about the identity of the protease(s) in charge of the cleavage or the sequence of proteolytic events at N-t and C-t sites. Moreover, increasing evidence has indicated that extracellular matrix metalloproteinases act as reelin proteases. The association between dysregulated reelin proteolysis and disease progression is recurrent.

A study proposed that extracellular matrix ADAMTS-3 metalloproteinases were more than likely the proteases that cleaved reelin in vivo at the N-t site, originating the 180 kDa (NR2) fragment [47]. On the other hand, other studies have found that ADAMTS-2, ADAMTS-4, and ADAMTS-5 are potential enzymes that could cleave reelin at the N-t site (discussed in [28,48]). ADAMTS-4 and ADAMTS-5 are also able of cleaving reelin at the C-t site, whilst the serine protease tissue plasminogen activator (tPA), as well as meprin α and β, are other potential reelin cleavage proteases at its C-t site [49,50], originating the 310 kDa fragment that appeared to be particularly increased in this study. Interestingly, meprin β is also a sheddase for the amyloid precursor protein (APP) [51,52]; moreover, meprin β appeared to be increased in the brain of AD patients [53]. Meanwhile, the alternative C-t protease of reelin, tPA, appeared to be decreased or unchanged in the brain [54], CSF, and plasma of AD patients [55,56]. In this puzzling scenario, as mentioned above, it is assumed that the main proteolytic processing of reelin occurs following apoER2 binding and, subsequently, reelin fragments are re-secreted [26]. The major reelin fragment generated following reelin–apoER2 interaction is the 180 kDa (NR2) fragment. The identity of the protease(s) that cleaves reelin in the endosome remains unknown, and it may or may not be the same as the extracellular matrix metalloproteinases.

A previous in vitro experiment demonstrated that N-terminal fragments could form larger complexes that, despite binding well to receptors, did not induce efficient signaling [21]. Thus, differences in the relative abundance of 180 and 310 kDa N-terminal fragments in AD CSF could be related to a higher formation of these complexes in the pathological brain. Regardless, the large imbalance in the C-terminal fragments in AD CSF strongly suggests a dysregulation in reelin processing by extracellular matrix metalloproteinases.

Our improved determination of the largest reelin species enabled the identification of a novel ~500 kDa reelin immunoreactive species that has not yet been described. The ~500 kDa reelin species were immunoreactive to the N-terminal antibodies but were not recognized by the C-terminal antibody. We hypothesized that these reelin species probably represented part of the multimers of N-terminal fragments suggested by in vitro experiments [21]. These species are stable under denaturing conditions but are seen in very low amounts and are sensitive to heating during electrophoresis preparation, a common feature for all reelin species resulting in laddering [18,34], which complicates further analysis. These large reelin species were present in ~80% of the AD cases and in a HEK-293 cellular model over-expressing reelin treated with Aβ42 but were absent or very weak in the NDC cases and in the media of cells treated with a scrambled Aβ peptide. Despite the fact that HEK-293 is not a neuronal (-like) cell line, it is a widely used cellular model for over-expressing and studying reelin, as it shows the capacity to form N-terminal fragments and large multimers. In a previous study, reelin multimers were induced by chemical crosslinking [21]. Here, we replicated the occurrence of the ~500 kDa reelin in AD CSF by treating the cells with amyloidogenic Aβ42. Interestingly, complexes of several CSF proteins, such as presenilins [57,58], cholinesterase [59], and apoE [60,61], formed under amyloidogenic conditions appear to be particularly stable. Reelin interacts with Aβ both in vitro [62] and in vivo [19], as it is recruited into amyloid fibrils; thus, we hypothesized that Aβ played a direct role in the formation of the 500 kDa reelin species detected in AD CSF. A full characterization of said species is necessary for a correct interpretation of their potential pathological significance. As mentioned, we cannot discard that the 500 kDa reelin species were mostly composed by the 180 kDa fragments, which may offer an alternative explanation for the imbalance in the generation of N-terminal reelin fragments.

Furthermore, the *APOE* genotypes of the analyzed samples were considered in our analysis. In the AD group, only the 310 kDa reelin fragments exhibited lower levels in *APOE* ε4/ε4 when compared with *APOE* ε3/ε3 individuals. Interestingly, the levels of the ecto-apoER2 fragments also appeared to be decreased in *APOE* ε4/ε4 when compared with *APOE* ε3/ε3. ApoE competes with reelin for binding to apoER2 and VLDLR, and apoER2 also participates in the internalization of apoE-containing lipoprotein particles to incorporate cholesterol and other lipids that are essential for normal neuronal function in

the cell [63,64]. Interestingly, apoE3 and apoE4 consistently inhibited reelin from binding to VLDLR and apoER2; this study also indicated that apoE interfered with the ability of reelin to activate a Dab1–dependent signaling pathway [12]. A later study also saw that, unlike reelin, apoE failed to elevate apoER2 processing [65], whereas others have found that the Dab1-dependent pathway was activated by apoE [66] and that apoE and apoER2 co-localized in endosomes [67].

Canonically, only dimeric ligand-binding induces effective signaling and the subsequent clustering of apoER2 [68]. The amino acid substitution of Cys-112 by Arg in apoE4 leads to the inability to form disulfide-linked homodimers and may impact some of the biological roles of apoE, particularly on receptor-binding activity [69]. Thus, despite similar affinities of apoE3 and apoE4 isoforms to the receptor [12,66], monomeric apoE4 can interact with apoER2 but may fail to drive signaling and subsequent reelin and apoER2 proteolytic processing; this would explain why the *APOE* $\varepsilon4/\varepsilon4$ individuals displayed lower levels of apoER2 and 310 kDa reelin compared with *APOE* $\varepsilon3/\varepsilon3$ individuals. Thus, apoE4 could block apoER2, impeding the binding of reelin. In this regard, was reported that apoE4 caused prolonged retention of the receptor inside the cell and impaired the signaling cascade [70]. Interestingly, in a recent study, the levels of membrane-bound apoER2 C-terminal fragments appeared to be significantly lower in AD extracts from advanced Braak stages of *APOE* $\varepsilon4$ noncarriers, but not in carriers [40]. Thus, we hypothesized that, in *APOE* $\varepsilon4$ carriers, apoER2 proteolysis was hampered, resulting in a reduction in ecto-apoER2 fragment release.

In *APOE* $\varepsilon4/\varepsilon4$ subjects, the generation of proteolytic fragments of reelin only appeared to be significantly reduced for the 320 kDa N-terminal fragment compared with *APOE* $\varepsilon3/\varepsilon3$, but nonsignificant trends were observed for reduced 180 kDa and increased 420 kDa levels. Similarly, the 100 kDa C-terminal fragment appeared to be nonsignificantly reduced in *APOE* $\varepsilon4/\varepsilon4$ compared with *APOE* $\varepsilon3/\varepsilon3$. Altogether, in agreement with decreased ecto-apoER2 generation, the results indicated that, in *APOE* $\varepsilon4/\varepsilon4$ AD patients, the efficiency of the reelin/apoE signaling pathways had a basal compromise due to the inability of apoE4 to biologically interact with the receptor. However, the effect of different *APOE* allelic variants on reelin signaling was more difficult to decipher due to the possibility that *APOE* allelic variants may also affect the activity and levels of reelin-cleaving metalloproteinases. For instance, apoE4 displayed a weaker ability to inhibit the function of matrix metallopeptidase 9 (MMP-9) than apoE2 or apoE3, given that MMP-9 expression and activity was elevated in the cerebrovasculature of both human and animal AD brains from specimens with the *APOE* $\varepsilon4$ genotype [71]. A study showed that MMP-9 could induce reelin processing at both the N-t and C-t sites indirectly through the activation of ADAMTS-4 [51]; however, another study failed to demonstrate the effect of MMP-9 inhibitor II on reelin cleavage [72].

In conclusion, we demonstrated the existence of an imbalance in reelin fragments in the CSF of AD patients, and we discovered an aberrant reelin species associated specifically with the amyloidogenic condition. This aberrant 500 kDa reelin species probably represented stable complexes of N-terminal fragments. Moreover, in AD patients with an *APOE* $\varepsilon4/\varepsilon4$ genotype, the generation of reelin and apoER2 fragments appeared to be distinctly different. Our results confirmed that reelin levels were altered associated with AD, probably reflecting an impairment in signaling. Our results also suggested that these changes may result, at least in part, from the activity of reelin-cleaving metalloproteinases. Interestingly, increasing reelin activity has been proposed as a therapeutic option for AD to protect against Aβ [62,73,74], as well as for others neuropsychiatric disorders [75]. In fact, reelin supplementation can enhance cognitive ability and synaptic plasticity [76]. However, for an effective acute activation of the reelin pathway, in addition to designing an adequate supplementation strategy, it seems necessary to monitor its efficiency in a pathological context where Aβ can interfere in the signaling, and the upregulation of reelin-cleaving metalloproteinases can reduce its effect. Thus, the determination of altered CSF reelin and

apoER2 fragments may also be applicable as biomarkers for disease progression and for the efficiency of therapeutic agents targeting reelin.

4. Materials and Methods

4.1. Human CSF Samples

Human CSF samples were provided by the Clinical Neurochemistry Laboratory (Mölndal, Sweden). CSF was obtained through lumbar puncture and collected in polypropylene tubes. It was gently mixed to avoid gradient effects, centrifuged at 2000× *g* for 10 min at 4 °C to remove cells and other insoluble materials, aliquoted, and stored at −80 °C until use. The cohort studied consisted of CSF samples from 43 AD patients subgrouped according to their *APOE* genotype: 15 *APOE* ε3/ε3 subjects (4 female/11 male; 79 ± 2 of age), 13 *APOE* ε3/ε4 subjects (10 female/3 male; 78 ± 1 of age), 15 AD *APOE* ε4/ε4 subjects (9 female/6 male; 74 ± 1 of age), and 14 non-disease control (NDC) subjects (9 *APOE* ε3 (2 *APOE* ε3/ε2 and 7 *APOE* ε3/ε3; 5 female/4 male; 69 ± 2 of age) and 5 *APOE* ε3/ε4 (2 female/3 male; 62 ± 5 of age)). No sample calculation was performed. The patients were designated as AD according to CSF biomarker levels using cut-offs that were >90% specific for AD: Aβ42 < 550ng/L and total tau (T-tau) > 400ng/L [36] (see Table 1). The samples were retrospectively selected to balance age, sex, and *APOE* status.

All the AD patients fulfilled the NIAA-AA criteria for dementia [35]. Exclusion criteria were refusing lumbar puncture or neuropsychological investigation and current alcohol or substance misuse. No blinding was performed in this study. This study was not pre-registered. The variants rs7412 and rs429358 (which define the ε2, ε3, and, ε4 alleles) in the *APOE* gene were genotyped by mini-sequencing, as previously described in detail [77].

4.2. Cell Culture and Aβ Treatment

The effects of Aβ42 on cellular reelin levels were tested in HEK-293T cells that were stably transfected with reelin (kindly provided by Drs. E. Soriano and L. Pujadas, Department of Cell Biology, University of Barcelona, Barcelona, Spain). No further authentication was performed in the laboratory. A maximum of 5 cell passages was used. To obtain conditioned cell culture medium, 2×10^6 cells/dish were grown in six-well plates in Dulbecco's modified Eagle's medium (DMEM) supplemented with 10% fetal bovine serum (FBS; Gibco), 100 μg/mL penicillin/streptomycin (Gibco), and 250 μg/mL G418 (Sigma). After 24 h, the medium was changed to a modified Eagle's Minimum Essential Media (Opti-MEM; Gibco), and the cells were treated with 2.5 μM β-amyloid 1-42 peptide (Aβ42) or a β-amyloid scrambled control peptide (Aβsc; AIAEGDSHVLKEGAYMEIFDVQGHVFGGKIFRVVDL-GSHNVA) (American Peptide Co., USA) for 2 consecutive days without changing the medium. After 3 days, the cell medium was filtered through 0.2 μm pores and concentrated with an Amicon Ultra 100 kDa size exclusion filter (Merk Millipore, Darmstadt, Germany), followed by analysis using Western blot [19,20].

4.3. Western Blot

For the analysis of reelin under denaturing conditions, CSF samples (13 μL) or culture media (13 μL) were resolved on 4–15% gradient SDS-PAGE (Mini-PROTEAN® TGX™ Precast Gels; Bio-Rad) and transferred to 0.45 μm nitrocellulose membranes (Bio-Rad). The samples were boiled at 98 °C in reducing Laemmli SDS sample buffer containing 2-mercaptoethanol (Thermo Scientific™) for only 3 min, given that storage and heat affect reelin determination noticeably, particularly through fragmentation of the full-length species [18,34]. Likewise, freezing–thawing cycles before electrophoresis were avoided. The transferred proteins were detected with fluorescent-based imaging using an anti N-terminal reelin mouse monoclonal antibody (1:1000; Millipore MAB5366; epitope 164–189; clone 142) or an anti C-terminal reelin rabbit monoclonal antibody (1:1000; Abcam ab139691; epitope 3250–3350). The transferred proteins were also detected using a Y186 antibody for apoER2 (rabbit monoclonal anti-N-terminal apoER2 186 antibody; 1:4000; generously provided by Prof. Johannes Nimpf, Department of Medical Biochemistry, Max F. Perutz Laboratories,

Medical University of Vienna, Vienna, Austria). Pre-stained molecular weight markers for electrophoresis were obtained from Thermo Scientific (PageRuler™ Plus, ref code# 26,620, or HiMark pre-stained protein standard, ref code# LC5699). A control CSF sample that was previously aliquoted was included into every blot and was used to normalize the immunoreactive signal between immunoblots. The immunoreactivity of each individual band of reelin was corrected with the immunoreactivity of the 180-kDa band (in the case of N-terminal bands) or with the 100-kDa band (in the case of C-terminal bands) from the control sample, reducing interblot variability and allowing for comparisons across blots. For apoER2, the immunoreactivity of the 70 kDa band was also corrected using the same strategy. The blots were then probed with the appropriate conjugated secondary IRDye antibodies (IRDye 680RD goat anti-mouse and IRDye 800RD goat anti-rabbit) and recorded with an Odyssey CLx Infrared Imaging system (LI-COR Biosciences GmbH). Multiplex fluorescence with the two independent antibodies served to simultaneously assess N- and C-terminal reelin. Band intensities were analyzed using LI-COR software (Image Studio Lite). To estimate the quotients between the different reelin bands of each sample, the unprocessed immunoreactivity for each of the bands was considered. All the samples were analyzed in duplicate. All the samples were determined at least in duplicate (duplicates in separate gels) and distributed in the gels to ensure comparison by disease condition and *APOE* genotype. The distribution of the samples in the gels was performed by a member of the team, and the experiment was performed by another, the experimenter, in a blind way.

4.4. Measurement of T-tau and Aβ42 by ELISA

The levels of the AD core biomarkers T-tau and Aβ42 were measured in the CSF using INNOTEST ELISAs (Fujirebio Europe, Gent, Belgium). All the samples were analyzed as part of a clinical routine by board-certified laboratory technicians following strict procedures for the batch-bridging, analysis, and quality control of the individual ELISA plates [78].

4.5. Statistical Analyses

All the data were analyzed using GraphPad Prism 6.0 (GraphPad Software, San Diego, CA, USA). The Kolmogorov–Smirnov test was used to analyze the distribution of each variable. ANOVA was used for parametric variables, and the Kruskal–Wallis test was used for nonparametric variables for comparison between the groups. Student's *t*-test for parametric variables and the Mann–Whitney U test for nonparametric variables were employed for comparison between the means of two groups and for determining *p*-values. Outliers were not excluded. For correlations, Pearson and Spearman tests were used. The results are presented as means ± SEM.

Abbreviations

Aβ: β-amyloid protein; AD: Alzheimer's disease; apoE: apolipoprotein E; apoER2: apolipoprotein E receptor 2; CSF: cerebrospinal fluid; NDC: non-disease control; T-tau: total tau protein.

References

1. Scheltens, P.; de Strooper, B.; Kivipelto, M.; Holstege, H.; Chételat, G.; Teunissen, C.E.; Cummings, J.; van der Flier, W.M. Alzheimer's disease. *Lancet* **2021**, *397*, 1577–1590. [CrossRef]
2. Selkoe, D.J.; Hardy, J. The amyloid hypothesis of Alzheimer's disease at 25 years. *EMBO Mol. Med.* **2016**, *8*, 595–608. [CrossRef]
3. Ranson, J.M.; Rittman, T.; Hayat, S.; Brayne, C.; Jessen, F.; Blennow, K.; van Duijn, C.; Barkhof, F.; Tang, E.; Mummery, C.J.; et al. Modifiable risk factors for dementia and dementia risk profiling. A user manual for Brain Health Services-part 2 of 6. *Alzheimers Res. Ther.* **2021**, *13*, 169. [CrossRef]
4. Rabaneda-Bueno, R.; Mena-Montes, B.; Torres-Castro, S.; Torres-Carrillo, N.; Torres-Carrillo, N.M. Advances in Genetics and Epigenetic Alterations in Alzheimer's Disease: A Notion for Therapeutic Treatment. *Genes* **2021**, *12*, 1959.
5. Panpalli, A.M.; Karaman, Y.; Guntekin, S.; Ergun, M.A. Analysis of genetics and risk factors of Alzheimer's Disease. *Neuroscience* **2016**, *325*, 124–131. [CrossRef]
6. Zhao, N.; Liu, C.C.; Qiao, W.; Bu, G. Apolipoprotein, E, receptors, and modulation of Alzheimer's Disease. *Biol. Psychiatry* **2018**, *83*, 347–357. [CrossRef]
7. Corder, E.H.; Saunders, A.M.; Strittmatter, W.J.; Schmechel, D.E.; Gaskell, P.C.; Small, G.W.; Roses, A.D.; Haines, J.L.; Pericak-Vance, M.A. Gene dose of apolipoprotein E type 4 allele and the risk of Alzheimer's disease in late onset families. *Science* **1993**, *261*, 921–923. [CrossRef]
8. Holtzman, D.M.; Herz, J.; Bu, G. Apolipoprotein E and apolipoprotein E receptors: Normal biology and roles in Alzheimer disease. *Cold Spring Harb. Perspect. Med.* **2012**, *2*, a006312. [CrossRef]

9. Angelopoulou, E.; Paudel, Y.N.; Papageorgiou, S.G.; Piperi, C. APOE Genotype and Alzheimer's Disease: The Influence of Lifestyle and Environmental Factors. *ACS Chem. Neurosci.* **2021**, *12*, 2749–2764. [CrossRef]

10. Dyer, C.A.; Smith, R.S.; Curtiss, L.K. Only multimers of a synthetic peptide of human apolipoprotein E are biologically active. *J. Biol. Chem.* **1991**, *266*, 15009–15015. [CrossRef]

11. DeSilva, U.; D'Arcangelo, G.; Braden, V.V.; Chen, J.; Miao, G.G.; Curran, T.; Green, E.D. The human reelin gene: Isolation, sequencing and mapping on chromosome 7. *Genome Res.* **1997**, *7*, 157–164. [CrossRef]

12. D'Arcangelo, G.; Homayouni, R.; Keshvara, L.; Rice, D.S.; Sheldon, M.; Curran, T. Reelin is a ligand for lipoprotein receptors. *Neuron* **1999**, *24*, 471–479. [CrossRef]

13. Hiesberger, T.; Trommsdorff, M.; Howell, B.W.; Goffinet, A.; Mumby, M.C.; Cooper, J.A.; Herz, J. Direct binding of Reelin to VLDL receptor and ApoE receptor 2 induces tyrosine phosphorylation of disabled-1 and modulates tau phosphorylation. *Neuron* **1999**, *24*, 481–489. [CrossRef]

14. Tissir, F.; Goffinet, A.M. Reelin and brain development. *Nat. Rev. Neurosci.* **2003**, *4*, 496–505. [CrossRef]

15. Chai, X.; Frotscher, M. How does Reelin signaling regulate the neuronal cytoskeleton during migration? *Neurogenesis* **2016**, *3*, e1242455. [CrossRef]

16. Lane-Donovan, C.; Herz, J. The ApoE receptors Vldlr and Apoer2 in central nervous system function and disease. *J. Lipid Res.* **2017**, *58*, 1036–1043. [CrossRef]

17. Sáez-Valero, J.; Costell, M.; Sjögren, M.; Andreasen, N.; Blennow, K.; Luque, J.M. Altered levels of cerebrospinal fluid reelin in frontotemporal dementia and Alzheimer's disease. *J. Neurosci. Res.* **2003**, *72*, 132–136. [CrossRef]

18. Botella-Lopez, A.; Burgaya, F.; Gavin, R.; Garcia-Ayllon, M.S.; Gomez-Tortosa, E.; Peña-Casanova, J.; Urena, J.M.; del Rio, J.A.; Blesa, R.; Soriano, E.; et al. Reelin expression and glycosylation patterns are altered in Alzheimer's disease. *Proc. Natl. Acad. Sci. USA* **2006**, *103*, 5573–5578. [CrossRef]

19. Cuchillo-Ibañez, I.; Mata-Balaguer, T.; Balmaceda, V.; Arranz, J.J.; Nimpf, J.; Sáez-Valero, J. The beta-amyloid peptide compromises Reelin signaling in Alzheimer's disease. *Sci. Rep.* **2016**, *6*, 31646. [CrossRef]

20. Cuchillo-Ibañez, I.; Balmaceda, V.; Botella-Lopez, A.; Rabano, A.; Avila, J.; Sáez-Valero, J. Beta-amyloid impairs reelin signaling. *PLoS ONE* **2013**, *8*, e72297. [CrossRef]

21. Kubo, K.; Mikoshiba, K.; Nakajima, K. Secreted Reelin molecules form homodimers. *Neurosci. Res.* **2002**, *43*, 381–388. [CrossRef]

22. Yasui, N.; Kitago, Y.; Beppu, A.; Kohno, T.; Morishita, S.; Gomi, H.; Nagae, M.; Hattori, M.; Takagi, J. Functional importance of covalent homodimer of reelin protein linked via its central region. *J. Biol. Chem.* **2011**, *286*, 35247–35256. [CrossRef] [PubMed]

23. Dlugosz, P.; Tresky, R.; Nimpf, J. Differential Action of Reelin on Oligomerization of ApoER2 and VLDL Receptor in HEK293 Cells Assessed by Time-Resolved Anisotropy and Fluorescence Lifetime Imaging Microscopy. *Front. Mol. Neurosci.* **2019**, *12*, 53. [CrossRef] [PubMed]

24. Jossin, Y.; Gui, L.; Goffinet, A.M. Processing of Reelin by embryonic neurons is important for function in tissue but not in dissociated cultured neurons. *J. Neurosci.* **2007**, *27*, 4243–4252. [CrossRef] [PubMed]

25. Hoe, H.S.; Cooper, M.J.; Burns, M.P.; Lewis, P.A.; van der Brug, M.; Chakraborty, G.; Cartagena, C.M.; Pak, D.T.; Cookson, M.R.; Rebeck, G.W. The metalloprotease inhibitor TIMP-3 regulates amyloid precursor protein and apolipoprotein E receptor proteolysis. *J. Neurosci.* **2007**, *27*, 10895–10905. [CrossRef] [PubMed]

26. Hibi, T.; Hattori, M. The N-terminal fragment of Reelin is generated after endocytosis and released through the pathway regulated by Rab11. *FEBS Lett.* **2009**, *583*, 1299–1303. [CrossRef]

27. Balmaceda, V.; Cuchillo-Ibáñez, I.; Pujadas, L.; García-Ayllón, M.S.; Saura, C.A.; Nimpf, J.; Soriano, E.; Sáez-Valero, J. ApoER2 processing by presenilin-1 modulates reelin expression. *FASEB J.* **2014**, *28*, 1543–1554. [CrossRef]

28. Hattori, M.; Kohno, T. Regulation of Reelin functions by specific proteolytic processing in the brain. *J. Biochem.* **2021**, *169*, 511–516. [CrossRef]

29. Turk, L.S.; Kuang, X.; Dal Pozzo, V.; Patel, K.; Chen, M.; Huynh, K.; Currie, M.J.; Mitchell, D.; Dobson, R.C.J.; D'Arcangelo, G.; et al. The structure-function relationship of a signaling-competent; dimeric Reelin fragment. *Structure* **2021**, *29*, 1156–1170. [CrossRef]

30. Koch, S.; Strasser, V.; Hauser, C.; Fasching, D.; Brandes, C.; Bajari, T.M.; Schneider, W.J.; Nimpf, J. A secreted soluble form of ApoE receptor 2 acts as a dominant-negative receptor and inhibits Reelin signaling. *EMBO J.* **2002**, *21*, 5996–6004. [CrossRef]

31. Smalheiser, N.R.; Costa, E.; Guidotti, A.; Impagnatiello, F.; Auta, J.; Lacor, P.; Kriho, V.; Pappas, G.D. Expression of reelin in adult mammalian blood; liver; pituitary pars intermedia; and adrenal chromaffin cells. *Proc. Natl. Acad. Sci. USA* **2000**, *97*, 1281–1286. [CrossRef] [PubMed]

32. Kohno, T.; Honda, T.; Kubo, K.; Nakano, Y.; Tsuchiya, A.; Murakami, T.; Banno, H.; Nakajima, K.; Hattori, M. Importance of Reelin C-terminal region in the development and maintenance of the postnatal cerebral cortex and its regulation by specific proteolysis. *J. Neurosci.* **2015**, *35*, 4776–4787. [CrossRef] [PubMed]

33. Ignatova, N.; Sindic, C.J.; Goffinet, A.M. Characterization of the various forms of the Reelin protein in the cerebrospinal fluid of normal subjects and in neurological diseases. *Neurobiol. Dis.* **2004**, *15*, 326–330. [CrossRef] [PubMed]

34. Lugli, G.; Krueger, J.M.; Davis, J.M.; Persico, A.M.; Keller, F.; Smalheiser, N.R. Methodological factors influencing measurement and processing of plasma reelin in humans. *BMC Biochem.* **2003**, *4*, 9. [CrossRef] [PubMed]

35. Jack, C.R., Jr.; Bennett, D.A.; Blennow, K.; Carrillo, M.C.; Dunn, B.; Haeberlein, S.B.; Holtzman, D.M.; Jagust, W.; Jessen, F.; Karlawish, J.; et al. NIA-AA Research Framework: Toward a biological definition of Alzheimer's disease. *Alzheimers Dement.* **2018**, *14*, 535–562. [CrossRef] [PubMed]

36. Hansson, O.; Zetterberg, H.; Buchhave, P.; Londos, E.; Blennow, K.; Minthon, L. Association between CSF biomarkers and incipient Alzheimer's disease in patients with mild cognitive impairment: A follow-up study. *Lancet Neurol.* **2006**, *5*, 228–234. [CrossRef]

37. Strasser, V.; Fasching, D.; Hauser, C.; Mayer, H.; Bock, H.H.; Hiesberger, T.; Herz, J.; Weeber, E.J.; Sweatt, J.D.; Pramatarova, A.; et al. Receptor clustering is involved in Reelin signaling. *Mol. Cell Biol.* **2004**, *24*, 1378–1386. [CrossRef]

38. Lopez-Font, I.; Iborra-Lazaro, G.; Sanchez-Valle, R.; Molinuevo, J.L.; Cuchillo-Ibañez, I.; Sáez-Valero, J. CSF-ApoER2 fragments as a read-out of reelin signaling: Distinct patterns in sporadic and autosomal-dominant Alzheimer disease. *Clin. Chim. Acta* **2019**, *490*, 6–11. [CrossRef]

39. Botella-Lopez, A.; Cuchillo-Ibañez, I.; Cotrufo, T.; Mok, S.S.; Li, Q.X.; Barquero, M.S.; Dierssen, M.; Soriano, E.; Sáez-Valero, J. Beta-amyloid controls altered Reelin expression and processing in Alzheimer's disease. *Neurobiol. Dis.* **2010**, *37*, 682–691. [CrossRef]

40. Mata-Balaguer, T.; Cuchillo-Ibañez, I.; Calero, M.; Ferrer, I.; Sáez-Valero, J. Decreased generation of C-terminal fragments of ApoER2 and increased reelin expression in Alzheimer's disease. *FASEB J.* **2018**, *32*, 3536–3546. [CrossRef]

41. Wirths, O.; Multhaup, G.; Czech, C.; Blanchard, V.; Tremp, G.; Pradier, L.; Beyreuther, K.; Bayer, T.A. Reelin in plaques of beta-amyloid precursor protein and presenilin-1 double-transgenic mice. *Neurosci. Lett.* **2001**, *316*, 145–148. [CrossRef]

42. Chin, J.; Massaro, C.M.; Palop, J.J.; Thwin, M.T.; Yu, G.Q.; Bien-Ly, N.; Bender, A.; Mucke, L. Reelin depletion in the entorhinal cortex of human amyloid precursor protein transgenic mice and humans with Alzheimer's disease. *J. Neurosci.* **2007**, *27*, 2727–2733. [CrossRef]

43. Herring, A.; Donath, A.; Steiner, K.M.; Widera, M.P.; Hamzehian, S.; Kanakis, D.; Kolble, K.; ElAli, A.; Hermann, D.M.; Paulus, W.; et al. Reelin depletion is an early phenomenon of Alzheimer's pathology. *J. Alzheimers Dis.* **2012**, *30*, 963–979. [CrossRef] [PubMed]

44. Cuchillo-Ibañez, I.; Balmaceda, V.; Mata-Balaguer, T.; Lopez-Font, I.; Sáez-Valero, J. Reelin in Alzheimer's Disease; Increased Levels but Impaired Signaling: When More is Less. *J. Alzheimers Dis.* **2016**, *52*, 403–416. [CrossRef] [PubMed]

45. Mathews, S.T.; Plaisance, E.P.; Kim, T. Imaging systems for westerns: Chemiluminescence vs. infrared detection. *Methods Mol. Biol.* **2009**, *536*, 499–513. [PubMed]

46. Gingrich, J.C.; Davis, D.R.; Nguyen, Q. Multiplex detection and quantitation of proteins on western blots using fluorescent probes. *Biotechniques* **2000**, *29*, 636–642. [CrossRef]

47. Ogino, H.; Hisanaga, A.; Kohno, T.; Kondo, Y.; Okumura, K.; Kamei, T.; Sato, T.; Asahara, H.; Tsuiji, H.; Fukata, M.; et al. Secreted Metalloproteinase ADAMTS-3 Inactivates Reelin. *J. Neurosci.* **2017**, *37*, 3181–3191. [CrossRef]

48. Jossin, Y. Reelin Functions; Mechanisms of Action and Signaling Pathways During Brain Development and Maturation. *Biomolecules* **2020**, *10*, 964. [CrossRef]

49. Krstic, D.; Rodriguez, M.; Knuesel, I. Regulated proteolytic processing of Reelin through interplay of tissue plasminogen activator (tPA), ADAMTS-4, ADAMTS-5 and their modulators. *PLoS ONE* **2012**, *7*, e47793. [CrossRef]

50. Tsuneura, Y.; Sawahata, M.; Itoh, N.; Miyajima, R.; Mori, D.; Kohno, T.; Hattori, M.; Sobue, A.; Nagai, T.; Mizoguchi, H.; et al. Analysis of Reelin signaling and neurodevelopmental trajectory in primary cultured cortical neurons with RELN deletion identified in schizophrenia. *Neurochem. Int.* **2021**, *144*, 104954. [CrossRef]

51. Jefferson, T.; Čaušević, M.; auf dem Keller, U.; Schilling, O.; Isbert, S.; Geyer, R.; Maier, W.; Tschickardt, S.; Jumpertz, T.; Weggen, S.; et al. Metalloprotease meprin beta generates nontoxic N-terminal amyloid precursor protein fragments in vivo. *J. Biol. Chem.* **2011**, *286*, 27741–27750. [CrossRef]

52. Bien, J.; Jefferson, T.; Causevic, M.; Jumpertz, T.; Munter, L.; Multhaup, G.; Weggen, S.; Becker-Pauly, C.; Pietrzik, C.U. The metalloprotease meprin beta generates amino terminal-truncated amyloid beta peptide species. *J. Biol. Chem.* **2012**, *287*, 33304–33313. [CrossRef]

53. Medoro, A.; Bartollino, S.; Mignogna, D.; Marziliano, N.; Porcile, C.; Nizzari, M.; Florio, T.; Pagano, A.; Raimo, G.; Intrieri, M.; et al. Proteases Upregulation in Sporadic Alzheimer's Disease Brain. *J. Alzheimers Dis.* **2019**, *68*, 931–938. [CrossRef]

54. Angelucci, F.; Cechova, K.; Prusa, R.; Hort, J. Amyloid beta soluble forms and plasminogen activation system in Alzheimer's disease: Consequences on extracellular maturation of brain-derived neurotrophic factor and therapeutic implications. *CNS Neurosci. Ther.* **2019**, *25*, 303–313. [CrossRef]

55. Hanzel, C.E.; Iulita, M.F.; Eyjolfsdottir, H.; Hjorth, E.; Schultzberg, M.; Eriksdotter, M.; Cuello, A.C. Analysis of matrix metalloproteases and the plasminogen system in mild cognitive impairment and Alzheimer's disease cerebrospinal fluid. *J. Alzheimers Dis.* **2014**, *40*, 667–678. [CrossRef]

56. Whelan, C.D.; Mattsson, N.; Nagle, M.W.; Vijayaraghavan, S.; Hyde, C.; Janelidze, S.; Stomrud, E.; Lee, J.; Fitz, L.; Samad, T.A.; et al. Multiplex proteomics identifies novel CSF and plasma biomarkers of early Alzheimer's disease. *Acta Neuropathol. Commun.* **2019**, *7*, 169. [CrossRef]

57. Garcia-Ayllón, M.S.; Campanari, M.L.; Brinkmalm, G.; Rabano, A.; Alom, J.; Saura, C.A.; Andreasen, N.; Blennow, K.; Sáez-Valero, J. CSF Presenilin-1 complexes are increased in Alzheimer's disease. *Acta Neuropathol. Commun.* **2013**, *1*, 46. [CrossRef]

58. Sogorb-Esteve, A.; Garcia-Ayllon, M.S.; Fortea, J.; Sanchez-Valle, R.; Lleo, A.; Molinuevo, J.L.; Sáez-Valero, J. Cerebrospinal fluid Presenilin-1 increases at asymptomatic stage in genetically determined Alzheimer's disease. *Mol. Neurodegener.* **2016**, *11*, 66. [CrossRef]

59. Kumar, R.; Nordberg, A.; Darreh-Shori, T. Amyloid-beta peptides act as allosteric modulators of cholinergic signalling through formation of soluble BAbetaACs. *Brain* **2016**, *139*, 174–192. [CrossRef]

60. Kanekiyo, T.; Xu, H.; Bu, G. ApoE and Abeta in Alzheimer's disease: Accidental encounters or partners? *Neuron* **2014**, *81*, 740–754. [CrossRef]

61. Tai, L.M.; Mehra, S.; Shete, V.; Estus, S.; Rebeck, G.W.; Bu, G.; LaDu, M.J. Soluble apoE/Abeta complex: Mechanism and therapeutic target for APOE4-induced AD risk. *Mol. Neurodegener.* **2014**, *9*, 2. [CrossRef]

62. Pujadas, L.; Rossi, D.; Andres, R.; Teixeira, C.M.; Serra-Vidal, B.; Parcerisas, A.; Maldonado, R.; Giralt, E.; Carulla, N.; Soriano, E. Reelin delays amyloid-beta fibril formation and rescues cognitive deficits in a model of Alzheimer's disease. *Nat. Commun.* **2014**, *5*, 3443. [CrossRef] [PubMed]

63. Beffert, U.; Weeber, E.J.; Durudas, A.; Qiu, S.; Masiulis, I.; Sweatt, J.D.; Li, W.P.; Adelmann, G.; Frotscher, M.; Hammer, R.E.; et al. Modulation of synaptic plasticity and memory by Reelin involves differential splicing of the lipoprotein receptor Apoer2. *Neuron* **2005**, *47*, 567–579. [CrossRef] [PubMed]

64. He, X.; Cooley, K.; Chung, C.H.; Dashti, N.; Tang, J. Apolipoprotein receptor 2 and X11 alpha/beta mediate apolipoprotein E-induced endocytosis of amyloid-beta precursor protein and beta-secretase, leading to amyloid-beta production. *J. Neurosci.* **2007**, *27*, 4052–4060. [CrossRef] [PubMed]

65. Wang, W.; Moerman-Herzog, A.M.; Slaton, A.; Barger, S.W. Presenilin 1 mutations influence processing and trafficking of the ApoE receptor apoER2. *Neurobiol. Aging* **2017**, *49*, 145–153. [CrossRef]

66. Huang, Z.J.; Cao, F.; Wu, Y.; Peng, J.H.; Zhong, J.J.; Jiang, Y.; Yin, C.; Guo, Z.D.; Sun, X.C.; Jiang, L.; et al. Apolipoprotein E promotes white matter remodeling via the Dab1-dependent pathway after traumatic brain injury. *CNS Neurosci. Ther.* **2020**, *26*, 698–710. [CrossRef]

67. Xian, X.; Pohlkamp, T.; Durakoglugil, M.S.; Wong, C.H.; Beck, J.K.; Lane-Donovan, C.; Plattner, F.; Herz, J. Reversal of ApoE4-induced recycling block as a novel prevention approach for Alzheimer's disease. *eLife* **2018**, *30*, e40048. [CrossRef]

68. Divekar, S.D.; Burrell, T.C.; Lee, J.E.; Weeber, E.J.; Rebeck, G.W. Ligand-induced homotypic and heterotypic clustering of apolipoprotein E receptor 2. *J. Biol. Chem.* **2014**, *289*, 15894–15903. [CrossRef]

69. Weisgraber, K.H.; Shinto, L.H. Identification of the disulfide-linked homodimer of apolipoprotein E3 in plasma. Impact on receptor binding activity. *J. Biol. Chem.* **1991**, *266*, 12029–12034. [CrossRef]

70. Chen, Y.; Durakoglugil, M.S.; Xian, X.; Herz, J. ApoE4 reduces glutamate receptor function and synaptic plasticity by selectively impairing ApoE receptor recycling. *Proc. Natl. Acad. Sci. USA* **2010**, *107*, 12011–12016. [CrossRef]

71. Ringland, C.; Schweig, J.E.; Paris, D.; Shackleton, B.; Lynch, C.E.; Eisenbaum, M.; Mullan, M.; Crawford, F.; Abdullah, L.; Bachmeier, C. Apolipoprotein E isoforms differentially regulate matrix metallopeptidase 9 function in Alzheimer's disease. *Neurobiol. Aging* **2020**, *95*, 56–68. [CrossRef]

72. Hisanaga, A.; Morishita, S.; Suzuki, K.; Sasaki, K.; Koie, M.; Kohno, T.; Hattori, M. A disintegrin and metalloproteinase with thrombospondin motifs 4 (ADAMTS-4) cleaves Reelin in an isoform-dependent manner. *FEBS Lett.* **2012**, *586*, 3349–3353. [CrossRef] [PubMed]

73. Lane-Donovan, C.; Philips, G.T.; Wasser, C.R.; Durakoglugil, M.S.; Masiulis, I.; Upadhaya, A.; Pohlkamp, T.; Coskun, C.; Kotti, T.; Steller, L.; et al. Reelin protects against amyloid β toxicity in vivo. *Sci. Signal.* **2015**, *8*, ra67. [CrossRef] [PubMed]

74. Durakoglugil, M.S.; Chen, Y.; White, C.L.; Kavalali, E.T.; Herz, J. Reelin signaling antagonizes beta-amyloid at the synapse. *Proc. Natl. Acad. Sci. USA* **2009**, *106*, 15938–15943. [CrossRef] [PubMed]

75. Tsuneura, Y.; Nakai, T.; Mizoguchi, H.; Yamada, K. New Strategies for the Treatment of Neuropsychiatric Disorders Based on Reelin Dysfunction. *Int. J. Mol. Sci.* **2022**, *23*, 1829. [CrossRef]

76. Rogers, J.T.; Rusiana, I.; Trotter, J.; Zhao, L.; Donaldson, E.; Pak, D.T.; Babus, L.W.; Peters, M.; Banko, J.L.; Chavis, P.; et al. Reelin supplementation enhances cognitive ability, synaptic plasticity, and dendritic spine density. *Learn. Mem.* **2011**, *18*, 558–564. [CrossRef]

77. Blennow, K.; Ricksten, A.; Prince, J.A.; Brookes, A.J.; Emahazion, T.; Wasslavik, C.; Bogdanovic, N.; Andreasen, N.; Batsman, S.; Marcusson, J.; et al. No association between the alpha2-macroglobulin (A2M) deletion and Alzheimer's disease, and no change in A2M mRNA, protein or protein expression. *J. Neural Transm.* **2000**, *107*, 1065–1079. [CrossRef]

78. Palmqvist, S.; Zetterberg, H.; Blennow, K.; Vestberg, S.; Andreasson, U.; Brooks, D.J.; Owenius, R.; Hagerstrom, D.; Wollmer, P.; Minthon, L.; et al. Accuracy of brain amyloid detection in clinical practice using cerebrospinal fluid beta-amyloid 42: A cross-validation study against amyloid positron emission tomography. *JAMA Neurol.* **2014**, *71*, 1282–1289. [CrossRef]

120

ARTICLE #3: THE APOLIPOPROTEIN RECEPTOR LRP3 COMPROMISES APP LEVELS

Inmaculada Cuchillo-Ibáñez, **Matthew Paul Lennol**, Sergio Escamilla, Trinidad Mata-Balaguer, Lucía Valverde-Vozmediano, Inmaculada López-Font, Isidro Ferrer & Javier Sáez-Valero

RESEARCH

The apolipoprotein receptor LRP3 compromises APP levels

Inmaculada Cuchillo-Ibañez[1,2,3*] ●, Matthew P. Lennol[1,2], Sergio Escamilla[1,2], Trinidad Mata-Balaguer[1,2], Lucía Valverde-Vozmediano[1], Inmaculada Lopez-Font[1,2,3], Isidro Ferrer[2,4] and Javier Sáez-Valero[1,2,3*]

Abstract

Background: Members of the low-density lipoprotein (LDL) receptor family are involved in endocytosis and in transducing signals, but also in amyloid precursor protein (APP) processing and β-amyloid secretion. ApoER2/LRP8 is a member of this family with key roles in synaptic plasticity in the adult brain. ApoER2 is cleaved after the binding of its ligand, the reelin protein, generating an intracellular domain (ApoER2-ICD) that modulates reelin gene transcription itself. We have analyzed whether ApoER2-ICD is able to regulate the expression of other LDL receptors, and we focused on LRP3, the most unknown member of this family. We analyzed LRP3 expression in middle-aged individuals (MA) and in cases with Alzheimer's disease (AD)-related pathology, and the relation of LRP3 with APP.

Methods: The effects of full-length ApoER2 and ApoER2-ICD overexpression on protein levels, in the presence of recombinant reelin or Aβ42 peptide, were evaluated by microarray, qRT-PCRs, and western blots in SH-SY5Y cells. LRP3 expression was analyzed in human frontal cortex extracts from MA subjects (mean age 51.8 ± 4.8 years) and AD-related pathology subjects [Braak neurofibrillary tangle stages I–II, 68.4 ± 8.8 years; III–IV, 80.4 ± 8.8 years; V–VI, 76.5 ± 9.7 years] by qRT-PCRs and western blot; LRP3 interaction with other proteins was assessed by immunoprecipitation. In CHO cells overexpressing LRP3, protein levels of full-length APP and fragments were evaluated by western blots. Chloroquine was employed to block the lysosomal/autophagy function.

Results: We have identified that ApoER2 overexpression increases LRP3 expression, also after reelin stimulation of ApoER2 signaling. The same occurred following ApoER2-ICD overexpression. In extracts from subjects with AD-related pathology, the levels of LRP3 mRNA and protein were lower than those in MA subjects. Interestingly, LRP3 transfection in CHO-PS70 cells induced a decrease of full-length APP levels and APP-CTF, particularly in the membrane fraction. In cell supernatants, levels of APP fragments from the amyloidogenic (sAPPα) or non-amyloidogenic (sAPPβ) pathways, as well as Aβ peptides, were drastically reduced with respect to mock-transfected cells. The inhibitor of lysosomal/autophagy function, chloroquine, significantly increased full-length APP, APP-CTF, and sAPPα levels.

Conclusions: ApoER2/reelin signaling regulates LRP3 expression, whose levels are affected in AD; LRP3 is involved in the regulation of APP levels.

Keywords: sAPP, ApoER2, ApoER2-ICD, Beta-amyloid, Alzheimer's disease, Chloroquine, Differential centrifugation, Autophagy

*Correspondence: icuchillo@umh.es; j.saez@umh.es
[1] Instituto de Neurociencias de Alicante, Universidad Miguel Hernández de Elche-CSIC, Sant Joan d'Alacant, Spain
[2] Centro de Investigación Biomédica en Red sobre Enfermedades Neurodegenerativas (CIBERNED), Madrid, Spain
Full list of author information is available at the end of the article

Introduction

The members of the family of low-density lipoprotein (LDL) receptors are endocytic receptors that mediate the uptake of lipoproteins and have been classically studied for their role in cholesterol transport and metabolism. Robust evidence indicates that LDL receptor family

Cuchillo-Ibañez et al. Alz Res Therapy   (2021) 13:181

Page 2 of 17

members are involved in synaptic plasticity regulation and neuronal migration (extensively reviewed in [1–6]). LDL receptors are related to Alzheimer's disease (AD) pathogenesis as receptors of apolipoprotein E (apoE) [7], being the APOE4 variant the largest known genetic risk factor for late-onset sporadic AD [8, 9]. Additionally, several members of the LDL receptor family are able to modulate the amyloid precursor (APP) proteolytic processing, either by regulation of the generation of the β-amyloid peptide (Aβ) or through Aβ clearance [10–13].

An important member of the LDL receptor family, ApoER2/LRP8, can exert a modulatory effect in transcriptional expression. ApoER2 interaction with its ligand, the reelin protein, drives to a sequential proteolytic processing, resulting in the cleavage of the receptor by α-secretase, which generates a membrane-tethered C-terminal fragment (ApoER2-CTF), followed by the cleavage by γ-secretase. The action of γ-secretase generates an intracellular domain fragment (ApoER2-ICD) capable of decreasing the expression of reelin mRNA [14, 15]. Using the same brain extracts as in [14], we found later that the generation of ApoER2-CTF appeared lower and, accordingly, reelin expression resulted higher with respect to those in control brain extracts [16].

In this study, we have further explored the modulatory transcriptional activity of ApoER2/reelin signaling, and we have observed that this pathway can modulate the expression of the LDL-related protein 3 (LRP3). LRP3 is probably the most unknown member of a new subfamily of LDL receptors [17], whose precise role in the central nervous system is still undetermined. We have estimated LRP3 expression in the frontal cortex of middle-aged (MA) individuals and in cases with Alzheimer's disease (AD)-related pathology, and after overexpression in CHO cells. We have demonstrated that LRP3 is able to modulate APP expression.

Material and methods

Human brain samples

This study was approved by the ethics committee of Universidad Miguel Hernández de Elche, Spain, and it was carried out in accordance with the WMA Declaration of Helsinki. Brain samples (frontal cortex; see Table 1) were obtained from the Brain Bank of the Institute of Neuropathology, Bellvitge University Hospital. Cases with AD-related pathology were considered those showing neurofibrillary tangles (NFT) and/or senile plaques with the distribution established by Braak and Braak at the post-mortem neuropathological examination [18]. These were categorized as Braak NFT stages I–II $n = 14$, 1 female/13 males, 68.4 ± 8.8 years; Braak stages III–IV, $n = 14$, 7 females/7 males, 80.4 ± 8.2 years; and Braak

stages V–VI, $n = 12$, 5 females/7 males, 76.5 ± 9.7 years. Cases at NFT stages I–II showed no or moderate numbers of senile plaques (mostly scores 0 and A); cases at stages III–IV usually had moderate numbers of senile plaques (mostly score B); cases at stages V–VI had heavy senile plaque burden (mostly score C; Table 1). Cases at stages I, II, and III did not have cognitive impairment; three cases at stage IV had moderate cognitive impairment, and cases at stages V and VI had suffered from dementia. Special care was taken not to include cases with combined pathologies to avoid bias in the pathological series. Samples from middle-aged (MA) subjects (3 females/8 males; average age 51.8 ± 4.8 years) corresponded to individuals with no neurological diseases and no evidence of NFTs and senile plaques. The mean post-mortem interval of the tissue was ~8 h in all cases, with no significant difference between the groups.

A major concern in the design of the study is the age of the different groups of human cases. MA individuals are younger (51.8 ± 4.8 years) when compared with cases with AD-related pathology (NFT I–II 68.4 ± 8.8, III–IV 80.4 ± 8.2, and V–VI 76.5 ± 9.7). This selection is due to the fact that the majority of individuals aged 65 years or older have stages I–III of NFT pathology, and, therefore, it is difficult to have samples of age-matched controls without AD-related pathology and morbidities considered in the selection of NFT series that could have an impact on the results [20].

Cell cultures

SH-SY5Y cells, a human neuroblastoma cell line, were seeded at a density of 1×10^5 cells/well in 6-well plates and cultured in Dulbecco's modified Eagle medium (DMEM) supplemented with Glutamax (GIBCO Thermo Fisher Scientific, Rockford, USA), 1% heat-inactivated fetal bovine serum (FBS), penicillin (100 U/ml), and streptomycin (100 µg/ml) in a 5% CO_2 incubator. To neuro-differentiate the cells, all-trans-retinoic acid (RA, Sigma-Aldrich Co, MO, USA) was employed. RA enhances neuronal markers, reelin and ApoER2 expression [21, 22]. Ten micromolar RA diluted in DMEM with 1% FBS was added every 2 days. After 6 days, cells were treated with recombinant reelin, 12 µg/ml for 24 h. Other cells were treated with suspensions of β-amyloid 1–42 (Aβ$_{42}$) or scrambled control peptide (Aβsc; AIAEGDSH-VLKEGAYMEIFDVQGHVFGGKIFRVVDLGSHNVA) (both from Anaspec Peptide, Eurogentec) in DMEM with 1% FBS, for two consecutive days without changing the media, at a final concentration of 500 nM, 1 µM, or 5 µM.

Non-differentiated SH-SY5Y cells were transfected with Lipofectamine 3000 (ThermoFisher) following manufacturer's instructions, with a construct encoding

Table 1 Human samples

	Age (y)	Gender	PM (h)	SP	ApoE
MA NFT					
0	46	f	9.5	0	e2/e3
	46	m	19		e3/e4
	47	m	5		e3/e3
	49	m	7.5		e3/e3
	50	m	17		e3/e3
	52	m	5		e3/e3
	52	f	6		e4/e4
	53	m	7.5		e3/e3
	56	m	4		e2/e3
	59	m	6.5		e3/e3
	60	f	11.5		e3/e3
AD NFT					
Braak I	53	m	6.25	A	e3/e4
	64	m	6.5	0	e3/e3
	67	m	14.5	0	e3/e3
	68	m	11	0	e2/e3
Braak II	57	m	4.5	0	e3/e4
	60	f	9.5	A	e3/e3
	65	m	16.3	0	e3/e3
	67	m	7.25	0	e3/e4
	69	m	3.5	A	e3/e4
	72	m	6.25	A	e3/e3
	74	m	5.5	A	e2/e3
	78	m	16	0	e3/e3
	78	m	10.75	B	e3/e4
	86	m	5.5	A	e2/e3
Braak III	68	f	4.5	A	e3/e3
	71	m	7.5	0	e2/e3
	73	m	4	0	e3/e3
	76	f	4	B	e3/e3
	77	m	13.3	C	e3/e4
	77	m	5.5	A	e3/e3
	79	f	3.5	B	e3/e3
	82	f	5	A	e3/e3
	90	f	4	B	e3/e3
Braak IV	79	m	5	A	e4/e4
	81	f	5	C	e3/e3
	85	m	14	B	e3/e4
	89	m	3.5	B	e3/e4
	99	f	5	B	e3/e3
Braak V	72	m	2.75	C	e3/e4
	73	m	4.5	B	e3/e4
	74	f	9	A	e3/e4
	75	m	11.3	B	e3/e4
	77	m	16	C	e3/e3
	78	m	17	0	e3/e3
	81	f	5.5	C	e3/e4
	87	m	7	C	e3/e3
	93	m	3	C	e3/e3

Table 1 (continued)

	Age (y)	Gender	PM (h)	SP	ApoE
Braak VI	56	f	7	C	e3/e3
	67	f	8	C	e3/e4
	86	f	20.3	C	e3/e3

Middle-aged (MA) cases and cases with AD-related pathology (AD). Subjects were categorized according to the Braak stage of neurofibrillary tangle (NFT I–VI) and senile plaque staging (0–C) [18, 19]. Age (y years), gender (m male, f female), post-mortem (PM, h hours), SP senile plaques, APOE (APOE alleles, e2, e3, and e4)

full-length ApoER2 (pEGFPN1-*Mus musculus* ApoER2, residues 1–842) and ApoER2-ICD-HA expressing only the cytoplasmic domain (residues 728–842) (both generously provided by Dr W. Rebeck; see ref. [23, 24]), or with GFP/cDNA3.1 as mock transfection as in [14] for 48 h. After 24 h post-transfection, some CHO-PS70 cells were treated with 10 µM chloroquine for another 24 h.

CHO cells stably overexpressing wild-type human APP (CHO-PS70, [25]) were grown in DMEM® containing 10% FBS, 0.1% Puromycin (Sigma-Aldrich), and 0.2% G418 disulfate salt (Sigma-Aldrich). CHO-PS70 cells were transfected with full-length human LRP3 cDNA (3×FLAG-LRP3 in pCMV7.1; a kind gift from Christine Lavoie, [26]) for 48 h. After 24 h post-transfection, some CHO-PS70 cells were treated with 10 µM chloroquine for 24 h.

Brain membrane-enriched fractions

Brain cortex samples were homogenized using a polytron Heidolph RZR-1 at 600–800 rpm, in a glass potter applying 10–15 pulses in buffer at 10% (w/v) (Hepes 1mM, sucrose 0.32 M, Cl_2Mg mM, EDTA 1mM, $NaHCO_3$ 1mM, PMSF, protease inhibitors (Cocktail Complete EDTA free, Roche), antiphosphatase inhibitor (PhosS-TOP, Sigma)). The homogenate was centrifuged at 1000 $\times g$ during 20 min at 4°C. The supernatant (post-nuclear fraction) was centrifuged at 13000 $\times g$ during 15 min at 4°C. The supernatant (cytosolic fraction) was aliquoted, and the resulting pellet (membrane-enriched fraction) was resuspended in buffer (Hepes 1mM, Cl_2Mg mM, EDTA 1mM, $NaHCO_3$ 1mM, PMSF, protease inhibitor cocktail (Sigma-Aldrich), antiphosphatase inhibitor (Sigma-Aldrich)).

In some CHO-PS70 cells, we performed a differential centrifugation. After homogenization of cell extracts in sucrose buffer (0.32 M sucrose, 10 mM Tris pH 7.4, EGTA, 1 mM Na_3VO_4, 5 mM NaF, 1 mM EDTA, 1 mM Hepes), the homogenate was centrifuged at 1000 $\times g$ for 10 min. The supernatant was centrifuged at 15000 $\times g$ for 15 min. The resultant supernatant (fraction containing mainly the plasma membrane and soluble proteins from the cytosol) and the pellet (containing mainly membranes

125

from the endoplasmic reticulum, mitochondria, lysosomes, peroxisomes, and endosomes) were quantified and stored.

Microarray analysis

Gene expression was analyzed 48 h after transfection with human full-length ApoER2, using microarrays Sure-Print G3 Human Microarrays (ID 039494, Agilent Technologies, Spain) and performed by Bioarray SL. (http://www.bioarray.es). The concentration and purity of the total RNA extracted were measured by a NanoDrop spectrophotometer, and RNA quality was determined with the kit R6K Screen Tape (Agilent Technologies, Spain). The estimated RNA integrity number ranged between 9.5 and 9.7. Each sample (four samples and four controls) was labeled with Cy3 using the One-Color Microarray-Based Gene Expression Microarrays Analysis v.6.6 (Agilent Technologies, Spain). Data were imported to the linear models for microarray data Bioconductor software (Limma, Marray, affy, pcaMethods and EMA). Raw data were first subjected to background subtraction, then to within-array loess normalization. Finally, across-array normalization was performed. Normalized data were fitted to a linear model. The significance of the gene expression changes was analyzed according to the adjusted p value (adj. $p < 0.05$).

qRT-PCR analysis

RNA was extracted from human brains, SH-SY5Y cells, or CHO-PS70 cells using the TRIzol® Reagent in the PureLink™ Micro-to-Midi Total RNA Purification System (Life Technologies, Carlsbad, CA, USA) following the manufacturer's instructions. SuperScript™ III Reverse Transcriptase (Life Technologies, Carlsbad, CA, USA) was used to synthesize cDNAs from this total RNA (2 µg) using random primers according to the manufacturer's instructions. Quantitative PCR amplification was performed on a StepOne™ Real-Time PCR System (Applied Biosystems, Thermo Fisher Scientific, Rockford, USA) with TaqMan probes specific for human *LRP3* (assay ID: HS01041220_m1), *LDLR* (assay ID: HS00181192_m1) (Applied Biosystems, Thermo Fisher Scientific, Rockford, USA), and human *18S* as a housekeeping gene (Applied Biosystems, Thermo Fisher Scientific, Rockford, USA) for the human brain and SH-SY5Y cell samples. In CHO-PS70, mRNA expression was measured with primers for human APP (forward: AAC CAGTGACCATCCAGAAC; reverse: ACTTGTCAG GAACGAGAAGG) and for glyceraldehyde 3-phosphate dehydrogenase (GAPDH, forward: AGAAGGTGGTGA AGCAGGCAT; reverse: AGGTCCACCACTCTGTTG CTGT) to normalize the expression levels of the target gene by the ΔCt method curves.

APOE genotyping was performed by qRT-PCR according to a previously described method [27].

Recombinant reelin

HEK-293T cells stably transfected with full-length mouse reelin clone pCrl or GFP (mock) (kindly provided by Dr. E. Soriano, Department of Cell Biology, University of Barcelona, Barcelona, Spain) were seeded in 175-cm^2 flasks at a density of 10×10^6 cells/flask. After 3 days in culture in Optimem, the supernatants were filtered through 0.2-µm pores and concentrated with an Amicon Ultra 100-kDa size exclusion filter (Merk Millipore, Darmstadt, Germany). For quantification, a coomasie gel was loaded with different volumes of the concentrated supernatants as well as with different bovine serum albumin solutions to perform an extrapolation.

Western blotting

Brain membrane-enriched fractions, SH-SY5Y extracts, or CHO-PS70 extracts (30 µg) were run on SDS-PAGE (7.5%, 12%, precast 4–15% gradient, or Tris-tricine 16%) after boiling at 98°C for 5 min in 6× Laemmli sample buffer. Proteins were transferred by electrophoresis to nitrocellulose membranes and detected with antibodies against the C-terminal of LRP3 (mouse, 1:100, Sigma-Aldrich, St. Louis, MO, USA), N-terminal of LRP3 (rabbit, 1:100, Sigma-Aldrich), Flag (mouse, 1:1000, Sigma-Aldrich), C-terminal of LDLR (rabbit, 1:200, Sigma-Aldrich), C-terminal of ApoER2 (rabbit, 1: 2000, Abcam, Cambridge, UK), C-terminal of APP (rabbit, 1: 2000, Sigma-Aldrich), N-terminal of APP (rabbit, 1: 2000, Sigma-Aldrich), sAPPα (mouse, 1:1000; IBL, Hamburg, Germany), sAPPβ (rabbit 1:1000; IBL), LC3B (rabbit, 1:2000; Abcam), or α-tubulin (1:4000, Sigma-Aldrich) as a loading control. Primary antibody binding was visualized with fluorescent secondary antibodies (IRDye, 1: 10000), and images were acquired using an Odyssey CLx Infrared Imaging system (LI-COR Biosciences GmbH). Representative whole blots are shown as Supp Fig. 1.

Immunoprecipitation

Brain extracts (100 µL) or CHO-PS70 extracts (50 µL) were incubated on a roller for 2.5 h at room temperature with 100 µL of magnetic beads (Dynabeads, Merck Millipore) coupled to the C-terminal LRP3 (mouse, Sigma-Aldrich) for brain extracts, C-terminal APP (rabbit, Biolegend) for CHO-PS170 extracts, or mouse/rabbit IgG (negative controls). The input, bound, and unbound fractions were analyzed by western blotting using specific antibodies.

Immunofluorescence

CHO-PS70 cells overexpressing LRP3-flag were washed with cold Hank-buffered salt solution and fixed with 4%

126

Cuchillo-Ibañez et al. Alz Res Therapy   (2021) 13:181

Page 5 of 17

Table 2 Expression of genes upregulated by full-length ApoER2 overexpression

Symbol	Gene name	Genomic location	Function	logFC	adj p
LRP3	Low-density lipoprotein receptor-related protein 3	19q13.11	Internalization of lipophilic molecules and/or signal transduction Precise role is unclear	0.48	0.047
LDLR	Low-density lipoprotein receptor	19p13.2	Mediates endocytosis of cholesterol-rich LDL	0.43	0.018
APOL1	apolipoprotein L, 1	22q12.3	Minor apoprotein component of HDL	1.28	0.003
INSIG1	Insulin-induced gene 1	7q36.3	Regulation of cholesterol cell concentration	0.72	0.001
DHCR24	24-Dehydrocholesterol reductase	1p32.3	Cholesterol metabolic process	0.35	0.008
MVK	Mevalonate kinase	12q24.11	Cholesterol metabolic process	0.33	0.019

Genes associated with lipid binding and transport, and cholesterol metabolism, whose transcripts were upregulated in ApoER2 overexpressing SH-SY5Y cells compared with control cells transfected with an empty vector. The expression of the genes was analyzed on DNA microarrays. The fold change (logFC) in gene expression between samples and controls, as well the adj p (p value adjusted for multiple testing) is indicated

paraformaldehyde and 0.1 M EGTA for 10 min. To stain the plasma membrane, cells were incubated with WGA-FITC (WGA: lectin from *Triticum vulgaris*, FITC (fluorescein) conjugate, Sigma-Aldrich) for 15 min at room temperature, and the nonspecific sites were blocked with 10% (w/v) bovine serum albumin for 30 min. No permeabilization steps were included before or during the incubation with the primary antibodies. Cells were incubated with a primary antibody against Flag (1:200; mouse; Sigma-Aldrich) for 1 h, followed by the secondary antibody (1:200, Cy5 anti-mouse; GE-Healthcare) for 1 h. After washes with PBS, cells were incubated briefly with Hoechst dye to label nuclei (Invitrogen). Pictures were acquired in a Leica SPEII upright TCL-SL confocal microscope using an oil-immersion 40× objective

Double-labeling immunofluorescence and confocal microscopy

The frontal cortex and hippocampus of 14 cases at Braak NFT stages 0–I, IV, and V–VI and senile plaque stages 0–C were used in the study. Formalin-fixed, paraffin-embedded, de-waxed sections, 4 μm thick, were stained with a saturated solution of Sudan black B (Merck) for 15 min to block autofluorescence of lipofuscin granules present in cell bodies and then rinsed in 70% ethanol and washed in distilled water. The sections were boiled in citrate buffer to enhance antigenicity and blocked for 30 min at room temperature with 10% fetal bovine serum diluted in PBS. Then, the sections were incubated at 4°C overnight with combinations of primary antibodies: LRP3-C-term (Sigma-Aldrich, ref SAB1300316, polyclonal rabbit, diluted at 1:50) and apoER2 (Invitrogen, ref MA5-36130, mouse monoclonal, diluted 1:50). After washing, the sections were incubated with Alexa488 or Alexa546 (1:400, Molecular Probes) fluorescent secondary antibodies against the corresponding host species. Nuclei were stained with DRAQ5™ (1:2000, Biostatus). After washing, the sections were mounted in an

Immuno-Fluore mounting medium (ICN Biomedicals), sealed, and dried overnight. Sections were examined with a Leica TCS-SL confocal microscope.

Statistical analysis

The distribution of data was tested for normality using a D'Agostino-Pearson test. ANOVA was used for parametric variables and the Kruskal-Wallis test for non-parametric variables for comparison between groups. A Student's t-test for parametric variables and a Mann-Whitney U test for non-parametric variables were employed for comparison between two groups and for determining p values. For data analyzed using unpaired Student's t-test, a Welch's correction was employed in data with different standard deviations. Correlation between variables was assessed by linear regression analyses. The results are presented as the means ± SE, and all the analyses were performed using GraphPad Prism (version 7; GraphPad Software, Inc). p value < 0.05 was considered significant.

Results

ApoER2 overexpression increases the expression of LRP3

SH-SY5Y cells were transfected with full-length ApoER2, and after 48 h, a microarray was performed. Among the genes affected, we focused on the analysis of LDL receptors and apolipoprotein-related genes (Table 2). The receptors LRP3 and LDLR appeared significantly upregulated, both of which are members of the LDL receptor family. Upregulation of LRP3 was confirmed by qRT-PCR, with a significant increase in mRNA LRP3 level compared to its expression in non-transfected cells. However, increments in LDLR mRNA expression were not significant when assessed by qRT-PCR (Fig. 1a).

Although SH-SY5Y cells secrete reelin to the media and it can act in a paracrine mode, recombinant reelin was employed to treat overexpressing-ApoER2 cells to potentiate the ApoER2 signaling. This treatment induced ApoER2 cleavage and, consequently, reduced the amount

127

Cuchillo-Ibañez et al. Alz Res Therapy   (2021) 13:181

Page 6 of 17
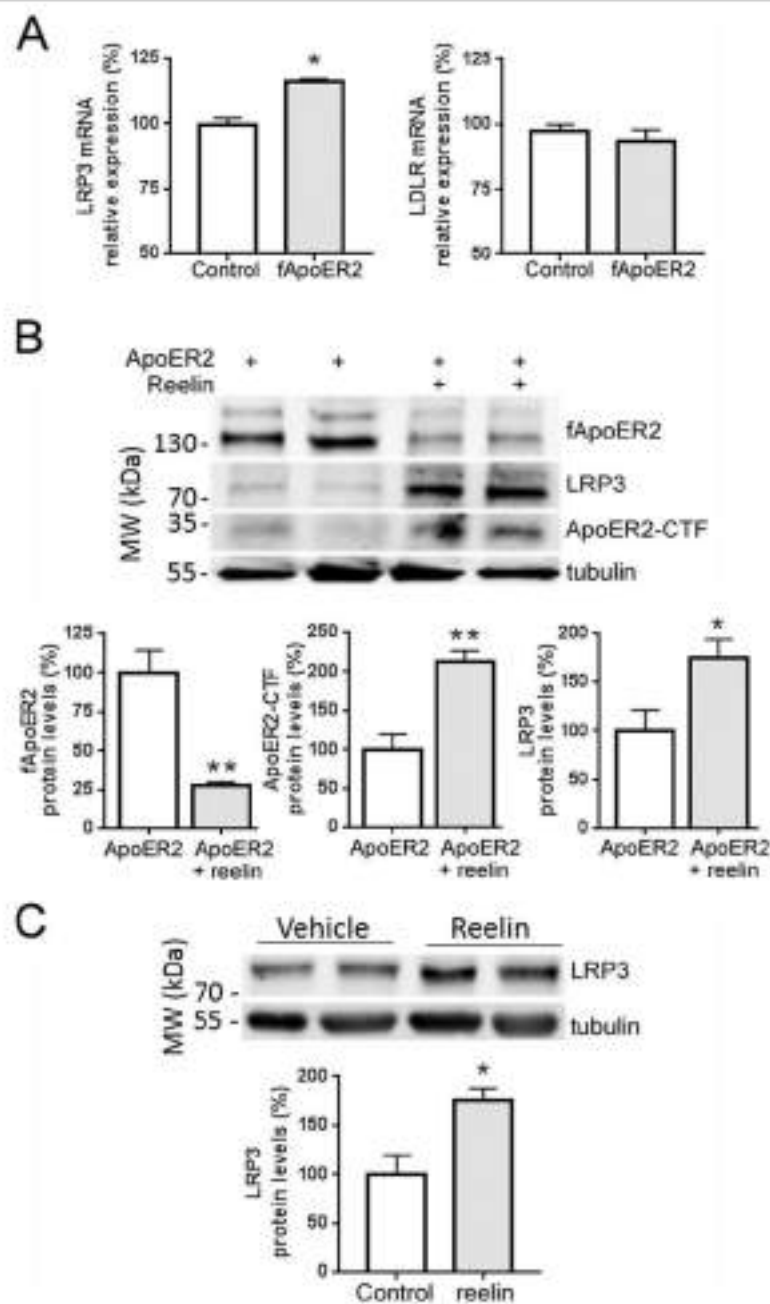
Fig. 1 ApoER2/reelin signaling upregulates LRP3 expression. **a** qRT-PCR analysis showing expression of LRP3 mRNA and LDLR mRNA after transfection with GFP cDNA (control) and full-length ApoER2 cDNA (fApoER2) in SH-SY5H cells. 18S was used as an internal control for mRNA expression ($n = 10–12$ for each condition, $p < 0.001$ for control versus fApoER2; t-test with Welch's correction). Note that the X axis begins at 50%. **b** Quantification and western blot showing the expression of full-length ApoER2, ApoER2-CTF, and LRP3 proteins after fApoER2 transfection and reelin (12 µg/ml) treatment for 24 h in SH-SY5Y cells. Tubulin was used as an internal control ($n = 9$ for each condition, **$p < 0.001$ for expression of fApoER2, t-test with Welch's correction, and ApoER2-CTF, t-test; *$p < 0.05$ for expression of LRP3, t-test). **c** Quantification and western blot showing the expression of LRP3 protein after reelin (12 µg/ml) treatment for 24 h or vehicle (Hanks's media) in neuro-differentiated SH-SY5Y cells with retinoic acid ($n = 9$ for each condition, *$p < 0.05$ t-test)

Fig. 2 ApoER2-ICD increases LRP3 expression. **a** Representative western blot showing the expression of ApoER2-ICD after transfection with full-length ApoER2 cDNA (ApoER2) and reelin treatment (12μg/ml, ApoER2 + reelin) for 24 h in SH-SY5Y cells. For comparison, the expression of the ApoER2-ICD construct (ApoER2-ICD) is also shown. **b** Western blot and **c** quantification of LRP3 protein expression after ApoER2-ICD transfection in SH-SY5Y cells. Tubulin was used as an internal control (n = 6 for each condition, *p < 0.001, t-test). **d** qRT-PCR analysis showing the expression of LRP3 mRNA (n = 7 for each condition, *p < 0.05, t-test) and **e** LDLR mRNA (n = 10 for each condition) after transfection with GFP cDNA (control) and ApoER2-ICD cDNA in SH-SY5Y cells. Note that the X axis in **d** begins at 50%. 18S was used as an internal control for mRNA expression

of full-length ApoER2 and increased the generation of the ApoER2-CTF. Importantly, reelin treatment induced an increment of LRP3 protein levels (Fig. 1b). In RA neuro-differentiated SH-SY5Y cells, reelin treatment was also able to induce an increase in LRP3 protein levels compared to non-stimulated cells (Fig. 1c).

Expression of ApoER2-ICD upregulates LRP3 expression

We considered the possibility that increments of LRP3 expression were induced by ApoER2-ICD, a fragment with transcriptional regulatory activity [14], generated by the proteolytic cleavage of ApoER2-CTF. This small fragment was observed in ApoER2-overexpressing cells after treatment with reelin (Fig. 2a). Thus, we overexpressed a chimeric ApoER2-ICD (amino acid residues 728–842) and measured LRP3 expression. LRP3 mRNA expression and protein levels increased significantly with respect to non-transfected cells (Fig. 2b–d), while LDLR mRNA levels were not significantly affected by ApoER2-ICD (Fig. 2e).

Expression levels of LRP3 in Aβ42-treated cells

On the contrary to the upregulation of LRP3 mRNA and protein that we observed after overexpression of full-length ApoER2 or ApoER2-ICD, we expected to find less LRP3 expression in Aβ42-treated cells, due to the fact that Aβ treatment reduces the generation of

ApoER2-CTF [16]. In agreement with this view, we found that treatment of neuro-differentiated SH-SY5Y cells with 1 μM and 5μM Aβ42 decreased the LRP3 protein levels, but 500 nM did not have the same effect, in comparison to scrambled peptide treatment (control, Fig. 3a). Five micromolar Aβ42 also reduced LRP3 mRNA expression (Fig. 3b).

Expression levels of LRP3 in AD brain

Next, we examined LRP3 levels in human frontal cortex extracts. Considering all cases with AD-related pathology, LRP3 mRNA expression was lower with respect to MA subjects ($p = 0.02$; t-test) (Fig. 4a). However, when cases with AD-related pathology were categorized by Braak NFT stages, the reduction was significant only at Braak stages NFT I–II ($p = 0.03$; t-test), while NFT III–IV or NFT V–VI displayed the same trend but failed to reach statistical significance ($p = 0.10$; $p = 0.15$, respectively, t-test). No significant modifications were found between Braak stages NFT I–II and NFT III–IV or NFT V–VI ($p = 0.56$; $p = 0.65$, respectively, t-test; Fig. 4b). Despite the difference in age between MA and AD-related pathology cases, age did not correlate with LRP3 mRNA in MA ($n = 11$; $R = 0.058$, $p = 0.87$) or AD-related pathology individuals ($n = 40$; $R = 0.067$; $p = 0.68$).

Gender did not contribute to differences in LRP3 mRNA expression either. The comparison between
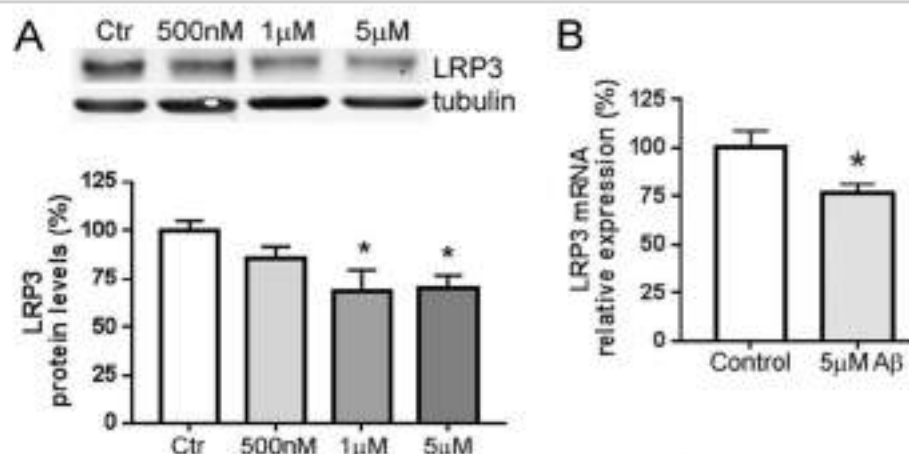
Fig. 3 Aβ42 reduces LRP3 expression. **a** Quantification and western blot showing the expression of LRP3 proteins in neuro-differentiated SH-SYSY cells treated with 5 μM Aβ42 or scrambled Aβ42 (control). Tubulin was used as an internal control (n = 9 for each condition, *p < 0.05, t-test). **b** qRT-PCR analysis showing expression of LRP3 mRNA in neuro-differentiated SH-5YSY cells treated with 500 nM, 1μM, 5 μM Aβ42, or scrambled Aβ42 (control). 18S was used as an internal control for mRNA expression (n = 8 for each condition, p < 0.05, t-test)
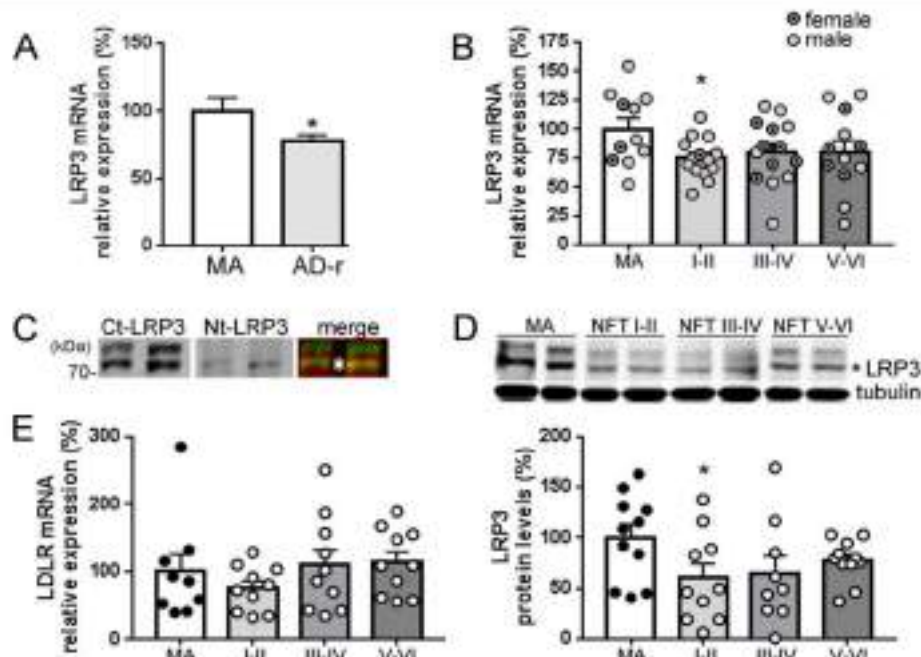
Fig. 4 Low levels of LRP3 in AD frontal cortex. **a** qRT-PCR analysis showing expression of LRP3 mRNA in brain extracts from MA and Alzheimer's disease-related (AD-r) subjects, and **b** categorized by Braak NFT stages (I–II, III–IV, and V–VI). 18S was used as an internal control for mRNA expression (n = 11 for MA, n = 12–14 for each AD-r Braak stage, *p < 0.05, t-test for MA v AD-r, t-test with Welch's correction for MA v AD-r I–II). **c** Western blots showing different LRP3 immunoreactivities in human cortex extracts. Two bands were observed using an anti-C-terminal LRP3, but a single band was observed when an anti-N-terminal LRP3 was used, all between 70 and 100kDa. One of the bands immunoreacted to both antibodies, likely representing the full-length receptor. Accordingly, the overlapping band (*) was selected for quantification. **d** Western blot using an anti-C-terminal LRP3 in brain extracts from MA and AD-r subjects, categorized by Braak's stages (NFT I–II, NFT III–IV, and NFT V–VI) and quantification of the lower band (marked with a *). Tubulin was used as an internal control (n = 11 for MA, n = 10–11 for each NFT Braak's stage, *p < 0.05, Mann-Whitney test). **e** qRT-PCR analysis showing expression of LDLR mRNA in brain extracts from MA and AD-r subjects, categorized by Braak's stages. 18s was used as an internal control for mRNA expression (n = 9 for MA, n = 10 for each Braak's stage)

130

females and males from MA and from AD-related pathology groups was not statistically significative ($p = 0.13$, one-way ANOVA). When female values were subtracted from both groups, LRP3 mRNA expression in males was still different between MA and AD-related pathology overall ($p = 0.042$, t-test). However, the difference observed in Braak stages I–II failed to maintain statistical significance, probably due to the smaller sample size ($p = 0.060$, t-test). Braak stages III–IV and V–VI remained without differences in males compared to MA males ($p = 0.20$ and $p = 0.22$, respectively, t-test). The *APOE* genotype did not account for LRP3 mRNA expression either ($p = 0.47$ e4 carriers v non-e4 carrier AD-related cases).

To evaluate LRP3 protein levels in the cortex from MA and cases with AD-related pathology, membrane-enriched fractions were isolated from brain samples. Due to the lack of reports about LRP3 in the brain, two antibodies were tested to corroborate the identity of LRP3 immunoreactive bands (Fig. 4c). We found that LRP3 expression levels were lower at Braak stages I–II compared to those in MA individuals ($p = 0.048$, t-test, Fig. 4d). No further differences were seen at stages III–IV and V–VI when compared with MA ($p = 0.11$ and $p = 0.12$, respectively, t-test) and compared with Braak NFT stages I–II ($p = 0.84$ and $p = 0.26$ respectively, t-test).

The estimated expression of LDLR mRNA was not significantly different between MA individuals and AD-related pathology subjects when the extracts were compared overall ($p = 0.73$ Mann-Whitney) or when compared discriminating Braak stages ($p = 0.73$ one-way ANOVA; Fig. 4e).

LRP3 interacts with apoE and APP, but not with reelin in the human brain

Double-labeling immunofluorescence and confocal resolution showed that the LRP3 antibody recognized small granules localized in the cytoplasm and proximal dendrites of all neurons, and around the nucleus of glial cells in the hippocampus and frontal cortex. ApoER2 antibody also showed small granules in the cytoplasm of neurons and small glial cells. The immunostaining was variable in the MA group and in cases with NFT pathology with marked individual disparities, probably due to the vulnerability of the protein to the pre-mortem status and post-mortem delay (Fig. 5a). This individual variability did not permit any attempt to quantify inter-group immunostaining densitometry.

We also evaluated, by means of immunoprecipitation assays, whether reelin acts as a ligand for LRP3, as it does for ApoER2, in frontal cortex extracts from MA and AD-related pathology cases. Reelin was not co-immunoprecipitated from any brain extracts. We next assessed whether LRP3 interacts with apoE and APP, in the same way as many members of the LDL receptor family do. After immunoprecipitation, both proteins were co-immunoprecipitated with LRP3 in MA and cases with AD-related pathology (Fig. 5b).

LRP3 modulates APP expression levels

We tested whether LRP3 was able to influence APP processing and Aβ generation in a similar manner to other members of the LDL receptor family. In order to do so, we overexpressed LRP3 in CHO-PS70 cells, a cell line that expresses the wild-type APP770 isoform. LRP3 was located at discrete areas of the soma and in the plasma membrane of CHO-PS70 cells (Fig. 6a). Moreover, LRP3 and APP co-immunoprecipitated in these cells (Fig. 6b). Overexpression of LRP3 did not affect APP mRNA levels (Fig. 6c), but it drastically reduced full-length APP levels, as well as APP-CTF in cell extracts (Fig. 6d). In the supernatant, the levels of sAPPα, sAPPβ, and soluble Aβ decreased in transfected CHO-PS70 cells compared to mock-transfected cells (Fig. 6e). Interestingly, when lysosomal function was impaired by chloroquine, full-length APP and sAPPα levels increased in a significant manner with regard to non-treated cells ($p = 0.0044$; $p = 0.031$, respectively, t-test; Fig. 7). sAPPβ levels showed a tendency to be higher than non-treated cells ($p = 0.065$).

To determine in more detail whether LRP3 is involved in APP degradation by lysosomes, we performed a differential centrifugation of CHO-PS70 cell homogenates. Two different fractions were obtained: a cytosol and plasma membrane-containing fraction, and an intracellular membrane-containing fraction. In CHO cells overexpressing LRP3, full-length APP levels were lower in both fractions, but APP-CTF levels were lower only in the intracellular membrane-containing fractions compared to those in CHO controls (Fig. 8a). Treatment with chloroquine did not affect APP levels in CHO cell controls in any fraction (Fig. 8b). In CHO cells overexpressing LRP3, full-length APP and APP-CTF levels increased in the cytosol and plasma membrane-containing fractions after chloroquine treatment. This could indicate that chloroquine is affecting LRP3 capacity of inducing APP endocytosis from the plasma membrane as observed in Fig. 8a. However, only APP-CTF levels were higher than those in CHO controls in the intracellular membrane-containing fractions (Fig. 8c). This could indicate an accumulation of APP-CTF in vesicles such as endosomes or autophagosomes, whose fusion with lysosomes is inhibited by chloroquine.

Discussion

Our results suggest that reelin signaling, through the cleavage of its receptor ApoER2, can ultimately influence the expression of other liporeceptors, such as LRP3.
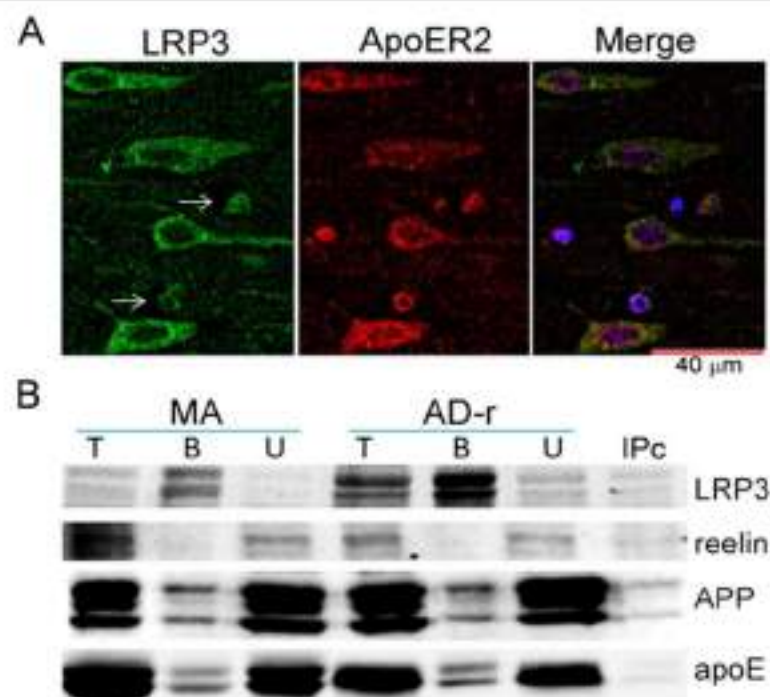
Fig. 5 LRP3 co-immunoprecipitates with apoE and APP. **a** Representative immunofluorescence photomicrograph showing LRP3 and ApoER2 labeling in the same cells in a hippocampus slice of a MA subject. Neurons (large cells) show LRP3 and ApoER2 co-localization; in addition, oligodendroglia-like cells (thin arrows) also co-localize both antibodies. **b** Representative western blots showing immunoprecipitation of LRP3 and co-immunoprecipitation of reelin (no immunoprecipitation), apoE, and APP, from non-demented (ND) and Alzheimer's disease (AD) extracts. T total input, B bound fraction, U unbound fraction, IPc bound fraction of the negative control

Many LDL receptor family members, such as ApoER2, LDLR, LRP1, LRP1b, LRP6, and SorLA (LRP11), as well as other alternative apoE receptors such as Trem2, are γ-secretase substrates [28, 29]. For many of these receptors, the nuclear translocation of the respective ICDs and their transcriptional functions have been demonstrated or inferred [13, 30–32]. Here, we demonstrate that reelin-induced generation of ApoER2-ICD, as well as ApoER2-ICD overexpression, increases LRP3 expression. This supports a link between ApoER2 processing and the regulation of the alternative apoE liporeceptor LRP3.

In frontal cortex extracts from AD, where ApoER2/reelin signaling is impaired and ApoER2 processing is lessened (reviewed in [33]), we found lower LRP3 protein and mRNA levels. LRP3 expression was mainly affected at early Braak stages of NFT pathology (stages I–II), in which the trans-entorhinal region shows neurofibrillary tangles and neuropil threads [18]. However, since the same decreasing trend was determined in advanced Braak stages, additional studies are needed to determine whether LRP3 decrease is only an early phenomenon associated to AD-related progression.

In the microarray, after overexpression of full-length ApoER2, the expression of another LDL receptor family member, LDLR, also appears to be upregulated. Interestingly, both LRP3 and LDLR are encoded by genes located on chromosome 19, locus 19q13 [34, 35]. The *APOE* gene also maps in chromosome 19, on locus 19q13.32 [36], in a cluster together with the apolipoprotein C1 and C2 genes. Genetic linkage studies suggest the presence of AD risk genes on chromosome 19 that would act in an independent manner from apoE, such as *ABCA7* (19p13.3) and *CD33* (19q13.41) [37]. Indeed, *LDLR* was analyzed as a potential AD risk factor, but the study concluded that the genetic variants in LDLR did not make a significant contribution to AD risk in the general population [38]. Interestingly, recent multiplex proteomics studies have identified that LDLR levels are modestly decreased in CSF from early AD patients, suggesting that this receptor could represent a new specific biomarker for AD [39]. Other genes encoding LDL receptor family members, such as LRP1, LRP1b, LRP2, LRP4, LRP6, and SorLA, have been associated to AD risk (reviewed in [13]), as well as ApoER2 [40]. Despite the results from the microarray study, the *q*RT-PCR failed to corroborate the modulation of LDLR by ApoER2 and did not find changes on LDLR expression in AD extracts.

Fig. 6 LRP3 overexpression in CHO-PS70 cells decreases APP levels. **a** Representative immunofluorescence photomicrographs showing LRP3 and WGA labeling at the plasma membrane and discrete cytosolic areas of CHO-PS70 cells transfected with LRP3-flag cDNA. Nuclei were stained with the DNA dye Hoechst. **b** Western blots from CHO-PS70 cells transfected with LRP3-flag (CHO-LRP3) or pcDNA3.1 (CHO control) showing immunoprecipitation of APP (using a C-terminal APP antibody) and co-immunoprecipitation of APP (using an N-terminal APP antibody) and LRP3. T input, B bound fraction, U unbound fraction, IPc negative control. **c** qRT-PCR analysis showing expression of APP mRNA in CHO-PS70 transfected with LRP3-flag (LRP3) or pcDNA3.1 (Ctr, control). G4PDH was used as an internal control for mRNA expression (n = 13 for each condition). **d** Western blots and quantification of CHO-PS70 cells transfected with LRP3-flag (LRP3) or pcDNA3.1 (Ctr, CHO control) showing the expression in the cell extracts of LRP3, full-length APP, APP-CTF proteins, and tubulin, as an internal control (n = 6 for each condition, *p<0.001, t-test). **d** Western blots and quantification of CHO-PS70 cells transfected with LRP3-flag (LRP3) or pcDNA3.1 (Ctr, CHO control) showing the expression in the supernatants of sAPPα, sAPPβ, and Aβ, and the total protein as the internal control (n = 6 for each condition, *p<0.001, t-test)

The reelin receptors ApoER2 and VLDLR are core members of the LDL family that share the same extracellular domain structure, the ligand binding-type repeat domains (LBDs) and the EGF-precursor homology domains. The intracellular domain of each of the core members contains at least one NPxY (Asn-Pro-X-Tyr) motif, which plays a role in protein interaction/signal transduction [41–43] and endocytosis [44]. In comparison, LRP3 is smaller than the core members of the LDL receptor family. LRP3 belongs to a subfamily, together with LRP10 (murine LRP9), LRP12, and Lrad3 (ST7/Mig13). These subfamily members are characterized by the sole presence of LBDs and CUB-domains (which binds Complement, Uegf, and Bmp1) in their extracellular domain and lack the EGF-like repeats [13]. The short LBD in LRP3 is likely the domain responsible for the co-immunoprecipitation of apoE, as this is the competent region that binds several ligands [45]. However, reelin did not co-immunoprecipitate, in the same manner as receptor-associated protein (RAP), another ApoER2 ligand, which does not bind to LRP3 either [17, 34, 45, 46]. In the intracellular domain, LRP3 lacks the NPxY motifs, but instead contains a similar tyrosine-based sequence (EDFPVY) [34, 47]. Therefore, the domain by which APP is able to interact with LRP3 is yet to be determined. In vitro data showed that the extracellular domain of LRP10 interacts with APP [48], while Lrad3, the LDL receptor family member with the shortest extracellular domain [49], is also able to interact with APP and to modulate APP processing pathways. ApoER2 and APP are linked extracellularly by binding different domains of F-spondin [50] and intracellularly through the adaptor proteins Dab-1 and Fe65, which interact with the NPxY motif of ApoER2 and APP [24, 51, 52]. Therefore, more studies are needed to explore the direct or indirect interaction between LRP3 and APP.

We observed that overexpression of LRP3 decreased the levels of full-length APP and APP-CTF in the fraction containing the plasma membrane, as well as Aβ and soluble APP fragment levels generated after amyloidogenic and non-amyloidogenic processing pathways. In CHO-PS70 cells overexpressing LRP3, chloroquine treatment increased the levels of full-length APP and APP-CTF in the fraction containing the plasma membrane, and of sAPPα in the media; furthermore, APP-CTF levels in the fraction containing intracellular vesicles were higher when autophagy was inhibited compared to non-treated cells. This suggests that LRP3, described as
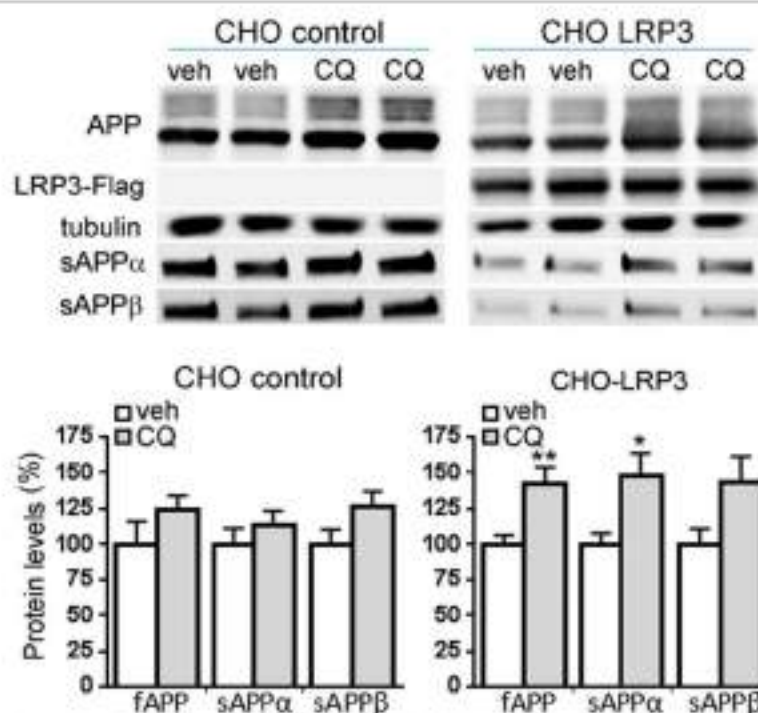
Fig. 7 Inhibition of lysosomal/autophagy function increases APP and sAPP levels. Western blots and quantification of CHO-P570 cells transfected with LRP3-flag (CHO LRP3) or pcDNA3.1 (CHO) for 24h and then treated with 10 mM chloroquine (CQ) for another 24 h or with vehicle (veh, Hank's media). Western blots show the expression in the cell extracts of LRP3, full-length APP (fAPP), and tubulin, and the expression of sAPPα and sAPPβ from the supernatants (n = 6–14 for each condition, **p<0.01 for fAPP respect to control; **p<0.05 for sAPPα respect to control; p = 0.065 for sAPPβ)

an endocytosis receptor [34], could be involved in APP processing through lysosomal degradation/autophagy mechanisms. The blockage of LRP3-mediated APP internalization by chloroquine could explain the increase in sAPPα levels, but not sAPPβ, as it has been proposed that the cleavage of APP by α-secretase occurs mainly at the cell surface [53], and also the increase of APP-CTF in intracellular vesicles, as endosomes would not be able to fuse with autophagosomes, thus leading to the accumulation of APP-CTF. Core members of the LDL receptor family have also been associated with APP trafficking and internalization, thus determining APP proteolytic processing and Aβ production, which could play a role in AD pathogenesis [54–57]. For example, LRP1 increases APP endocytosis and generation of Aβ [58–60], while LRP1B retains APP at the cell surface [61]. ApoER2 is able to alter APP subcellular distribution, increasing the generation of Aβ; this effect depends on the integrity of the NPxY motif in ApoER2 [62]. In a mouse model in which the ApoER2 isoform lacks three LBDs, the non-amyloidogenic processing of APP predominates [63]. In this line, LRP1 endocytosis impairment favors non-amyloidogenic processing of APP due to reduced internalization,

resulting in less extracellular Aβ [64, 65]. Additionally, mechanisms related to the APP secretory pathways are also possible, such as for LRP1, whose retention in the endoplasmic reticulum by the expression of a specific motif leads to a decrease in full-length APP and CTF levels at the plasma membrane as well as in Aβ secretion [1, 66]. A direct downregulation of APP mRNA would be unlikely given our *q*RT-PCR data.

Interestingly, LRP1 has been shown to constitute a major regulator of tau uptake and spread [67]. Therefore, the potential tau-LRP3 interactions appear to be an interesting possibility to study. A thorough investigation of possible interactions of LRP3 with AD hallmarks and key proteins could serve to decipher the physiological role and potential participation in pathological processes of this LDL receptor family member.

LRP3 expression is highest in skeletal muscle and in the ovaries, but it is also present at relatively high levels in the brain and heart, among other tissues [17]. LRP3 has been involved so far in osteogenic and adipocytic differentiation [68], and systemic use of steroids has been associated with site-specific differential methylation of the LRP3 gene [69], but its role in neuronal
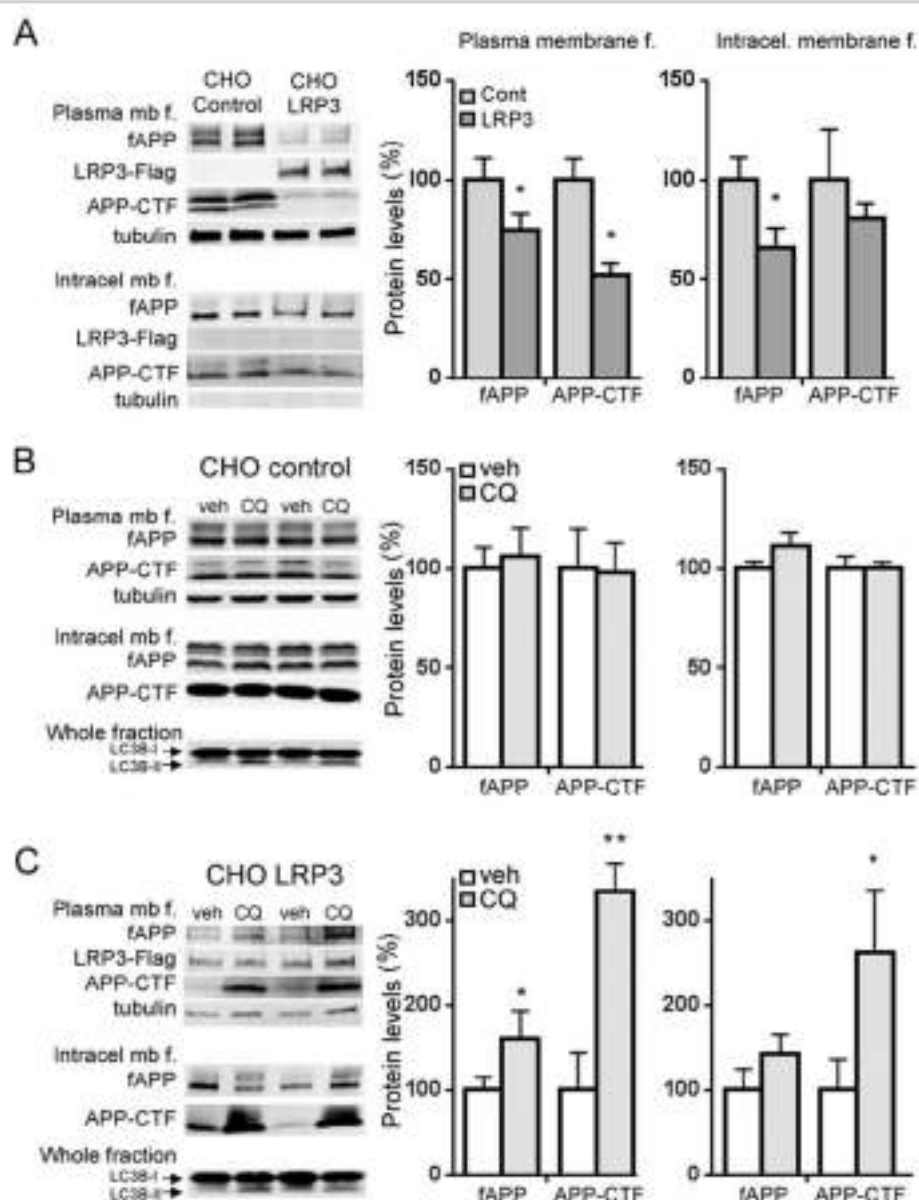
Fig. 8 Chloroquine increases full-length APP and sAPP levels at the membrane fraction. Western blots and quantification of the expression of full-length APP (fAPP), APP-CTF, Flag (LRP3-flag), and tubulin in cytosol and plasma membrane-containing fractions (plasma membrane f. or plasma mb f.) and in intracellular membrane-containing fractions (intracell membrane f. or intracell mb f) from CHO-PS70 cell homogenates. The presence of LRP3-flag was only observed in the cytosol and plasma membrane fraction, and tubulin was not present in the intracellular membrane-containing fraction. For LC3B-I conversion to LC3B-II to monitor autophagy, the whole cell extracts were used. **a** Comparison between CHO-PS70 cells transfected with LRP3-flag (CHO LRP3) or pcDNA3.1 (CHO control). **b** Comparison between CHO cells transfected with pcDNA3.1 (CHO control) for 24h and then treated with 10 mM chloroquine (CQ) for another 24 h or with vehicle (veh, Hank's media). **c** Comparison between CHO cells transfected with LRP3-flag (CHO LRP3) for 24h and then treated with 10 mM chloroquine (CQ) for another 24 h or with vehicle (veh, Hank's media). (n = 6–10 for each condition, **p<0.01; *p<0.05 z-test)

activity is still unknown. *LRP3* has been identified as a gene upregulated for a short window of 2 h, exclusively following learning, in the rat dentate gyrus [70]. To clarify LRP3s biological functions, it is essential to define the significance of LRP3 expression in the brain in aging and AD-related pathology with disease progression. An alteration in the expression of LRP3 may influence the processing and expression of APP,

135

affecting its synaptic function and, therefore, contributing to the AD pathology.

Conclusions

ApoER2/reelin signaling is able to regulate LRP3 expression, and LRP3 reduces APP protein levels, including sAPP fragments and Aβ peptide. The mechanism involved is yet to be determined, although it may be related to APP endocytosis. This study could contribute to find new strategies in aging and AD research, given that LRP3 modulation could participate in the regulation of Aβ levels.

Limitations

The main limitation of this study is the scarce knowledge of the physiological function of LRP3 in the brain, as there are few reports about it as a neuronal receptor. We employed a well-characterized brain collection, but it would be interesting to validate our findings with an alternative collection of post-mortem cortex samples from MA individuals and cases with AD-related pathology. Despite the difference in age between non-demented and control subjects, age does not appear to be related with decreased LRP3 expression in the AD-related pathological group, but the validation of the data in age-matched groups is desirable. Development of in vivo knockouts or knockdowns of LRP3 would contribute to the understanding of the mechanism that links this receptor and APP, given that, for example, knockdown of LRP10 led to increased processing of APP to generate Aβ [48].

Abbreviations

Aβ42: β-Amyloid protein (amino acid residues 1–42); AD: Alzheimer's disease; APP: Amyloid β precursor protein; ApoE: Apolipoprotein E; ApoER2/LRP8: Apolipoprotein E receptor 2; ApoER2-ICD: ApoER2 intracytoplasmic domain; ApoER2-CTF: ApoER2 C-terminal fragment; CQ: Chloroquine; LDLR: Low-density lipoprotein receptor; ND: Non-demented; VLDLR: Very low-density lipoprotein receptor.

Supplementary Information

The online version contains supplementary material available at https://doi.org/10.1186/s13195-021-00921-5.

Additional file 1: Supplemental Figure 1. Representatives whole blots. Whole blots from SH-SY5Y cell extracts, human frontal cortex from non-demented and Alzheimer's disease subjects, and from CHO cell extracts and supernatants. The antibody employed in every blot is indicated. T = total input, B = bound fraction, U = unbound fraction, Bc: bound fraction of the negative control, Uc: bound fraction of the negative control.

Additional file 2. Complete microarray.

Declarations

Author details
¹Instituto de Neurociencias de Alicante, Universidad Miguel Hernández de Elche-CSIC, Sant Joan d'Alacant, Spain. ²Centro de Investigación Biomédica en Red sobre Enfermedades Neurodegenerativas (CIBERNED), Madrid, Spain. ³Instituto de Investigación Sanitaria y Biomédica de Alicante (ISABIAL), Alicante, Spain. ⁴Instituto de Neuropatología, Hospital Universitario de Bellvitge, Universidad de Barcelona, Hospitalet de Llobregat, Barcelona, Spain.

References
1. Waldron E, Heilig C, Schweitzer A, Nadella N, Jaeger S, Martin AM, et al. LRP1 modulates APP trafficking along early compartments of the secretory pathway. Neurobiol Dis. 2008;31:188–97 Available from: https://pubmed.ncbi.nlm.nih.gov/18559293/. Cited 2020 Dec 27.

Cuchillo-Ibañez et al. Alz Res Therapy   (2021) 13:181

Page 15 of 17

2. Gilat-Frenkel M, Boehm-Cagan A, Liraz O, Xian X, Herz J, Michaelson DM. Involvement of the Apoer2 and Lrp1 receptors in mediating the pathological effects of ApoE4 in vivo. Curr Alzheimer Res. 2014;11:549–57 Bentham Science Publishers Ltd. Available from: http://www.ncbi.nlm. nih.gov/pubmed/24251389. Cited 2020 Feb 13.

3. Kim J, Yoon H, Basak J, Kim J. Apolipoprotein E in synaptic plasticity and Alzheimer's disease: potential cellular and molecular mechanisms. Mol Cells. 2014;833–40 Korean Society for Molecular and Cellular Biology. Available from: http://www.ncbi.nlm.nih.gov/pubmed/25358504. Cited 2020 Feb 13.

4. Bock HH, May P. Canonical and non-canonical reelin signaling. Front Cell Neurosci. 2016;10:166 Frontiers Media S.A. Available from: http://www. ncbi.nlm.nih.gov/pubmed/27445693. Cited 2020 Feb 13.

5. Lane-Donovan C, Herz J. Building a better blood-brain barrier. Elife. 2017;6:e31808 eLife Sciences Publications Ltd. Available from: http:// www.ncbi.nlm.nih.gov/pubmed/28994392. Cited 2020 Feb 13.

6. May P, Herz J, Bock HH. Molecular mechanisms of lipoprotein receptor signalling. Cell Mol Life Sci. 2005;62(19-20):2325–38 Springer. Available from: https://link.springer.com/article/10.1007/s00018-005-5231-z. Cited 2021 Jan 18.

7. Herz J, Chen Y. Reelin, lipoprotein receptors and synaptic plasticity. Nat Rev Neurosci. 2006;(7):850–9 Available from: http://www.ncbi.nlm.nih. gov/pubmed/17053810. Cited 2019 Jul 23.

8. Schmechel DE, Saunders AM, Strittmatter WJ, Crain BJ, Hulette CM, Joo SH, et al. Increased amyloid β-peptide deposition in cerebral cortex as a consequence of apolipoprotein E genotype in late-onset Alzheimer disease. Proc Natl Acad Sci U S A. 1993;90:9649–53 National Academy of Sciences.

9. Pinto D, Delaby E, Merico D, Barbosa M, Merikangas A, Klei L, et al. Convergence of genes and cellular pathways dysregulated in autism spectrum disorders. Am J Hum Genet. 2014;94:677–94 Available from: https://linki nghub.elsevier.com/retrieve/pii/S0002929714001505. Cited 2019 Jan 14.

10. Jaeger S, Pietrzik CU. Functional role of lipoprotein receptors in Alzheimer's disease. Curr Alzheimer Res. 2008;5:15–25 Available from: http:// www.ncbi.nlm.nih.gov/pubmed/18288927. Cited 2020 Feb 13.

11. Marzolo MP, Bu G. Lipoprotein receptors and cholesterol in APP trafficking and proteolytic processing, implications for Alzheimer's disease. Semin Cell Dev Biol. 2009;20(2):191–200 Elsevier Ltd. Available from: http://www.ncbi.nlm.nih.gov/pubmed/19041409. Cited 2020 Feb 13.

12. Lane-Donovan C, Phillips GT, Herz J. More than cholesterol transporters: lipoprotein receptors in CNS function and neurodegeneration. Neuron. 2014;83:771–87 Available from: http://www.ncbi.nlm.nih.gov/pubmed/ 25144875. Cited 2020 Feb 13.

13. Pohlkamp T, Wasser CR, Herz J. Functional roles of the interaction of APP and lipoprotein receptors. Front Mol Neurosci. 2017;10:54 Frontiers Media S.A. Available from: http://www.ncbi.nlm.nih.gov/pubmed/28298885. Cited 2020 Feb 13.

14. Balmaceda V, Cuchillo-Ibáñez I, Pujadas L, García-Ayllón M-S, Saura CA, Nimpf J, et al. ApoER2 processing by presenilin-1 modulates reelin expression. FASEB J. 2014;28(4):1543–54.

15. Telese F, Ma Q, Perez PM, Notani D, Oh S, Li W, et al. LRP8-reelin-regulated neuronal enhancer signature underlying learning and memory formation. Neuron. 2015;86:696–710 Cell Press. Available from: http://www. ncbi.nlm.nih.gov/pubmed/25892301. Cited 2020 Feb 13.

16. Mata-Balaguer T, Cuchillo-Ibañez I, Calero M, Ferrer I, Sáez-Valero J. Decreased generation of C-terminal fragments of ApoER2 and increased reelin expression in Alzheimer's disease. FASEB J. 2018;32:3536–46 Available from: https://www.fasebj.org/doi/10.1096/fj.201700736RR. Cited 2019 Jan 10.

17. Battle MA, Maher VM, McCormick JJ. ST7 is a novel low-density lipoprotein receptor-related protein (LRP) with a cytoplasmic tail that interacts with proteins related to signal transduction pathways. Biochemistry. 2003;42:7270–82 Available from: http://pubs.acs.org/doi/abs/10.1021/ bi034081y. Cited 2019 Feb 22.

18. Braak H, Braak E. Neuropathological stageing of Alzheimer-related changes. Acta Neuropathol. 1991;82:239–59 Available from: http://www. ncbi.nlm.nih.gov/pubmed/1759558. Cited 2019 Jul 15.

19. Braak H, Alafuzoff I, Arzberger T, Kretzschmar H, Del Tredici K. Staging of Alzheimer disease-associated neurofibrillary pathology using paraffin sections and immunocytochemistry. Acta Neuropathol.

20. Ferrer I. Defining Alzheimer as a common age-related neurodegenerative process not inevitably leading to dementia. Prog Neurobiol. 2012;97:38–51 Available from: https://pubmed.ncbi.nlm.nih.gov/22459297/. Cited 2021 Sep 27.

21. Chen Y, Kundakovic M, Agis-Balboa RC, Pinna G, Grayson DR. Induction of the reelin promoter by retinoic acid is mediated by Sp1. J Neurochem. 2007;103:650–65 Available from: https://pubmed.ncbi.nlm.nih.gov/17666 047/. Cited 2021 Apr 8.

22. Jämsä A, Hasslund K, Cowburn RF, Bäckström A, Vasänge M. The retinoic acid and brain-derived neurotrophic factor differentiated SH-SY5Y cell line as a model for Alzheimer's disease-like tau phosphorylation. Biochem Biophys Res Commun. 2004;319:993–1000 Available from: https://pub med.ncbi.nlm.nih.gov/15184080/. Cited 2021 Apr 12.

23. Dumanis SB, Cha HJ, Song JM, Trotter JH, Spitzer M, Lee JY, et al. ApoE receptor 2 regulates synapse and dendritic spine formation. PLoS One. 2011;6(2):e17203 Available from: https://pubmed.ncbi.nlm.nih.gov/21347 244/. Cited 2021 Mar 22.

24. Hoe H-S, Wessner D, Beffert U, Becker AG, Matsuoka Y, Rebeck GW. F-spondin interaction with the apolipoprotein E receptor ApoEr2 affects processing of amyloid precursor protein. Mol Cell Biol. 2005;25:9259–68 Available from: http://www.ncbi.nlm.nih.gov/pubmed/16227578. Cited 2020 Feb 14.

25. Xia W, Zhang J, Kholodenko D, Citron M, Podlisny MB, Teplow DB, et al. Enhanced production and oligomerization of the 42-residue amyloid β-protein by Chinese hamster ovary cells stably expressing mutant presenilins. J Biol Chem. 1997;272:7977–82 American Society for Biochemistry and Molecular Biology. Available from: http://www.jbc.stanford.edu/jbc/. Cited 2020 Dec 26.

26. Brodeur J, Larkin H, Boucher R, Thériault C, St-Louis SC, Gagnon H, et al. Calnuc binds to LRP9 and affects its endosomal sorting. Traffic. 2009;10:1098–114 Blackwell Munksgaard. Available from: https://pub med.ncbi.nlm.nih.gov/19497050/. Cited 2020 Dec 26.

27. Calero O, García-Albert L, Rodríguez-Martín A, Veiga S, Calero M. A fast and cost-effective method for apolipoprotein e isotyping as an alternative to APOE genotyping for patient screening and stratification. Sci Rep. 2018;8(1):1–8 Nature Publishing Group. Available from: https://pubmed. ncbi.nlm.nih.gov/29654261/. Cited 2021 Jun 15.

28. Lleó A, Saura CA. γ-secretase substrates and their implications for drug development in Alzheimer's disease. Curr Top Med Chem. 2011;11:1513–27 Available from: http://www.ncbi.nlm.nih.gov/pubmed/21510835. Cited 2020 Feb 13.

29. Güner G, Lichtenthaler SF. The substrate repertoire of γ-secretase/presenilin. Semin Cell Dev Biol. 2020;105:27–42 Elsevier Ltd.

30. Mi K, Johnson GVW. Regulated proteolytic processing of LRP6 results in release of its intracellular domain. J Neurochem. 2007;101:517–29 Available from: http://www.ncbi.nlm.nih.gov/pubmed/17326769. Cited 2020 Feb 13.

31. May P, Woldt E, Matz RL, Boucher P. The LDL receptor-related protein (LRP) family: an old family of proteins with new physiological functions. Ann Med. 2007;39:219–28 Available from: http://www.ncbi.nlm.nih.gov/ pubmed/17457719. Cited 2020 Feb 13.

32. Wakabayashi T, De Strooper B. Presenilins: members of the γ-secretase quartets, but part-time soloists too. Physiology. 2008;23(4):194–204 Physiology (Bethesda). Available from: https://pubmed.ncbi.nlm.nih.gov/ 18697993/. Cited 2020 Dec 26.

33. Cuchillo-Ibañez I, Balmaceda V, Mata-Balaguer T, Lopez-Font I, Sáez-Valero J. Reelin in Alzheimer's disease, increased levels but impaired signaling: when more is less. J Alzheimer's Dis. 2016;52:403–16 Available from: http://www.medra.org/servlet/aliasResolver?alias=iospress&doi=10. 3233/JAD-151193. Cited 2019 Mar 28.

34. Ishii H, Kim D-H, Fujita T, Endo Y, Saeki S, Yamamoto TT. cDNA cloning of a new low-density lipoprotein receptor-related protein and mapping of its gene (LRP3) to chromosome bands 19q12–q13.2. Genomics. 1998;51:132–5 Available from: http://www.ncbi.nlm.nih.gov/pubmed/ 9693042. Cited 2019 Feb 22.

35. Francke U, Brown MS, Goldstein JL. Assignment of the human gene for the low density lipoprotein receptor to chromosome 19: synteny of a receptor, a ligand, and a genetic disease. Proc Natl Acad Sci U S A. 1984;81:2826–30.

36. Shaw DJ, Brook JD, Meredith AL, Harley HG, Sarfarazi M, Harper PS. Gene mapping and chromosome 19. J Med Genet. 1986;23:2–10 Available from: http://www.ncbi.nlm.nih.gov/pubmed/3081724. Cited 2020 Feb 14.

37. Moreno-Grau S, Hernández I, Heilmann-Heimbach S, Ruiz S, Rosende-Roca M, Mauleón A, et al. Genome-wide significant risk factors on chromosome 19 and the APOE locus. Oncotarget. 2018;9:24590–600 Impact Journals LLC. Available from: http://www.ncbi.nlm.nih.gov/pubmed/29872490. Cited 2020 Feb 14.

38. Bertram L, Hsiao M, McQueen MB, Parkinson M, Mullin K, Blacker D, et al. The LDLR locus in Alzheimer's disease: a family-based study and meta-analysis of case-control data. Neurobiol Aging. 2007;28:18.e1–4 Elsevier Inc. Available from: http://www.ncbi.nlm.nih.gov/pubmed/16378661. Cited 2020 Feb 14.

39. Whelan CD, Mattsson N, Nagle MW, Vijayaraghavan S, Hyde C, Janelidze S, et al. Multiplex proteomics identifies novel CSF and plasma biomarkers of early Alzheimer's disease. Acta Neuropathol Commun. 2019;7:169 BioMed Central Ltd. Available from: http://www.ncbi.nlm.nih.gov/pubmed/31694701. Cited 2020 Feb 14.

40. Ma SL, Ng HK, Baum L, Pang JCS, Chiu HFK, Woo J, et al. Low-density lipoprotein receptor-related protein 8 (apolipoprotein E receptor 2) gene polymorphisms in Alzheimer's disease. Neurosci Lett. 2002;332:216–8 Elsevier Ireland Ltd.

41. Trommsdorff M, Borg JP, Margolis B, Herz J. Interaction of cytosolic adaptor proteins with neuronal apolipoprotein E receptors and the amyloid precursor protein. J Biol Chem. 1998;273:33556–60.

42. Howell BW, Lanier LM, Frank R, Gertler FB, Cooper JA. The disabled 1 phosphotyrosine-binding domain binds to the internalization signals of transmembrane glycoproteins and to phospholipids. Mol Cell Biol. 1999;19:5179–88 American Society for Microbiology. Available from: https://pubmed.ncbi.nlm.nih.gov/10373567/. Cited 2020 Dec 20.

43. Gotthardt M, Trommsdorff M, Nevitt MF, Shelton J, Richardson JA, Stockinger W, et al. Interactions of the low density lipoprotein receptor gene family with cytosolic adaptor and scaffold proteins suggest diverse biological functions in cellular communication and signal transduction. J Biol Chem. 2000;275:25616–24.

44. Chen WJ, Goldstein JL, Brown MS. NPXY, a sequence often found in cytoplasmic tails, is required for coated pit-mediated internalization of the low density lipoprotein receptor. J Biol Chem. 1990;265:3116–23.

45. Croy JE, Shin WD, Knauer MF, Knauer DJ, Komives EA. All three LDL receptor homology regions of the LDL receptor-related protein bind multiple ligands. Biochemistry. 2003;42:13049–57 Available from: http://pubs.acs.org/doi/abs/10.1021/bi034752s. Cited 2019 Feb 22.

46. Divekar SD, Burrell TC, Lee JE, Weeber EJ, Rebeck GW. Ligand-induced homotypic and heterotypic clustering of apolipoprotein E receptor 2. J Biol Chem. 2014;289:15894–903 American Society for Biochemistry and Molecular Biology Inc. Available from: https://pubmed.ncbi.nlm.nih.gov/24755222/. Cited 2020 Dec 20.

47. Boucher R, Larkin H, Brodeur J, Gagnon H, Thériault C, Lavoie C. Intracellular trafficking of LRP9 is dependent on two acidic cluster/dileucine motifs. Histochem Cell Biol. 2008;130:315–27 Springer Verlag. Available from: https://pubmed.ncbi.nlm.nih.gov/18461348/. Cited 2020 Aug 6.

48. Brodeur J, Thériault C, Lessard-Beaudoin M, Marcil A, Dahan S, Lavoie C. LDLR-related protein 10 (LRP10) regulates amyloid precursor protein (APP) trafficking and processing: evidence for a role in Alzheimer's disease. Mol Neurodegener. 2012;7:31 Available from: https://pubmed.ncbi.nlm.nih.gov/22734645/. Cited 2020 Jul 30.

49. Ranganathan S, Noyes NC, Migliorini M, Winkles JA, Battey FD, Hyman BT, et al. LRAD3, a novel low-density lipoprotein receptor family member that modulates amyloid precursor protein trafficking. J Neurosci. 2011;31:10836–46 Available from: https://pubmed.ncbi.nlm.nih.gov/21795536/. Cited 2020 Dec 26.

50. Ho A, Südhof TC. Binding of F-spondin to amyloid-β precursor protein: a candidate amyloid-β precursor protein ligand that modulates amyloid-β precursor protein cleavage. Proc Natl Acad Sci U S A. 2004;101:2548–53.

51. May P, Krishna Reddy Y, Herz J. Proteolytic processing of low density lipoprotein receptor-related protein mediates regulated release of its intracellular domain. J Biol Chem. 2002;277:18736–43 Available from: https://pubmed.ncbi.nlm.nih.gov/11907044/. Cited 2020 Aug 4.

52. Hoe HS, Tran TS, Matsuoka Y, Howell BW, Rebeck GW. DAB1 and reelin effects on amyloid precursor protein and ApoE receptor 2 trafficking and processing. J Biol Chem. 2006;281:35176–85 JBC Papers in Press. Available from: http://www.jbc.org/. Cited 2020 Dec 20.

53. Evrard C, Kienlen-Campard P, Coevoet M, Opsomer R, Tasiaux B, Melnyk P, et al. Contribution of the endosomal-lysosomal and proteasomal systems in amyloid-β precursor protein-derived fragments processing. Front Cell Neurosci. 2018;12:435 Frontiers Media S.A. Available from: www.frontiersin.org. Cited 2021 Jun 5.

54. Kounnas MZ, Moir RD, Rebeck GW, Bush AI, Argraves WS, Tanzi RE, et al. LDL receptor-related protein, a multifunctional ApoE receptor, binds secreted β-amyloid precursor protein and mediates its degradation. Cell. 1995;82:331–40.

55. Bu G, Cam J, Zerbinatti C. LRP in amyloid-beta production and metabolism. Ann N Y Acad Sci. 2006;1086:35–53 Available from: http://www.ncbi.nlm.nih.gov/pubmed/17185504. Cited 2020 Feb 14.

56. Holtzman DM, Herz J, Bu G. Apolipoprotein E and apolipoprotein E receptors: normal biology and roles in Alzheimer disease. Cold Spring Harb Perspect Med. 2012;2:a006312 Cold Spring Harbor Laboratory Press. Available from: http://www.ncbi.nlm.nih.gov/pubmed/22393530. Cited 2020 Feb 14.

57. Zhang H, Chen W, Tan Z, Zhang L, Dong Z, Cui W, et al. A role of low-density lipoprotein receptor-related protein 4 (LRP4) in astrocytic Aβ clearance. J Neurosci. 2020;40:JN-RM-0250-20 Society for Neuroscience. Available from: https://pubmed.ncbi.nlm.nih.gov/32457076/. Cited 2020 Jul 30.

58. Ulery PG, Beers J, Mikhailenko I, Tanzi RE, Rebeck GW, Hyman BT, et al. Modulation of β-amyloid precursor protein processing by the low density lipoprotein receptor-related protein (LRP). Evidence that LRP contributes to the pathogenesis of Alzheimer's disease. J Biol Chem. 2000;275:7410–5.

59. Pietrzik CU, Busse T, Merriam DE, Weggen S, Koo EH. The cytoplasmic domain of the LDL receptor-related protein regulates multiple steps in APP processing. EMBO J. 2002;21:5691–700.

60. Cam JA, Zerbinatti CV, Li Y, Bu G. Rapid endocytosis of the low density lipoprotein receptor-related protein modulates cell surface distribution and processing of the beta-amyloid precursor protein. J Biol Chem. 2005;280:15464–70 Available from: http://www.ncbi.nlm.nih.gov/pubmed/15705569. Cited 2020 Feb 14.

61. Cam JA, Zerbinatti CV, Knisely JM, Hecimovic S, Li Y, Bu G. The low density lipoprotein receptor-related protein 1B retains beta-amyloid precursor protein at the cell surface and reduces amyloid-beta peptide production. J Biol Chem. 2004;279:29639–46 Available from: http://www.ncbi.nlm.nih.gov/pubmed/15126508. Cited 2020 Feb 14.

62. Fuentealba RA, Barria MI, Lee J, Cam J, Araya C, Escudero CA, et al. ApoER2 expression increases Abeta production while decreasing Amyloid Precursor Protein (APP) endocytosis: possible role in the partitioning of APP into lipid rafts and in the regulation of gamma-secretase activity. Mol Neurodegener. 2007;2:14 Available from: http://www.ncbi.nlm.nih.gov/pubmed/17620134. Cited 2020 Feb 14.

63. Goto JJ, Tanzi RE. The role of the low-density lipoprotein receptor-related protein (LRP1) in Alzheimer's Aβ generation: development of a cell-based model system. J Mol Neurosci. 2002;19:37–41 Humana Press. Available from: http://www.ncbi.nlm.nih.gov/pubmed/12212791. Cited 2020 Apr 2.

64. Van Gool B, Storck SE, Reekmans SM, Lechat B, Gordts PLSM, Pradier L, et al. LRP1 has a predominant role in production over clearance of Aβ in a mouse model of Alzheimer's disease. Mol Neurobiol. 2019;56:7234–45 Humana Press Inc. Available from: https://pubmed.ncbi.nlm.nih.gov/31004319/. Cited 2020 Dec 28.

65. Eggert S, Gonzalez AC, Thomas C, Schilling S, Schwarz SM, Tischer C, et al. Dimerization leads to changes in APP (amyloid precursor protein) trafficking mediated by LRP1 and SorLA. Cell Mol Life Sci. 2018;75:301–22 Birkhauser Verlag AG. Available from: https://pubmed.ncbi.nlm.nih.gov/28799085/. Cited 2021 Jan 18.

66. Herr UM, Strecker P, Storck SE, Thomas C, Rabiej V, Junker A, et al. LRP1 modulates APP intraneuronal transport and processing in its monomeric and dimeric state. Front Mol Neurosci. 2017;10:118 Frontiers Research Foundation. Available from: https://pubmed.ncbi.nlm.nih.gov/28496400/. Cited 2020 Dec 27.

138

Cuchillo-Ibañez et al. Alz Res Therapy   (2021) 13:181

Page 17 of 17

67. Rauch JN, Luna G, Guzman E, Audouard M, Challis C, Sibih YE, et al. LRP1 is a master regulator of tau uptake and spread. Nature. 2020;580:381–5 Nature Research.

68. Elsafadi M, Manikandan M, Alajez NM, Hamam R, Dawud RA, Aldahmash A, et al. MicroRNA-4739 regulates osteogenic and adipocytic differentiation of immortalized human bone marrow stromal cells via targeting LRP3. Stem Cell Res. 2017;2094–104 Available from: http://www.ncbi.nlm.nih.gov/pubmed/28340487. Cited 2020 Feb 14.

69. Wan ES, Qiu W, Baccarelli A, Carey VJ, Bacherman H, Rennard SI, et al. Systemic steroid exposure is associated with differential methylation in chronic obstructive pulmonary disease. Am J Respir Crit Care Med.

2012;186:1248–55 Available from: http://www.ncbi.nlm.nih.gov/pubmed/23065012. Cited 2020 Feb 14.

70. O'Sullivan NC, McGettigan PA, Sheridan GK, Pickering M, Conboy L, O'Connor JJ, et al. Temporal change in gene expression in the rat dentate gyrus following passive avoidance learning. J Neurochem. 2007;101:1085–98 Available from: http://www.ncbi.nlm.nih.gov/pubmed/17298388. Cited 2020 Feb 14.

Publisher's Note

Springer Nature remains neutral with regard to jurisdictional claims in published maps and institutional affiliations.

139

DISCUSSION

AD is a multifactorial disease that involves many different mechanisms, amongst which reelin and apoE appear to play important roles. Our studies demonstrate that both proteins present an aberrant profile associated to the AD condition that may result in ineffective function, and this has been confirmed by other research groups. In AD CSF samples, total protein levels, glycosylation, dimerization, and fragmentation of apoE and reelin differ from control subjects. The articles included in the doctoral thesis suggest that specific proteins that link apoE and reelin receptor pathways, such as apoER2 or LRP3, could participate in AD-related mechanisms.

The first article included in this doctoral thesis was centred on apoE in the CSF from individuals with AD. We detected a net increase of apoE levels in the CSF samples of transgenic rats and AD patients. Increased apoE levels in transgenic rat CSF were also reported in a recent study (Bac et al., 2023), whereas mainly contradictory results have been presented in studies assessing apoE levels in AD CSF samples (Cruchaga et al., 2012). In our study, while a unique immunoreactive band was detected in the transgenic rat, two distinct apoE glycoforms of 34 and 36 kDa were detected in human CSF. Levels of the less glycosylated 34 kDa species were found to be particularly increased in AD samples, leading to an imbalance in the 36/34 kDa ratio, which was lower in AD patients. We partially validated the results in a second cohort, as higher 34 kDa apoE levels and a decreased 36/34 kDa ratio were observed in AD samples compared with controls. Therefore, despite the occurrence of increased total levels of apoE, the proportion of glycosylated apoE compared to less glycosylated apoE is reduced in AD, which could hinder the biological roles of the protein, as adequate glycosylation is essential for the correct functioning of apoE (Kacperczyk et al., 2021). Interestingly, in the first cohort the *APOE* ε4/ε4 cases presented a higher 36/34 kDa ratio than the AD samples with different *APOE* genotypes; however, these differences were not observed in the second cohort. Anyhow, due to the basal compromise in some of the biological functions of apoE4, *APOE* ε4-carriers may be more sensitive to the alterations in the balance

of glycoforms, and therefore smaller changes in apoE4 could have more direct consequences than in apoE3.

Many studies have associated changes in glycosylation to AD, reporting, for instance, changes in carbohydrate metabolism (Johnson et al., 2020) and N-glycosylation (Chen et al., 2021) in the pathology, and as such the glycosylation of proteins has been considered as a potential therapeutic target (Conroy et al., 2021). Alterations in organelles involved in glycosylation have also been reported in AD, such as endoplasmic reticulum stress (Imaizumi et al., 2001) and Golgi fragmentation (Haukedal et al., 2023). The apoE glycoform imbalance detected in the CSF should therefore come as no surprise, as it coincides with previous reports in AD describing an aberrant glycosylation pattern in many key proteins, including APP, BACE1, nicastrin, tau and PS (reviewed in Schedin-Weiss et al., 2013). For example, the modification of APP O-glycosylation has been linked to Aβ generation and, as such, some studies have proposed that maintaining APP glycosylation status at a state comparable to younger people could protect against AD (Akasaka-Manya & Manya, 2020). Therefore, the aberrant glycosylation in apoE leading to the progressive switch observed from the control condition, characterized by abundant 36 kDa species, to the pathological condition, in which the presence of 34 kDa species is increased, could explain the role that apoE plays in AD by slowly losing the protective functions, such as Aβ clearance, which are expected to be carried out by the mature 36 kDa species.

We also detected an aberrant apoE species of approximately 100 kDa exclusively in AD cases, regardless of the *APOE* genotype, probably representing dimers, but not linked by disulphide bonds, since they were resistant to β-mercaptoethanol. As discussed earlier (Rebeck et al., 1998), apoE4 lacks the ability to form stable dimers through the amino acid substitution at position 112 (Arg instead of Cys). Nonetheless, we confirmed the identity of these species as apoE via immunoprecipitation and mass spectrometry studies. Through trials under reducing and non-reducing conditions, these high molecular mass species were also detected in control samples when analysed in absence of the reducing agent β-mercaptoethanol. Furthermore, using an apoE4-specific antibody, we identified apoE4 as part of the aberrant dimers in AD cases, but not in disulphide-linked dimers from control *APOE* ε3/ε4 cases under non-reducing conditions, thus

indicating that apoE4 only participates in the aberrant aggregates. This phenomenon was corroborated under native conditions, in which dimers were detected in *APOE* ε4/ε4 AD subjects, and *APOE* ε3/ε4 AD cases presented a higher proportion of dimers compared to genotype-matched controls. The occurrence in human CSF of these SDS-stable dimers is highly unexpected, as they had only been described previously *in vitro* (Martel et al., 1997). Further studies are required to confirm their nature and composition. Interestingly, both apoE and reelin exhibit aberrant aggregates related to the AD condition. A similar phenomenon occurs in soluble CSF-PS1 complexes (Sogorb-Esteve et al., 2018), in which Aβ oligomers are identified as part of the complexes. Therefore, we hypothesize that Aβ oligomers could trigger and participate, as a cross-linking agent, in the formation of these SDS-stable complexes.

In addition to characterizing these apoE complexes to decipher their significance, it would be desirable to evaluate the potential of aberrant apoE dimerization as a read-out for AD progression. In this sense, it will also be of interest to determine whether apoE immature glycoforms are part of the aberrant complexes, as immature glycoforms are not expected to participate in disulphide-linked dimers.

Our preliminary studies in AD brain samples seem to replicate the imbalance of apoE glycoforms detected in the CSF. Results in AD brain samples suggest an inability to correctly produce fully glycosylated 36 kDa apoE species, particularly in samples from the temporal region, displaying a major depletion in these mature glycoforms. The levels of the less glycosylated 34 kDa species, on the other hand, remain unaltered in both temporal and frontal regions; thus, the capacity to synthetize apoE appears to be unaffected, and accordingly an altered post-translational mechanism is expected. ApoE glycosylation is of great functional importance (Flowers et al., 2020); therefore, these modifications could be indicative of a loss of function for apoE in AD, leading to a paradoxical situation in which apoE is incapable of adequately performing its functions, despite the increased total CSF levels in AD patients and the transgenic rat model.

Our initial results regarding saline solubilization of apoE, showing less soluble apoE in AD samples compared to controls, appear to support this hypothesis: apoE would be retained within the cell, thus hindering its biological

functions. It is worth noting that no higher molecular mass species comparable to the 100 kDa band in the CSF were detected in brain extracts, despite being reported in previous studies (Permanne et al., 1997). These complexes may exist in the AD brain but could be lost through the solubilization process (e.g., sonication); to confirm this, studies are required to assess how sensitive the SDS-stable aggregates obtained from the CSF are to the chemical treatments and gentle extraction protocols used for brain samples.

Recapitulating, apoE appears to suffer structural modifications in the human AD brain and CSF. It is worth noting that the CSF samples are usually obtained as a means to diagnose AD when the first clinical symptoms appear, so the structural modifications in apoE likely represent early stages of the pathology. In the brain, the large depletion of the mature apoE glycoforms in the earliest-affected areas suggests that these modifications could increase with the progression of AD. Analysis of ventricular CSF obtained from post-mortem subjects could be of value to demonstrate the depletion of the 36 kDa apoE species and the occurrence of apoE aggregates, as demonstrated previously for other soluble protein aggregates (García-Ayllón et al., 2013).

In the study regarding reelin processing in AD, we detected a decrease in full-length reelin levels, alongside an imbalance in the levels of reelin fragments present in the CSF of AD patients, when compared to controls. An increase of the N-terminal 310 kDa and C-terminal 100 kDa fragments was detected, indicative of enhanced cleavage at the C-terminal region. However, the N-terminal 180 kDa reelin fragment levels remained unaltered, whereas decreased 250 kDa C-terminal fragment levels were found, likely pointing towards reduced N-terminal region cleavage of reelin, which is expected to occur after reelin binding to apoER2 (Hibi & Hattori, 2009). Our group described an ineffective binding of reelin to apoER2 in AD (Cuchillo-Ibañez et al., 2016), which could be responsible for the reduced N-terminal cleavage. This ineffective binding could lead reelin to be processed by other mechanisms that are independent of its interaction with the apoER2 receptor, such as the activity of extracellular matrix metalloproteinases, which may be responsible for the imbalance in reelin fragments observed in the CSF (Hattori & Kohno, 2021). Therefore, AD samples

appear to be characterised by enhanced C-terminal region cleavage and reduced N-terminal region cleavage.

The imbalances detected allowed us to describe quotients for reelin N-terminal (310 kDa/180 kDa) and C-terminal (100 kDa/250 kDa) fragments that appear to be higher in AD than in controls, and these quotients could serve as a better read-out for the pathology than reelin concentrations alone, which present high inter-subject variability (Botella-López et al., 2010). In previous studies we focused on the determination in AD brain and CSF samples of the levels of the 180 kDa N-terminal fragment and the 420 kDa full-length reelin, and both were detected at higher levels in the pathology (Cuchillo-Ibáñez et al., 2016).

In our current study on reelin, we performed a more reliable quantification of the 420 kDa species, given that we used western blotting with an enhanced resolution, based on infrared-excitation of the fluorophores attached to the secondary antibodies, and we optimized the separation between higher molecular mass species by resolving the electrophoresis on 4-15% polyacrylamide-gradient gels. These changes allowed us to detect, unexpectedly, the presence of an additional 500 kDa reelin immunoreactive species exclusively in AD samples, regardless of the *APOE* genotype. In previous studies, these aberrant high molecular weight species of 500 kDa were probably mixed with full-length reelin (in previous analyses, 6% polyacrylamide gels were used), which could explain the contradiction in full-length reelin levels between studies (in previous reports increased full-length reelin was detected, whereas we found decreased full-length reelin levels). The 500 kDa reelin species appeared to lack the C-terminal domain, as they were only detected with the N-terminal antibody.

The *APOE* genotype of the individuals could influence the levels of reelin fragments, given that apoE proteins are competitors for binding to apoER2. Accordingly, the levels of the 310 kDa reelin fragment, as well as the levels of ectodomain fragments of apoER2, appeared to be decreased in *APOE* ε4/ε4 subjects. Interestingly, previous results in cultured neurons indicated that apoE4 is probably the most effective isoform in dampening reelin signalling by binding to apoER2 (D'Arcangelo et al., 1999). Due to the fact that the interaction of reelin with apoER2 generates fragments of the ligand, this would explain the lower generation of reelin fragments in *APOE* ε4-carriers. On the other hand, apoE2,

when compared with apoE4, promotes a greater accumulation of the C-terminal fragments of apoER2 generated after interaction with the receptor (Hoe & Rebeck, 2005). This apparent contradiction, in which apoE4 binds more efficiently to apoER2 but fails to effectively activate signalling, including the subsequent endocytosis and proteolysis of the ligand and receptor, could be related with the inability of apoE4 to form disulphide-linked dimers. Reelin (Kubo et al., 2002) and apoE2/3 homodimers (Dyer et al., 1991), linked by disulphide bonds, appear as the native forms able to bind to receptors. Thus, a basal compromise or impaired signalling could occur in *APOE* ε4/ε4, in which the reelin/apoER2 signalling pathway could be activated to a lower extent than in *APOE* ε3/ε3 subjects.

In sum, the decreased levels of the 420 kDa full-length reelin, taken together with the aberrant fragmentation and aggregation of the protein, suggest that reelin signalling is altered in AD, leading to imbalances in the distribution of species detected in CSF samples.

Finally, in the third article focused on LRP3, we described a significant reduction of the levels of this novel and mainly unknown apoE receptor in the brain of patients with AD. Moreover, we demonstrated that LRP3 expression is modulated by the apoER2/reelin signalling pathway. The up-regulation of the LRP3 receptor is probably exerted by the ICD fragment of apoER2, which is generated following reelin stimulation, as the up-regulation of LRP3 was also demonstrated when apoER2-ICD was overexpressed. Nonetheless, LRP3 does not seem to interact directly with reelin, whereas it may interact with apoE. We were able to demonstrate that LRP3 expression modulates APP levels, reducing the levels of APP proteins likely through a lysosomal/autophagy pathway, a mechanism that has been proposed in previous studies (Cao et al., 2019; van Acker et al., 2019). This modulation reduced the levels of Aβ, which is particularly relevant in the context of AD, but also sAPPα, which has been seen to have protective effects (Milosch et al., 2015) and has even been proposed as a potential therapeutic target for AD (Reinhardt et al., 2018). Therefore, any benefits gained from the reduction in Aβ could be countered by the lower sAPPα levels.

LRP3 could therefore play an important role in the pathogenesis of AD through its crosstalk with apoE signalling, APP, and the apoER2/reelin signalling pathway.

ApoE, reelin and LRP3 signalling: A common link

ApoE and reelin are both glycoproteins that are characterized in AD by an aberrant glycosylation profile and the appearance of SDS-stable complexes. ApoE, particularly apoE4, interferes in reelin binding to apoER2 (D'Arcangelo et al., 1991), both as monomeric apoE (Chen et al., 2010) and as dimers (Dyer et al., 1991). Therefore, the increase of monomers of apoE (especially in *APOE* ε4/ε4), in addition to the appearance of aberrant apoE and reelin dimers, could result in increased competition for binding to apoER2, and, as such, reelin signalling could be hindered. This interference in apoER2 signalling would thus lead to a complex scenario in which increased levels of the ligands do not necessarily represent increased signalling efficiency.

ApoER2 proteolytic processing down-regulates reelin expression through the ICD fragment generated following effective ligand-receptor interaction (Balmaceda et al., 2014). Therefore, the reduced activation and subsequent processing of apoER2 that occurs in AD should lead to increased levels of reelin, however in our study we detected decreased full-length reelin levels. This contradiction could be explained by the activity of alternative means of reelin proteolysis that are likely activated through the lack of binding to apoER2, such as extracellular matrix metalloproteinases (Kohno et al., 2015), which could in turn also explain the imbalance of reelin fragments detected in the CSF of AD subjects in our study. Given the importance of the apoER2/reelin-apoE pathway in protecting against AD progression, through the inhibition of tau phosphorylation (Hoe et al., 2006) and the regulation of APP levels and, thus, Aβ generation (Hoe et al., 2005), the impairment of this pathway may also contribute to the exacerbation of AD.

As apoER2/reelin signalling increases LRP3 expression, the decreased activation of the pathway could potentially be responsible for the reduced LRP3 levels detected in the AD brain. These reduced levels could in turn lead to

enhanced APP and, consequently, increased Aβ levels, thus contributing to the progression of the pathology, although the increase in sAPPα levels could potentially counteract this effect. ApoE may be the component that interacts directly with LRP3, although the nature of this interaction is yet unknown. Further studies are required to clarify the crosstalk between LRP3 and the apoER2/reelin signalling pathway, the role of apoE, and the interaction between APP and these mechanisms.

The apoE glycoform levels and reelin proteolytic processing, taken together with the formation of aberrant aggregates of both proteins in AD, could contribute to the altered pathway and play a role in the progression of the disease by reducing the protective effects of the apoER2/reelin signalling pathway, and through a new mechanism: the LRP3 receptor. The potential pathway connecting apoE, apoER2/reelin and LRP3 is illustrated in **Figure 11**.

In light of these results and taking into consideration the deleterious effects of apoE4 on many AD-related functions (Yu et al., 2014), and the enhanced competition for binding to apoER2, the increased risk of developing AD associated to the *APOE* ε4 genotype is comprehensible. Understanding the mechanisms underlying the imbalance in apoE glycoforms and the formation of aberrant dimers could therefore provide information regarding the pathogenesis of AD, and the correction of these alterations may even serve as a therapeutic target in the future.

The imbalance in apoE glycoforms, alongside the fragmentation profile in reelin, could serve as read-outs for AD progression and could be assessed in parallel to the other CSF core biomarkers: T-tau, P-tau and Aβ42. In this sense, the high molecular weight species of both apoE and reelin detected could serve as potential biomarkers for AD. Reelin 500 kDa species were detected in the majority of AD cases, but were missing in a considerable portion, thus limiting their potential. The 100 kDa apoE species, however, did appear consistently in practically all the AD cases, and could thus serve as a potential indicator of AD. In particular, the detection of apoE dimers in *APOE* ε4/ε4 subjects, and the detection specifically of apoE4 in these complexes in *APOE* ε3/ε4 subjects, presents considerable potential as a read-out for AD. Nonetheless, techniques that distinguish between specific protein species are required.
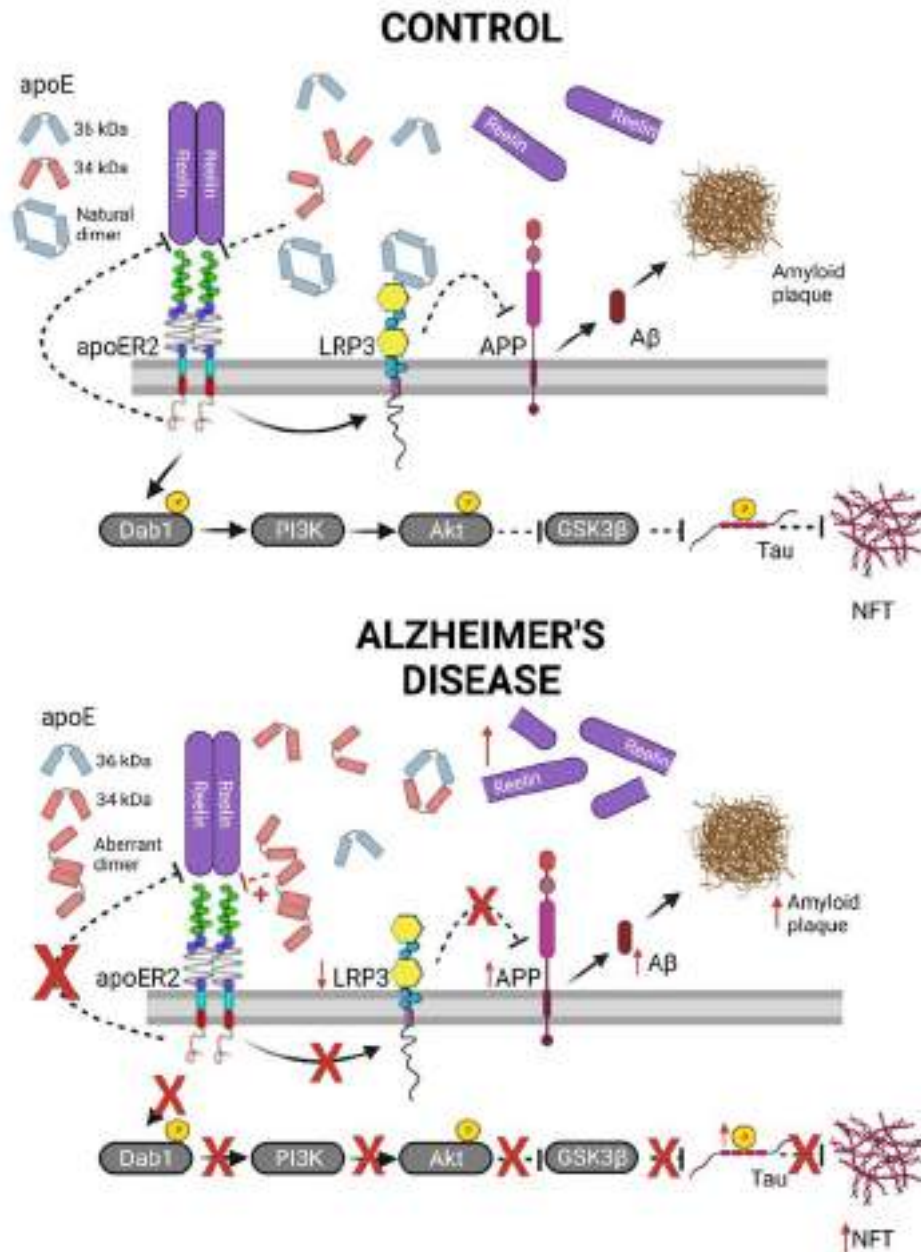
Figure 11. Illustrated pathway of potential interactions between apoE, reelin and LRP3. The control (above) and pathological (below) situations are illustrated. Reelin interaction with apoER2 leads to the processing of the receptor, forming the apoER2-ICD, which in turn inhibits reelin transcription. This ligand-receptor effective interaction also activates a downstream signalling pathway by the phosphorylation of Dab1, activating PI3K, which, in turn, phosphorylates Akt. Akt phosphorylation then inhibits GSK3β, thus preventing tau hyperphosphorylation and the subsequent formation of NFTs. The apoER2/reelin signalling activation also increases the expression of LRP3, which in turn decreases APP levels and, thus, Aβ production. ApoE competes with reelin for binding apoER2, including apoE monomers (apoE4 and maybe 34 kDa species) and aberrant dimers (represented as dimers including 34 kDa apoE with unorthodox

conformation). In AD the appearance of aberrant apoE dimers, alongside the increased presence of the less glycosylated 34 kDa apoE species, may block the apoER2/reelin signalling pathway. This blockage would also hinder the activity of the pathway, leading to decreased LRP3 levels, and consequentially an increased formation of amyloid plaques and NFTs. Reelin proteolysis through extracellular matrix metalloproteinases also appears to be enhanced, leading to an imbalance in reelin fragments. Created with BioRender.com

Limitations

All the studies reported in this doctoral thesis present limitations, some of which are already commented in the articles. The CSF studies for both apoE and reelin should be amplified in independent cohorts, preferably with a larger sample size, especially in the control groups, which included fewer subjects than the AD groups (e.g., 15 AD *APOE* ε3/ε4 subjects compared to 5 genotype-matched controls). In this sense, the inclusion of an *APOE* ε4/ε4 control group would be very interesting by allowing us to compare apoE4 from control and AD subjects, as disparities in the glycoform balance in this subgroup were detected amongst cohorts. However, it will be very difficult to obtain control samples with an *APOE* ε4/ε4 genotype, due to the high possibility of developing AD, and as such the majority of studies tend to distinguish between *APOE* ε4-carriers and non-carriers (van Harten et al., 2017).

Limitations regarding our studies in brain samples, in addition to the lack of *APOE* ε4/ε4 cases and *APOE* ε3/ε4 controls in the frontal cortex study, are focused on the absence of samples from earlier pathological stages in these cohorts. Extending the analysis with earlier Braak stage subjects and *APOE* genotypes would be desirable to enhance our understanding of the role of apoE in AD.

In the LRP3 study, very little is known regarding the function of the receptor in the brain and which proteins interact with it; as such, further studies to confirm our results in other brain cohorts could demonstrate a role for the receptor in AD. Studies using samples obtained from other brain areas would also be desirable, as LRP3 expression could vary across the brain in a similar fashion to apoER2 (Gallo et al., 2020).

The techniques used in our studies also present limitations. Western blotting, even when resolved by quantitative fluorescence, is not a reproducible

quantitative method like others, such as enzyme-linked immunosorbent assay (ELISA). The development of new sensitive and fully quantitative techniques that discriminate between particular species, such as glycoforms and aggregates, is highly desirable.

Future studies

The functional relevance of distinct apoE species is of great importance. The shift between the 36 kDa and the 34 kDa apoE glycoforms in AD may result in a decreased ability of the protein to perform its biological functions. In addition to the capacity to interact effectively with receptors, apoE glycosylation has been seen to affect its Aβ42 binding ability (Chua et al., 2010), and therefore the higher proportion of these immature glycoforms may also affect the role apoE plays in Aβ production and clearance. Studies separating the two glycoforms that assess the downstream activation of signalling pathways, alongside Aβ binding and clearance, are highly desirable. In this sense, a characterization of the glycosylation pattern of apoE glycoforms will require the examination of their interactions with different lectins, together with deglycosylation analysis.

The functional implications of the immature apoE species and aberrant dimers detected in AD, and how they interfere with natural apoE and reelin dimers, should be explored. As such, it would be interesting to develop a model (cellular or animal) that replicates the formation of aberrant dimers in order to understand how they are formed and their potential roles in AD.

In the AD human brain, we presume that the depletion of the 36 kDa apoE is related to alterations in post-translational mechanisms that do not give rise to mature apoE forms, but the studies should be completed by measuring *APOE* transcription levels, which we presume will remain unaltered. Future studies should be performed analysing apoE from different brain regions and different AD pathological stages, to assess the progression of apoE modifications throughout the brain and the pathology.

Future studies should also attempt to determine whether reelin proteolytic processing is altered in AD. The extent and regulation of reelin processing by extracellular matrix metalloproteinases remain unresolved. The functional

importance of all the reelin fragments described should also be assessed to determine if they merely interfere in signalling by interacting with full-length reelin or apoER2, or if they have additional roles. How these fragments interact/interfere in apoER2 signalling could shed some light on the impairment of reelin signalling in AD. Resolving the nature and composition of the aberrant 500 kDa species is also of interest.

Our results give rise to new questions in the field of neuronal receptors, and the exact function of LRP3 in the CNS should be described. It is plausible that LRP3 is proteolytically processed by secretases, in a similar fashion to the LRP family member apoER2 and APP. In this case, it would be interesting to study whether LRP3 fragments have specific functions. Furthermore, LRP3 modulation by apoE isoforms should be further described, and the mechanism by which reelin/apoER2 signalling affects LRP3 should be deciphered. Knowing more about the function and regulation of the receptor will help to determine whether it plays a role in AD pathogenesis.

Final remarks

In conclusion, apoE and reelin both suffer modifications in AD that could be either a cause or an effect of the disease. These modifications likely impair the functions of the proteins, leading to an exacerbation of the pathology. As they share common receptors, the aberrant dimerization of apoE and reelin, and the imbalance in apoE glycoforms and reelin fragments, may impede effective reelin/apoE binding to apoER2, thus inhibiting the protective functions of the apoER2/reelin-apoE signalling pathway. This scenario leads to the paradox in which increased levels of the ligand do not necessarily represent increased signalling, as the pathway appears to be compromised. Novel receptors, such as LRP3, that interact with key AD-related proteins, including APP, could also play a role in the regulation of apoE function in the disease process, and therefore warrant further investigation.

Despite the increased risk of developing AD associated specifically to the *APOE* ε4 allele, the majority of AD patients express the much more common ε3 allele, and thus research should not focus solely on the ε4 allelic variant. As such,

in our studies we also found important apoE modifications in *APOE* ε3 carriers, as originally hypothesized. Therefore, apoE alterations appear regardless of the *APOE* genotype, and the risk associated *APOE* ε4 allele appears to simply exacerbate the modifications present in apoE, rather than presenting unique alterations.

CONCLUSIONS

The results obtained and discussed in this Thesis can be summarized in the following points:

1) Total apoE protein levels are increased in the CSF of AD subjects, and in the CSF of transgenic rats, at early stages of the pathology.

2) SDS-PAGE-resistant apoE dimers appear in AD CSF, in all *APOE* genotypes, despite the inability of apoE4 to form disulphide-linked dimers.

3) In AD CSF samples, the less glycosylated 34 kDa apoE species is more abundant than in controls, leading to an altered glycoform balance.

4) The apoE glycoform imbalance and the aberrant dimers are consistent across all *APOE* genotypes, and do not appear to be exclusive to the risk associated *APOE* ε4 allele.

5) The altered apoE glycoform pattern is present in AD brain samples, especially in earliest-affected brain regions, such as the temporal cortex.

6) Reelin full-length protein levels and the fragment ratios described (N-terminal fragment ratio: 310/180 kDa; C-terminal fragment ratio: 100/250 kDa) increase in AD CSF samples.

7) AD CSF is characterized by the appearance of 500 kDa reelin aggregates containing the N-terminal domain.

8) The apoE glycoform imbalance and reelin fragmentation profile, as well as the aberrant dimers detected in both proteins, could serve as read-outs for AD onset and progression.

9) LRP3 is a novel receptor whose expression is modulated by the apoER2/reelin signalling pathway.

10) LRP3 affects APP levels and subsequent Aβ and sAPPα production through an autophagic/lysosomal mechanism.

Los resultados obtenidos y presentados en la presente memoria de tesis se pueden resumir en las siguientes conclusiones:

1) Los niveles totales de la proteína apoE aumentan en el LCR de sujetos con EA y ratas transgénicas en etapas tempranas de la patología.

2) En el LCR de sujetos con EA aparecen dímeros de apoE resistentes a SDS-PAGE, independientemente del genotipo *APOE*, a pesar de la incapacidad de apoE4 para formar dímeros unidos por enlaces disulfuro.

3) En las muestras de LCR de sujetos con EA se observa un desbalance en glicoformas de apoE, debido a que la especie menos glicosilada de 34 kDa es más abundante que en los controles.

4) El desequilibrio de glicoformas de apoE y los dímeros aberrantes aparecen en todos los genotipos *APOE*, y no parecen ser exclusivos del alelo *APOE* ε4, que está asociado a un mayor riesgo de padecer EA.

5) El desbalance de glicoformas de apoE también se observa en muestras de cerebro con EA, especialmente en las regiones con afectación temprana, como la corteza temporal.

6) Los niveles de reelina aumentan en el LCR de pacientes con EA; tanto los niveles de proteína completa como las proporciones de fragmentos descritas (fragmentos N-terminal: 310/180 kDa; fragmentos C-terminal: 100/250 kDa).

7) El LCR de sujetos con EA se caracteriza por la aparición de agregados de reelina de 500 kDa que contienen el dominio N-terminal de la proteína.

8) El desbalance de glicoformas de apoE y el perfil de fragmentación de la reelina, así como los dímeros aberrantes detectados en ambas proteínas., podrían servir como biomarcadores del inicio y la progresión de la EA.

9) El LRP3 es un receptor nuevo cuya expresión está modulada por la vía de señalización de apoER2/reelina.

10) El LRP3 afecta los niveles de APP y la producción de Aβ y sAPPα a través de un mecanismo autofágico/lisosomal.

REFERENCES

1- Alzheimer, A. (1907). Uber eine eigenartige Erkrankung der Hirnrinde. *Zentralbl. Nervenh. Psych.*, *18*, 177-179.

2- Gauthier S, Rosa-Neto P, Morais JA, Webster C. World Alzheimer Report 2021: Journey through the diagnosis of dementia. London: Alzheimer's Disease International; 2021.

3- 2022 Alzheimer's disease facts and figures. Alzheimers Dement. 2022 Apr;18(4):700-789. doi: 10.1002/alz.12638. Epub 2022 Mar 14. PMID: 35289055.

4- Wong W. Economic burden of Alzheimer disease and managed care considerations. Am J Manag Care. 2020 Aug;26(8 Suppl):S177-S183. doi: 10.37765/ajmc.2020.88482. PMID: 32840331.

5- Jack CR Jr, Knopman DS, Jagust WJ, Shaw LM, Aisen PS, Weiner MW, Petersen RC, Trojanowski JQ. Hypothetical model of dynamic biomarkers of the Alzheimer's pathological cascade. Lancet Neurol. 2010 Jan;9(1):119-28. doi: 10.1016/S1474-4422(09)70299-6. PMID: 20083042; PMCID: PMC2819840.

6- Ferrer I. Hypothesis review: Alzheimer's overture guidelines. Brain Pathol. 2022 Oct 12:e13122. doi: 10.1111/bpa.13122. Epub ahead of print. PMID: 36223647.

7- Braak H, Braak E. Neuropathological stageing of Alzheimer-related changes. Acta Neuropathol. 1991;82(4):239-59. doi: 10.1007/BF00308809. PMID: 1759558.

8- Braak H, Del Tredici K. The pathological process underlying Alzheimer's disease in individuals under thirty. Acta Neuropathol. 2011 Feb;121(2):171-81. doi: 10.1007/s00401-010-0789-4. Epub 2010 Dec 15. PMID: 21170538.

9- Braak H, Braak E. Frequency of stages of Alzheimer-related lesions in different age categories. Neurobiol Aging. 1997 Jul-Aug;18(4):351-7. doi: 10.1016/s0197-4580(97)00056-0. PMID: 9330961.Haass C, Kaether C, Thinakaran G, Sisodia S. Trafficking and proteolytic processing of APP. Cold Spring Harb Perspect Med. 2012 May;2(5):a006270. doi: 10.1101/cshperspect.a006270. PMID: 22553493; PMCID: PMC3331683.

10- Masters CL, Bateman R, Blennow K, Rowe CC, Sperling RA, Cummings JL. Alzheimer's disease. Nat Rev Dis Primers. 2015 Oct 15;1:15056. doi: 10.1038/nrdp.2015.56. PMID: 27188934.

11- Haass C, Kaether C, Thinakaran G, Sisodia S. Trafficking and proteolytic processing of APP. Cold Spring Harb Perspect Med. 2012 May;2(5):a006270. doi: 10.1101/cshperspect.a006270. PMID: 22553493; PMCID: PMC3331683.

12- Wasco W, Bupp K, Magendantz M, Gusella JF, Tanzi RE, Solomon F. Identification of a mouse brain cDNA that encodes a protein related to the Alzheimer disease-associated amyloid beta protein precursor. Proc Natl Acad Sci U S A. 1992 Nov 15;89(22):10758-62. doi: 10.1073/pnas.89.22.10758. PMID: 1279693; PMCID: PMC50421.

13- Coulson EJ, Paliga K, Beyreuther K, Masters CL. What the evolution of the amyloid protein precursor supergene family tells us about its function. Neurochem Int. 2000 Mar;36(3):175-84. doi: 10.1016/s0197-0186(99)00125-4. PMID: 10676850.

14- Young-Pearse TL, Bai J, Chang R, Zheng JB, LoTurco JJ, Selkoe DJ. A critical function for beta-amyloid precursor protein in neuronal migration revealed by in utero RNA interference. J Neurosci. 2007 Dec 26;27(52):14459-69. doi: 10.1523/JNEUROSCI.4701-07.2007. PMID: 18160654; PMCID: PMC6673432.

15- Zheng H, Koo EH. The amyloid precursor protein: beyond amyloid. Mol Neurodegener. 2006 Jul 3;1:5. doi: 10.1186/1750-1326-1-5. PMID: 16930452; PMCID: PMC1538601.

16- Goate A, Chartier-Harlin MC, Mullan M, Brown J, Crawford F, Fidani L, Giuffra L, Haynes A, Irving N, James L, et al. Segregation of a missense mutation in the amyloid precursor protein gene with familial Alzheimer's disease. Nature. 1991 Feb 21;349(6311):704-6. doi: 10.1038/349704a0. PMID: 1671712.

17- Menéndez-González M, Pérez-Pinera P, Martínez-Rivera M, Calatayud MT, Blázquez Menes B. APP processing and the APP-KPI domain involvement in the amyloid cascade. Neurodegener Dis. 2005;2(6):277-83. doi: 10.1159/000092315. PMID: 16909010.

18- Zhang YW, Thompson R, Zhang H, Xu H. APP processing in Alzheimer's disease. Mol Brain. 2011 Jan 7;4:3. doi: 10.1186/1756-6606-4-3. PMID: 21214928; PMCID: PMC3022812.

19- Sisodia SS. Beta-amyloid precursor protein cleavage by a membrane-bound protease. Proc Natl Acad Sci U S A. 1992 Jul 1;89(13):6075-9. doi: 10.1073/pnas.89.13.6075. PMID: 1631093; PMCID: PMC49440.

20- Spies PE, Verbeek MM, van Groen T, Claassen JA. Reviewing reasons for the decreased CSF Abeta42 concentration in Alzheimer disease. Front Biosci (Landmark Ed). 2012 Jun 1;17(6):2024-34. doi: 10.2741/4035. PMID: 22652762.

21- Furukawa K, Sopher BL, Rydel RE, Begley JG, Pham DG, Martin GM, Fox M, Mattson MP. Increased activity-regulating and neuroprotective efficacy of alpha-secretase-derived secreted amyloid precursor protein conferred by a C-terminal heparin-binding domain. J Neurochem. 1996 Nov;67(5):1882-96. doi: 10.1046/j.1471-4159.1996.67051882.x. Erratum in: J Neurochem 1997 Mar;68(3):1331. PMID: 8863493.

22- Mattson MP. Cellular actions of beta-amyloid precursor protein and its soluble and fibrillogenic derivatives. Physiol Rev. 1997 Oct;77(4):1081-132. doi: 10.1152/physrev.1997.77.4.1081. PMID: 9354812.

23- Caillé I, Allinquant B, Dupont E, Bouillot C, Langer A, Müller U, Prochiantz A. Soluble form of amyloid precursor protein regulates proliferation of progenitors in the adult subventricular zone. Development. 2004 May;131(9):2173-81. doi: 10.1242/dev.01103. Epub 2004 Apr 8. PMID: 15073156.

24- Lichtenthaler SF, Tschirner SK, Steiner H. Secretases in Alzheimer's disease: Novel insights into proteolysis of APP and TREM2. Curr Opin Neurobiol. 2022 Feb;72:101-110. doi: 10.1016/j.conb.2021.09.003. Epub 2021 Oct 22. PMID: 34689040.

25- Kuhn PH, Wang H, Dislich B, Colombo A, Zeitschel U, Ellwart JW, Kremmer E, Rossner S, Lichtenthaler SF. ADAM10 is the physiologically relevant, constitutive alpha-secretase of the amyloid precursor protein in primary neurons. EMBO J. 2010 Sep 1;29(17):3020-32. doi: 10.1038/emboj.2010.167. Epub 2010 Jul 30. PMID: 20676056; PMCID: PMC2944055.

26- Jorissen E, Prox J, Bernreuther C, Weber S, Schwanbeck R, Serneels L, Snellinx A, Craessaerts K, Thathiah A, Tesseur I, Bartsch U, Weskamp G, Blobel CP, Glatzel M, De Strooper B, Saftig P. The disintegrin/metalloproteinase ADAM10 is essential for the establishment of the brain cortex. J Neurosci. 2010 Apr 7;30(14):4833-44. doi: 10.1523/JNEUROSCI.5221-09.2010. PMID: 20371803; PMCID: PMC2921981.

27- Endres K, Fahrenholz F, Lotz J, Hiemke C, Teipel S, Lieb K, Tüscher O, Fellgiebel A. Increased CSF APPs-α levels in patients with Alzheimer disease treated with acitretin. Neurology. 2014 Nov 18;83(21):1930-5. doi: 10.1212/WNL.0000000000001017. Epub 2014 Oct 24. PMID: 25344383.

28- Colciaghi F, Borroni B, Pastorino L, Marcello E, Zimmermann M, Cattabeni F, Padovani A, Di Luca M. [alpha]-Secretase ADAM10 as well as [alpha]APPs is reduced in platelets and CSF of Alzheimer disease patients. Mol Med. 2002 Feb;8(2):67-74. PMID: 12080182; PMCID: PMC2039975.

29- Tyler SJ, Dawbarn D, Wilcock GK, Allen SJ. alpha- and beta-secretase: profound changes in Alzheimer's disease. Biochem Biophys Res Commun. 2002 Dec 6;299(3):373-6. doi: 10.1016/s0006-291x(02)02635-9. PMID: 12445809.

30- Sogorb-Esteve A, García-Ayllón MS, Gobom J, Alom J, Zetterberg H, Blennow K, Sáez-Valero J. Levels of ADAM10 are reduced in Alzheimer's disease CSF. J Neuroinflammation. 2018 Jul 25;15(1):213. doi: 10.1186/s12974-018-1255-9. PMID: 30045733; PMCID: PMC6060469.

31- Kimberly WT, LaVoie MJ, Ostaszewski BL, Ye W, Wolfe MS, Selkoe DJ. Gamma-secretase is a membrane protein complex comprised of presenilin, nicastrin, Aph-1, and Pen-2. Proc Natl Acad Sci U S A. 2003 May 27;100(11):6382-7. doi: 10.1073/pnas.1037392100. Epub 2003 May 9. PMID: 12740439; PMCID: PMC164455.

32- Takasugi N, Tomita T, Hayashi I, Tsuruoka M, Niimura M, Takahashi Y, Thinakaran G, Iwatsubo T. The role of presenilin cofactors in the gamma-secretase complex. Nature. 2003 Mar 27;422(6930):438-41. doi: 10.1038/nature01506. Epub 2003 Mar 16. PMID: 12660785.

33- Ahn K, Shelton CC, Tian Y, Zhang X, Gilchrist ML, Sisodia SS, Li YM. Activation and intrinsic gamma-secretase activity of presenilin 1. Proc Natl Acad Sci U S A. 2010 Dec 14;107(50):21435-40. doi: 10.1073/pnas.1013246107. Epub 2010 Nov 29. PMID: 21115843; PMCID: PMC3003001.

34- Arawaka S, Hasegawa H, Tandon A, Janus C, Chen F, Yu G, Kikuchi K, Koyama S, Kato T, Fraser PE, St George-Hyslop P. The levels of mature glycosylated nicastrin are regulated and correlate with gamma-secretase processing of amyloid beta-precursor protein. J Neurochem. 2002 Dec;83(5):1065-71. doi: 10.1046/j.1471-4159.2002.01207.x. PMID: 12437577.

35- Goutte C, Tsunozaki M, Hale VA, Priess JR. APH-1 is a multipass membrane protein essential for the Notch signaling pathway in Caenorhabditis elegans embryos. Proc Natl Acad Sci U S A. 2002 Jan 22;99(2):775-9. doi: 10.1073/pnas.022523499. Epub 2002 Jan 15. PMID: 11792846; PMCID: PMC117381.

36- Steiner H, Winkler E, Edbauer D, Prokop S, Basset G, Yamasaki A, Kostka M, Haass C. PEN-2 is an integral component of the gamma-secretase complex required for coordinated expression of presenilin and nicastrin. J Biol Chem. 2002 Oct 18;277(42):39062-5. doi: 10.1074/jbc.C200469200. Epub 2002 Aug 26. PMID: 12198112.

37- Sinha S, Anderson JP, Barbour R, Basi GS, Caccavello R, Davis D, Doan M, Dovey HF, Frigon N, Hong J, Jacobson-Croak K, Jewett N, Keim P, Knops J, Lieberburg I, Power M, Tan H, Tatsuno G, Tung J, Schenk D, Seubert P, Suomensaari SM, Wang S, Walker D, Zhao J, McConlogue L, John V. Purification and cloning of amyloid precursor protein beta-secretase from human brain. Nature. 1999 Dec 2;402(6761):537-40. doi: 10.1038/990114. PMID: 10591214.

38- Hampel H, Vassar R, De Strooper B, Hardy J, Willem M, Singh N, Zhou J, Yan R, Vanmechelen E, De Vos A, Nisticò R, Corbo M, Imbimbo BP, Streffer J, Voytyuk I, Timmers M, Tahami Monfared AA, Irizarry M, Albala B, Koyama A, Watanabe N, Kimura T, Yarenis L, Lista S, Kramer L, Vergallo A. The β-Secretase BACE1 in Alzheimer's Disease. Biol Psychiatry. 2021 Apr 15;89(8):745-756. doi: 10.1016/j.biopsych.2020.02.001. Epub 2020 Feb 13. PMID: 32223911; PMCID: PMC7533042.

39- Luo Y, Bolon B, Kahn S, Bennett BD, Babu-Khan S, Denis P, Fan W, Kha H, Zhang J, Gong Y, Martin L, Louis JC, Yan Q, Richards WG, Citron M, Vassar R. Mice deficient in BACE1, the Alzheimer's beta-secretase, have normal phenotype

and abolished beta-amyloid generation. Nat Neurosci. 2001 Mar;4(3):231-2. doi: 10.1038/85059. PMID: 11224535.

40- Dominguez D, Tournoy J, Hartmann D, Huth T, Cryns K, Deforce S, Serneels L, Camacho IE, Marjaux E, Craessaerts K, Roebroek AJ, Schwake M, D'Hooge R, Bach P, Kalinke U, Moechars D, Alzheimer C, Reiss K, Saftig P, De Strooper B. Phenotypic and biochemical analyses of BACE1- and BACE2-deficient mice. J Biol Chem. 2005 Sep 2;280(35):30797-806. doi: 10.1074/jbc.M505249200. Epub 2005 Jun 29. PMID: 15987683.

41- Ohno M, Sametsky EA, Younkin LH, Oakley H, Younkin SG, Citron M, Vassar R, Disterhoft JF. BACE1 deficiency rescues memory deficits and cholinergic dysfunction in a mouse model of Alzheimer's disease. Neuron. 2004 Jan 8;41(1):27-33. doi: 10.1016/s0896-6273(03)00810-9. PMID: 14715132.

42- Ohno M, Cole SL, Yasvoina M, Zhao J, Citron M, Berry R, Disterhoft JF, Vassar R. BACE1 gene deletion prevents neuron loss and memory deficits in 5XFAD APP/PS1 transgenic mice. Neurobiol Dis. 2007 Apr;26(1):134-45. doi: 10.1016/j.nbd.2006.12.008. Epub 2006 Dec 20. PMID: 17258906; PMCID: PMC1876698.

43- Yang LB, Lindholm K, Yan R, Citron M, Xia W, Yang XL, Beach T, Sue L, Wong P, Price D, Li R, Shen Y. Elevated beta-secretase expression and enzymatic activity detected in sporadic Alzheimer disease. Nat Med. 2003 Jan;9(1):3-4. doi: 10.1038/nm0103-3. PMID: 12514700.

44- Johnston JA, Liu WW, Todd SA, Coulson DT, Murphy S, Irvine GB, Passmore AP. Expression and activity of beta-site amyloid precursor protein cleaving enzyme in Alzheimer's disease. Biochem Soc Trans. 2005 Nov;33(Pt 5):1096-100. doi: 10.1042/BST20051096. PMID: 16246054.

45- Lopez-Font I, Boix CP, Zetterberg H, Blennow K, Sáez-Valero J. Characterization of Cerebrospinal Fluid BACE1 Species. Mol Neurobiol. 2019 Dec;56(12):8603-8616. doi: 10.1007/s12035-019-01677-8. Epub 2019 Jul 9. PMID: 31290061.

46- Egan MF, Kost J, Tariot PN, Aisen PS, Cummings JL, Vellas B, Sur C, Mukai Y, Voss T, Furtek C, Mahoney E, Harper Mozley L, Vandenberghe R, Mo Y, Michelson D. Randomized Trial of Verubecestat for Mild-to-Moderate Alzheimer's Disease. N Engl J Med. 2018 May 3;378(18):1691-1703. doi: 10.1056/NEJMoa1706441. PMID: 29719179; PMCID: PMC6776074.

47- Henley D, Raghavan N, Sperling R, Aisen P, Raman R, Romano G. Preliminary Results of a Trial of Atabecestat in Preclinical Alzheimer's Disease. N Engl J Med. 2019 Apr 11;380(15):1483-1485. doi: 10.1056/NEJMc1813435. PMID: 30970197.

48- Nikolaev A, McLaughlin T, O'Leary DD, Tessier-Lavigne M. APP binds DR6 to trigger axon pruning and neuron death via distinct caspases. Nature. 2009 Feb 19;457(7232):981-9. doi: 10.1038/nature07767. PMID: 19225519; PMCID: PMC2677572.

49- Zhao J, Fu Y, Yasvoina M, Shao P, Hitt B, O'Connor T, Logan S, Maus E, Citron M, Berry R, Binder L, Vassar R. Beta-site amyloid precursor protein cleaving enzyme 1 levels become elevated in neurons around amyloid plaques: implications for Alzheimer's disease pathogenesis. J Neurosci. 2007 Apr 4;27(14):3639-49. doi: 10.1523/JNEUROSCI.4396-06.2007. PMID: 17409228; PMCID: PMC6672403.

50- Kandalepas PC, Sadleir KR, Eimer WA, Zhao J, Nicholson DA, Vassar R. The Alzheimer's β-secretase BACE1 localizes to normal presynaptic terminals and to dystrophic presynaptic terminals surrounding amyloid plaques. Acta Neuropathol. 2013 Sep;126(3):329-52. doi: 10.1007/s00401-013-1152-3. Epub 2013 Jul 3. Erratum in: Acta Neuropathol. 2013 Oct;126(4):623. PMID: 23820808; PMCID: PMC3753469.

51- Sadleir KR, Kandalepas PC, Buggia-Prévot V, Nicholson DA, Thinakaran G, Vassar R. Presynaptic dystrophic neurites surrounding amyloid plaques are sites of microtubule disruption, BACE1 elevation, and increased Aβ generation in Alzheimer's disease. Acta Neuropathol. 2016 Aug;132(2):235-256. doi: 10.1007/s00401-016-1558-9. Epub 2016 Mar 18. PMID: 26993139; PMCID: PMC4947125.

52- Andrew RJ, Kellett KA, Thinakaran G, Hooper NM. A Greek Tragedy: The Growing Complexity of Alzheimer Amyloid Precursor Protein Proteolysis. J Biol Chem. 2016 Sep 9;291(37):19235-44. doi: 10.1074/jbc.R116.746032. Epub 2016 Jul 29. PMID: 27474742; PMCID: PMC5016663.

53- Jeong H, Shin H, Hong S, Kim Y. Physiological Roles of Monomeric Amyloid-β and Implications for Alzheimer's Disease Therapeutics. Exp Neurobiol. 2022 Apr 30;31(2):65-88. doi: 10.5607/en22004. PMID: 35673997; PMCID: PMC9194638.

54- Lane CA, Hardy J, Schott JM. Alzheimer's disease. Eur J Neurol. 2018 Jan;25(1):59-70. doi: 10.1111/ene.13439. Epub 2017 Oct 19. PMID: 28872215.

55- Grimmer T, Riemenschneider M, Förstl H, Henriksen G, Klunk WE, Mathis CA, Shiga T, Wester HJ, Kurz A, Drzezga A. Beta amyloid in Alzheimer's disease: increased deposition in brain is reflected in reduced concentration in cerebrospinal fluid. Biol Psychiatry. 2009 Jun 1;65(11):927-34. doi: 10.1016/j.biopsych.2009.01.027. Epub 2009 Mar 6. PMID: 19268916; PMCID: PMC2700302.

56- Strozyk D, Blennow K, White LR, Launer LJ. CSF Abeta 42 levels correlate with amyloid-neuropathology in a population-based autopsy study. Neurology. 2003 Feb 25;60(4):652-6. doi: 10.1212/01.wnl.0000046581.81650.d0. PMID: 12601108.

57- Wahlund LO, Blennow K. Cerebrospinal fluid biomarkers for disease stage and intensity in cognitively impaired patients. Neurosci Lett. 2003 Mar 20;339(2):99-102. doi: 10.1016/s0304-3940(02)01483-0. PMID: 12614904.

58- Blennow K, Zetterberg H. Biomarkers for Alzheimer's disease: current status and prospects for the future. J Intern Med. 2018 Dec;284(6):643-663. doi: 10.1111/joim.12816. Epub 2018 Aug 19. PMID: 30051512.

59- Hardy JA, Higgins GA. Alzheimer's disease: the amyloid cascade hypothesis. Science. 1992 Apr 10;256(5054):184-5. doi: 10.1126/science.1566067. PMID: 1566067.

60- Selkoe DJ, Hardy J. The amyloid hypothesis of Alzheimer's disease at 25 years. EMBO Mol Med. 2016 Jun 1;8(6):595-608. doi: 10.15252/emmm.201606210. PMID: 27025652; PMCID: PMC4888851.

61- Cline EN, Bicca MA, Viola KL, Klein WL. The Amyloid-β Oligomer Hypothesis: Beginning of the Third Decade. J Alzheimers Dis. 2018;64(s1):S567-S610. doi: 10.3233/JAD-179941. PMID: 29843241; PMCID: PMC6004937.

62- Chen GF, Xu TH, Yan Y, Zhou YR, Jiang Y, Melcher K, Xu HE. Amyloid beta: structure, biology and structure-based therapeutic development. Acta Pharmacol Sin. 2017 Sep;38(9):1205-1235. doi: 10.1038/aps.2017.28. Epub 2017 Jul 17. PMID: 28713158; PMCID: PMC5589967.

63- Reiss AB, Arain HA, Stecker MM, Siegart NM, Kasselman LJ. Amyloid toxicity in Alzheimer's disease. Rev Neurosci. 2018 Aug 28;29(6):613-627. doi: 10.1515/revneuro-2017-0063. PMID: 29447116.

64- Soria Lopez JA, González HM, Léger GC. Alzheimer's disease. Handb Clin Neurol. 2019;167:231-255. doi: 10.1016/B978-0-12-804766-8.00013-3. PMID: 31753135.

65- Grundke-Iqbal I, Iqbal K, George L, Tung YC, Kim KS, Wisniewski HM. Amyloid protein and neurofibrillary tangles coexist in the same neuron in Alzheimer

disease. Proc Natl Acad Sci U S A. 1989 Apr;86(8):2853-7. doi: 10.1073/pnas.86.8.2853. PMID: 2649895; PMCID: PMC287017.

66- Wood JG, Mirra SS, Pollock NJ, Binder LI. Neurofibrillary tangles of Alzheimer disease share antigenic determinants with the axonal microtubule-associated protein tau (tau). Proc Natl Acad Sci U S A. 1986 Jun;83(11):4040-3. doi: 10.1073/pnas.83.11.4040. Erratum in: Proc Natl Acad Sci U S A 1986 Dec;83(24):9773. PMID: 2424015; PMCID: PMC323661.

67- Robbins M, Clayton E, Kaminski Schierle GS. Synaptic tau: A pathological or physiological phenomenon? Acta Neuropathol Commun. 2021 Sep 9;9(1):149. doi: 10.1186/s40478-021-01246-y. PMID: 34503576; PMCID: PMC8428049.

68- Mandelkow EM, Mandelkow E. Biochemistry and cell biology of tau protein in neurofibrillary degeneration. Cold Spring Harb Perspect Med. 2012 Jul;2(7):a006247. doi: 10.1101/cshperspect.a006247. PMID: 22762014; PMCID: PMC3385935.

69- Kovacs GG. Tauopathies. Handb Clin Neurol. 2017;145:355-368. doi: 10.1016/B978-0-12-802395-2.00025-0. PMID: 28987182.

70- Boekhoorn K, Terwel D, Biemans B, Borghgraef P, Wiegert O, Ramakers GJ, de Vos K, Krugers H, Tomiyama T, Mori H, Joels M, van Leuven F, Lucassen PJ. Improved long-term potentiation and memory in young tau-P301L transgenic mice before onset of hyperphosphorylation and tauopathy. J Neurosci. 2006 Mar 29;26(13):3514-23. doi: 10.1523/JNEUROSCI.5425-05.2006. PMID: 16571759; PMCID: PMC6673867.

71- Shentu YP, Huo Y, Feng XL, Gilbert J, Zhang Q, Liuyang ZY, Wang XL, Wang G, Zhou H, Wang XC, Wang JZ, Lu YM, Westermarck J, Man HY, Liu R. CIP2A Causes Tau/APP Phosphorylation, Synaptopathy, and Memory Deficits in Alzheimer's Disease. Cell Rep. 2018 Jul 17;24(3):713-723. doi: 10.1016/j.celrep.2018.06.009. PMID: 30021167; PMCID: PMC6095478.

72- Selkoe DJ. Alzheimer's disease is a synaptic failure. Science. 2002 Oct 25;298(5594):789-91. doi: 10.1126/science.1074069. PMID: 12399581.

73- Sinsky J, Pichlerova K, Hanes J. Tau Protein Interaction Partners and Their Roles in Alzheimer's Disease and Other Tauopathies. Int J Mol Sci. 2021 Aug 26;22(17):9207. doi: 10.3390/ijms22179207. PMID: 34502116; PMCID: PMC8431036.

74- Goedert M, Spillantini MG, Cairns NJ, Crowther RA. Tau proteins of Alzheimer paired helical filaments: abnormal phosphorylation of all six brain isoforms. Neuron. 1992 Jan;8(1):159-68. doi: 10.1016/0896-6273(92)90117-v. PMID: 1530909.

75- He Z, Guo JL, McBride JD, Narasimhan S, Kim H, Changolkar L, Zhang B, Gathagan RJ, Yue C, Dengler C, Stieber A, Nitla M, Coulter DA, Abel T, Brunden KR, Trojanowski JQ, Lee VM. Amyloid-β plaques enhance Alzheimer's brain tau-seeded pathologies by facilitating neuritic plaque tau aggregation. Nat Med. 2018 Jan;24(1):29-38. doi: 10.1038/nm.4443. Epub 2017 Dec 4. PMID: 29200205; PMCID: PMC5760353.

76- Zhang Z, Obianyo O, Dall E, Du Y, Fu H, Liu X, Kang SS, Song M, Yu SP, Cabrele C, Schubert M, Li X, Wang JZ, Brandstetter H, Ye K. Inhibition of delta-secretase improves cognitive functions in mouse models of Alzheimer's disease. Nat Commun. 2017 Mar 27;8:14740. doi: 10.1038/ncomms14740. PMID: 28345579; PMCID: PMC5378956.

77- Braak H, Braak E. Neuropil threads occur in dendrites of tangle-bearing nerve cells. Neuropathol Appl Neurobiol. 1988 Jan-Feb;14(1):39-44. doi: 10.1111/j.1365-2990.1988.tb00864.x. PMID: 2453810.

78- Jie CVML, Treyer V, Schibli R, Mu L. Tauvid™: The First FDA-Approved PET Tracer for Imaging Tau Pathology in Alzheimer's Disease. Pharmaceuticals

(Basel). 2021 Jan 30;14(2):110. doi: 10.3390/ph14020110. PMID: 33573211; PMCID: PMC7911942.

79- Boros BD, Greathouse KM, Gentry EG, Curtis KA, Birchall EL, Gearing M, Herskowitz JH. Dendritic spines provide cognitive resilience against Alzheimer's disease. Ann Neurol. 2017 Oct;82(4):602-614. doi: 10.1002/ana.25049. Epub 2017 Oct 22. PMID: 28921611; PMCID: PMC5744899.

80- Wu HY, Hudry E, Hashimoto T, Kuchibhotla K, Rozkalne A, Fan Z, Spires-Jones T, Xie H, Arbel-Ornath M, Grosskreutz CL, Bacskai BJ, Hyman BT. Amyloid beta induces the morphological neurodegenerative triad of spine loss, dendritic simplification, and neuritic dystrophies through calcineurin activation. J Neurosci. 2010 Feb 17;30(7):2636-49. doi: 10.1523/JNEUROSCI.4456-09.2010. PMID: 20164348; PMCID: PMC2841957.

81- Burgold S, Bittner T, Dorostkar MM, Kieser D, Fuhrmann M, Mitteregger G, Kretzschmar H, Schmidt B, Herms J. In vivo multiphoton imaging reveals gradual growth of newborn amyloid plaques over weeks. Acta Neuropathol. 2011 Mar;121(3):327-35. doi: 10.1007/s00401-010-0787-6. Epub 2010 Dec 7. PMID: 21136067; PMCID: PMC3038220.

82- Reiss AB, Arain HA, Stecker MM, Siegart NM, Kasselman LJ. Amyloid toxicity in Alzheimer's disease. Rev Neurosci. 2018 Aug 28;29(6):613-627. doi: 10.1515/revneuro-2017-0063. PMID: 29447116.

83- Jack CR Jr, Bennett DA, Blennow K, Carrillo MC, Dunn B, Haeberlein SB, Holtzman DM, Jagust W, Jessen F, Karlawish J, Liu E, Molinuevo JL, Montine T, Phelps C, Rankin KP, Rowe CC, Scheltens P, Siemers E, Snyder HM, Sperling R; Contributors. NIA-AA Research Framework: Toward a biological definition of Alzheimer's disease. Alzheimers Dement. 2018 Apr;14(4):535-562. doi: 10.1016/j.jalz.2018.02.018. PMID: 29653606; PMCID: PMC5958625.

84- Pereira JB, Janelidze S, Ossenkoppele R, Kvartsberg H, Brinkmalm A, Mattsson-Carlgren N, Stomrud E, Smith R, Zetterberg H, Blennow K, Hansson O. Untangling the association of amyloid-β and tau with synaptic and axonal loss in Alzheimer's disease. Brain. 2021 Feb 12;144(1):310-324. doi: 10.1093/brain/awaa395. PMID: 33279949; PMCID: PMC8210638.

85- Calsolaro V, Edison P. Neuroinflammation in Alzheimer's disease: Current evidence and future directions. Alzheimers Dement. 2016 Jun;12(6):719-32. doi: 10.1016/j.jalz.2016.02.010. Epub 2016 May 11. PMID: 27179961.

86- Parhizkar S, Holtzman DM. APOE mediated neuroinflammation and neurodegeneration in Alzheimer's disease. Semin Immunol. 2022 Jan;59:101594. doi: 10.1016/j.smim.2022.101594. Epub 2022 Feb 26. PMID: 35232622; PMCID: PMC9411266.

87- Sastre M, Klockgether T, Heneka MT. Contribution of inflammatory processes to Alzheimer's disease: molecular mechanisms. Int J Dev Neurosci. 2006 Apr-May;24(2-3):167-76. doi: 10.1016/j.ijdevneu.2005.11.014. Epub 2006 Feb 10. PMID: 16472958.

88- Morales I, Guzmán-Martínez L, Cerda-Troncoso C, Farías GA, Maccioni RB. Neuroinflammation in the pathogenesis of Alzheimer's disease. A rational framework for the search of novel therapeutic approaches. Front Cell Neurosci. 2014 Apr 22;8:112. doi: 10.3389/fncel.2014.00112. PMID: 24795567; PMCID: PMC4001039.

89- Guo JT, Yu J, Grass D, de Beer FC, Kindy MS. Inflammation-dependent cerebral deposition of serum amyloid a protein in a mouse model of amyloidosis. J Neurosci. 2002 Jul 15;22(14):5900-9. doi: 10.1523/JNEUROSCI.22-14-05900.2002. PMID: 12122052; PMCID: PMC6757908.

90- Sastre M, Dewachter I, Landreth GE, Willson TM, Klockgether T, van Leuven F, Heneka MT. Nonsteroidal anti-inflammatory drugs and peroxisome proliferator-

activated receptor-gamma agonists modulate immunostimulated processing of amyloid precursor protein through regulation of beta-secretase. J Neurosci. 2003 Oct 29;23(30):9796-804. doi: 10.1523/JNEUROSCI.23-30-09796.2003. PMID: 14586007; PMCID: PMC6740896.

91-   Chen Z, Zhong C. Oxidative stress in Alzheimer's disease. Neurosci Bull. 2014 Apr;30(2):271-81. doi: 10.1007/s12264-013-1423-y. Epub 2014 Mar 24. PMID: 24664866; PMCID: PMC5562667.

92-   Li JQ, Yu JT, Jiang T, Tan L. Endoplasmic reticulum dysfunction in Alzheimer's disease. Mol Neurobiol. 2015 Feb;51(1):383-95. doi: 10.1007/s12035-014-8695-8. Epub 2014 Apr 9. PMID: 24715417.

93-   Lennol MP, Canelles S, Guerra-Cantera S, Argente J, García-Segura LM, de Ceballos ML, Chowen JA, Frago LM. Amyloid-β_{1-40} differentially stimulates proliferation, activation of oxidative stress and inflammatory responses in male and female hippocampal astrocyte cultures. Mech Ageing Dev. 2021 Apr;195:111462. doi: 10.1016/j.mad.2021.111462. Epub 2021 Feb 17. PMID: 33609535.

94-   Kao YC, Ho PC, Tu YK, Jou IM, Tsai KJ. Lipids and Alzheimer's Disease. Int J Mol Sci. 2020 Feb 22;21(4):1505. doi: 10.3390/ijms21041505. PMID: 32098382; PMCID: PMC7073164.

95-   Vance JE, Hayashi H, Karten B. Cholesterol homeostasis in neurons and glial cells. Semin Cell Dev Biol. 2005 Apr;16(2):193-212. doi: 10.1016/j.semcdb.2005.01.005. PMID: 15797830.

96-   Di Paolo G, Kim TW. Linking lipids to Alzheimer's disease: cholesterol and beyond. Nat Rev Neurosci. 2011 May;12(5):284-96. doi: 10.1038/nrn3012. Epub 2011 Mar 30. Erratum in: Nat Rev Neurosci. 2011 Aug;12(8):484. PMID: 21448224; PMCID: PMC3321383.

97-   Kojro E, Gimpl G, Lammich S, Marz W, Fahrenholz F. Low cholesterol stimulates the nonamyloidogenic pathway by its effect on the alpha -secretase ADAM 10. Proc Natl Acad Sci U S A. 2001 May 8;98(10):5815-20. doi: 10.1073/pnas.081612998. Epub 2001 Apr 17. PMID: 11309494; PMCID: PMC33296.

98-   Puglielli L, Tanzi RE, Kovacs DM. Alzheimer's disease: the cholesterol connection. Nat Neurosci. 2003 Apr;6(4):345-51. doi: 10.1038/nn0403-345. PMID: 12658281.

99-   Testa G, Staurenghi E, Zerbinati C, Gargiulo S, Iuliano L, Giaccone G, Fantò F, Poli G, Leonarduzzi G, Gamba P. Changes in brain oxysterols at different stages of Alzheimer's disease: Their involvement in neuroinflammation. Redox Biol. 2016 Dec;10:24-33. doi: 10.1016/j.redox.2016.09.001. Epub 2016 Sep 16. PMID: 27687218; PMCID: PMC5040635.

100-   Harold D, Abraham R, Hollingworth P, Sims R, Gerrish A, Hamshere ML, Pahwa JS, Moskvina V, Dowzell K, Williams A, Jones N, Thomas C, Stretton A, Morgan AR, Lovestone S, Powell J, Proitsi P, Lupton MK, Brayne C, Rubinsztein DC, Gill M, Lawlor B, Lynch A, Morgan K, Brown KS, Passmore PA, Craig D, McGuinness B, Todd S, Holmes C, Mann D, Smith AD, Love S, Kehoe PG, Hardy J, Mead S, Fox N, Rossor M, Collinge J, Maier W, Jessen F, Schürmann B, Heun R, van den Bussche H, Heuser I, Kornhuber J, Wiltfang J, Dichgans M, Frölich L, Hampel H, Hüll M, Rujescu D, Goate AM, Kauwe JS, Cruchaga C, Nowotny P, Morris JC, Mayo K, Sleegers K, Bettens K, Engelborghs S, De Deyn PP, Van Broeckhoven C, Livingston G, Bass NJ, Gurling H, McQuillin A, Gwilliam R, Deloukas P, Al-Chalabi A, Shaw CE, Tsolaki M, Singleton AB, Guerreiro R, Mühleisen TW, Nöthen MM, Moebus S, Jöckel KH, Klopp N, Wichmann HE, Carrasquillo MM, Pankratz VS, Younkin SG, Holmans PA, O'Donovan M, Owen MJ, Williams J. Genome-wide association study identifies variants at CLU and PICALM

associated with Alzheimer's disease. Nat Genet. 2009 Oct;41(10):1088-93. doi: 10.1038/ng.440. Epub 2009 Sep 6. Erratum in: Nat Genet. 2009 Oct;41(10):1156. Erratum in: Nat Genet. 2013 Jun;45(6):712. Haun, Reinhard [added]. PMID: 19734902; PMCID: PMC2845877.

101- Van Cauwenberghe C, Van Broeckhoven C, Sleegers K. The genetic landscape of Alzheimer disease: clinical implications and perspectives. Genet Med. 2016 May;18(5):421-30. doi: 10.1038/gim.2015.117. Epub 2015 Aug 27. PMID: 26312828; PMCID: PMC4857183.

102- Sherrington R, Froelich S, Sorbi S, Campion D, Chi H, Rogaeva EA, Levesque G, Rogaev EI, Lin C, Liang Y, Ikeda M, Mar L, Brice A, Agid Y, Percy ME, Clerget-Darpoux F, Piacentini S, Marcon G, Nacmias B, Amaducci L, Frebourg T, Lannfelt L, Rommens JM, St George-Hyslop PH. Alzheimer's disease associated with mutations in presenilin 2 is rare and variably penetrant. Hum Mol Genet. 1996 Jul;5(7):985-8. doi: 10.1093/hmg/5.7.985. PMID: 8817335.

103- Levy-Lahad E, Wasco W, Poorkaj P, Romano DM, Oshima J, Pettingell WH, Yu CE, Jondro PD, Schmidt SD, Wang K, et al. Candidate gene for the chromosome 1 familial Alzheimer's disease locus. Science. 1995 Aug 18;269(5226):973-7. doi: 10.1126/science.7638622. PMID: 7638622.

104- Canevelli M, Piscopo P, Talarico G, Vanacore N, Blasimme A, Crestini A, Tosto G, Troili F, Lenzi GL, Confaloni A, Bruno G. Familial Alzheimer's disease sustained by presenilin 2 mutations: systematic review of literature and genotype-phenotype correlation. Neurosci Biobehav Rev. 2014 May;42:170-9. doi: 10.1016/j.neubiorev.2014.02.010. Epub 2014 Mar 2. PMID: 24594196.

105- Cruts M, Theuns J, Van Broeckhoven C. Locus-specific mutation databases for neurodegenerative brain diseases. Hum Mutat. 2012 Sep;33(9):1340-4. doi: 10.1002/humu.22117. Epub 2012 Jul 2. PMID: 22581678; PMCID: PMC3465795.

106- Selkoe DJ. Alzheimer's disease: genes, proteins, and therapy. Physiol Rev. 2001 Apr;81(2):741-66. doi: 10.1152/physrev.2001.81.2.741. PMID: 11274343.

107- Walker ES, Martinez M, Brunkan AL, Goate A. Presenilin 2 familial Alzheimer's disease mutations result in partial loss of function and dramatic changes in Abeta 42/40 ratios. J Neurochem. 2005 Jan;92(2):294-301. doi: 10.1111/j.1471-4159.2004.02858.x. PMID: 15663477.

108- Cacace R, Sleegers K, Van Broeckhoven C. Molecular genetics of early-onset Alzheimer's disease revisited. Alzheimers Dement. 2016 Jun;12(6):733-48. doi: 10.1016/j.jalz.2016.01.012. Epub 2016 Mar 24. PMID: 27016693.

109- Ayodele T, Rogaeva E, Kurup JT, Beecham G, Reitz C. Early-Onset Alzheimer's Disease: What Is Missing in Research? Curr Neurol Neurosci Rep. 2021 Jan 19;21(2):4. doi: 10.1007/s11910-020-01090-y. PMID: 33464407; PMCID: PMC7815616.

110- Andersen OM, Rudolph IM, Willnow TE. Risk factor SORL1: from genetic association to functional validation in Alzheimer's disease. Acta Neuropathol. 2016 Nov;132(5):653-665. doi: 10.1007/s00401-016-1615-4. Epub 2016 Sep 16. PMID: 27638701; PMCID: PMC5073117.

111- Bellenguez C, Charbonnier C, Grenier-Boley B, Quenez O, Le Guennec K, Nicolas G, Chauhan G, Wallon D, Rousseau S, Richard AC, Boland A, Bourque G, Munter HM, Olaso R, Meyer V, Rollin-Sillaire A, Pasquier F, Letenneur L, Redon R, Dartigues JF, Tzourio C, Frebourg T, Lathrop M, Deleuze JF, Hannequin D, Genin E, Amouyel P, Debette S, Lambert JC, Campion D; CNR MAJ collaborators. Contribution to Alzheimer's disease risk of rare variants in TREM2, SORL1, and ABCA7 in 1779 cases and 1273 controls. Neurobiol Aging. 2017 Nov;59:220.e1-220.e9. doi: 10.1016/j.neurobiolaging.2017.07.001. Epub 2017 Jul 14. PMID: 28789839.

112- Guerreiro R, Wojtas A, Bras J, Carrasquillo M, Rogaeva E, Majounie E, Cruchaga C, Sassi C, Kauwe JS, Younkin S, Hazrati L, Collinge J, Pocock J, Lashley T, Williams J, Lambert JC, Amouyel P, Goate A, Rademakers R, Morgan K, Powell J, St George-Hyslop P, Singleton A, Hardy J; Alzheimer Genetic Analysis Group. TREM2 variants in Alzheimer's disease. N Engl J Med. 2013 Jan 10;368(2):117-27. doi: 10.1056/NEJMoa1211851. Epub 2012 Nov 14. PMID: 23150934; PMCID: PMC3631573.

113- Jonsson T, Stefansson H, Steinberg S, Jonsdottir I, Jonsson PV, Snaedal J, Bjornsson S, Huttenlocher J, Levey AI, Lah JJ, Rujescu D, Hampel H, Giegling I, Andreassen OA, Engedal K, Ulstein I, Djurovic S, Ibrahim-Verbaas C, Hofman A, Ikram MA, van Duijn CM, Thorsteinsdottir U, Kong A, Stefansson K. Variant of TREM2 associated with the risk of Alzheimer's disease. N Engl J Med. 2013 Jan 10;368(2):107-16. doi: 10.1056/NEJMoa1211103. Epub 2012 Nov 14. PMID: 23150908; PMCID: PMC3677583.

114- Pottier C, Hannequin D, Coutant S, Rovelet-Lecrux A, Wallon D, Rousseau S, Legallic S, Paquet C, Bombois S, Pariente J, Thomas-Anterion C, Michon A, Croisile B, Etcharry-Bouyx F, Berr C, Dartigues JF, Amouyel P, Dauchel H, Boutoleau-Bretonnière C, Thauvin C, Frebourg T, Lambert JC, Campion D; PHRC GMAJ Collaborators. High frequency of potentially pathogenic SORL1 mutations in autosomal dominant early-onset Alzheimer disease. Mol Psychiatry. 2012 Sep;17(9):875-9. doi: 10.1038/mp.2012.15. Epub 2012 Apr 3. PMID: 22472873.

115- Naj AC, Jun G, Beecham GW, Wang LS, Vardarajan BN, Buros J, Gallins PJ, Buxbaum JD, Jarvik GP, Crane PK, Larson EB, Bird TD, Boeve BF, Graff-Radford NR, De Jager PL, Evans D, Schneider JA, Carrasquillo MM, Ertekin-Taner N, Younkin SG, Cruchaga C, Kauwe JS, Nowotny P, Kramer P, Hardy J, Huentelman MJ, Myers AJ, Barmada MM, Demirci FY, Baldwin CT, Green RC, Rogaeva E, St George-Hyslop P, Arnold SE, Barber R, Beach T, Bigio EH, Bowen JD, Boxer A, Burke JR, Cairns NJ, Carlson CS, Carney RM, Carroll SL, Chui HC, Clark DG, Corneveaux J, Cotman CW, Cummings JL, DeCarli C, DeKosky ST, Diaz-Arrastia R, Dick M, Dickson DW, Ellis WG, Faber KM, Fallon KB, Farlow MR, Ferris S, Frosch MP, Galasko DR, Ganguli M, Gearing M, Geschwind DH, Ghetti B, Gilbert JR, Gilman S, Giordani B, Glass JD, Growdon JH, Hamilton RL, Harrell LE, Head E, Honig LS, Hulette CM, Hyman BT, Jicha GA, Jin LW, Johnson N, Karlawish J, Karydas A, Kaye JA, Kim R, Koo EH, Kowall NW, Lah JJ, Levey AI, Lieberman AP, Lopez OL, Mack WJ, Marson DC, Martiniuk F, Mash DC, Masliah E, McCormick WC, McCurry SM, McDavid AN, McKee AC, Mesulam M, Miller BL, Miller CA, Miller JW, Parisi JE, Perl DP, Peskind E, Petersen RC, Poon WW, Quinn JF, Rajbhandary RA, Raskind M, Reisberg B, Ringman JM, Roberson ED, Rosenberg RN, Sano M, Schneider LS, Seeley W, Shelanski ML, Slifer MA, Smith CD, Sonnen JA, Spina S, Stern RA, Tanzi RE, Trojanowski JQ, Troncoso JC, Van Deerlin VM, Vinters HV, Vonsattel JP, Weintraub S, Welsh-Bohmer KA, Williamson J, Woltjer RL, Cantwell LB, Dombroski BA, Beekly D, Lunetta KL, Martin ER, Kamboh MI, Saykin AJ, Reiman EM, Bennett DA, Morris JC, Montine TJ, Goate AM, Blacker D, Tsuang DW, Hakonarson H, Kukull WA, Foroud TM, Haines JL, Mayeux R, Pericak-Vance MA, Farrer LA, Schellenberg GD. Common variants at MS4A4/MS4A6E, CD2AP, CD33 and EPHA1 are associated with late-onset Alzheimer's disease. Nat Genet. 2011 May;43(5):436-41. doi: 10.1038/ng.801. Epub 2011 Apr 3. PMID: 21460841; PMCID: PMC3090745.

116- Agüero P, Sainz MJ, García-Ayllón MS, Sáez-Valero J, Téllez R, Guerrero-López R, Pérez-Pérez J, Jiménez-Escrig A, Gómez-Tortosa E. α-Secretase nonsense mutation (ADAM10 Tyr167*) in familial Alzheimer's disease. Alzheimers Res

Ther. 2020 Oct 31;12(1):139. doi: 10.1186/s13195-020-00708-0. PMID: 33129344; PMCID: PMC7603780.

117- Corder EH, Saunders AM, Strittmatter WJ, Schmechel DE, Gaskell PC, Small GW, Roses AD, Haines JL, Pericak-Vance MA. Gene dose of apolipoprotein E type 4 allele and the risk of Alzheimer's disease in late onset families. Science. 1993 Aug 13;261(5123):921-3. doi: 10.1126/science.8346443. PMID: 8346443.

118- Xu W, Tan L, Wang HF, Jiang T, Tan MS, Tan L, Zhao QF, Li JQ, Wang J, Yu JT. Meta-analysis of modifiable risk factors for Alzheimer's disease. J Neurol Neurosurg Psychiatry. 2015 Dec;86(12):1299-306. doi: 10.1136/jnnp-2015-310548. Epub 2015 Aug 20. PMID: 26294005.

119- Qizilbash N, Gregson J, Johnson ME, Pearce N, Douglas I, Wing K, Evans SJW, Pocock SJ. BMI and risk of dementia in two million people over two decades: a retrospective cohort study. Lancet Diabetes Endocrinol. 2015 Jun;3(6):431-436. doi: 10.1016/S2213-8587(15)00033-9. Epub 2015 Apr 9. PMID: 25866264.

120- Barnes DE, Yaffe K. The projected effect of risk factor reduction on Alzheimer's disease prevalence. Lancet Neurol. 2011 Sep;10(9):819-28. doi: 10.1016/S1474-4422(11)70072-2. Epub 2011 Jul 19. PMID: 21775213; PMCID: PMC3647614.

121- Nordestgaard LT, Christoffersen M, Frikke-Schmidt R. Shared Risk Factors between Dementia and Atherosclerotic Cardiovascular Disease. Int J Mol Sci. 2022 Aug 29;23(17):9777. doi: 10.3390/ijms23179777. PMID: 36077172; PMCID: PMC9456552.

122- De la Rosa A, Olaso-Gonzalez G, Arc-Chagnaud C, Millan F, Salvador-Pascual A, García-Lucerga C, Blasco-Lafarga C, Garcia-Dominguez E, Carretero A, Correas AG, Viña J, Gomez-Cabrera MC. Physical exercise in the prevention and treatment of Alzheimer's disease. J Sport Health Sci. 2020 Sep;9(5):394-404. doi: 10.1016/j.jshs.2020.01.004. Epub 2020 Feb 4. PMID: 32780691; PMCID: PMC7498620.

123- Petersson SD, Philippou E. Mediterranean Diet, Cognitive Function, and Dementia: A Systematic Review of the Evidence. Adv Nutr. 2016 Sep 15;7(5):889-904. doi: 10.3945/an.116.012138. PMID: 27633105; PMCID: PMC5015034.

124- Stern Y. Cognitive reserve in ageing and Alzheimer's disease. Lancet Neurol. 2012 Nov;11(11):1006-12. doi: 10.1016/S1474-4422(12)70191-6. PMID: 23079557; PMCID: PMC3507991.

125- Livingston G, Huntley J, Sommerlad A, Ames D, Ballard C, Banerjee S, Brayne C, Burns A, Cohen-Mansfield J, Cooper C, Costafreda SG, Dias A, Fox N, Gitlin LN, Howard R, Kales HC, Kivimäki M, Larson EB, Ogunniyi A, Orgeta V, Ritchie K, Rockwood K, Sampson EL, Samus Q, Schneider LS, Selbæk G, Teri L, Mukadam N. Dementia prevention, intervention, and care: 2020 report of the Lancet Commission. Lancet. 2020 Aug 8;396(10248):413-446. doi: 10.1016/S0140-6736(20)30367-6. Epub 2020 Jul 30. PMID: 32738937; PMCID: PMC7392084.

126- Kockx M, Traini M, Kritharides L. Cell-specific production, secretion, and function of apolipoprotein E. J Mol Med (Berl). 2018 May;96(5):361-371. doi: 10.1007/s00109-018-1632-y. Epub 2018 Mar 7. PMID: 29516132.

127- Boyles JK, Pitas RE, Wilson E, Mahley RW, Taylor JM. Apolipoprotein E associated with astrocytic glia of the central nervous system and with nonmyelinating glia of the peripheral nervous system. J Clin Invest. 1985 Oct;76(4):1501-13. doi: 10.1172/JCI112130. PMID: 3932467; PMCID: PMC424114.

128- Bruinsma IB, Wilhelmus MM, Kox M, Veerhuis R, de Waal RM, Verbeek MM. Apolipoprotein E protects cultured pericytes and astrocytes from D-Abeta(1-40)-

mediated cell death. Brain Res. 2010 Feb 22;1315:169-80. doi: 10.1016/j.brainres.2009.12.039. Epub 2009 Dec 23. PMID: 20034483.

129- Buttini M, Masliah E, Yu GQ, Palop JJ, Chang S, Bernardo A, Lin C, Wyss-Coray T, Huang Y, Mucke L. Cellular source of apolipoprotein E4 determines neuronal susceptibility to excitotoxic injury in transgenic mice. Am J Pathol. 2010 Aug;177(2):563-9. doi: 10.2353/ajpath.2010.090973. Epub 2010 Jul 1. PMID: 20595630; PMCID: PMC2913361.

130- Kockx M, Guo DL, Huby T, Lesnik P, Kay J, Sabaretnam T, Jary E, Hill M, Gaus K, Chapman J, Stow JL, Jessup W, Kritharides L. Secretion of apolipoprotein E from macrophages occurs via a protein kinase A and calcium-dependent pathway along the microtubule network. Circ Res. 2007 Sep 14;101(6):607-16. doi: 10.1161/CIRCRESAHA.107.157198. Epub 2007 Jul 27. PMID: 17660382.

131- Haukedal H, Freude KK. Implications of Glycosylation in Alzheimer's Disease. Front Neurosci. 2021 Jan 13;14:625348. doi: 10.3389/fnins.2020.625348. PMID: 33519371; PMCID: PMC7838500.

132- Mahley RW. Central Nervous System Lipoproteins: ApoE and Regulation of Cholesterol Metabolism. Arterioscler Thromb Vasc Biol. 2016 Jul;36(7):1305-15. doi: 10.1161/ATVBAHA.116.307023. Epub 2016 May 12. PMID: 27174096; PMCID: PMC4942259.

133- Lane-Donovan C, Wong WM, Durakoglugil MS, Wasser CR, Jiang S, Xian X, Herz J. Genetic Restoration of Plasma ApoE Improves Cognition and Partially Restores Synaptic Defects in ApoE-Deficient Mice. J Neurosci. 2016 Sep 28;36(39):10141-50. doi: 10.1523/JNEUROSCI.1054-16.2016. Epub 2016 Sep 28. PMID: 27683909; PMCID: PMC5039258.

134- Tensaouti Y, Yu TS, Kernie SG. Apolipoprotein E regulates the maturation of injury-induced adult-born hippocampal neurons following traumatic brain injury. PLoS One. 2020 Mar 2;15(3):e0229240. doi: 10.1371/journal.pone.0229240. PMID: 32119690; PMCID: PMC7051085.

135- Vance JE, Hayashi H. Formation and function of apolipoprotein E-containing lipoproteins in the nervous system. Biochim Biophys Acta. 2010 Aug;1801(8):806-18. doi: 10.1016/j.bbalip.2010.02.007. Epub 2010 Feb 17. PMID: 20170744.

136- Jacobo-Albavera L, Domínguez-Pérez M, Medina-Leyte DJ, González-Garrido A, Villarreal-Molina T. The Role of the ATP-Binding Cassette A1 (ABCA1) in Human Disease. Int J Mol Sci. 2021 Feb 5;22(4):1593. doi: 10.3390/ijms22041593. PMID: 33562440; PMCID: PMC7915494.

137- Feingold KR. Lipid and Lipoprotein Metabolism. Endocrinol Metab Clin North Am. 2022 Sep;51(3):437-458. doi: 10.1016/j.ecl.2022.02.008. Epub 2022 Jul 4. PMID: 35963623.

138- Fernández-Calle R, Konings SC, Frontiñán-Rubio J, García-Revilla J, Camprubí-Ferrer L, Svensson M, Martinson I, Boza-Serrano A, Venero JL, Nielsen HM, Gouras GK, Deierborg T. APOE in the bullseye of neurodegenerative diseases: impact of the APOE genotype in Alzheimer's disease pathology and brain diseases. Mol Neurodegener. 2022 Sep 24;17(1):62. doi: 10.1186/s13024-022-00566-4. PMID: 36153580; PMCID: PMC9509584.

139- Hong C, Tontonoz P. Liver X receptors in lipid metabolism: opportunities for drug discovery. Nat Rev Drug Discov. 2014 Jun;13(6):433-44. doi: 10.1038/nrd4280. Epub 2014 May 16. PMID: 24833295.

140- Koldamova R, Lefterov I. Role of LXR and ABCA1 in the pathogenesis of Alzheimer's disease - implications for a new therapeutic approach. Curr Alzheimer Res. 2007 Apr;4(2):171-8. doi: 10.2174/156720507780362227. PMID: 17430243.

141- Li Z, Shue F, Zhao N, Shinohara M, Bu G. APOE2: protective mechanism and therapeutic implications for Alzheimer's disease. Mol Neurodegener. 2020 Nov 4;15(1):63. doi: 10.1186/s13024-020-00413-4. PMID: 33148290; PMCID: PMC7640652.

142- Eisenberg DT, Kuzawa CW, Hayes MG. Worldwide allele frequencies of the human apolipoprotein E gene: climate, local adaptations, and evolutionary history. Am J Phys Anthropol. 2010 Sep;143(1):100-11. doi: 10.1002/ajpa.21298. PMID: 20734437.

143- Husain MA, Laurent B, Plourde M. APOE and Alzheimer's Disease: From Lipid Transport to Physiopathology and Therapeutics. Front Neurosci. 2021 Feb 17;15:630502. doi: 10.3389/fnins.2021.630502. PMID: 33679311; PMCID: PMC7925634.

144- Sando SB, Melquist S, Cannon A, Hutton ML, Sletvold O, Saltvedt I, White LR, Lydersen S, Aasly JO. APOE epsilon 4 lowers age at onset and is a high risk factor for Alzheimer's disease; a case control study from central Norway. BMC Neurol. 2008 Apr 16;8:9. doi: 10.1186/1471-2377-8-9. PMID: 18416843; PMCID: PMC2375917.

145- Yamazaki Y, Zhao N, Caulfield TR, Liu CC, Bu G. Apolipoprotein E and Alzheimer disease: pathobiology and targeting strategies. Nat Rev Neurol. 2019 Sep;15(9):501-518. doi: 10.1038/s41582-019-0228-7. Epub 2019 Jul 31. PMID: 31367008; PMCID: PMC7055192.

146- Roses AD. Apolipoprotein E alleles as risk factors in Alzheimer's disease. Annu Rev Med. 1996;47:387-400. doi: 10.1146/annurev.med.47.1.387. PMID: 8712790.

147- Farrer LA, Cupples LA, Haines JL, Hyman B, Kukull WA, Mayeux R, Myers RH, Pericak-Vance MA, Risch N, van Duijn CM. Effects of age, sex, and ethnicity on the association between apolipoprotein E genotype and Alzheimer disease. A meta-analysis. APOE and Alzheimer Disease Meta Analysis Consortium. JAMA. 1997 Oct 22-29;278(16):1349-56. PMID: 9343467.

148- Belloy ME, Napolioni V, Greicius MD. A Quarter Century of APOE and Alzheimer's Disease: Progress to Date and the Path Forward. Neuron. 2019 Mar 6;101(5):820-838. doi: 10.1016/j.neuron.2019.01.056. PMID: 30844401; PMCID: PMC6407643.

149- Rasmussen KL, Tybjaerg-Hansen A, Nordestgaard BG, Frikke-Schmidt R. Plasma levels of apolipoprotein E and risk of dementia in the general population. Ann Neurol. 2015 Feb;77(2):301-11. doi: 10.1002/ana.24326. Epub 2015 Jan 13. PMID: 25469919.

150- Shinohara M, Kanekiyo T, Yang L, Linthicum D, Shinohara M, Fu Y, Price L, Frisch-Daiello JL, Han X, Fryer JD, Bu G. APOE2 eases cognitive decline during Aging: Clinical and preclinical evaluations. Ann Neurol. 2016 May;79(5):758-774. doi: 10.1002/ana.24628. Epub 2016 Mar 29. PMID: 26933942; PMCID: PMC5010530.

151- Wildsmith KR, Basak JM, Patterson BW, Pyatkivskyy Y, Kim J, Yarasheski KE, Wang JX, Mawuenyega KG, Jiang H, Parsadanian M, Yoon H, Kasten T, Sigurdson WC, Xiong C, Goate A, Holtzman DM, Bateman RJ. In vivo human apolipoprotein E isoform fractional turnover rates in the CNS. PLoS One. 2012;7(6):e38013. doi: 10.1371/journal.pone.0038013. Epub 2012 Jun 4. PMID: 22675504; PMCID: PMC3366983.

152- Cruchaga C, Kauwe JS, Nowotny P, Bales K, Pickering EH, Mayo K, Bertelsen S, Hinrichs A; Alzheimer's Disease Neuroimaging Initiative; Fagan AM, Holtzman DM, Morris JC, Goate AM. Cerebrospinal fluid APOE levels: an endophenotype for genetic studies for Alzheimer's disease. Hum Mol Genet. 2012 Oct

15;21(20):4558-71. doi: 10.1093/hmg/dds296. Epub 2012 Jul 20. PMID: 22821396; PMCID: PMC3459471.flowers

153- Lin YT, Seo J, Gao F, Feldman HM, Wen HL, Penney J, Cam HP, Gjoneska E, Raja WK, Cheng J, Rueda R, Kritskiy O, Abdurrob F, Peng Z, Milo B, Yu CJ, Elmsaouri S, Dey D, Ko T, Yankner BA, Tsai LH. APOE4 Causes Widespread Molecular and Cellular Alterations Associated with Alzheimer's Disease Phenotypes in Human iPSC-Derived Brain Cell Types. Neuron. 2018 Jun 27;98(6):1141-1154.e7. doi: 10.1016/j.neuron.2018.05.008. Epub 2018 May 31. Erratum in: Neuron. 2018 Jun 27;98 (6):1294. PMID: 29861287; PMCID: PMC6023751.

154- Zhao J, Fu Y, Yamazaki Y, Ren Y, Davis MD, Liu CC, Lu W, Wang X, Chen K, Cherukuri Y, Jia L, Martens YA, Job L, Shue F, Nguyen TT, Younkin SG, Graff-Radford NR, Wszolek ZK, Brafman DA, Asmann YW, Ertekin-Taner N, Kanekiyo T, Bu G. APOE4 exacerbates synapse loss and neurodegeneration in Alzheimer's disease patient iPSC-derived cerebral organoids. Nat Commun. 2020 Nov 2;11(1):5540. doi: 10.1038/s41467-020-19264-0. Erratum in: Nat Commun. 2021 May 5;12(1):2707. PMID: 33139712; PMCID: PMC7608683.

155- Sullivan PM, Han B, Liu F, Mace BE, Ervin JF, Wu S, Koger D, Paul S, Bales KR. Reduced levels of human apoE4 protein in an animal model of cognitive impairment. Neurobiol Aging. 2011 May;32(5):791-801. doi: 10.1016/j.neurobiolaging.2009.05.011. Epub 2009 Jul 4. PMID: 19577821.

156- Garcia AR, Finch C, Gatz M, Kraft T, Eid Rodriguez D, Cummings D, Charifson M, Buetow K, Beheim BA, Allayee H, Thomas GS, Stieglitz J, Gurven MD, Kaplan H, Trumble BC. *APOE4* is associated with elevated blood lipids and lower levels of innate immune biomarkers in a tropical Amerindian subsistence population. Elife. 2021 Sep 29;10:e68231. doi: 10.7554/eLife.68231. PMID: 34586066; PMCID: PMC8480980.

157- Li H, Dhanasekaran P, Alexander ET, Rader DJ, Phillips MC, Lund-Katz S. Molecular mechanisms responsible for the differential effects of apoE3 and apoE4 on plasma lipoprotein-cholesterol levels. Arterioscler Thromb Vasc Biol. 2013 Apr;33(4):687-93. doi: 10.1161/ATVBAHA.112.301193. Epub 2013 Feb 14. PMID: 23413428; PMCID: PMC3660844.

158- Weisgraber KH. Apolipoprotein E: structure-function relationships. Adv Protein Chem. 1994;45:249-302. doi: 10.1016/s0065-3233(08)60642-7. PMID: 8154371.

159- Frieden C, Garai K. Concerning the structure of apoE. Protein Sci. 2013 Dec;22(12):1820-5. doi: 10.1002/pro.2379. Epub 2013 Oct 19. PMID: 24115173; PMCID: PMC3843636.

160- Chen Y, Strickland MR, Soranno A, Holtzman DM. Apolipoprotein E: Structural Insights and Links to Alzheimer Disease Pathogenesis. Neuron. 2021 Jan 20;109(2):205-221. doi: 10.1016/j.neuron.2020.10.008. Epub 2020 Nov 10. PMID: 33176118; PMCID: PMC7931158.

161- Yu JT, Tan L, Hardy J. Apolipoprotein E in Alzheimer's disease: an update. Annu Rev Neurosci. 2014;37:79-100. doi: 10.1146/annurev-neuro-071013-014300. Epub 2014 Apr 21. PMID: 24821312. Yu JT, Tan L, Hardy J. Apolipoprotein E in Alzheimer's disease: an update. Annu Rev Neurosci. 2014;37:79-100. doi: 10.1146/annurev-neuro-071013-014300. Epub 2014 Apr 21. PMID: 24821312.hardy

162- Elliott DA, Halliday GM, Garner B. Apolipoprotein-E forms dimers in human frontal cortex and hippocampus. BMC Neurosci. 2010 Feb 20;11:23. doi: 10.1186/1471-2202-11-23. PMID: 20170526; PMCID: PMC2837047.

163- Weisgraber KH, Innerarity TL, Mahley RW. Abnormal lipoprotein receptor-binding activity of the human E apoprotein due to cysteine-arginine interchange at a single site. J Biol Chem. 1982 Mar 10;257(5):2518-21. PMID: 6277903.

164- Hubin E, Verghese PB, van Nuland N, Broersen K. Apolipoprotein E associated with reconstituted high-density lipoprotein-like particles is protected from aggregation. FEBS Lett. 2019 Jun;593(11):1144-1153. doi: 10.1002/1873-3468.13428. Epub 2019 May 27. PMID: 31058310; PMCID: PMC6617784.

165- Wardell MR, Brennan SO, Janus ED, Fraser R, Carrell RW. Apolipoprotein E2-Christchurch (136 Arg----Ser). New variant of human apolipoprotein E in a patient with type III hyperlipoproteinemia. J Clin Invest. 1987 Aug;80(2):483-90. doi: 10.1172/JCI113096. PMID: 3038959; PMCID: PMC442261.

166- Arboleda-Velasquez JF, Lopera F, O'Hare M, Delgado-Tirado S, Marino C, Chmielewska N, Saez-Torres KL, Amarnani D, Schultz AP, Sperling RA, Leyton-Cifuentes D, Chen K, Baena A, Aguillon D, Rios-Romenets S, Giraldo M, Guzmán-Vélez E, Norton DJ, Pardilla-Delgado E, Artola A, Sanchez JS, Acosta-Uribe J, Lalli M, Kosik KS, Huentelman MJ, Zetterberg H, Blennow K, Reiman RA, Luo J, Chen Y, Thiyyagura P, Su Y, Jun GR, Naymik M, Gai X, Bootwalla M, Ji J, Shen L, Miller JB, Kim LA, Tariot PN, Johnson KA, Reiman EM, Quiroz YT. Resistance to autosomal dominant Alzheimer's disease in an APOE3 Christchurch homozygote: a case report. Nat Med. 2019 Nov;25(11):1680-1683. doi: 10.1038/s41591-019-0611-3. Epub 2019 Nov 4. PMID: 31686034; PMCID: PMC6898984.

167- Hernandez I, Gelpi E, Molina-Porcel L, Bernal S, Rodríguez-Santiago B, Dols-Icardo O, Ruiz A, Alcolea D, Boada M, Lleó A, Clarimón J. Heterozygous APOE Christchurch in familial Alzheimer's disease without mutations in other Mendelian genes. Neuropathol Appl Neurobiol. 2021 Jun;47(4):579-582. doi: 10.1111/nan.12670. Epub 2020 Nov 5. PMID: 33095930.

168- Le Guen Y, Belloy ME, Grenier-Boley B, de Rojas I, Castillo-Morales A, Jansen I, Nicolas A, Bellenguez C, Dalmasso C, Küçükali F, Eger SJ, Rasmussen KL, Thomassen JQ, Deleuze JF, He Z, Napolioni V, Amouyel P, Jessen F, Kehoe PG, van Duijn C, Tsolaki M, Sánchez-Juan P, Sleegers K, Ingelsson M, Rossi G, Hiltunen M, Sims R, van der Flier WM, Ramirez A, Andreassen OA, Frikke-Schmidt R, Williams J, Ruiz A, Lambert JC, Greicius MD; Members of the EADB, GR@ACE, DEGESCO, DemGene, GERAD, and EADI Groups; Arosio B, Benussi L, Boland A, Borroni B, Caffarra P, Daian D, Daniele A, Debette S, Dufouil C, Düzel E, Galimberti D, Giedraitis V, Grimmer T, Graff C, Grünblatt E, Hanon O, Hausner L, Heilmann-Heimbach S, Holstege H, Hort J, Jürgen D, Kuulasmaa T, van der Lugt A, Masullo C, Mecocci P, Mehrabian S, de Mendonça A, Moebus S, Nacmias B, Nicolas G, Olaso R, Papenberg G, Parnetti L, Pasquier F, Peters O, Pijnenburg YAL, Popp J, Rainero I, Ramakers I, Riedel-Heller S, Scarmeas N, Scheltens P, Scherbaum N, Schneider A, Seripa D, Soininen H, Solfrizzi V, Spalletta G, Squassina A, van Swieten J, Tegos TJ, Tremolizzo L, Verhey F, Vyhnalek M, Wiltfang J, Boada M, García-González P, Puerta R, Real LM, Álvarez V, Bullido MJ, Clarimon J, García-Alberca JM, Mir P, Moreno F, Pastor P, Piñol-Ripoll G, Molina-Porcel L, Pérez-Tur J, Rodríguez-Rodríguez E, Royo JL, Sánchez-Valle R, Dichgans M, Rujescu D. Association of Rare APOE Missense Variants V236E and R251G With Risk of Alzheimer Disease. JAMA Neurol. 2022 Jul 1;79(7):652-663. doi: 10.1001/jamaneurol.2022.1166. PMID: 35639372; PMCID: PMC9157381.Shuvaev VV, Fujii J, Kawasaki Y, Itoh H, Hamaoka R, Barbier A, Ziegler O, Siest G, Taniguchi N. Glycation of apolipoprotein E impairs its binding to heparin: identification of the major glycation site. Biochim Biophys Acta. 1999 Aug 30;1454(3):296-308. doi: 10.1016/s0925-4439(99)00047-2. PMID: 10452964.

169- Jaros JA, Martins-de-Souza D, Rahmoune H, Rothermundt M, Leweke FM, Guest PC, Bahn S. Protein phosphorylation patterns in serum from schizophrenia

patients and healthy controls. J Proteomics. 2012 Dec 5;76 Spec No.:43-55. doi: 10.1016/j.jprot.2012.05.027. Epub 2012 May 26. PMID: 22641159.

170- Jolivalt C, Leininger-Muller B, Drozdz R, Naskalski JW, Siest G. Apolipoprotein E is highly susceptible to oxidation by myeloperoxidase, an enzyme present in the brain. Neurosci Lett. 1996 May 24;210(1):61-4. doi: 10.1016/0304-3940(96)12661-6. PMID: 8762192.

171- Shuvaev VV, Fujii J, Kawasaki Y, Itoh H, Hamaoka R, Barbier A, Ziegler O, Siest G, Taniguchi N. Glycation of apolipoprotein E impairs its binding to heparin: identification of the major glycation site. Biochim Biophys Acta. 1999 Aug 30;1454(3):296-308. doi: 10.1016/s0925-4439(99)00047-2. PMID: 10452964.

172- Ke LY, Chan HC, Chen CC, Chang CF, Lu PL, Chu CS, Lai WT, Shin SJ, Liu FT, Chen CH. Increased APOE glycosylation plays a key role in the atherogenicity of L5 low-density lipoprotein. FASEB J. 2020 Jul;34(7):9802-9813. doi: 10.1096/fj.202000659R. Epub 2020 Jun 5. PMID: 32501643.

173- Martens YA, Zhao N, Liu CC, Kanekiyo T, Yang AJ, Goate AM, Holtzman DM, Bu G. ApoE Cascade Hypothesis in the pathogenesis of Alzheimer's disease and related dementias. Neuron. 2022 Apr 20;110(8):1304-1317. doi: 10.1016/j.neuron.2022.03.004. Epub 2022 Mar 16. PMID: 35298921; PMCID: PMC9035117.

174- Flowers SA, Grant OC, Woods RJ, Rebeck GW. O-glycosylation on cerebrospinal fluid and plasma apolipoprotein E differs in the lipid-binding domain. Glycobiology. 2020 Jan 28;30(2):74-85. doi: 10.1093/glycob/cwz084. PMID: 31616924; PMCID: PMC7335482.

175- Lee Y, Kockx M, Raftery MJ, Jessup W, Griffith R, Kritharides L. Glycosylation and sialylation of macrophage-derived human apolipoprotein E analyzed by SDS-PAGE and mass spectrometry: evidence for a novel site of glycosylation on Ser290. Mol Cell Proteomics. 2010 Sep;9(9):1968-81. doi: 10.1074/mcp.M900430-MCP200. Epub 2010 May 28. PMID: 20511397; PMCID: PMC2938105.

176- Lanfranco MF, Sepulveda J, Kopetsky G, Rebeck GW. Expression and secretion of apoE isoforms in astrocytes and microglia during inflammation. Glia. 2021 Jun;69(6):1478-1493. doi: 10.1002/glia.23974. Epub 2021 Feb 8. PMID: 33556209; PMCID: PMC8717762.

177- Holtzman DM, Herz J, Bu G. Apolipoprotein E and apolipoprotein E receptors: normal biology and roles in Alzheimer disease. Cold Spring Harb Perspect Med. 2012 Mar;2(3):a006312. doi: 10.1101/cshperspect.a006312. PMID: 22393530; PMCID: PMC3282491.

178- May P, Woldt E, Matz RL, Boucher P. The LDL receptor-related protein (LRP) family: an old family of proteins with new physiological functions. Ann Med. 2007;39(3):219-28. doi: 10.1080/07853890701214881. PMID: 17457719.

179- Chen J, Li Q, Wang J. Topology of human apolipoprotein E3 uniquely regulates its diverse biological functions. Proc Natl Acad Sci U S A. 2011 Sep 6;108(36):14813-8. doi: 10.1073/pnas.1106420108. Epub 2011 Aug 22. PMID: 21873229; PMCID: PMC3169138.

180- Bu G. Apolipoprotein E and its receptors in Alzheimer's disease: pathways, pathogenesis and therapy. Nat Rev Neurosci. 2009 May;10(5):333-44. doi: 10.1038/nrn2620. Epub 2009 Apr 2. PMID: 19339974; PMCID: PMC2908393.

181- Zhao N, Liu CC, Qiao W, Bu G. Apolipoprotein E, Receptors, and Modulation of Alzheimer's Disease. Biol Psychiatry. 2018 Feb 15;83(4):347-357. doi: 10.1016/j.biopsych.2017.03.003. Epub 2017 Mar 14. PMID: 28434655; PMCID: PMC5599322.

182- Shinohara M, Tachibana M, Kanekiyo T, Bu G. Role of LRP1 in the pathogenesis of Alzheimer's disease: evidence from clinical and preclinical studies. J Lipid Res.

2017 Jul;58(7):1267-1281. doi: 10.1194/jlr.R075796. Epub 2017 Apr 4. PMID: 28381441; PMCID: PMC5496044.

183- Cooper JM, Lathuiliere A, Migliorini M, Arai AL, Wani MM, Dujardin S, Muratoglu SC, Hyman BT, Strickland DK. Regulation of tau internalization, degradation, and seeding by LRP1 reveals multiple pathways for tau catabolism. J Biol Chem. 2021 Jan-Jun;296:100715. doi: 10.1016/j.jbc.2021.100715. Epub 2021 Apr 28. PMID: 33930462; PMCID: PMC8164048.

184- Campion D, Charbonnier C, Nicolas G. SORL1 genetic variants and Alzheimer disease risk: a literature review and meta-analysis of sequencing data. Acta Neuropathol. 2019 Aug;138(2):173-186. doi: 10.1007/s00401-019-01991-4. Epub 2019 Mar 25. PMID: 30911827.

185- Yajima R, Tokutake T, Koyama A, Kasuga K, Tezuka T, Nishizawa M, Ikeuchi T. ApoE-isoform-dependent cellular uptake of amyloid-β is mediated by lipoprotein receptor LR11/SorLA. Biochem Biophys Res Commun. 2015 Jan 2;456(1):482-8. doi: 10.1016/j.bbrc.2014.11.111. Epub 2014 Dec 5. PMID: 25482438.

186- Spoelgen R, von Arnim CA, Thomas AV, Peltan ID, Koker M, Deng A, Irizarry MC, Andersen OM, Willnow TE, Hyman BT. Interaction of the cytosolic domains of sorLA/LR11 with the amyloid precursor protein (APP) and beta-secretase beta-site APP-cleaving enzyme. J Neurosci. 2006 Jan 11;26(2):418-28. doi: 10.1523/JNEUROSCI.3882-05.2006. PMID: 16407538; PMCID: PMC6674411.

187- Saito H, Dhanasekaran P, Nguyen D, Baldwin F, Weisgraber KH, Wehrli S, Phillips MC, Lund-Katz S. Characterization of the heparin binding sites in human apolipoprotein E. J Biol Chem. 2003 Apr 25;278(17):14782-7. doi: 10.1074/jbc.M213207200. Epub 2003 Feb 14. PMID: 12588864.

188- Lalazar A, Weisgraber KH, Rall SC Jr, Giladi H, Innerarity TL, Levanon AZ, Boyles JK, Amit B, Gorecki M, Mahley RW, et al. Site-specific mutagenesis of human apolipoprotein E. Receptor binding activity of variants with single amino acid substitutions. J Biol Chem. 1988 Mar 15;263(8):3542-5. PMID: 2831187.

189- D'Arcangelo G, Homayouni R, Keshvara L, Rice DS, Sheldon M, Curran T. Reelin is a ligand for lipoprotein receptors. Neuron. 1999 Oct;24(2):471-9. doi: 10.1016/s0896-6273(00)80860-0. PMID: 10571240.

190- He X, Cooley K, Chung CH, Dashti N, Tang J. Apolipoprotein receptor 2 and X11 alpha/beta mediate apolipoprotein E-induced endocytosis of amyloid-beta precursor protein and beta-secretase, leading to amyloid-beta production. J Neurosci. 2007 Apr 11;27(15):4052-60. doi: 10.1523/JNEUROSCI.3993-06.2007. PMID: 17428983; PMCID: PMC6672528.

191- Beffert U, Stolt PC, Herz J. Functions of lipoprotein receptors in neurons. J Lipid Res. 2004 Mar;45(3):403-9. doi: 10.1194/jlr.R300017-JLR200. Epub 2003 Dec 1. PMID: 14657206.

192- Hoe HS, Rebeck GW. Regulation of ApoE receptor proteolysis by ligand binding. Brain Res Mol Brain Res. 2005 Jun 13;137(1-2):31-9. doi: 10.1016/j.molbrainres.2005.02.013. Epub 2005 Mar 23. PMID: 15950758.

193- Elsafadi M, Manikandan M, Alajez NM, Hamam R, Dawud RA, Aldahmash A, Iqbal Z, Alfayez M, Kassem M, Mahmood A. MicroRNA-4739 regulates osteogenic and adipocytic differentiation of immortalized human bone marrow stromal cells via targeting LRP3. Stem Cell Res. 2017 Apr;20:94-104. doi: 10.1016/j.scr.2017.03.001. Epub 2017 Mar 8. PMID: 28340487.

194- Dyer CA, Smith RS, Curtiss LK. Only multimers of a synthetic peptide of human apolipoprotein E are biologically active. J Biol Chem. 1991 Aug 15;266(23):15009-15. PMID: 1869538.

195- Rebeck GW, Alonzo NC, Berezovska O, Harr SD, Knowles RB, Growdon JH, Hyman BT, Mendez AJ. Structure and functions of human cerebrospinal fluid

lipoproteins from individuals of different APOE genotypes. Exp Neurol. 1998 Jan;149(1):175-82. doi: 10.1006/exnr.1997.6710. PMID: 9454626.

196- Minagawa H, Gong JS, Jung CG, Watanabe A, Lund-Katz S, Phillips MC, Saito H, Michikawa M. Mechanism underlying apolipoprotein E (ApoE) isoform-dependent lipid efflux from neural cells in culture. J Neurosci Res. 2009 Aug 15;87(11):2498-508. doi: 10.1002/jnr.22073. PMID: 19326444; PMCID: PMC3065888.

197- DeSilva U, D'Arcangelo G, Braden VV, Chen J, Miao GG, Curran T, Green ED. The human reelin gene: isolation, sequencing, and mapping on chromosome 7. Genome Res. 1997 Feb;7(2):157-64. doi: 10.1101/gr.7.2.157. PMID: 9049633.

198- Alcántara S, Ruiz M, D'Arcangelo G, Ezan F, de Lecea L, Curran T, Sotelo C, Soriano E. Regional and cellular patterns of reelin mRNA expression in the forebrain of the developing and adult mouse. J Neurosci. 1998 Oct 1;18(19):7779-99. doi: 10.1523/JNEUROSCI.18-19-07779.1998. PMID: 9742148; PMCID: PMC6792998.beffer

199- Frotscher M. Role for Reelin in stabilizing cortical architecture. Trends Neurosci. 2010 Sep;33(9):407-14. doi: 10.1016/j.tins.2010.06.001. Epub 2010 Jul 1. PMID: 20598379.

200- Jossin Y. Reelin Functions, Mechanisms of Action and Signaling Pathways During Brain Development and Maturation. Biomolecules. 2020 Jun 26;10(6):964. doi: 10.3390/biom10060964. PMID: 32604886; PMCID: PMC7355739.

201- Ventruti A, Kazdoba TM, Niu S, D'Arcangelo G. Reelin deficiency causes specific defects in the molecular composition of the synapses in the adult brain. Neuroscience. 2011 Aug 25;189:32-42. doi: 10.1016/j.neuroscience.2011.05.050. Epub 2011 Jun 2. PMID: 21664258.

202- Knuesel I. Reelin-mediated signaling in neuropsychiatric and neurodegenerative diseases. Prog Neurobiol. 2010 Aug;91(4):257-74. doi: 10.1016/j.pneurobio.2010.04.002. Epub 2010 Apr 22. PMID: 20417248.

203- Kubo K, Mikoshiba K, Nakajima K. Secreted Reelin molecules form homodimers. Neurosci Res. 2002 Aug;43(4):381-8. doi: 10.1016/s0168-0102(02)00068-8. PMID: 12135781.

204- Krstic D, Rodriguez M, Knuesel I. Regulated proteolytic processing of Reelin through interplay of tissue plasminogen activator (tPA), ADAMTS-4, ADAMTS-5, and their modulators. PLoS One. 2012;7(10):e47793. doi: 10.1371/journal.pone.0047793. Epub 2012 Oct 17. PMID: 23082219; PMCID: PMC3474754.

205- Kohno T, Honda T, Kubo K, Nakano Y, Tsuchiya A, Murakami T, Banno H, Nakajima K, Hattori M. Importance of Reelin C-terminal region in the development and maintenance of the postnatal cerebral cortex and its regulation by specific proteolysis. J Neurosci. 2015 Mar 18;35(11):4776-87. doi: 10.1523/JNEUROSCI.4119-14.2015. PMID: 25788693; PMCID: PMC6605132.

206- Smalheiser NR, Costa E, Guidotti A, Impagnatiello F, Auta J, Lacor P, Kriho V, Pappas GD. Expression of reelin in adult mammalian blood, liver, pituitary pars intermedia, and adrenal chromaffin cells. Proc Natl Acad Sci U S A. 2000 Feb 1;97(3):1281-6. doi: 10.1073/pnas.97.3.1281. PMID: 10655522; PMCID: PMC15597.

207- May P, Bock HH, Nimpf J, Herz J. Differential glycosylation regulates processing of lipoprotein receptors by gamma-secretase. J Biol Chem. 2003 Sep 26;278(39):37386-92. doi: 10.1074/jbc.M305858200. Epub 2003 Jul 18. PMID: 12871934.

208- Hoe HS, Tran TS, Matsuoka Y, Howell BW, Rebeck GW. DAB1 and Reelin effects on amyloid precursor protein and ApoE receptor 2 trafficking and

processing. J Biol Chem. 2006 Nov 17;281(46):35176-85. doi: 10.1074/jbc.M602162200. Epub 2006 Sep 1. PMID: 16951405.

209- Koch S, Strasser V, Hauser C, Fasching D, Brandes C, Bajari TM, Schneider WJ, Nimpf J. A secreted soluble form of ApoE receptor 2 acts as a dominant-negative receptor and inhibits Reelin signaling. EMBO J. 2002 Nov 15;21(22):5996-6004. doi: 10.1093/emboj/cdf599. PMID: 12426372; PMCID: PMC137191.

210- Chow VW, Mattson MP, Wong PC, Gleichmann M. An overview of APP processing enzymes and products. Neuromolecular Med. 2010 Mar;12(1):1-12. doi: 10.1007/s12017-009-8104-z. PMID: 20232515; PMCID: PMC2889200.

211- Balmaceda V, Cuchillo-Ibáñez I, Pujadas L, García-Ayllón MS, Saura CA, Nimpf J, Soriano E, Sáez-Valero J. ApoER2 processing by presenilin-1 modulates reelin expression. FASEB J. 2014 Apr;28(4):1543-54. doi: 10.1096/fj.13-239350. Epub 2013 Dec 16. PMID: 24344333.

212- Howell BW, Herrick TM, Cooper JA. Reelin-induced tyrosine [corrected] phosphorylation of disabled 1 during neuronal positioning. Genes Dev. 1999 Mar 15;13(6):643-8. doi: 10.1101/gad.13.6.643. Erratum in: Genes Dev. 1999 Jun 15;13(12):1642. PMID: 10090720; PMCID: PMC316552.

213- Bock HH, Jossin Y, Liu P, Förster E, May P, Goffinet AM, Herz J. Phosphatidylinositol 3-kinase interacts with the adaptor protein Dab1 in response to Reelin signaling and is required for normal cortical lamination. J Biol Chem. 2003 Oct 3;278(40):38772-9. doi: 10.1074/jbc.M306416200. Epub 2003 Jul 25. PMID: 12882964.

214- Jossin Y, Goffinet AM. Reelin signals through phosphatidylinositol 3-kinase and Akt to control cortical development and through mTor to regulate dendritic growth. Mol Cell Biol. 2007 Oct;27(20):7113-24. doi: 10.1128/MCB.00928-07. Epub 2007 Aug 13. PMID: 17698586; PMCID: PMC2168915.

215- Beffert U, Morfini G, Bock HH, Reyna H, Brady ST, Herz J. Reelin-mediated signaling locally regulates protein kinase B/Akt and glycogen synthase kinase 3beta. J Biol Chem. 2002 Dec 20;277(51):49958-64. doi: 10.1074/jbc.M209205200. Epub 2002 Oct 9. PMID: 12376533.

216- Avila J, León-Espinosa G, García E, García-Escudero V, Hernández F, Defelipe J. Tau Phosphorylation by GSK3 in Different Conditions. Int J Alzheimers Dis. 2012;2012:578373. doi: 10.1155/2012/578373. Epub 2012 May 17. PMID: 22675648; PMCID: PMC3362846.

217- Meseke M, Cavus E, Förster E. Reelin promotes microtubule dynamics in processes of developing neurons. Histochem Cell Biol. 2013 Feb;139(2):283-97. doi: 10.1007/s00418-012-1025-1. Epub 2012 Sep 19. PMID: 22990595.

218- Krstic D, Knuesel I. Deciphering the mechanism underlying late-onset Alzheimer disease. Nat Rev Neurol. 2013 Jan;9(1):25-34. doi: 10.1038/nrneurol.2012.236. Epub 2012 Nov 27. PMID: 23183882.

219- Trommsdorff M, Borg JP, Margolis B, Herz J. Interaction of cytosolic adaptor proteins with neuronal apolipoprotein E receptors and the amyloid precursor protein. J Biol Chem. 1998 Dec 11;273(50):33556-60. doi: 10.1074/jbc.273.50.33556. PMID: 9837937.

220- Hoe HS, Lee KJ, Carney RS, Lee J, Markova A, Lee JY, Howell BW, Hyman BT, Pak DT, Bu G, Rebeck GW. Interaction of reelin with amyloid precursor protein promotes neurite outgrowth. J Neurosci. 2009 Jun 10;29(23):7459-73. doi: 10.1523/JNEUROSCI.4872-08.2009. PMID: 19515914; PMCID: PMC2759694.

221- Hoe HS, Wessner D, Beffert U, Becker AG, Matsuoka Y, Rebeck GW. F-spondin interaction with the apolipoprotein E receptor ApoEr2 affects processing of amyloid precursor protein. Mol Cell Biol. 2005 Nov;25(21):9259-68. doi: 10.1128/MCB.25.21.9259-9268.2005. PMID: 16227578; PMCID: PMC1265841.

222- Deutsch SI, Rosse RB, Deutsch LH. Faulty regulation of tau phosphorylation by the reelin signal transduction pathway is a potential mechanism of pathogenesis and therapeutic target in Alzheimer's disease. Eur Neuropsychopharmacol. 2006 Dec;16(8):547-51. doi: 10.1016/j.euroneuro.2006.01.006. Epub 2006 Feb 28. PMID: 16504486.

223- Flowers SA, Rebeck GW. APOE in the normal brain. Neurobiol Dis. 2020 Mar;136:104724. doi: 10.1016/j.nbd.2019.104724. Epub 2020 Jan 3. PMID: 31911114; PMCID: PMC7002287.

224- McIntosh AM, Bennett C, Dickson D, Anestis SF, Watts DP, Webster TH, Fontenot MB, Bradley BJ. The apolipoprotein E (APOE) gene appears functionally monomorphic in chimpanzees (Pan troglodytes). PLoS One. 2012;7(10):e47760. doi: 10.1371/journal.pone.0047760. Epub 2012 Oct 24. PMID: 23112842; PMCID: PMC3480407.

225- Maloney B, Ge YW, Alley GM, Lahiri DK. Important differences between human and mouse APOE gene promoters: limitation of mouse APOE model in studying Alzheimer's disease. J Neurochem. 2007 Nov;103(3):1237-57. doi: 10.1111/j.1471-4159.2007.04831.x. Epub 2007 Sep 8. PMID: 17854398.

226- Liao F, Zhang TJ, Jiang H, Lefton KB, Robinson GO, Vassar R, Sullivan PM, Holtzman DM. Murine versus human apolipoprotein E4: differential facilitation of and co-localization in cerebral amyloid angiopathy and amyloid plaques in APP transgenic mouse models. Acta Neuropathol Commun. 2015 Nov 10;3:70. doi: 10.1186/s40478-015-0250-y. PMID: 26556230; PMCID: PMC4641345.

227- Fryer JD, Simmons K, Parsadanian M, Bales KR, Paul SM, Sullivan PM, Holtzman DM. Human apolipoprotein E4 alters the amyloid-beta 40:42 ratio and promotes the formation of cerebral amyloid angiopathy in an amyloid precursor protein transgenic model. J Neurosci. 2005 Mar 16;25(11):2803-10. doi: 10.1523/JNEUROSCI.5170-04.2005. PMID: 15772340; PMCID: PMC6725147.

228- Lewandowski CT, Maldonado Weng J, LaDu MJ. Alzheimer's disease pathology in APOE transgenic mouse models: The Who, What, When, Where, Why, and How. Neurobiol Dis. 2020 Jun;139:104811. doi: 10.1016/j.nbd.2020.104811. Epub 2020 Feb 20. PMID: 32087290; PMCID: PMC7150653.

229- Namba Y, Tomonaga M, Kawasaki H, Otomo E, Ikeda K. Apolipoprotein E immunoreactivity in cerebral amyloid deposits and neurofibrillary tangles in Alzheimer's disease and kuru plaque amyloid in Creutzfeldt-Jakob disease. Brain Res. 1991 Feb 8;541(1):163-6. doi: 10.1016/0006-8993(91)91092-f. PMID: 2029618.

230- LaDu MJ, Falduto MT, Manelli AM, Reardon CA, Getz GS, Frail DE. Isoform-specific binding of apolipoprotein E to beta-amyloid. J Biol Chem. 1994 Sep 23;269(38):23403-6. PMID: 8089103.

231- Wisniewski T, Golabek A, Matsubara E, Ghiso J, Frangione B. Apolipoprotein E: binding to soluble Alzheimer's beta-amyloid. Biochem Biophys Res Commun. 1993 Apr 30;192(2):359-65. doi: 10.1006/bbrc.1993.1423. PMID: 8484748.

232- Strittmatter WJ, Weisgraber KH, Huang DY, Dong LM, Salvesen GS, Pericak-Vance M, Schmechel D, Saunders AM, Goldgaber D, Roses AD. Binding of human apolipoprotein E to synthetic amyloid beta peptide: isoform-specific effects and implications for late-onset Alzheimer disease. Proc Natl Acad Sci U S A. 1993 Sep 1;90(17):8098-102. doi: 10.1073/pnas.90.17.8098. PMID: 8367470; PMCID: PMC47295.

233- Wisniewski T, Drummond E. APOE-amyloid interaction: Therapeutic targets. Neurobiol Dis. 2020 May;138:104784. doi: 10.1016/j.nbd.2020.104784. Epub 2020 Feb 4. PMID: 32027932; PMCID: PMC7118587.

234- Brunden KR, Richter-Cook NJ, Chaturvedi N, Frederickson RC. pH-dependent binding of synthetic beta-amyloid peptides to glycosaminoglycans. J Neurochem.

1993 Dec;61(6):2147-54. doi: 10.1111/j.1471-4159.1993.tb07453.x. PMID: 8245966.

235- Verghese PB, Castellano JM, Garai K, Wang Y, Jiang H, Shah A, Bu G, Frieden C, Holtzman DM. ApoE influences amyloid-β (Aβ) clearance despite minimal apoE/Aβ association in physiological conditions. Proc Natl Acad Sci U S A. 2013 May 7;110(19):E1807-16. doi: 10.1073/pnas.1220484110. Epub 2013 Apr 25. PMID: 23620513; PMCID: PMC3651443.

236- LaDu MJ, Pederson TM, Frail DE, Reardon CA, Getz GS, Falduto MT. Purification of apolipoprotein E attenuates isoform-specific binding to beta-amyloid. J Biol Chem. 1995 Apr 21;270(16):9039-42. doi: 10.1074/jbc.270.16.9039. PMID: 7721816.

237- Petrlova J, Hong HS, Bricarello DA, Harishchandra G, Lorigan GA, Jin LW, Voss JC. A differential association of Apolipoprotein E isoforms with the amyloid-β oligomer in solution. Proteins. 2011 Feb;79(2):402-16. doi: 10.1002/prot.22891. PMID: 21069870; PMCID: PMC3016465.

238- Tai LM, Bilousova T, Jungbauer L, Roeske SK, Youmans KL, Yu C, Poon WW, Cornwell LB, Miller CA, Vinters HV, Van Eldik LJ, Fardo DW, Estus S, Bu G, Gylys KH, Ladu MJ. Levels of soluble apolipoprotein E/amyloid-β (Aβ) complex are reduced and oligomeric Aβ increased with APOE4 and Alzheimer disease in a transgenic mouse model and human samples. J Biol Chem. 2013 Feb 22;288(8):5914-26. doi: 10.1074/jbc.M112.442103. Epub 2013 Jan 4. PMID: 23293020; PMCID: PMC3581407.

239- Gouras GK, Tsai J, Naslund J, Vincent B, Edgar M, Checler F, Greenfield JP, Haroutunian V, Buxbaum JD, Xu H, Greengard P, Relkin NR. Intraneuronal Abeta42 accumulation in human brain. Am J Pathol. 2000 Jan;156(1):15-20. doi: 10.1016/s0002-9440(10)64700-1. PMID: 10623648; PMCID: PMC1868613.

240- Zhao W, Dumanis SB, Tamboli IY, Rodriguez GA, Jo Ladu M, Moussa CE, William Rebeck G. Human APOE genotype affects intraneuronal Aβ1-42 accumulation in a lentiviral gene transfer model. Hum Mol Genet. 2014 Mar 1;23(5):1365-75. doi: 10.1093/hmg/ddt525. Epub 2013 Oct 23. PMID: 24154541; PMCID: PMC3919009.

241- Huang YA, Zhou B, Wernig M, Südhof TC. ApoE2, ApoE3, and ApoE4 Differentially Stimulate APP Transcription and Aβ Secretion. Cell. 2017 Jan 26;168(3):427-441.e21. doi: 10.1016/j.cell.2016.12.044. Epub 2017 Jan 19. PMID: 28111074; PMCID: PMC5310835.

242- Tiraboschi P, Hansen LA, Masliah E, Alford M, Thal LJ, Corey-Bloom J. Impact of APOE genotype on neuropathologic and neurochemical markers of Alzheimer disease. Neurology. 2004 Jun 8;62(11):1977-83. doi: 10.1212/01.wnl.0000128091.92139.0f. PMID: 15184600.

243- Fagan AM, Watson M, Parsadanian M, Bales KR, Paul SM, Holtzman DM. Human and murine ApoE markedly alters A beta metabolism before and after plaque formation in a mouse model of Alzheimer's disease. Neurobiol Dis. 2002 Apr;9(3):305-18. doi: 10.1006/nbdi.2002.0483. PMID: 11950276.

244- Holtzman DM, Fagan AM, Mackey B, Tenkova T, Sartorius L, Paul SM, Bales K, Ashe KH, Irizarry MC, Hyman BT. Apolipoprotein E facilitates neuritic and cerebrovascular plaque formation in an Alzheimer's disease model. Ann Neurol. 2000 Jun;47(6):739-47. PMID: 10852539.

245- Morris JC, Roe CM, Xiong C, Fagan AM, Goate AM, Holtzman DM, Mintun MA. APOE predicts amyloid-beta but not tau Alzheimer pathology in cognitively normal aging. Ann Neurol. 2010 Jan;67(1):122-31. doi: 10.1002/ana.21843. PMID: 20186853; PMCID: PMC2830375.

246- Hashimoto T, Serrano-Pozo A, Hori Y, Adams KW, Takeda S, Banerji AO, Mitani A, Joyner D, Thyssen DH, Bacskai BJ, Frosch MP, Spires-Jones TL, Finn MB,

Holtzman DM, Hyman BT. Apolipoprotein E, especially apolipoprotein E4, increases the oligomerization of amyloid β peptide. J Neurosci. 2012 Oct 24;32(43):15181-92. doi: 10.1523/JNEUROSCI.1542-12.2012. PMID: 23100439; PMCID: PMC3493562.

247- Cerf E, Gustot A, Goormaghtigh E, Ruysschaert JM, Raussens V. High ability of apolipoprotein E4 to stabilize amyloid-β peptide oligomers, the pathological entities responsible for Alzheimer's disease. FASEB J. 2011 May;25(5):1585-95. doi: 10.1096/fj.10-175976. Epub 2011 Jan 25. PMID: 21266538.

248- Harper JD, Lansbury PT Jr. Models of amyloid seeding in Alzheimer's disease and scrapie: mechanistic truths and physiological consequences of the time-dependent solubility of amyloid proteins. Annu Rev Biochem. 1997;66:385-407. doi: 10.1146/annurev.biochem.66.1.385. PMID: 9242912.

249- Liu CC, Zhao N, Fu Y, Wang N, Linares C, Tsai CW, Bu G. ApoE4 Accelerates Early Seeding of Amyloid Pathology. Neuron. 2017 Dec 6;96(5):1024-1032.e3. doi: 10.1016/j.neuron.2017.11.013. PMID: 29216449; PMCID: PMC5948105.

250- Castano EM, Prelli F, Wisniewski T, Golabek A, Kumar RA, Soto C, Frangione B. Fibrillogenesis in Alzheimer's disease of amyloid beta peptides and apolipoprotein E. Biochem J. 1995 Mar 1;306 (Pt 2)(Pt 2):599-604. doi: 10.1042/bj3060599. PMID: 7534068; PMCID: PMC1136559.

251- Wood SJ, Chan W, Wetzel R. Seeding of A beta fibril formation is inhibited by all three isotypes of apolipoprotein E. Biochemistry. 1996 Sep 24;35(38):12623-8. doi: 10.1021/bi961074j. PMID: 8823200.

252- Wahrle SE, Jiang H, Parsadanian M, Hartman RE, Bales KR, Paul SM, Holtzman DM. Deletion of Abca1 increases Abeta deposition in the PDAPP transgenic mouse model of Alzheimer disease. J Biol Chem. 2005 Dec 30;280(52):43236-42. doi: 10.1074/jbc.M508780200. Epub 2005 Oct 5. PMID: 16207708.

253- Bales KR, Verina T, Cummins DJ, Du Y, Dodel RC, Saura J, Fishman CE, DeLong CA, Piccardo P, Petegnief V, Ghetti B, Paul SM. Apolipoprotein E is essential for amyloid deposition in the APP(V717F) transgenic mouse model of Alzheimer's disease. Proc Natl Acad Sci U S A. 1999 Dec 21;96(26):15233-8. doi: 10.1073/pnas.96.26.15233. PMID: 10611368; PMCID: PMC24803.

254- Ulrich JD, Ulland TK, Mahan TE, Nyström S, Nilsson KP, Song WM, Zhou Y, Reinartz M, Choi S, Jiang H, Stewart FR, Anderson E, Wang Y, Colonna M, Holtzman DM. ApoE facilitates the microglial response to amyloid plaque pathology. J Exp Med. 2018 Apr 2;215(4):1047-1058. doi: 10.1084/jem.20171265. Epub 2018 Feb 26. PMID: 29483128; PMCID: PMC5881464.

255- Huynh TV, Liao F, Francis CM, Robinson GO, Serrano JR, Jiang H, Roh J, Finn MB, Sullivan PM, Esparza TJ, Stewart FR, Mahan TE, Ulrich JD, Cole T, Holtzman DM. Age-Dependent Effects of apoE Reduction Using Antisense Oligonucleotides in a Model of β-amyloidosis. Neuron. 2017 Dec 6;96(5):1013-1023.e4. doi: 10.1016/j.neuron.2017.11.014. PMID: 29216448; PMCID: PMC5728673.

256- Tarasoff-Conway JM, Carare RO, Osorio RS, Glodzik L, Butler T, Fieremans E, Axel L, Rusinek H, Nicholson C, Zlokovic BV, Frangione B, Blennow K, Ménard J, Zetterberg H, Wisniewski T, de Leon MJ. Clearance systems in the brain-implications for Alzheimer disease. Nat Rev Neurol. 2015 Aug;11(8):457-70. doi: 10.1038/nrneurol.2015.119. Epub 2015 Jul 21. Erratum in: Nat Rev Neurol. 2016 Apr;12(4):248. PMID: 26195256; PMCID: PMC4694579.

257- Kanekiyo T, Xu H, Bu G. ApoE and Aβ in Alzheimer's disease: accidental encounters or partners? Neuron. 2014 Feb 19;81(4):740-54. doi: 10.1016/j.neuron.2014.01.045. PMID: 24559670; PMCID: PMC3983361.

258- Castellano JM, Kim J, Stewart FR, Jiang H, DeMattos RB, Patterson BW, Fagan AM, Morris JC, Mawuenyega KG, Cruchaga C, Goate AM, Bales KR, Paul SM, Bateman RJ, Holtzman DM. Human apoE isoforms differentially regulate brain amyloid-β peptide clearance. Sci Transl Med. 2011 Jun 29;3(89):89ra57. doi: 10.1126/scitranslmed.3002156. PMID: 21715678; PMCID: PMC3192364.

259- Saido T, Leissring MA. Proteolytic degradation of amyloid β-protein. Cold Spring Harb Perspect Med. 2012 Jun;2(6):a006379. doi: 10.1101/cshperspect.a006379. PMID: 22675659; PMCID: PMC3367539.

260- Jiang Q, Lee CY, Mandrekar S, Wilkinson B, Cramer P, Zelcer N, Mann K, Lamb B, Willson TM, Collins JL, Richardson JC, Smith JD, Comery TA, Riddell D, Holtzman DM, Tontonoz P, Landreth GE. ApoE promotes the proteolytic degradation of Abeta. Neuron. 2008 Jun 12;58(5):681-93. doi: 10.1016/j.neuron.2008.04.010. PMID: 18549781; PMCID: PMC2493297.

261- Miners JS, Van Helmond Z, Chalmers K, Wilcock G, Love S, Kehoe PG. Decreased expression and activity of neprilysin in Alzheimer disease are associated with cerebral amyloid angiopathy. J Neuropathol Exp Neurol. 2006 Oct;65(10):1012-21. doi: 10.1097/01.jnen.0000240463.87886.9a. PMID: 17021406.

262- Ma Q, Zhao Z, Sagare AP, Wu Y, Wang M, Owens NC, Verghese PB, Herz J, Holtzman DM, Zlokovic BV. Blood-brain barrier-associated pericytes internalize and clear aggregated amyloid-β42 by LRP1-dependent apolipoprotein E isoform-specific mechanism. Mol Neurodegener. 2018 Oct 19;13(1):57. doi: 10.1186/s13024-018-0286-0. Erratum in: Mol Neurodegener. 2022 Nov 3;17(1):71. PMID: 30340601; PMCID: PMC6194676.

263- Montagne A, Nation DA, Sagare AP, Barisano G, Sweeney MD, Chakhoyan A, Pachicano M, Joe E, Nelson AR, D'Orazio LM, Buennagel DP, Harrington MG, Benzinger TLS, Fagan AM, Ringman JM, Schneider LS, Morris JC, Reiman EM, Caselli RJ, Chui HC, Tcw J, Chen Y, Pa J, Conti PS, Law M, Toga AW, Zlokovic BV. APOE4 leads to blood-brain barrier dysfunction predicting cognitive decline. Nature. 2020 May;581(7806):71-76. doi: 10.1038/s41586-020-2247-3. Epub 2020 Apr 29. PMID: 32376954; PMCID: PMC7250000.

264- Deane R, Sagare A, Hamm K, Parisi M, Lane S, Finn MB, Holtzman DM, Zlokovic BV. apoE isoform-specific disruption of amyloid beta peptide clearance from mouse brain. J Clin Invest. 2008 Dec;118(12):4002-13. doi: 10.1172/JCI36663. Epub 2008 Nov 13. PMID: 19033669; PMCID: PMC2582453.

265- DeMattos RB, Cirrito JR, Parsadanian M, May PC, O'Dell MA, Taylor JW, Harmony JA, Aronow BJ, Bales KR, Paul SM, Holtzman DM. ApoE and clusterin cooperatively suppress Abeta levels and deposition: evidence that ApoE regulates extracellular Abeta metabolism in vivo. Neuron. 2004 Jan 22;41(2):193-202. doi: 10.1016/s0896-6273(03)00850-x. PMID: 14741101.

266- Li J, Kanekiyo T, Shinohara M, Zhang Y, LaDu MJ, Xu H, Bu G. Differential regulation of amyloid-β endocytic trafficking and lysosomal degradation by apolipoprotein E isoforms. J Biol Chem. 2012 Dec 28;287(53):44593-601. doi: 10.1074/jbc.M112.420224. Epub 2012 Nov 6. PMID: 23132858; PMCID: PMC3531774.

267- Carlo AS, Gustafsen C, Mastrobuoni G, Nielsen MS, Burgert T, Hartl D, Rohe M, Nykjaer A, Herz J, Heeren J, Kempa S, Petersen CM, Willnow TE. The pro-neurotrophin receptor sortilin is a major neuronal apolipoprotein E receptor for catabolism of amyloid-β peptide in the brain. J Neurosci. 2013 Jan 2;33(1):358-70. doi: 10.1523/JNEUROSCI.2425-12.2013. PMID: 23283348; PMCID: PMC3744345.

268- Basak JM, Verghese PB, Yoon H, Kim J, Holtzman DM. Low-density lipoprotein receptor represents an apolipoprotein E-independent pathway of Aβ uptake and

degradation by astrocytes. J Biol Chem. 2012 Apr 20;287(17):13959-71. doi: 10.1074/jbc.M111.288746. Epub 2012 Mar 1. PMID: 22383525; PMCID: PMC3340151.

269- Fernandez CG, Hamby ME, McReynolds ML, Ray WJ. The Role of APOE4 in Disrupting the Homeostatic Functions of Astrocytes and Microglia in Aging and Alzheimer's Disease. Front Aging Neurosci. 2019 Feb 11;11:14. doi: 10.3389/fnagi.2019.00014. PMID: 30804776; PMCID: PMC6378415.

270- Gendron TF, Petrucelli L. The role of tau in neurodegeneration. Mol Neurodegener. 2009 Mar 11;4:13. doi: 10.1186/1750-1326-4-13. PMID: 19284597; PMCID: PMC2663562.

271- Bejanin A, Schonhaut DR, La Joie R, Kramer JH, Baker SL, Sosa N, Ayakta N, Cantwell A, Janabi M, Lauriola M, O'Neil JP, Gorno-Tempini ML, Miller ZA, Rosen HJ, Miller BL, Jagust WJ, Rabinovici GD. Tau pathology and neurodegeneration contribute to cognitive impairment in Alzheimer's disease. Brain. 2017 Dec 1;140(12):3286-3300. doi: 10.1093/brain/awx243. PMID: 29053874; PMCID: PMC5841139.

272- Rohn TT, Catlin LW, Coonse KG, Habig JW. Identification of an amino-terminal fragment of apolipoprotein E4 that localizes to neurofibrillary tangles of the Alzheimer's disease brain. Brain Res. 2012 Sep 26;1475:106-15. doi: 10.1016/j.brainres.2012.08.003. Epub 2012 Aug 8. PMID: 22902767.

273- Sanchez JS, Becker JA, Jacobs HIL, Hanseeuw BJ, Jiang S, Schultz AP, Properzi MJ, Katz SR, Beiser A, Satizabal CL, O'Donnell A, DeCarli C, Killiany R, El Fakhri G, Normandin MD, Gómez-Isla T, Quiroz YT, Rentz DM, Sperling RA, Seshadri S, Augustinack J, Price JC, Johnson KA. The cortical origin and initial spread of medial temporal tauopathy in Alzheimer's disease assessed with positron emission tomography. Sci Transl Med. 2021 Jan 20;13(577):eabc0655. doi: 10.1126/scitranslmed.abc0655. PMID: 33472953; PMCID: PMC7978042.

274- Vogel JW, Young AL, Oxtoby NP, Smith R, Ossenkoppele R, Strandberg OT, La Joie R, Aksman LM, Grothe MJ, Iturria-Medina Y; Alzheimer's Disease Neuroimaging Initiative; Pontecorvo MJ, Devous MD, Rabinovici GD, Alexander DC, Lyoo CH, Evans AC, Hansson O. Four distinct trajectories of tau deposition identified in Alzheimer's disease. Nat Med. 2021 May;27(5):871-881. doi: 10.1038/s41591-021-01309-6. Epub 2021 Apr 29. PMID: 33927414; PMCID: PMC8686688.

275- Robinson AC, Davidson YS, Roncaroli F, Minshull J, Tinkler P, Horan MA, Payton A, Pendleton N, Mann DMA. Influence of APOE genotype in primary age-related tauopathy. Acta Neuropathol Commun. 2020 Dec 7;8(1):215. doi: 10.1186/s40478-020-01095-1. PMID: 33287896; PMCID: PMC7720601.

276- Wang C, Xiong M, Gratuze M, Bao X, Shi Y, Andhey PS, Manis M, Schroeder C, Yin Z, Madore C, Butovsky O, Artyomov M, Ulrich JD, Holtzman DM. Selective removal of astrocytic APOE4 strongly protects against tau-mediated neurodegeneration and decreases synaptic phagocytosis by microglia. Neuron. 2021 May 19;109(10):1657-1674.e7. doi: 10.1016/j.neuron.2021.03.024. Epub 2021 Apr 7. PMID: 33831349; PMCID: PMC8141024.

277- Kang SS, Ahn EH, Liu X, Bryson M, Miller GW, Weinshenker D, Ye K. ApoE4 inhibition of VMAT2 in the locus coeruleus exacerbates Tau pathology in Alzheimer's disease. Acta Neuropathol. 2021 Jul;142(1):139-158. doi: 10.1007/s00401-021-02315-1. Epub 2021 Apr 25. PMID: 33895869; PMCID: PMC8217363.

278- Shi Y, Yamada K, Liddelow SA, Smith ST, Zhao L, Luo W, Tsai RM, Spina S, Grinberg LT, Rojas JC, Gallardo G, Wang K, Roh J, Robinson G, Finn MB, Jiang H, Sullivan PM, Baufeld C, Wood MW, Sutphen C, McCue L, Xiong C, Del-Aguila JL, Morris JC, Cruchaga C; Alzheimer's Disease Neuroimaging Initiative; Fagan

AM, Miller BL, Boxer AL, Seeley WW, Butovsky O, Barres BA, Paul SM, Holtzman DM. ApoE4 markedly exacerbates tau-mediated neurodegeneration in a mouse model of tauopathy. Nature. 2017 Sep 28;549(7673):523-527. doi: 10.1038/nature24016. Epub 2017 Sep 20. PMID: 28959956; PMCID: PMC5641217.

279- Litvinchuk A, Huynh TV, Shi Y, Jackson RJ, Finn MB, Manis M, Francis CM, Tran AC, Sullivan PM, Ulrich JD, Hyman BT, Cole T, Holtzman DM. Apolipoprotein E4 Reduction with Antisense Oligonucleotides Decreases Neurodegeneration in a Tauopathy Model. Ann Neurol. 2021 May;89(5):952-966. doi: 10.1002/ana.26043. Epub 2021 Feb 24. PMID: 33550655; PMCID: PMC8260038.

280- Andrews-Zwilling Y, Bien-Ly N, Xu Q, Li G, Bernardo A, Yoon SY, Zwilling D, Yan TX, Chen L, Huang Y. Apolipoprotein E4 causes age- and Tau-dependent impairment of GABAergic interneurons, leading to learning and memory deficits in mice. J Neurosci. 2010 Oct 13;30(41):13707-17. doi: 10.1523/JNEUROSCI.4040-10.2010. PMID: 20943911; PMCID: PMC2988475.

281- Wadhwani AR, Affaneh A, Van Gulden S, Kessler JA. Neuronal apolipoprotein E4 increases cell death and phosphorylated tau release in alzheimer disease. Ann Neurol. 2019 May;85(5):726-739. doi: 10.1002/ana.25455. Epub 2019 Mar 27. PMID: 30840313; PMCID: PMC8123085.

282- Wang C, Najm R, Xu Q, Jeong DE, Walker D, Balestra ME, Yoon SY, Yuan H, Li G, Miller ZA, Miller BL, Malloy MJ, Huang Y. Gain of toxic apolipoprotein E4 effects in human iPSC-derived neurons is ameliorated by a small-molecule structure corrector. Nat Med. 2018 May;24(5):647-657. doi: 10.1038/s41591-018-0004-z. Epub 2018 Apr 9. PMID: 29632371; PMCID: PMC5948154.

283- Koch G, Di Lorenzo F, Loizzo S, Motta C, Travaglione S, Baiula M, Rimondini R, Ponzo V, Bonnì S, Toniolo S, Sallustio F, Bozzali M, Caltagirone C, Campana G, Martorana A. CSF tau is associated with impaired cortical plasticity, cognitive decline and astrocyte survival only in APOE4-positive Alzheimer's disease. Sci Rep. 2017 Oct 23;7(1):13728. doi: 10.1038/s41598-017-14204-3. PMID: 29062035; PMCID: PMC5653826.

284- Wattmo C, Blennow K, Hansson O. Cerebro-spinal fluid biomarker levels: phosphorylated tau (T) and total tau (N) as markers for rate of progression in Alzheimer's disease. BMC Neurol. 2020 Jan 9;20(1):10. doi: 10.1186/s12883-019-1591-0. PMID: 31918679; PMCID: PMC6951013.

285- Liu Y, Song JH, Xu W, Hou XH, Li JQ, Yu JT, Tan L, Chi S; and Alzheimer's Disease Neuroimaging Initiative. The Associations of Cerebrospinal Fluid ApoE and Biomarkers of Alzheimer's Disease: Exploring Interactions With Sex. Front Neurosci. 2021 Mar 3;15:633576. doi: 10.3389/fnins.2021.633576. PMID: 33746700; PMCID: PMC7968417.

286- Rodriguez-Vieitez E, Nielsen HM. Associations Between APOE Variants, Tau and α-Synuclein. Adv Exp Med Biol. 2019;1184:177-186. doi: 10.1007/978-981-32-9358-8_15. PMID: 32096038.

287- Whitwell JL, Graff-Radford J, Tosakulwong N, Weigand SD, Machulda M, Senjem ML, Schwarz CG, Spychalla AJ, Jones DT, Drubach DA, Knopman DS, Boeve BF, Ertekin-Taner N, Petersen RC, Lowe VJ, Jack CR Jr, Josephs KA. [18 F]AV-1451 clustering of entorhinal and cortical uptake in Alzheimer's disease. Ann Neurol. 2018 Feb;83(2):248-257. doi: 10.1002/ana.25142. Epub 2018 Feb 6. PMID: 29323751; PMCID: PMC5821532.

288- Holmes BB, DeVos SL, Kfoury N, Li M, Jacks R, Yanamandra K, Ouidja MO, Brodsky FM, Marasa J, Bagchi DP, Kotzbauer PT, Miller TM, Papy-Garcia D, Diamond MI. Heparan sulfate proteoglycans mediate internalization and propagation of specific proteopathic seeds. Proc Natl Acad Sci U S A. 2013 Aug

13;110(33):E3138-47. doi: 10.1073/pnas.1301440110. Epub 2013 Jul 29. PMID: 23898162; PMCID: PMC3746848.

289- Jablonski AM, Warren L, Usenovic M, Zhou H, Sugam J, Parmentier-Batteur S, Voleti B. Astrocytic expression of the Alzheimer's disease risk allele, ApoEε4, potentiates neuronal tau pathology in multiple preclinical models. Sci Rep. 2021 Feb 9;11(1):3438. doi: 10.1038/s41598-021-82901-1. PMID: 33564035; PMCID: PMC7873246.

290- Rauch JN, Luna G, Guzman E, Audouard M, Challis C, Sibih YE, Leshuk C, Hernandez I, Wegmann S, Hyman BT, Gradinaru V, Kampmann M, Kosik KS. LRP1 is a master regulator of tau uptake and spread. Nature. 2020 Apr;580(7803):381-385. doi: 10.1038/s41586-020-2156-5. Epub 2020 Apr 1. PMID: 32296178; PMCID: PMC7687380.

291- Shi Y, Andhey PS, Ising C, Wang K, Snipes LL, Boyer K, Lawson S, Yamada K, Qin W, Manis M, Serrano JR, Benitez BA, Schmidt RE, Artyomov M, Ulrich JD, Holtzman DM. Overexpressing low-density lipoprotein receptor reduces tau-associated neurodegeneration in relation to apoE-linked mechanisms. Neuron. 2021 Aug 4;109(15):2413-2426.e7. doi: 10.1016/j.neuron.2021.05.034. Epub 2021 Jun 21. PMID: 34157306; PMCID: PMC8349883.

292- Gratuze M, Jiang H, Wang C, Xiong M, Bao X, Holtzman DM. APOE Antibody Inhibits Aβ-Associated Tau Seeding and Spreading in a Mouse Model. Ann Neurol. 2022 Jun;91(6):847-852. doi: 10.1002/ana.26351. Epub 2022 Mar 31. PMID: 35285073; PMCID: PMC9285984.

293- Baek MS, Cho H, Lee HS, Lee JH, Ryu YH, Lyoo CH. Effect of APOE ε4 genotype on amyloid-β and tau accumulation in Alzheimer's disease. Alzheimers Res Ther. 2020 Oct 31;12(1):140. doi: 10.1186/s13195-020-00710-6. PMID: 33129364; PMCID: PMC7603688.

294- Therriault J, Benedet AL, Pascoal TA, Mathotaarachchi S, Chamoun M, Savard M, Thomas E, Kang MS, Lussier F, Tissot C, Parsons M, Qureshi MNI, Vitali P, Massarweh G, Soucy JP, Rej S, Saha-Chaudhuri P, Gauthier S, Rosa-Neto P. Association of Apolipoprotein E ε4 With Medial Temporal Tau Independent of Amyloid-β. JAMA Neurol. 2020 Apr 1;77(4):470-479. doi: 10.1001/jamaneurol.2019.4421. PMID: 31860000; PMCID: PMC6990684.

295- Scheff SW, Price DA, Schmitt FA, Mufson EJ. Hippocampal synaptic loss in early Alzheimer's disease and mild cognitive impairment. Neurobiol Aging. 2006 Oct;27(10):1372-84. doi: 10.1016/j.neurobiolaging.2005.09.012. Epub 2005 Nov 9. PMID: 16289476.

296- Reddy PH, Mani G, Park BS, Jacques J, Murdoch G, Whetsell W Jr, Kaye J, Manczak M. Differential loss of synaptic proteins in Alzheimer's disease: implications for synaptic dysfunction. J Alzheimers Dis. 2005 Apr;7(2):103-17; discussion 173-80. doi: 10.3233/jad-2005-7203. PMID: 15851848.

297- Tu S, Okamoto S, Lipton SA, Xu H. Oligomeric Aβ-induced synaptic dysfunction in Alzheimer's disease. Mol Neurodegener. 2014 Nov 14;9:48. doi: 10.1186/1750-1326-9-48. PMID: 25394486; PMCID: PMC4237769.

298- Klementieva O, Willén K, Martinsson I, Israelsson B, Engdahl A, Cladera J, Uvdal P, Gouras GK. Pre-plaque conformational changes in Alzheimer's disease-linked Aβ and APP. Nat Commun. 2017 Mar 13;8:14726. doi: 10.1038/ncomms14726. PMID: 28287086; PMCID: PMC5355803.

299- Liu CC, Liu CC, Kanekiyo T, Xu H, Bu G. Apolipoprotein E and Alzheimer disease: risk, mechanisms and therapy. Nat Rev Neurol. 2013 Feb;9(2):106-18. doi: 10.1038/nrneurol.2012.263. Epub 2013 Jan 8. Erratum in: Nat Rev Neurol. 2013. doi: 10.1038/nmeurol.2013.32. Liu, Chia-Chan [corrected to Liu, Chia-Chen]. PMID: 23296339; PMCID: PMC3726719.

300- Mahley RW, Huang Y. Apolipoprotein e sets the stage: response to injury triggers neuropathology. Neuron. 2012 Dec 6;76(5):871-85. doi: 10.1016/j.neuron.2012.11.020. PMID: 23217737; PMCID: PMC4891195.

301- Perdigão C, Barata MA, Araújo MN, Mirfakhar FS, Castanheira J, Guimas Almeida C. Intracellular Trafficking Mechanisms of Synaptic Dysfunction in Alzheimer's Disease. Front Cell Neurosci. 2020 Apr 17;14:72. doi: 10.3389/fncel.2020.00072. PMID: 32362813; PMCID: PMC7180223.

302- Wang C, Wilson WA, Moore SD, Mace BE, Maeda N, Schmechel DE, Sullivan PM. Human apoE4-targeted replacement mice display synaptic deficits in the absence of neuropathology. Neurobiol Dis. 2005 Mar;18(2):390-8. doi: 10.1016/j.nbd.2004.10.013. PMID: 15686968.

303- Dumanis SB, Tesoriero JA, Babus LW, Nguyen MT, Trotter JH, Ladu MJ, Weeber EJ, Turner RS, Xu B, Rebeck GW, Hoe HS. ApoE4 decreases spine density and dendritic complexity in cortical neurons in vivo. J Neurosci. 2009 Dec 2;29(48):15317-22. doi: 10.1523/JNEUROSCI.4026-09.2009. PMID: 19955384; PMCID: PMC2846754.

304- Jain S, Yoon SY, Leung L, Knoferle J, Huang Y. Cellular source-specific effects of apolipoprotein (apo) E4 on dendrite arborization and dendritic spine development. PLoS One. 2013;8(3):e59478. doi: 10.1371/journal.pone.0059478. Epub 2013 Mar 19. PMID: 23527202; PMCID: PMC3602301.

305- Trommer BL, Shah C, Yun SH, Gamkrelidze G, Pasternak ES, Ye GL, Sotak M, Sullivan PM, Pasternak JF, LaDu MJ. ApoE isoform affects LTP in human targeted replacement mice. Neuroreport. 2004 Dec 3;15(17):2655-8. doi: 10.1097/00001756-200412030-00020. PMID: 15570172.

306- Korwek KM, Trotter JH, Ladu MJ, Sullivan PM, Weeber EJ. ApoE isoform-dependent changes in hippocampal synaptic function. Mol Neurodegener. 2009 May 27;4:21. doi: 10.1186/1750-1326-4-21. PMID: 19725929; PMCID: PMC2695436.

307- Rodriguez GA, Burns MP, Weeber EJ, Rebeck GW. Young APOE4 targeted replacement mice exhibit poor spatial learning and memory, with reduced dendritic spine density in the medial entorhinal cortex. Learn Mem. 2013 Apr 16;20(5):256-66. doi: 10.1101/lm.030031.112. PMID: 23592036; PMCID: PMC3630489.

308- Koffie RM, Hashimoto T, Tai HC, Kay KR, Serrano-Pozo A, Joyner D, Hou S, Kopeikina KJ, Frosch MP, Lee VM, Holtzman DM, Hyman BT, Spires-Jones TL. Apolipoprotein E4 effects in Alzheimer's disease are mediated by synaptotoxic oligomeric amyloid-β. Brain. 2012 Jul;135(Pt 7):2155-68. doi: 10.1093/brain/aws127. Epub 2012 May 26. PMID: 22637583; PMCID: PMC3381721.

309- Xian X, Pohlkamp T, Durakoglugil MS, Wong CH, Beck JK, Lane-Donovan C, Plattner F, Herz J. Reversal of ApoE4-induced recycling block as a novel prevention approach for Alzheimer's disease. Elife. 2018 Oct 30;7:e40048. doi: 10.7554/eLife.40048. PMID: 30375977; PMCID: PMC6261251.

310- Heeren J, Grewal T, Laatsch A, Becker N, Rinninger F, Rye KA, Beisiegel U. Impaired recycling of apolipoprotein E4 is associated with intracellular cholesterol accumulation. J Biol Chem. 2004 Dec 31;279(53):55483-92. doi: 10.1074/jbc.M409324200. Epub 2004 Oct 12. PMID: 15485881.

311- Chen Y, Durakoglugil MS, Xian X, Herz J. ApoE4 reduces glutamate receptor function and synaptic plasticity by selectively impairing ApoE receptor recycling. Proc Natl Acad Sci U S A. 2010 Jun 29;107(26):12011-6. doi: 10.1073/pnas.0914984107. Epub 2010 Jun 14. PMID: 20547867; PMCID: PMC2900641.

312- Weeber EJ, Beffert U, Jones C, Christian JM, Forster E, Sweatt JD, Herz J. Reelin and ApoE receptors cooperate to enhance hippocampal synaptic plasticity and learning. J Biol Chem. 2002 Oct 18;277(42):39944-52. doi: 10.1074/jbc.M205147200. Epub 2002 Aug 7. PMID: 12167620.

313- Guzman-Martinez L, Maccioni RB, Andrade V, Navarrete LP, Pastor MG, Ramos-Escobar N. Neuroinflammation as a Common Feature of Neurodegenerative Disorders. Front Pharmacol. 2019 Sep 12;10:1008. doi: 10.3389/fphar.2019.01008. PMID: 31572186; PMCID: PMC6751310.

314- Shabab T, Khanabdali R, Moghadamtousi SZ, Kadir HA, Mohan G. Neuroinflammation pathways: a general review. Int J Neurosci. 2017 Jul;127(7):624-633. doi: 10.1080/00207454.2016.1212854. Epub 2016 Aug 9. PMID: 27412492.

315- Cudaback E, Li X, Montine KS, Montine TJ, Keene CD. Apolipoprotein E isoform-dependent microglia migration. FASEB J. 2011 Jun;25(6):2082-91. doi: 10.1096/fj.10-176891. Epub 2011 Mar 8. PMID: 21385991; PMCID: PMC3101033.

316- Ngkelo A, Meja K, Yeadon M, Adcock I, Kirkham PA. LPS induced inflammatory responses in human peripheral blood mononuclear cells is mediated through NOX4 and Giα dependent PI-3kinase signalling. J Inflamm (Lond). 2012 Jan 12;9(1):1. doi: 10.1186/1476-9255-9-1. PMID: 22239975; PMCID: PMC3293082.

317- Carmona S, Zahs K, Wu E, Dakin K, Bras J, Guerreiro R. The role of TREM2 in Alzheimer's disease and other neurodegenerative disorders. Lancet Neurol. 2018 Aug;17(8):721-730. doi: 10.1016/S1474-4422(18)30232-1. Epub 2018 Jul 17. PMID: 30033062.

318- Gratuze M, Leyns CEG, Holtzman DM. New insights into the role of TREM2 in Alzheimer's disease. Mol Neurodegener. 2018 Dec 20;13(1):66. doi: 10.1186/s13024-018-0298-9. PMID: 30572908; PMCID: PMC6302500.

319- Ulland TK, Colonna M. TREM2 - a key player in microglial biology and Alzheimer disease. Nat Rev Neurol. 2018 Nov;14(11):667-675. doi: 10.1038/s41582-018-0072-1. PMID: 30266932.

320- Gosselin D, Skola D, Coufal NG, Holtman IR, Schlachetzki JCM, Sajti E, Jaeger BN, O'Connor C, Fitzpatrick C, Pasillas MP, Pena M, Adair A, Gonda DD, Levy ML, Ransohoff RM, Gage FH, Glass CK. An environment-dependent transcriptional network specifies human microglia identity. Science. 2017 Jun 23;356(6344):eaal3222. doi: 10.1126/science.aal3222. Epub 2017 May 25. PMID: 28546318; PMCID: PMC5858585.

321- Zhong L, Chen XF, Wang T, Wang Z, Liao C, Wang Z, Huang R, Wang D, Li X, Wu L, Jia L, Zheng H, Painter M, Atagi Y, Liu CC, Zhang YW, Fryer JD, Xu H, Bu G. Soluble TREM2 induces inflammatory responses and enhances microglial survival. J Exp Med. 2017 Mar 6;214(3):597-607. doi: 10.1084/jem.20160844. Epub 2017 Feb 16. PMID: 28209725; PMCID: PMC5339672.

322- Leyns CEG, Ulrich JD, Finn MB, Stewart FR, Koscal LJ, Remolina Serrano J, Robinson GO, Anderson E, Colonna M, Holtzman DM. TREM2 deficiency attenuates neuroinflammation and protects against neurodegeneration in a mouse model of tauopathy. Proc Natl Acad Sci U S A. 2017 Oct 24;114(43):11524-11529. doi: 10.1073/pnas.1710311114. Epub 2017 Oct 9. PMID: 29073081; PMCID: PMC5663386.

323- Bemiller SM, McCray TJ, Allan K, Formica SV, Xu G, Wilson G, Kokiko-Cochran ON, Crish SD, Lasagna-Reeves CA, Ransohoff RM, Landreth GE, Lamb BT. TREM2 deficiency exacerbates tau pathology through dysregulated kinase signaling in a mouse model of tauopathy. Mol Neurodegener. 2017 Oct 16;12(1):74. doi: 10.1186/s13024-017-0216-6. PMID: 29037207; PMCID: PMC5644120.

324- Leyns CEG, Gratuze M, Narasimhan S, Jain N, Koscal LJ, Jiang H, Manis M, Colonna M, Lee VMY, Ulrich JD, Holtzman DM. TREM2 function impedes tau seeding in neuritic plaques. Nat Neurosci. 2019 Aug;22(8):1217-1222. doi: 10.1038/s41593-019-0433-0. Epub 2019 Jun 24. PMID: 31235932; PMCID: PMC6660358.

325- Parhizkar S, Arzberger T, Brendel M, Kleinberger G, Deussing M, Focke C, Nuscher B, Xiong M, Ghasemigharagoz A, Katzmarski N, Krasemann S, Lichtenthaler SF, Müller SA, Colombo A, Monasor LS, Tahirovic S, Herms J, Willem M, Pettkus N, Butovsky O, Bartenstein P, Edbauer D, Rominger A, Ertürk A, Grathwohl SA, Neher JJ, Holtzman DM, Meyer-Luehmann M, Haass C. Loss of TREM2 function increases amyloid seeding but reduces plaque-associated ApoE. Nat Neurosci. 2019 Feb;22(2):191-204. doi: 10.1038/s41593-018-0296-9. Epub 2019 Jan 7. PMID: 30617257; PMCID: PMC6417433.

326- Andreone BJ, Przybyla L, Llapashtica C, Rana A, Davis SS, van Lengerich B, Lin K, Shi J, Mei Y, Astarita G, Di Paolo G, Sandmann T, Monroe KM, Lewcock JW. Alzheimer's-associated PLCγ2 is a signaling node required for both TREM2 function and the inflammatory response in human microglia. Nat Neurosci. 2020 Aug;23(8):927-938. doi: 10.1038/s41593-020-0650-6. Epub 2020 Jun 8. PMID: 32514138.

327- McQuade A, Kang YJ, Hasselmann J, Jairaman A, Sotelo A, Coburn M, Shabestari SK, Chadarevian JP, Fote G, Tu CH, Danhash E, Silva J, Martinez E, Cotman C, Prieto GA, Thompson LM, Steffan JS, Smith I, Davtyan H, Cahalan M, Cho H, Blurton-Jones M. Gene expression and functional deficits underlie TREM2-knockout microglia responses in human models of Alzheimer's disease. Nat Commun. 2020 Oct 23;11(1):5370. doi: 10.1038/s41467-020-19227-5. PMID: 33097708; PMCID: PMC7584603.

328- Shen X, Venero JL, Joseph B, Burguillos MA. Caspases orchestrate microglia instrumental functions. Prog Neurobiol. 2018 Dec;171:50-71. doi: 10.1016/j.pneurobio.2018.09.007. Epub 2018 Oct 2. PMID: 30290215.

329- Zhu Y, Kodvawala A, Hui DY. Apolipoprotein E inhibits toll-like receptor (TLR)-3- and TLR-4-mediated macrophage activation through distinct mechanisms. Biochem J. 2010 Apr 28;428(1):47-54. doi: 10.1042/BJ20100016. PMID: 20218969; PMCID: PMC3050041.

330- Krasemann S, Madore C, Cialic R, Baufeld C, Calcagno N, El Fatimy R, Beckers L, O'Loughlin E, Xu Y, Fanek Z, Greco DJ, Smith ST, Tweet G, Humulock Z, Zrzavy T, Conde-Sanroman P, Gacias M, Weng Z, Chen H, Tjon E, Mazaheri F, Hartmann K, Madi A, Ulrich JD, Glatzel M, Worthmann A, Heeren J, Budnik B, Lemere C, Ikezu T, Heppner FL, Litvak V, Holtzman DM, Lassmann H, Weiner HL, Ochando J, Haass C, Butovsky O. The TREM2-APOE Pathway Drives the Transcriptional Phenotype of Dysfunctional Microglia in Neurodegenerative Diseases. Immunity. 2017 Sep 19;47(3):566-581.e9. doi: 10.1016/j.immuni.2017.08.008. PMID: 28930663; PMCID: PMC5719893.

331- Wong MY, Lewis M, Doherty JJ, Shi Y, Cashikar AG, Amelianchik A, Tymchuk S, Sullivan PM, Qian M, Covey DF, Petsko GA, Holtzman DM, Paul SM, Luo W. 25-Hydroxycholesterol amplifies microglial IL-1β production in an apoE isoform-dependent manner. J Neuroinflammation. 2020 Jun 17;17(1):192. doi: 10.1186/s12974-020-01869-3. PMID: 32552741; PMCID: PMC7298825.

332- Chuang TY, Guo Y, Seki SM, Rosen AM, Johanson DM, Mandell JW, Lucchinetti CF, Gaultier A. LRP1 expression in microglia is protective during CNS autoimmunity. Acta Neuropathol Commun. 2016 Jul 11;4(1):68. doi: 10.1186/s40478-016-0343-2. PMID: 27400748; PMCID: PMC4940960.

333- Brifault C, Kwon H, Campana WM, Gonias SL. LRP1 deficiency in microglia blocks neuro-inflammation in the spinal dorsal horn and neuropathic pain

processing. Glia. 2019 Jun;67(6):1210-1224. doi: 10.1002/glia.23599. Epub 2019 Feb 11. PMID: 30746765; PMCID: PMC6462253.

334- He Y, Ruganzu JB, Zheng Q, Wu X, Jin H, Peng X, Ding B, Lin C, Ji S, Ma Y, Yang W. Silencing of LRP1 Exacerbates Inflammatory Response Via TLR4/NF-κB/MAPKs Signaling Pathways in APP/PS1 Transgenic Mice. Mol Neurobiol. 2020 Sep;57(9):3727-3743. doi: 10.1007/s12035-020-01982-7. Epub 2020 Jun 22. PMID: 32572761.

335- Pocivavsek A, Mikhailenko I, Strickland DK, Rebeck GW. Microglial low-density lipoprotein receptor-related protein 1 modulates c-Jun N-terminal kinase activation. J Neuroimmunol. 2009 Sep 29;214(1-2):25-32. doi: 10.1016/j.jneuroim.2009.06.010. Epub 2009 Jul 7. PMID: 19586665; PMCID: PMC2745483.

336- Schmukler E, Solomon S, Simonovitch S, Goldshmit Y, Wolfson E, Michaelson DM, Pinkas-Kramarski R. Altered mitochondrial dynamics and function in APOE4-expressing astrocytes. Cell Death Dis. 2020 Jul 24;11(7):578. doi: 10.1038/s41419-020-02776-4. PMID: 32709881; PMCID: PMC7382473.

337- Farmer BC, Williams HC, Devanney NA, Piron MA, Nation GK, Carter DJ, Walsh AE, Khanal R, Young LEA, Kluemper JC, Hernandez G, Allenger EJ, Mooney R, Golden LR, Smith CT, Brandon JA, Gupta VA, Kern PA, Gentry MS, Morganti JM, Sun RC, Johnson LA. APOE4 lowers energy expenditure in females and impairs glucose oxidation by increasing flux through aerobic glycolysis. Mol Neurodegener. 2021 Sep 6;16(1):62. doi: 10.1186/s13024-021-00483-y. PMID: 34488832; PMCID: PMC8420022.

338- Zhang J, Liu Q. Cholesterol metabolism and homeostasis in the brain. Protein Cell. 2015 Apr;6(4):254-64. doi: 10.1007/s13238-014-0131-3. Epub 2015 Feb 15. PMID: 25682154; PMCID: PMC4383754.

339- Gong JS, Kobayashi M, Hayashi H, Zou K, Sawamura N, Fujita SC, Yanagisawa K, Michikawa M. Apolipoprotein E (ApoE) isoform-dependent lipid release from astrocytes prepared from human ApoE3 and ApoE4 knock-in mice. J Biol Chem. 2002 Aug 16;277(33):29919-26. doi: 10.1074/jbc.M203934200. Epub 2002 May 31. PMID: 12042316.

340- Zhao J, Davis MD, Martens YA, Shinohara M, Graff-Radford NR, Younkin SG, Wszolek ZK, Kanekiyo T, Bu G. APOE ε4/ε4 diminishes neurotrophic function of human iPSC-derived astrocytes. Hum Mol Genet. 2017 Jul 15;26(14):2690-2700. doi: 10.1093/hmg/ddx155. PMID: 28444230; PMCID: PMC5886091.

341- Tcw J, Qian L, Pipalia NH, Chao MJ, Liang SA, Shi Y, Jain BR, Bertelsen SE, Kapoor M, Marcora E, Sikora E, Andrews EJ, Martini AC, Karch CM, Head E, Holtzman DM, Zhang B, Wang M, Maxfield FR, Poon WW, Goate AM. Cholesterol and matrisome pathways dysregulated in astrocytes and microglia. Cell. 2022 Jun 23;185(13):2213-2233.e25. doi: 10.1016/j.cell.2022.05.017. PMID: 35750033; PMCID: PMC9340815.

342- Rawat V, Wang S, Sima J, Bar R, Liraz O, Gundimeda U, Parekh T, Chan J, Johansson JO, Tang C, Chui HC, Harrington MG, Michaelson DM, Yassine HN. ApoE4 Alters ABCA1 Membrane Trafficking in Astrocytes. J Neurosci. 2019 Nov 27;39(48):9611-9622. doi: 10.1523/JNEUROSCI.1400-19.2019. Epub 2019 Oct 22. PMID: 31641056; PMCID: PMC6880458.

343- Papassotiropoulos A, Lütjohann D, Bagli M, Locatelli S, Jessen F, Buschfort R, Ptok U, Björkhem I, von Bergmann K, Heun R. 24S-hydroxycholesterol in cerebrospinal fluid is elevated in early stages of dementia. J Psychiatr Res. 2002 Jan-Feb;36(1):27-32. doi: 10.1016/s0022-3956(01)00050-4. PMID: 11755458.

344- Kawarabayashi T, Shoji M, Younkin LH, Wen-Lang L, Dickson DW, Murakami T, Matsubara E, Abe K, Ashe KH, Younkin SG. Dimeric amyloid beta protein rapidly accumulates in lipid rafts followed by apolipoprotein E and phosphorylated tau

accumulation in the Tg2576 mouse model of Alzheimer's disease. J Neurosci. 2004 Apr 14;24(15):3801-9. doi: 10.1523/JNEUROSCI.5543-03.2004. PMID: 15084661; PMCID: PMC6729359.

345- El Gaamouch F, Jing P, Xia J, Cai D. Alzheimer's Disease Risk Genes and Lipid Regulators. J Alzheimers Dis. 2016 Apr 23;53(1):15-29. doi: 10.3233/JAD-160169. PMID: 27128373.

346- Schengrund CL. Lipid rafts: keys to neurodegeneration. Brain Res Bull. 2010 Apr 29;82(1-2):7-17. doi: 10.1016/j.brainresbull.2010.02.013. Epub 2010 Mar 3. PMID: 20206240.

347- Okada T, Ikeda K, Wakabayashi M, Ogawa M, Matsuzaki K. Formation of toxic Abeta(1-40) fibrils on GM1 ganglioside-containing membranes mimicking lipid rafts: polymorphisms in Abeta(1-40) fibrils. J Mol Biol. 2008 Oct 17;382(4):1066-74. doi: 10.1016/j.jmb.2008.07.072. Epub 2008 Jul 30. PMID: 18692507.

348- Nordestgaard LT, Tybjærg-Hansen A, Nordestgaard BG, Frikke-Schmidt R. Loss-of-function mutation in ABCA1 and risk of Alzheimer's disease and cerebrovascular disease. Alzheimers Dement. 2015 Dec;11(12):1430-1438. doi: 10.1016/j.jalz.2015.04.006. Epub 2015 Jun 13. PMID: 26079414.

349- Wahrle SE, Jiang H, Parsadanian M, Kim J, Li A, Knoten A, Jain S, Hirsch-Reinshagen V, Wellington CL, Bales KR, Paul SM, Holtzman DM. Overexpression of ABCA1 reduces amyloid deposition in the PDAPP mouse model of Alzheimer disease. J Clin Invest. 2008 Feb;118(2):671-82. doi: 10.1172/JCI33622. PMID: 18202749; PMCID: PMC2200302.

350- Wahrle SE, Jiang H, Parsadanian M, Legleiter J, Han X, Fryer JD, Kowalewski T, Holtzman DM. ABCA1 is required for normal central nervous system ApoE levels and for lipidation of astrocyte-secreted apoE. J Biol Chem. 2004 Sep 24;279(39):40987-93. doi: 10.1074/jbc.M407963200. Epub 2004 Jul 21. PMID: 15269217.

351- Fitz NF, Cronican AA, Saleem M, Fauq AH, Chapman R, Lefterov I, Koldamova R. Abca1 deficiency affects Alzheimer's disease-like phenotype in human ApoE4 but not in ApoE3-targeted replacement mice. J Neurosci. 2012 Sep 19;32(38):13125-36. doi: 10.1523/JNEUROSCI.1937-12.2012. PMID: 22993429; PMCID: PMC3646580.

352- Liu L, MacKenzie KR, Putluri N, Maletić-Savatić M, Bellen HJ. The Glia-Neuron Lactate Shuttle and Elevated ROS Promote Lipid Synthesis in Neurons and Lipid Droplet Accumulation in Glia via APOE/D. Cell Metab. 2017 Nov 7;26(5):719-737.e6. doi: 10.1016/j.cmet.2017.08.024. Epub 2017 Sep 28. PMID: 28965825; PMCID: PMC5677551.

353- Schönfeld P, Reiser G. Why does brain metabolism not favor burning of fatty acids to provide energy? Reflections on disadvantages of the use of free fatty acids as fuel for brain. J Cereb Blood Flow Metab. 2013 Oct;33(10):1493-9. doi: 10.1038/jcbfm.2013.128. Epub 2013 Aug 7. PMID: 23921897; PMCID: PMC3790936.

354- Ioannou MS, Jackson J, Sheu SH, Chang CL, Weigel AV, Liu H, Pasolli HA, Xu CS, Pang S, Matthies D, Hess HF, Lippincott-Schwartz J, Liu Z. Neuron-Astrocyte Metabolic Coupling Protects against Activity-Induced Fatty Acid Toxicity. Cell. 2019 May 30;177(6):1522-1535.e14. doi: 10.1016/j.cell.2019.04.001. Epub 2019 May 23. PMID: 31130380.

355- Nguyen TB, Louie SM, Daniele JR, Tran Q, Dillin A, Zoncu R, Nomura DK, Olzmann JA. DGAT1-Dependent Lipid Droplet Biogenesis Protects Mitochondrial Function during Starvation-Induced Autophagy. Dev Cell. 2017 Jul 10;42(1):9-21.e5. doi: 10.1016/j.devcel.2017.06.003. PMID: 28697336; PMCID: PMC5553613.

356- Qi G, Mi Y, Shi X, Gu H, Brinton RD, Yin F. ApoE4 Impairs Neuron-Astrocyte Coupling of Fatty Acid Metabolism. Cell Rep. 2021 Jan 5;34(1):108572. doi: 10.1016/j.celrep.2020.108572. PMID: 33406436; PMCID: PMC7837265.

357- Sienski G, Narayan P, Bonner JM, Kory N, Boland S, Arczewska AA, Ralvenius WT, Akay L, Lockshin E, He L, Milo B, Graziosi A, Baru V, Lewis CA, Kellis M, Sabatini DM, Tsai LH, Lindquist S. *APOE4* disrupts intracellular lipid homeostasis in human iPSC-derived glia. Sci Transl Med. 2021 Mar 3;13(583):eaaz4564. doi: 10.1126/scitranslmed.aaz4564. PMID: 33658354; PMCID: PMC8218593.

358- Boix CP, Lopez-Font I, Cuchillo-Ibañez I, Sáez-Valero J. Amyloid precursor protein glycosylation is altered in the brain of patients with Alzheimer's disease. Alzheimers Res Ther. 2020 Aug 12;12(1):96. doi: 10.1186/s13195-020-00664-9. PMID: 32787955; PMCID: PMC7425076.

359- Almansoub HAMM, Tang H, Wu Y, Wang DQ, Mahaman YAR, Wei N, Almansob YAM, He W, Liu D. Tau Abnormalities and the Potential Therapy in Alzheimer's Disease. J Alzheimers Dis. 2019;67(1):13-33. doi: 10.3233/JAD-180868. PMID: 30507581.

360- Frenkel-Pinter M, Shmueli MD, Raz C, Yanku M, Zilberzwige S, Gazit E, Segal D. Interplay between protein glycosylation pathways in Alzheimer's disease. Sci Adv. 2017 Sep 15;3(9):e1601576. doi: 10.1126/sciadv.1601576. PMID: 28929132; PMCID: PMC5600531.

361- Kacperczyk M, Kmieciak A, Kratz EM. The Role of ApoE Expression and Variability of Its Glycosylation in Human Reproductive Health in the Light of Current Information. Int J Mol Sci. 2021 Jul 4;22(13):7197. doi: 10.3390/ijms22137197. PMID: 34281251; PMCID: PMC8268793.

362- Chua CC, Lim ML, Wong BS. Altered apolipoprotein E glycosylation is associated with Abeta(42) accumulation in an animal model of Niemann-Pick Type C disease. J Neurochem. 2010 Mar;112(6):1619-26. doi: 10.1111/j.1471-4159.2010.06586.x. Epub 2010 Jan 13. PMID: 20070866.

363- Sugano M, Yamauchi K, Kawasaki K, Tozuka M, Fujita K, Okumura N, Ota H. Sialic acid moiety of apolipoprotein E3 at Thr(194) affects its interaction with beta-amyloid(1-42) peptides. Clin Chim Acta. 2008 Feb;388(1-2):123-9. doi: 10.1016/j.cca.2007.10.024. Epub 2007 Oct 30. PMID: 18023277.

364- Montine KS, Bassett CN, Ou JJ, Markesbery WR, Swift LL, Montine TJ. Apolipoprotein E allelic influence on human cerebrospinal fluid apolipoproteins. J Lipid Res. 1998 Dec;39(12):2443-51. PMID: 9831633.

365- Patra K, Giannisis A, Edlund AK, Sando SB, Lauridsen C, Berge G, Grøntvedt GR, Bråthen G, White LR, Nielsen HM. Plasma Apolipoprotein E Monomer and Dimer Profile and Relevance to Alzheimer's Disease. J Alzheimers Dis. 2019;71(4):1217-1231. doi: 10.3233/JAD-190175. PMID: 31524156.

366- Martel CL, Mackic JB, Matsubara E, Governale S, Miguel C, Miao W, McComb JG, Frangione B, Ghiso J, Zlokovic BV. Isoform-specific effects of apolipoproteins E2, E3, and E4 on cerebral capillary sequestration and blood-brain barrier transport of circulating Alzheimer's amyloid beta. J Neurochem. 1997 Nov;69(5):1995-2004. doi: 10.1046/j.1471-4159.1997.69051995.x. PMID: 9349544.

367- Permanne B, Perez C, Soto C, Frangione B, Wisniewski T. Detection of apolipoprotein E/dimeric soluble amyloid beta complexes in Alzheimer's disease brain supernatants. Biochem Biophys Res Commun. 1997 Nov 26;240(3):715-20. doi: 10.1006/bbrc.1997.7727. PMID: 9398632.

368- Deroo S, Stengel F, Mohammadi A, Henry N, Hubin E, Krammer EM, Aebersold R, Raussens V. Chemical cross-linking/mass spectrometry maps the amyloid β peptide binding region on both apolipoprotein E domains. ACS Chem Biol. 2015

Apr 17;10(4):1010-6. doi: 10.1021/cb500994j. Epub 2015 Jan 21. PMID: 25546376.

369- Safaiyan S, Besson-Girard S, Kaya T, Cantuti-Castelvetri L, Liu L, Ji H, Schifferer M, Gouna G, Usifo F, Kannaiyan N, Fitzner D, Xiang X, Rossner MJ, Brendel M, Gokce O, Simons M. White matter aging drives microglial diversity. Neuron. 2021 Apr 7;109(7):1100-1117.e10. doi: 10.1016/j.neuron.2021.01.027. Epub 2021 Feb 18. PMID: 33606969.

370- Ji F, Pasternak O, Ng KK, Chong JSX, Liu S, Zhang L, Shim HY, Loke YM, Tan BY, Venketasubramanian N, Chen CL, Zhou JH. White matter microstructural abnormalities and default network degeneration are associated with early memory deficit in Alzheimer's disease continuum. Sci Rep. 2019 Mar 18;9(1):4749. doi: 10.1038/s41598-019-41363-2. PMID: 30894627; PMCID: PMC6426923.

371- Heise V, Filippini N, Ebmeier KP, Mackay CE. The APOE ε4 allele modulates brain white matter integrity in healthy adults. Mol Psychiatry. 2011 Sep;16(9):908-16. doi: 10.1038/mp.2010.90. Epub 2010 Sep 7. PMID: 20820167.

372- Mirza SS, Saeed U, Knight J, Ramirez J, Stuss DT, Keith J, Nestor SM, Yu D, Swardfager W, Rogaeva E, St George Hyslop P, Black SE, Masellis M; Alzheimer's Disease Neuroimaging Initiative. *APOE* ε4, white matter hyperintensities, and cognition in Alzheimer and Lewy body dementia. Neurology. 2019 Nov 5;93(19):e1807-e1819. doi: 10.1212/WNL.0000000000008377. Epub 2019 Oct 1. PMID: 31575706; PMCID: PMC6946485.

373- Van Acker ZP, Bretou M, Annaert W. Endo-lysosomal dysregulations and late-onset Alzheimer's disease: impact of genetic risk factors. Mol Neurodegener. 2019 Jun 3;14(1):20. doi: 10.1186/s13024-019-0323-7. PMID: 31159836; PMCID: PMC6547588.

374- Xiao Q, Yan P, Ma X, Liu H, Perez R, Zhu A, Gonzales E, Tripoli DL, Czerniewski L, Ballabio A, Cirrito JR, Diwan A, Lee JM. Neuronal-Targeted TFEB Accelerates Lysosomal Degradation of APP, Reducing Aβ Generation and Amyloid Plaque Pathogenesis. J Neurosci. 2015 Sep 2;35(35):12137-51. doi: 10.1523/JNEUROSCI.0705-15.2015. PMID: 26338325; PMCID: PMC4556784.

375- Cho MH, Cho K, Kang HJ, Jeon EY, Kim HS, Kwon HJ, Kim HM, Kim DH, Yoon SY. Autophagy in microglia degrades extracellular β-amyloid fibrils and regulates the NLRP3 inflammasome. Autophagy. 2014 Oct 1;10(10):1761-75. doi: 10.4161/auto.29647. Epub 2014 Jul 22. PMID: 25126727; PMCID: PMC4198361.

376- Nixon RA. Amyloid precursor protein and endosomal-lysosomal dysfunction in Alzheimer's disease: inseparable partners in a multifactorial disease. FASEB J. 2017 Jul;31(7):2729-2743. doi: 10.1096/fj.201700359. PMID: 28663518; PMCID: PMC6137496.

377- François A, Terro F, Janet T, Rioux Bilan A, Paccalin M, Page G. Involvement of interleukin-1β in the autophagic process of microglia: relevance to Alzheimer's disease. J Neuroinflammation. 2013 Dec 13;10:151. doi: 10.1186/1742-2094-10-151. PMID: 24330807; PMCID: PMC3878742.

378- Lambert JC, Ibrahim-Verbaas CA, Harold D, Naj AC, Sims R, Bellenguez C, DeStafano AL, Bis JC, Beecham GW, Grenier-Boley B, Russo G, Thorton-Wells TA, Jones N, Smith AV, Chouraki V, Thomas C, Ikram MA, Zelenika D, Vardarajan BN, Kamatani Y, Lin CF, Gerrish A, Schmidt H, Kunkle B, Dunstan ML, Ruiz A, Bihoreau MT, Choi SH, Reitz C, Pasquier F, Cruchaga C, Craig D, Amin N, Berr C, Lopez OL, De Jager PL, Deramecourt V, Johnston JA, Evans D, Lovestone S, Letenneur L, Morón FJ, Rubinsztein DC, Eiriksdottir G, Sleegers K, Goate AM, Fiévet N, Huentelman MW, Gill M, Brown K, Kamboh MI, Keller L,

Barberger-Gateau P, McGuiness B, Larson EB, Green R, Myers AJ, Dufouil C, Todd S, Wallon D, Love S, Rogaeva E, Gallacher J, St George-Hyslop P, Clarimon J, Lleo A, Bayer A, Tsuang DW, Yu L, Tsolaki M, Bossù P, Spalletta G, Proitsi P, Collinge J, Sorbi S, Sanchez-Garcia F, Fox NC, Hardy J, Deniz Naranjo MC, Bosco P, Clarke R, Brayne C, Galimberti D, Mancuso M, Matthews F; European Alzheimer's Disease Initiative (EADI); Genetic and Environmental Risk in Alzheimer's Disease; Alzheimer's Disease Genetic Consortium; Cohorts for Heart and Aging Research in Genomic Epidemiology; Moebus S, Mecocci P, Del Zompo M, Maier W, Hampel H, Pilotto A, Bullido M, Panza F, Caffarra P, Nacmias B, Gilbert JR, Mayhaus M, Lannefelt L, Hakonarson H, Pichler S, Carrasquillo MM, Ingelsson M, Beekly D, Alvarez V, Zou F, Valladares O, Younkin SG, Coto E, Hamilton-Nelson KL, Gu W, Razquin C, Pastor P, Mateo I, Owen MJ, Faber KM, Jonsson PV, Combarros O, O'Donovan MC, Cantwell LB, Soininen H, Blacker D, Mead S, Mosley TH Jr, Bennett DA, Harris TB, Fratiglioni L, Holmes C, de Bruijn RF, Passmore P, Montine TJ, Bettens K, Rotter JI, Brice A, Morgan K, Foroud TM, Kukull WA, Hannequin D, Powell JF, Nalls MA, Ritchie K, Lunetta KL, Kauwe JS, Boerwinkle E, Riemenschneider M, Boada M, Hiltuenen M, Martin ER, Schmidt R, Rujescu D, Wang LS, Dartigues JF, Mayeux R, Tzourio C, Hofman A, Nöthen MM, Graff C, Psaty BM, Jones L, Haines JL, Holmans PA, Lathrop M, Pericak-Vance MA, Launer LJ, Farrer LA, van Duijn CM, Van Broeckhoven C, Moskvina V, Seshadri S, Williams J, Schellenberg GD, Amouyel P. Meta-analysis of 74,046 individuals identifies 11 new susceptibility loci for Alzheimer's disease. Nat Genet. 2013 Dec;45(12):1452-8. doi: 10.1038/ng.2802. Epub 2013 Oct 27. PMID: 24162737; PMCID: PMC3896259.

379- Simonovitch S, Schmukler E, Bespalko A, Iram T, Frenkel D, Holtzman DM, Masliah E, Michaelson DM, Pinkas-Kramarski R. Impaired Autophagy in APOE4 Astrocytes. J Alzheimers Dis. 2016;51(3):915-27. doi: 10.3233/JAD-151101. PMID: 26923027.

380- Nuriel T, Peng KY, Ashok A, Dillman AA, Figueroa HY, Apuzzo J, Ambat J, Levy E, Cookson MR, Mathews PM, Duff KE. The Endosomal-Lysosomal Pathway Is Dysregulated by *APOE4* Expression *in Vivo*. Front Neurosci. 2017 Dec 12;11:702. doi: 10.3389/fnins.2017.00702. PMID: 29311783; PMCID: PMC5733017.

381- Simonovitch S, Schmukler E, Masliah E, Pinkas-Kramarski R, Michaelson DM. The Effects of APOE4 on Mitochondrial Dynamics and Proteins in vivo. J Alzheimers Dis. 2019;70(3):861-875. doi: 10.3233/JAD-190074. PMID: 31306119; PMCID: PMC7478177.

382- Parcon PA, Balasubramaniam M, Ayyadevara S, Jones RA, Liu L, Shmookler Reis RJ, Barger SW, Mrak RE, Griffin WST. Apolipoprotein E4 inhibits autophagy gene products through direct, specific binding to CLEAR motifs. Alzheimers Dement. 2018 Feb;14(2):230-242. doi: 10.1016/j.jalz.2017.07.754. Epub 2017 Sep 22. PMID: 28945989; PMCID: PMC6613789.

383- Tzioras M, Davies C, Newman A, Jackson R, Spires-Jones T. Invited Review: APOE at the interface of inflammation, neurodegeneration and pathological protein spread in Alzheimer's disease. Neuropathol Appl Neurobiol. 2019 Jun;45(4):327-346. doi: 10.1111/nan.12529. Epub 2018 Nov 28. PMID: 30394574; PMCID: PMC6563457.

384- Krstic D, Pfister S, Notter T, Knuesel I. Decisive role of Reelin signaling during early stages of Alzheimer's disease. Neuroscience. 2013 Aug 29;246:108-16. doi: 10.1016/j.neuroscience.2013.04.042. Epub 2013 Apr 28. PMID: 23632168.

385- Ohkubo N, Lee YD, Morishima A, Terashima T, Kikkawa S, Tohyama M, Sakanaka M, Tanaka J, Maeda N, Vitek MP, Mitsuda N. Apolipoprotein E and Reelin ligands modulate tau phosphorylation through an apolipoprotein E

receptor/disabled-1/glycogen synthase kinase-3beta cascade. FASEB J. 2003 Feb;17(2):295-7. doi: 10.1096/fj.02-0434fje. Epub 2002 Dec 18. PMID: 12490540.

386- Beffert U, Weeber EJ, Morfini G, Ko J, Brady ST, Tsai LH, Sweatt JD, Herz J. Reelin and cyclin-dependent kinase 5-dependent signals cooperate in regulating neuronal migration and synaptic transmission. J Neurosci. 2004 Feb 25;24(8):1897-906. doi: 10.1523/JNEUROSCI.4084-03.2004. PMID: 14985430; PMCID: PMC6730409.

387- Hoe HS, Rebeck GW. Functional interactions of APP with the apoE receptor family. J Neurochem. 2008 Sep;106(6):2263-71. doi: 10.1111/j.1471-4159.2008.05517.x. Epub 2008 Jun 28. PMID: 18554321.

388- Durakoglugil MS, Chen Y, White CL, Kavalali ET, Herz J. Reelin signaling antagonizes beta-amyloid at the synapse. Proc Natl Acad Sci U S A. 2009 Sep 15;106(37):15938-43. doi: 10.1073/pnas.0908176106. Epub 2009 Sep 2. PMID: 19805234; PMCID: PMC2747222.

389- Kobayashi M, Ishiguro K, Katoh-Fukui Y, Yokoyama M, Fujita SC. Phosphorylation state of tau in the hippocampus of apolipoprotein E4 and E3 knock-in mice. Neuroreport. 2003 Apr 15;14(5):699-702. doi: 10.1097/00001756-200304150-00008. PMID: 12692466.

390- Chin J, Massaro CM, Palop JJ, Thwin MT, Yu GQ, Bien-Ly N, Bender A, Mucke L. Reelin depletion in the entorhinal cortex of human amyloid precursor protein transgenic mice and humans with Alzheimer's disease. J Neurosci. 2007 Mar 14;27(11):2727-33. doi: 10.1523/JNEUROSCI.3758-06.2007. PMID: 17360894; PMCID: PMC6672562.

391- Herring A, Donath A, Steiner KM, Widera MP, Hamzehian S, Kanakis D, Kölble K, ElAli A, Hermann DM, Paulus W, Keyvani K. Reelin depletion is an early phenomenon of Alzheimer's pathology. J Alzheimers Dis. 2012;30(4):963-79. doi: 10.3233/JAD-2012-112069. PMID: 22495348.

392- Botella-López A, Burgaya F, Gavín R, García-Ayllón MS, Gómez-Tortosa E, Peña-Casanova J, Ureña JM, Del Río JA, Blesa R, Soriano E, Sáez-Valero J. Reelin expression and glycosylation patterns are altered in Alzheimer's disease. Proc Natl Acad Sci U S A. 2006 Apr 4;103(14):5573-8. doi: 10.1073/pnas.0601279103. Epub 2006 Mar 27. PMID: 16567613; PMCID: PMC1414634.

393- Sáez-Valero J, Costell M, Sjögren M, Andreasen N, Blennow K, Luque JM. Altered levels of cerebrospinal fluid reelin in frontotemporal dementia and Alzheimer's disease. J Neurosci Res. 2003 Apr 1;72(1):132-6. doi: 10.1002/jnr.10554. PMID: 12645087.

394- Notter T, Knuesel I. Reelin immunoreactivity in neuritic varicosities in the human hippocampal formation of non-demented subjects and Alzheimer's disease patients. Acta Neuropathol Commun. 2013 Jun 26;1:27. doi: 10.1186/2051-5960-1-27. PMID: 24252415; PMCID: PMC3893416.

395- Knuesel I, Nyffeler M, Mormède C, Muhia M, Meyer U, Pietropaolo S, Yee BK, Pryce CR, LaFerla FM, Marighetto A, Feldon J. Age-related accumulation of Reelin in amyloid-like deposits. Neurobiol Aging. 2009 May;30(5):697-716. doi: 10.1016/j.neurobiolaging.2007.08.011. Epub 2007 Sep 27. PMID: 17904250.

396- Cuchillo-Ibañez I, Balmaceda V, Mata-Balaguer T, Lopez-Font I, Sáez-Valero J. Reelin in Alzheimer's Disease, Increased Levels but Impaired Signaling: When More is Less. J Alzheimers Dis. 2016 Mar 26;52(2):403-16. doi: 10.3233/JAD-151193. PMID: 27031488.

397- Mata-Balaguer T, Cuchillo-Ibañez I, Calero M, Ferrer I, Sáez-Valero J. Decreased generation of C-terminal fragments of ApoER2 and increased reelin

expression in Alzheimer's disease. FASEB J. 2018 Jul;32(7):3536-3546. doi: 10.1096/fj.201700736RR. Epub 2018 Feb 9. PMID: 29442527.

398- Doehner J, Madhusudan A, Konietzko U, Fritschy JM, Knuesel I. Co-localization of Reelin and proteolytic AbetaPP fragments in hippocampal plaques in aged wild-type mice. J Alzheimers Dis. 2010;19(4):1339-57. doi: 10.3233/JAD-2010-1333. PMID: 20061602.

399- Kocherhans S, Madhusudan A, Doehner J, Breu KS, Nitsch RM, Fritschy JM, Knuesel I. Reduced Reelin expression accelerates amyloid-beta plaque formation and tau pathology in transgenic Alzheimer's disease mice. J Neurosci. 2010 Jul 7;30(27):9228-40. doi: 10.1523/JNEUROSCI.0418-10.2010. PMID: 20610758; PMCID: PMC6632461.

400- Botella-López A, Cuchillo-Ibáñez I, Cotrufo T, Mok SS, Li QX, Barquero MS, Dierssen M, Soriano E, Sáez-Valero J. Beta-amyloid controls altered Reelin expression and processing in Alzheimer's disease. Neurobiol Dis. 2010 Mar;37(3):682-91. doi: 10.1016/j.nbd.2009.12.006. Epub 2009 Dec 16. PMID: 20025970.

401- Helbecque N, Cottel D, Amouyel P. Low-density lipoprotein receptor-related protein 8 gene polymorphisms and dementia. Neurobiol Aging. 2009 Feb;30(2):266-71. doi: 10.1016/j.neurobiolaging.2007.05.024. Epub 2007 Jul 5. PMID: 17614163.

402- Cuchillo-Ibañez I, Mata-Balaguer T, Balmaceda V, Arranz JJ, Nimpf J, Sáez-Valero J. The β-amyloid peptide compromises Reelin signaling in Alzheimer's disease. Sci Rep. 2016 Aug 17;6:31646. doi: 10.1038/srep31646. PMID: 27531658; PMCID: PMC4987719.

403- Müller T, Loosse C, Schrötter A, Schnabel A, Helling S, Egensperger R, Marcus K. The AICD interacting protein DAB1 is up-regulated in Alzheimer frontal cortex brain samples and causes deregulation of proteins involved in gene expression changes. Curr Alzheimer Res. 2011 Aug;8(5):573-82. doi: 10.2174/156720511796391827. PMID: 21453247.

404- Parisiadou L, Efthimiopoulos S. Expression of mDab1 promotes the stability and processing of amyloid precursor protein and this effect is counteracted by X11alpha. Neurobiol Aging. 2007 Mar;28(3):377-88. doi: 10.1016/j.neurobiolaging.2005.12.015. Epub 2006 Feb 3. PMID: 16458391.

405- Gao H, Tao Y, He Q, Song F, Saffen D. Functional enrichment analysis of three Alzheimer's disease genome-wide association studies identities DAB1 as a novel candidate liability/protective gene. Biochem Biophys Res Commun. 2015 Aug 7;463(4):490-5. doi: 10.1016/j.bbrc.2015.05.044. Epub 2015 May 29. PMID: 26028559.

406- Beach TG, Monsell SE, Phillips LE, Kukull W. Accuracy of the clinical diagnosis of Alzheimer disease at National Institute on Aging Alzheimer Disease Centers, 2005-2010. J Neuropathol Exp Neurol. 2012 Apr;71(4):266-73. doi: 10.1097/NEN.0b013e31824b211b. PMID: 22437338; PMCID: PMC3331862.

407- Blennow K, Hampel H, Weiner M, Zetterberg H. Cerebrospinal fluid and plasma biomarkers in Alzheimer disease. Nat Rev Neurol. 2010 Mar;6(3):131-44. doi: 10.1038/nrneurol.2010.4. Epub 2010 Feb 16. PMID: 20157306.

408- Blennow K, Wallin A, Agren H, Spenger C, Siegfried J, Vanmechelen E. Tau protein in cerebrospinal fluid: a biochemical marker for axonal degeneration in Alzheimer disease? Mol Chem Neuropathol. 1995 Dec;26(3):231-45. doi: 10.1007/BF02815140. PMID: 8748926.

409- Andreasen N, Hesse C, Davidsson P, Minthon L, Wallin A, Winblad B, Vanderstichele H, Vanmechelen E, Blennow K. Cerebrospinal fluid beta-amyloid(1-42) in Alzheimer disease: differences between early- and late-onset

Alzheimer disease and stability during the course of disease. Arch Neurol. 1999 Jun;56(6):673-80. doi: 10.1001/archneur.56.6.673. PMID: 10369305.

410- Seubert P, Vigo-Pelfrey C, Esch F, Lee M, Dovey H, Davis D, Sinha S, Schlossmacher M, Whaley J, Swindlehurst C, et al. Isolation and quantification of soluble Alzheimer's beta-peptide from biological fluids. Nature. 1992 Sep 24;359(6393):325-7. doi: 10.1038/359325a0. PMID: 1406936.

411- Olsson B, Lautner R, Andreasson U, Öhrfelt A, Portelius E, Bjerke M, Hölttä M, Rosén C, Olsson C, Strobel G, Wu E, Dakin K, Petzold M, Blennow K, Zetterberg H. CSF and blood biomarkers for the diagnosis of Alzheimer's disease: a systematic review and meta-analysis. Lancet Neurol. 2016 Jun;15(7):673-684. doi: 10.1016/S1474-4422(16)00070-3. Epub 2016 Apr 8. PMID: 27068280.

412- Strozyk D, Blennow K, White LR, Launer LJ. CSF Abeta 42 levels correlate with amyloid-neuropathology in a population-based autopsy study. Neurology. 2003 Feb 25;60(4):652-6. doi: 10.1212/01.wnl.0000046581.81650.d0. PMID: 12601108.

413- Blennow K, Mattsson N, Schöll M, Hansson O, Zetterberg H. Amyloid biomarkers in Alzheimer's disease. Trends Pharmacol Sci. 2015 May;36(5):297-309. doi: 10.1016/j.tips.2015.03.002. Epub 2015 Apr 1. PMID: 25840462.

414- Hansson O, Zetterberg H, Buchhave P, Andreasson U, Londos E, Minthon L, Blennow K. Prediction of Alzheimer's disease using the CSF Abeta42/Abeta40 ratio in patients with mild cognitive impairment. Dement Geriatr Cogn Disord. 2007;23(5):316-20. doi: 10.1159/000100926. Epub 2007 Mar 19. PMID: 17374949.

415- Lewczuk P, Matzen A, Blennow K, Parnetti L, Molinuevo JL, Eusebi P, Kornhuber J, Morris JC, Fagan AM. Cerebrospinal Fluid Aβ42/40 Corresponds Better than Aβ42 to Amyloid PET in Alzheimer's Disease. J Alzheimers Dis. 2017;55(2):813-822. doi: 10.3233/JAD-160722. PMID: 27792012; PMCID: PMC5147502.

416- Shoji M, Matsubara E, Kanai M, Watanabe M, Nakamura T, Tomidokoro Y, Shizuka M, Wakabayashi K, Igeta Y, Ikeda Y, Mizushima K, Amari M, Ishiguro K, Kawarabayashi T, Harigaya Y, Okamoto K, Hirai S. Combination assay of CSF tau, A beta 1-40 and A beta 1-42(43) as a biochemical marker of Alzheimer's disease. J Neurol Sci. 1998 Jun 30;158(2):134-40. doi: 10.1016/s0022-510x(98)00122-1. PMID: 9702683.

417- Lewczuk P, Lelental N, Spitzer P, Maler JM, Kornhuber J. Amyloid-β 42/40 cerebrospinal fluid concentration ratio in the diagnostics of Alzheimer's disease: validation of two novel assays. J Alzheimers Dis. 2015;43(1):183-91. doi: 10.3233/JAD-140771. PMID: 25079805.

418- Blennow K, Hampel H. CSF markers for incipient Alzheimer's disease. Lancet Neurol. 2003 Oct;2(10):605-13. doi: 10.1016/s1474-4422(03)00530-1. PMID: 14505582.

419- Zetterberg H, Hietala MA, Jonsson M, Andreasen N, Styrud E, Karlsson I, Edman A, Popa C, Rasulzada A, Wahlund LO, Mehta PD, Rosengren L, Blennow K, Wallin A. Neurochemical aftermath of amateur boxing. Arch Neurol. 2006 Sep;63(9):1277-80. doi: 10.1001/archneur.63.9.1277. PMID: 16966505.

420- Buchhave P, Minthon L, Zetterberg H, Wallin AK, Blennow K, Hansson O. Cerebrospinal fluid levels of β-amyloid 1-42, but not of tau, are fully changed already 5 to 10 years before the onset of Alzheimer dementia. Arch Gen Psychiatry. 2012 Jan;69(1):98-106. doi: 10.1001/archgenpsychiatry.2011.155. PMID: 22213792.

421- Wallin AK, Blennow K, Zetterberg H, Londos E, Minthon L, Hansson O. CSF biomarkers predict a more malignant outcome in Alzheimer disease. Neurology. 2010 May 11;74(19):1531-7. doi: 10.1212/WNL.0b013e3181dd4dd8. PMID: 20458070.

422- Skillbäck T, Rosén C, Asztely F, Mattsson N, Blennow K, Zetterberg H. Diagnostic performance of cerebrospinal fluid total tau and phosphorylated tau in Creutzfeldt-Jakob disease: results from the Swedish Mortality Registry. JAMA Neurol. 2014 Apr;71(4):476-83. doi: 10.1001/jamaneurol.2013.6455. PMID: 24566866.

423- Gordon BA, Friedrichsen K, Brier M, Blazey T, Su Y, Christensen J, Aldea P, McConathy J, Holtzman DM, Cairns NJ, Morris JC, Fagan AM, Ances BM, Benzinger TL. The relationship between cerebrospinal fluid markers of Alzheimer pathology and positron emission tomography tau imaging. Brain. 2016 Aug;139(Pt 8):2249-60. doi: 10.1093/brain/aww139. Epub 2016 Jun 10. PMID: 27286736; PMCID: PMC4958902.

424- Blennow K, Zetterberg H. Biomarkers for Alzheimer's disease: current status and prospects for the future. J Intern Med. 2018 Dec;284(6):643-663. doi: 10.1111/joim.12816. Epub 2018 Aug 19. PMID: 30051512.

425- Hansson O, Zetterberg H, Buchhave P, Londos E, Blennow K, Minthon L. Association between CSF biomarkers and incipient Alzheimer's disease in patients with mild cognitive impairment: a follow-up study. Lancet Neurol. 2006 Mar;5(3):228-34. doi: 10.1016/S1474-4422(06)70355-6. Erratum in: Lancet Neurol. 2006 Apr;5(4):293. PMID: 16488378.

426- Gustafson DR, Skoog I, Rosengren L, Zetterberg H, Blennow K. Cerebrospinal fluid beta-amyloid 1-42 concentration may predict cognitive decline in older women. J Neurol Neurosurg Psychiatry. 2007 May;78(5):461-4. doi: 10.1136/jnnp.2006.100529. Epub 2006 Nov 10. PMID: 17098843; PMCID: PMC2117838.

427- Jack CR Jr, Bennett DA, Blennow K, Carrillo MC, Feldman HH, Frisoni GB, Hampel H, Jagust WJ, Johnson KA, Knopman DS, Petersen RC, Scheltens P, Sperling RA, Dubois B. A/T/N: An unbiased descriptive classification scheme for Alzheimer disease biomarkers. Neurology. 2016 Aug 2;87(5):539-47. doi: 10.1212/WNL.0000000000002923. Epub 2016 Jul 1. PMID: 27371494; PMCID: PMC4970664.

428- Kvartsberg H, Portelius E, Andreasson U, Brinkmalm G, Hellwig K, Lelental N, Kornhuber J, Hansson O, Minthon L, Spitzer P, Maler JM, Zetterberg H, Blennow K, Lewczuk P. Characterization of the postsynaptic protein neurogranin in paired cerebrospinal fluid and plasma samples from Alzheimer's disease patients and healthy controls. Alzheimers Res Ther. 2015 Jul 1;7(1):40. doi: 10.1186/s13195-015-0124-3. PMID: 26136856; PMCID: PMC4487851.

429- Portelius E, Zetterberg H, Skillbäck T, Törnqvist U, Andreasson U, Trojanowski JQ, Weiner MW, Shaw LM, Mattsson N, Blennow K; Alzheimer's Disease Neuroimaging Initiative. Cerebrospinal fluid neurogranin: relation to cognition and neurodegeneration in Alzheimer's disease. Brain. 2015 Nov;138(Pt 11):3373-85. doi: 10.1093/brain/awv267. Epub 2015 Sep 15. PMID: 26373605; PMCID: PMC4643642.

430- Johnson SC, Suárez-Calvet M, Suridjan I, Minguillón C, Gispert JD, Jonaitis E, Michna A, Carboni M, Bittner T, Rabe C, Kollmorgen G, Zetterberg H, Blennow K. Identifying clinically useful biomarkers in neurodegenerative disease through a collaborative approach: the NeuroToolKit. Alzheimers Res Ther. 2023 Jan 28;15(1):25. doi: 10.1186/s13195-023-01168-y. PMID: 36709293; PMCID: PMC9883877.

431- O'Bryant SE, Gupta V, Henriksen K, Edwards M, Jeromin A, Lista S, Bazenet C, Soares H, Lovestone S, Hampel H, Montine T, Blennow K, Foroud T, Carrillo M, Graff-Radford N, Laske C, Breteler M, Shaw L, Trojanowski JQ, Schupf N, Rissman RA, Fagan AM, Oberoi P, Umek R, Weiner MW, Grammas P, Posner H, Martins R; STAR-B and BBBIG working groups. Guidelines for the

standardization of preanalytic variables for blood-based biomarker studies in Alzheimer's disease research. Alzheimers Dement. 2015 May;11(5):549-60. doi: 10.1016/j.jalz.2014.08.099. Epub 2014 Oct 1. PMID: 25282381; PMCID: PMC4414664.

432- Andreasson U, Blennow K, Zetterberg H. Update on ultrasensitive technologies to facilitate research on blood biomarkers for central nervous system disorders. Alzheimers Dement (Amst). 2016 Jun 25;3:98-102. doi: 10.1016/j.dadm.2016.05.005. PMID: 27453931; PMCID: PMC4941042.

433- Hansson O, Zetterberg H, Vanmechelen E, Vanderstichele H, Andreasson U, Londos E, Wallin A, Minthon L, Blennow K. Evaluation of plasma Abeta(40) and Abeta(42) as predictors of conversion to Alzheimer's disease in patients with mild cognitive impairment. Neurobiol Aging. 2010 Mar;31(3):357-67. doi: 10.1016/j.neurobiolaging.2008.03.027. Epub 2008 May 19. PMID: 18486992.

434- Janelidze S, Stomrud E, Palmqvist S, Zetterberg H, van Westen D, Jeromin A, Song L, Hanlon D, Tan Hehir CA, Baker D, Blennow K, Hansson O. Plasma β-amyloid in Alzheimer's disease and vascular disease. Sci Rep. 2016 May 31;6:26801. doi: 10.1038/srep26801. PMID: 27241045; PMCID: PMC4886210.

435- Zetterberg H, Wilson D, Andreasson U, Minthon L, Blennow K, Randall J, Hansson O. Plasma tau levels in Alzheimer's disease. Alzheimers Res Ther. 2013 Mar 28;5(2):9. doi: 10.1186/alzrt163. PMID: 23551972; PMCID: PMC3707015.

436- Mattsson N, Zetterberg H, Janelidze S, Insel PS, Andreasson U, Stomrud E, Palmqvist S, Baker D, Tan Hehir CA, Jeromin A, Hanlon D, Song L, Shaw LM, Trojanowski JQ, Weiner MW, Hansson O, Blennow K; ADNI Investigators. Plasma tau in Alzheimer disease. Neurology. 2016 Oct 25;87(17):1827-1835. doi: 10.1212/WNL.0000000000003246. Epub 2016 Sep 30. PMID: 27694257; PMCID: PMC5089525.

437- Palmqvist S, Janelidze S, Quiroz YT, Zetterberg H, Lopera F, Stomrud E, Su Y, Chen Y, Serrano GE, Leuzy A, Mattsson-Carlgren N, Strandberg O, Smith R, Villegas A, Sepulveda-Falla D, Chai X, Proctor NK, Beach TG, Blennow K, Dage JL, Reiman EM, Hansson O. Discriminative Accuracy of Plasma Phospho-tau217 for Alzheimer Disease vs Other Neurodegenerative Disorders. JAMA. 2020 Aug 25;324(8):772-781. doi: 10.1001/jama.2020.12134. PMID: 32722745; PMCID: PMC7388060.

438- Gaetani L, Blennow K, Calabresi P, Di Filippo M, Parnetti L, Zetterberg H. Neurofilament light chain as a biomarker in neurological disorders. J Neurol Neurosurg Psychiatry. 2019 Aug;90(8):870-881. doi: 10.1136/jnnp-2018-320106. Epub 2019 Apr 9. PMID: 30967444.

439- Gisslén M, Price RW, Andreasson U, Norgren N, Nilsson S, Hagberg L, Fuchs D, Spudich S, Blennow K, Zetterberg H. Plasma Concentration of the Neurofilament Light Protein (NFL) is a Biomarker of CNS Injury in HIV Infection: A Cross-Sectional Study. EBioMedicine. 2015 Nov 22;3:135-140. doi: 10.1016/j.ebiom.2015.11.036. Erratum in: EBioMedicine. 2016 May;7:287-288. PMID: 26870824; PMCID: PMC4739412.

440- Mattsson N, Andreasson U, Zetterberg H, Blennow K; Alzheimer's Disease Neuroimaging Initiative. Association of Plasma Neurofilament Light With Neurodegeneration in Patients With Alzheimer Disease. JAMA Neurol. 2017 May 1;74(5):557-566. doi: 10.1001/jamaneurol.2016.6117. PMID: 28346578; PMCID: PMC5822204.

441- Weston PSJ, Poole T, Ryan NS, Nair A, Liang Y, Macpherson K, Druyeh R, Malone IB, Ahsan RL, Pemberton H, Klimova J, Mead S, Blennow K, Rossor MN, Schott JM, Zetterberg H, Fox NC. Serum neurofilament light in familial Alzheimer disease: A marker of early neurodegeneration. Neurology. 2017 Nov

21;89(21):2167-2175. doi: 10.1212/WNL.0000000000004667. Epub 2017 Oct 25. PMID: 29070659; PMCID: PMC5696646.

442- Rohrer JD, Woollacott IO, Dick KM, Brotherhood E, Gordon E, Fellows A, Toombs J, Druyeh R, Cardoso MJ, Ourselin S, Nicholas JM, Norgren N, Mead S, Andreasson U, Blennow K, Schott JM, Fox NC, Warren JD, Zetterberg H. Serum neurofilament light chain protein is a measure of disease intensity in frontotemporal dementia. Neurology. 2016 Sep 27;87(13):1329-36. doi: 10.1212/WNL.0000000000003154. Epub 2016 Aug 31. PMID: 27581216; PMCID: PMC5047041.

443- Gupta VB, Laws SM, Villemagne VL, Ames D, Bush AI, Ellis KA, Lui JK, Masters C, Rowe CC, Szoeke C, Taddei K, Martins RN; AIBL Research Group. Plasma apolipoprotein E and Alzheimer disease risk: the AIBL study of aging. Neurology. 2011 Mar 22;76(12):1091-8. doi: 10.1212/WNL.0b013e318211c352. PMID: 21422459.

444- Martínez-Morillo E, Hansson O, Atagi Y, Bu G, Minthon L, Diamandis EP, Nielsen HM. Total apolipoprotein E levels and specific isoform composition in cerebrospinal fluid and plasma from Alzheimer's disease patients and controls. Acta Neuropathol. 2014 May;127(5):633-43. doi: 10.1007/s00401-014-1266-2. Epub 2014 Mar 15. PMID: 24633805.

445- Gregg RE, Zech LA, Schaefer EJ, Stark D, Wilson D, Brewer HB Jr. Abnormal in vivo metabolism of apolipoprotein E4 in humans. J Clin Invest. 1986 Sep;78(3):815-21. doi: 10.1172/JCI112645. PMID: 3745440; PMCID: PMC423680.

446- Fukumoto H, Ingelsson M, Gårevik N, Wahlund LO, Nukina N, Yaguchi Y, Shibata M, Hyman BT, Rebeck GW, Irizarry MC. APOE epsilon 3/ epsilon 4 heterozygotes have an elevated proportion of apolipoprotein E4 in cerebrospinal fluid relative to plasma, independent of Alzheimer's disease diagnosis. Exp Neurol. 2003 Sep;183(1):249-53. doi: 10.1016/s0014-4886(03)00088-8. PMID: 12957508.

447- Ramaswamy G, Xu Q, Huang Y, Weisgraber KH. Effect of domain interaction on apolipoprotein E levels in mouse brain. J Neurosci. 2005 Nov 16;25(46):10658-63. doi: 10.1523/JNEUROSCI.1922-05.2005. PMID: 16291938; PMCID: PMC6725862.

448- Riddell DR, Zhou H, Atchison K, Warwick HK, Atkinson PJ, Jefferson J, Xu L, Aschmies S, Kirksey Y, Hu Y, Wagner E, Parratt A, Xu J, Li Z, Zaleska MM, Jacobsen JS, Pangalos MN, Reinhart PH. Impact of apolipoprotein E (ApoE) polymorphism on brain ApoE levels. J Neurosci. 2008 Nov 5;28(45):11445-53. doi: 10.1523/JNEUROSCI.1972-08.2008. PMID: 18987181; PMCID: PMC6671315.

449- Darreh-Shori T, Forsberg A, Modiri N, Andreasen N, Blennow K, Kamil C, Ahmed H, Almkvist O, Långström B, Nordberg A. Differential levels of apolipoprotein E and butyrylcholinesterase show strong association with pathological signs of Alzheimer's disease in the brain in vivo. Neurobiol Aging. 2011 Dec;32(12):2320.e15-32. doi: 10.1016/j.neurobiolaging.2010.04.028. Epub 2010 Jun 9. PMID: 20538374.

450- Wahrle SE, Shah AR, Fagan AM, Smemo S, Kauwe JS, Grupe A, Hinrichs A, Mayo K, Jiang H, Thal LJ, Goate AM, Holtzman DM. Apolipoprotein E levels in cerebrospinal fluid and the effects of ABCA1 polymorphisms. Mol Neurodegener. 2007 Apr 12;2:7. doi: 10.1186/1750-1326-2-7. PMID: 17430597; PMCID: PMC1857699.

451- Minta K, Brinkmalm G, Janelidze S, Sjödin S, Portelius E, Stomrud E, Zetterberg H, Blennow K, Hansson O, Andreasson U. Quantification of total apolipoprotein E and its isoforms in cerebrospinal fluid from patients with neurodegenerative

diseases. Alzheimers Res Ther. 2020 Feb 13;12(1):19. doi: 10.1186/s13195-020-00585-7. PMID: 32054532; PMCID: PMC7020540.

452- Honda K, Saito Y, Saito H, Toyoda M, Abe R, Saito T, Saido TC, Michikawa M, Taru H, Sobu Y, Hata S, Nakaya T, Suzuki T. Accumulation of amyloid-β in the brain of mouse models of Alzheimer's disease is modified by altered gene expression in the presence of human apoE isoforms during aging. Neurobiol Aging. 2023 Mar;123:63-74. doi: 10.1016/j.neurobiolaging.2022.12.003. Epub 2022 Dec 17. PMID: 36638682.

453- Nielsen HM, Chen K, Lee W, Chen Y, Bauer RJ 3rd, Reiman E, Caselli R, Bu G. Peripheral apoE isoform levels in cognitively normal APOE ε3/ε4 individuals are associated with regional gray matter volume and cerebral glucose metabolism. Alzheimers Res Ther. 2017 Jan 30;9(1):5. doi: 10.1186/s13195-016-0231-9. PMID: 28137305; PMCID: PMC5282900.

454- Simon R, Girod M, Fonbonne C, Salvador A, Clément Y, Lantéri P, Amouyel P, Lambert JC, Lemoine J. Total ApoE and ApoE4 isoform assays in an Alzheimer's disease case-control study by targeted mass spectrometry (n=669): a pilot assay for methionine-containing proteotypic peptides. Mol Cell Proteomics. 2012 Nov;11(11):1389-403. doi: 10.1074/mcp.M112.018861. Epub 2012 Aug 23. PMID: 22918225; PMCID: PMC3494189.

455- Cruchaga C, Kauwe JS, Mayo K, Spiegel N, Bertelsen S, Nowotny P, Shah AR, Abraham R, Hollingworth P, Harold D, Owen MM, Williams J, Lovestone S, Peskind ER, Li G, Leverenz JB, Galasko D; Alzheimer's Disease Neuroimaging Initiative; Morris JC, Fagan AM, Holtzman DM, Goate AM. SNPs associated with cerebrospinal fluid phospho-tau levels influence rate of decline in Alzheimer's disease. PLoS Genet. 2010 Sep 16;6(9):e1001101. doi: 10.1371/journal.pgen.1001101. PMID: 20862329; PMCID: PMC2940763.

456- Morris JC, Roe CM, Xiong C, Fagan AM, Goate AM, Holtzman DM, Mintun MA. APOE predicts amyloid-beta but not tau Alzheimer pathology in cognitively normal aging. Ann Neurol. 2010 Jan;67(1):122-31. doi: 10.1002/ana.21843. PMID: 20186853; PMCID: PMC2830375.

457- Reiman EM, Chen K, Liu X, Bandy D, Yu M, Lee W, Ayutyanont N, Keppler J, Reeder SA, Langbaum JB, Alexander GE, Klunk WE, Mathis CA, Price JC, Aizenstein HJ, DeKosky ST, Caselli RJ. Fibrillar amyloid-beta burden in cognitively normal people at 3 levels of genetic risk for Alzheimer's disease. Proc Natl Acad Sci U S A. 2009 Apr 21;106(16):6820-5. doi: 10.1073/pnas.0900345106. Epub 2009 Apr 3. PMID: 19346482; PMCID: PMC2665196.

458- Deming Y, Li Z, Kapoor M, Harari O, Del-Aguila JL, Black K, Carrell D, Cai Y, Fernandez MV, Budde J, Ma S, Saef B, Howells B, Huang KL, Bertelsen S, Fagan AM, Holtzman DM, Morris JC, Kim S, Saykin AJ, De Jager PL, Albert M, Moghekar A, O'Brien R, Riemenschneider M, Petersen RC, Blennow K, Zetterberg H, Minthon L, Van Deerlin VM, Lee VM, Shaw LM, Trojanowski JQ, Schellenberg G, Haines JL, Mayeux R, Pericak-Vance MA, Farrer LA, Peskind ER, Li G, Di Narzo AF; Alzheimer's Disease Neuroimaging Initiative (ADNI); Alzheimer Disease Genetic Consortium (ADGC); Kauwe JS, Goate AM, Cruchaga C. Genome-wide association study identifies four novel loci associated with Alzheimer's endophenotypes and disease modifiers. Acta Neuropathol. 2017 May;133(5):839-856. doi: 10.1007/s00401-017-1685-y. Epub 2017 Feb 28. PMID: 28247064; PMCID: PMC5613285.

459- Hibi T, Hattori M. The N-terminal fragment of Reelin is generated after endocytosis and released through the pathway regulated by Rab11. FEBS Lett. 2009 Apr 17;583(8):1299-303. doi: 10.1016/j.febslet.2009.03.024. Epub 2009 Mar 20. PMID: 19303411.

460- Hattori M, Kohno T. Regulation of Reelin functions by specific proteolytic processing in the brain. J Biochem. 2021 Jul 3;169(5):511-516. doi: 10.1093/jb/mvab015. PMID: 33566063.

461- Lennol MP, Sánchez-Domínguez I, Cuchillo-Ibañez I, Camporesi E, Brinkmalm G, Alcolea D, Fortea J, Lleó A, Soria G, Aguado F, Zetterberg H, Blennow K, Sáez-Valero J. Apolipoprotein E imbalance in the cerebrospinal fluid of Alzheimer's disease patients. Alzheimers Res Ther. 2022 Nov 2;14(1):161. doi: 10.1186/s13195-022-01108-2. PMID: 36324176; PMCID: PMC9628034.

462- Lopez-Font I, Lennol MP, Iborra-Lazaro G, Zetterberg H, Blennow K, Sáez-Valero J. Altered Balance of Reelin Proteolytic Fragments in the Cerebrospinal Fluid of Alzheimer's Disease Patients. Int J Mol Sci. 2022 Jul 7;23(14):7522. doi: 10.3390/ijms23147522. PMID: 35886870; PMCID: PMC9318932.

463- Cuchillo-Ibañez I, Lennol MP, Escamilla S, Mata-Balaguer T, Valverde-Vozmediano L, Lopez-Font I, Ferrer I, Sáez-Valero J. The apolipoprotein receptor LRP3 compromises APP levels. Alzheimers Res Ther. 2021 Nov 2;13(1):181. doi: 10.1186/s13195-021-00921-5. PMID: 34727970; PMCID: PMC8565065.

464- Sáez-Valero J, Sberna G, McLean CA, Small DH. Molecular isoform distribution and glycosylation of acetylcholinesterase are altered in brain and cerebrospinal fluid of patients with Alzheimer's disease. J Neurochem. 1999 Apr;72(4):1600-8. doi: 10.1046/j.1471-4159.1999.721600.x. PMID: 10098867.

465- Bac B, Hicheri C, Weiss C, Buell A, Vilcek N, Spaeni C, Geula C, Savas JN, Disterhoft JF. The TgF344-AD rat: behavioral and proteomic changes associated with aging and protein expression in a transgenic rat model of Alzheimer's disease. Neurobiol Aging. 2023 Mar;123:98-110. doi: 10.1016/j.neurobiolaging.2022.12.015. Epub 2022 Dec 30. PMID: 36657371.

466- Sogorb-Esteve A, García-Ayllón MS, Fortea J, Sánchez-Valle R, Lleó A, Molinuevo JL, Sáez-Valero J. Cerebrospinal fluid Presenilin-1 increases at asymptomatic stage in genetically determined Alzheimer's disease. Mol Neurodegener. 2016 Sep 29;11(1):66. doi: 10.1186/s13024-016-0131-2. PMID: 27686161; PMCID: PMC5043603.

467- García-Ayllón MS, Campanari ML, Brinkmalm G, Rábano A, Alom J, Saura CA, Andreasen N, Blennow K, Sáez-Valero J. CSF Presenilin-1 complexes are increased in Alzheimer's disease. Acta Neuropathol Commun. 2013 Aug 6;1:46. doi: 10.1186/2051-5960-1-46. PMID: 24252417; PMCID: PMC3893612.

468- Johnson ECB, Dammer EB, Duong DM, Ping L, Zhou M, Yin L, Higginbotham LA, Guajardo A, White B, Troncoso JC, Thambisetty M, Montine TJ, Lee EB, Trojanowski JQ, Beach TG, Reiman EM, Haroutunian V, Wang M, Schadt E, Zhang B, Dickson DW, Ertekin-Taner N, Golde TE, Petyuk VA, De Jager PL, Bennett DA, Wingo TS, Rangaraju S, Hajjar I, Shulman JM, Lah JJ, Levey AI, Seyfried NT. Large-scale proteomic analysis of Alzheimer's disease brain and cerebrospinal fluid reveals early changes in energy metabolism associated with microglia and astrocyte activation. Nat Med. 2020 May;26(5):769-780. doi: 10.1038/s41591-020-0815-6. Epub 2020 Apr 13. PMID: 32284590; PMCID: PMC7405761.

469- Chen Z, Yu Q, Yu Q, Johnson J, Shipman R, Zhong X, Huang J, Asthana S, Carlsson C, Okonkwo O, Li L. In-depth Site-specific Analysis of N-glycoproteome in Human Cerebrospinal Fluid and Glycosylation Landscape Changes in Alzheimer's Disease. Mol Cell Proteomics. 2021;20:100081. doi: 10.1016/j.mcpro.2021.100081. Epub 2021 Apr 20. PMID: 33862227; PMCID: PMC8724636.

470- Conroy LR, Hawkinson TR, Young LEA, Gentry MS, Sun RC. Emerging roles of N-linked glycosylation in brain physiology and disorders. Trends Endocrinol

Metab. 2021 Dec;32(12):980-993. doi: 10.1016/j.tem.2021.09.006. Epub 2021 Oct 29. PMID: 34756776; PMCID: PMC8589112.

471- Imaizumi K, Miyoshi K, Katayama T, Yoneda T, Taniguchi M, Kudo T, Tohyama M. The unfolded protein response and Alzheimer's disease. Biochim Biophys Acta. 2001 May 31;1536(2-3):85-96. doi: 10.1016/s0925-4439(01)00049-7. PMID: 11406343.

472- Haukedal H, Corsi GI, Gadekar VP, Doncheva NT, Kedia S, de Haan N, Chandrasekaran A, Jensen P, Schiønning P, Vallin S, Marlet FR, Poon A, Pires C, Agha FK, Wandall HH, Cirera S, Simonsen AH, Nielsen TT, Nielsen JE, Hyttel P, Muddashetty R, Aldana BI, Gorodkin J, Nair D, Meyer M, Larsen MR, Freude K. Golgi fragmentation - One of the earliest organelle phenotypes in Alzheimer's disease neurons. Front Neurosci. 2023 Feb 16;17:1120086. doi: 10.3389/fnins.2023.1120086. PMID: 36875643; PMCID: PMC9978754.

473- Schedin-Weiss S, Winblad B, Tjernberg LO. The role of protein glycosylation in Alzheimer disease. FEBS J. 2014 Jan;281(1):46-62. doi: 10.1111/febs.12590. Epub 2013 Nov 26. PMID: 24279329.

474- Akasaka-Manya K, Manya H. The Role of APP *O*-Glycosylation in Alzheimer's Disease. Biomolecules. 2020 Nov 18;10(11):1569. doi: 10.3390/biom10111569. PMID: 33218200; PMCID: PMC7699271.

475- Milosch N, Tanriöver G, Kundu A, Rami A, François JC, Baumkötter F, Weyer SW, Samanta A, Jäschke A, Brod F, Buchholz CJ, Kins S, Behl C, Müller UC, Kögel D. Holo-APP and G-protein-mediated signaling are required for sAPPα-induced activation of the Akt survival pathway. Cell Death Dis. 2014 Aug 28;5(8):e1391. doi: 10.1038/cddis.2014.352. PMID: 25165877; PMCID: PMC4454324.

476- Reinhardt S, Stoye N, Luderer M, Kiefer F, Schmitt U, Lieb K, Endres K. Identification of disulfiram as a secretase-modulating compound with beneficial effects on Alzheimer's disease hallmarks. Sci Rep. 2018 Jan 22;8(1):1329. doi: 10.1038/s41598-018-19577-7. PMID: 29358714; PMCID: PMC5778060.

477- Gallo CM, Ho A, Beffert U. ApoER2: Functional Tuning Through Splicing. Front Mol Neurosci. 2020 Jul 31;13:144. doi: 10.3389/fnmol.2020.00144. PMID: 32848602; PMCID: PMC7410921.

478- van Harten AC, Jongbloed W, Teunissen CE, Scheltens P, Veerhuis R, van der Flier WM. CSF ApoE predicts clinical progression in nondemented APOEε4 carriers. Neurobiol Aging. 2017 Sep;57:186-194. doi: 10.1016/j.neurobiolaging.2017.04.002. Epub 2017 Apr 12. PMID: 28571653.

ACKNOWLDGEMENTS

First and foremost, I would like to thank the members of my lab for all the support they've given me over the last 3 and a half years. I've learned loads over the course of my PhD, and I feel I've become much more competent thanks to all the experience. I thank Inma C for her feedback on this manuscript and assistance; Inma L for helping me adapt to the lab and making it more enjoyable; Salu for being a great source of knowledge and wisdom, and always being available and willing to help; and my fellow PhD students: Sergio, Mari, and Adriana, for sharing the journey and killing all those cells with me. I've never been the easiest person to deal with, but that never stopped you from taking an interest, being patient, and being willing to help and teach me, for which I am grateful. I take with me loads of experiences, post-it notes, memories, and people that I will always cherish. I would also like to thank all the hard-working staff at the INA for making our day-to-day work so much easier and enjoyable.

On a professional level, there are a few names that warrant special mention for the impact they had on my career. Ferran, for nurturing my interest in research and in more fundamental science, for all the guidance, all the opportunities, and all the laughs over the many years of collaboration. You're a fantastic professional, the best the whole faculty has to offer (without a doubt), and a real inspiration in this time of excessive political correctness.

Laura and Sandra. My time in Madrid was hard, and finding a lab that was willing to teach a student with absolutely no experience was troublesome to say the least. From the first time we met, you made it clear that you would do your utmost to help my career as much as possible, and you achieved just that, more than you can possibly imagine. Everything I know, every success that has followed since my time with you, is your merit as much as my own. Going to that interview was one of the 2 best decisions I've made in my career. Learning from you was one of the very few positives I took from my time in Madrid, and you made the lab somewhere fun and enjoyable, so thank you both for everything.

A very special mention must go to Javier. From the first phone call in January of 2018 (the other one of the 2 best decisions I've made), when I had no

idea where my future lied, you've been understanding, supportive and patient. I have the genuine feeling that, given the ups and downs of the last few years, I wouldn't be in this position if you hadn't taken me under your wing. You've been more than just a director, you've been a friend, a mentor, a colleague. You've taught as much about science as you have about life, and that is something that you deserve eternal gratitude for. You took a risk with me, and from the first moment you never gave up, never backed away, never doubted my potential, and you've been true to your word. All I hope is that, with everything, I've been able to make you think it was the right choice (even if I still don't separate the kDa from the numbers).

On a personal level, I would like to start by making it clear that this thesis, and everything that comes with it, isn't my success: it belongs to all of us, to everyone who has been at my side and helped me, from friends to family, even to my precious little Piglett (Meow or "Matt" to you too).

To my friends, who have stuck with me for many, many years. There aren't many names to mention, but I've always preferred quality over quantity. A special mention goes out to Marc and Jordi, for both being so supportive, understanding, and for genuinely caring about me, especially in the hardest of times, and for all the laughs.

V. This paragraph isn't the easiest to write because I hate summarizing, and I could write a whole thesis about you. Through all the years, all the experiences, the right (and wrong) decisions, you've been there. I wouldn't be the person I am today, finishing this thesis, without you. The lives we've shared, the paths we've walked, the cities we've seen: I never believed that anyone could possibly play such a big role in someone else's life, but you have. I'm still in awe of you, after all these years. Gracias mon, por todo. "*You without end*".

I thank my grandparents for being caring, nurturing, loving, and for each contributing in your own way to this achievement, and to me as a person. I feel I've been blessed with this family unit, that has luckily been with me this whole time. I've learnt so much from you all, and the pride you abundantly show has been a real motivating factor over the years.

To my brother from the same mother, Chris. I genuinely feel I'm the luckiest person to have you as a brother. You've been there for me, helped in everything you could, and put up with me being a difficult person at times. You're one of my best friends, and you're always there for anything that's needed, be it a serious chat, be it some light-hearted laughs, or be it just a late night on the PlayStation. I know just how proud you are of me, but you should know I'm just as proud of you, for everything you do, and everything you are. You are worth your weight in gold, and never let anyone say otherwise.

To my Mum and Dad. I can't express how grateful I am for everything you've done for me over the years. For the decisions and sacrifices made, and all the support; for sticking by my side at some of the lowest points; for teaching me to be the man I am today, with assertiveness but mainly with care; for nudging me in the right direction when I was lost; for putting up with the difficult side of me, always with a smile. I thank you for all the laughs, all the lessons, all the guidance, all the love. I feel so fortunate to have you, both as parents and as friends. I hope that this whole thesis, in some way, has made it all worthwhile. Again, thank you for making it possible.

I wouldn't be in this position without each and every one of you, and you know that just as well as I do. So, I would not only like to thank you, as I'd also like to congratulate you all for your part in the story. I am but a Vessel of all the energy, love, support, and belief you've poured into me over the years, and I hope I've been able to convert it all into something that makes you all feel just a little bit proud of me, and more importantly of yourselves.

This is too politically correct for me so... Hail Satan and hail the apoE-calypse.

As I tiptoed off the plane of existence,
And drifted listlessly,
Through the velvet blackness of Oblivion,
I am what I always was:
Gleaming and Empty.

"From the Kettle Onto the Coil" - Deafheaven